Nitrogen Isotopic Systematics in Ureilites

A THESIS

submitted for the Award of Ph. D. degree of

Mohan Lal Sukhadia University

in the

Faculty of Science

BY

Vinai Kumar Rai

Under the Supervision of

Prof. S. V. S. Murty

DEPARTMENT OF SOLAR SYSTEM STUDIES AND GEOCHRONOLOGY

PHYSICAL RESEARCH LABORATORY, AHMEDABAD

MOHANLAL SUKHADIA UNIVERSITY, UDAIPUR

Year of submission: 2001

to

My Babu Ji & Amma

Certificate

I hereby declare that the work presented in this thesis is original and has not formed the basis for the award of any degree or diploma by any university or Institution.

Vinai Kumar Rai

(Author)

Certified by:

Prof. S. V. S. Murty

Physical Research Laboratory,

Ahmedabad, 380 009, India

(May, 2001)

Acknowledgements

Writing acknowledgement for my thesis work was very important to me. This was in my mind for quite for some time during the last few months when I was finalizing the chapters, which constitute the present work. So many persons have helped me in coming up at different stages during the last five years of doctoral work that my indebtedness to them needed a big space for proper articulation. I am really grateful to all of those persons who helped me by giving me courage at difficult times, by imparting the necessary knowledge and by tolerating me when I was imperfect.

It will be an injustice on my part if I call Prof. S. V. S. Murty as only my 'thesis supervisor'. He is much more than that to me. He inculcated tremendous interest in me for this fascinating branch of science, which deals with the study of the 'extra-terrestrial' messenger's to our planet called 'meteorite'. I was a newcomer to this field. There are thousands of moments, I remember, when I asked foolish questions, there are thousands of instances when I didn't know how to properly articulate the scientific ideas and non-scientific issues. He was having patience all the time beyond my imagination. His patience, guidance and 'personal touch's made me comfortable and spontaneous with time. He is truly my 'mentor' who stood by me in all my 'deficient' moments.

Ratan was not just a 'senior' to me. He taught me the intricacies of the 'mass spectrometer' (his 'sweet heart' as he call it) and the associated techniques. The discussions, which I used to have with him helped me to strengthen my foundation in this field. Its very nice to have 'little' Sudeshna and 'Martian' Ramakant as my associates in the lab. They made life entertaining through out these years.

Most of the ureilite samples used in present study have been very generously provided by Prof. Ulrich Ott, Max-Planck-Institut für Chemie, Mainz, Germany. I am very grateful to him and to Sudek Christa, who has prepared the acid residues. I thank Dr. Roale, Institute of Plasma Research for helping in SEM work. Thanks are due to Prof. U. Ott and Prof. K. Marti for sparing their valuable time for me and discussing illuminating aspect of science. My thanks are also due to Prof. D. Lal, who's suggestions have been brief but very useful for this work.

I would like to thank Prof. J. N. Goswami, Prof N. Bhandari, Prof. T. R. Venkatesan, Dr. Kanchan Pande and J. R. Trivedi for their affectionate concern and timely help at various stages. I am grateful to Dr. P. N. Shukla for helping me in INAA analysis and Prof. S. K. Bhattacharya in carbon isotopic measurements. My sincere appreciation to the members of academic committee at PRL for critically reviewing my work at various stages. I wish to thank all the members of SOS-

Abstract

Ureilites are an enigmatic group of achondritic meteorites and contain several unusual features. Origin of diamonds in ureilites has been an actively pursued research topic for more than two decades and is not yet settled. In addition, ureilites exhibit several primitive features that are inconsistent with their igneous origin. Ureilites contain large amounts of fractionated (planetary) noble gases that are mostly carried by diamonds. Though ureilites are a highly recrystallized body, very low values of $^{40}Ar/^{36}Ar$ suggest that the carbon in ureilites has been formed very early in the solar system. Study of nitrogen and noble gases in various separated phases of ureilites might help in understanding the enigmatic features of ureilites and may also provide clues to the physicochemical conditions in which various carbon phases in ureilites have been formed.

The aim of the present study is to understand the origin of diamond in ureilites using nitrogen and noble gases as tracers. The primordial noble gases are trapped in diamond very early and remained least altered since then because of the highly refractory nature (in low fO_2 condition) of the diamond. The nitrogen coreleased with these primordial noble gases may provide primordial nitrogen composition, which is unknown so far. Bulk samples from ten ureilites (three polymict and seven monomict), HF-HCl resistant residues from eight of them and HF-HCl-HClO$_4$ residues from seven of them, have been analyzed for nitrogen and noble gases simultaneously by stepwise heating techniques (combustion and pyrolysis). The morphology and elemental composition of some of these acid residues have been studied by SEM and INAA analysis respectively.

The results of present study suggest the presence of two major nitrogen components in ureilites with very distinct isotopic composition. In addition, at least two more (minor) nitrogen components are needed to explain the observed N systematics of ureilites. The first major nitrogen component present in both monomict and polymict ureilites is very light with $\delta^{15}N \leq -100‰$ and is accompanied by most of the noble gases. This is most likely carried by the diamonds. The second nitrogen component that is carried by the

amorphous carbon, is heavier with very variable nitrogen composition. $\delta^{15}N$ of this nitrogen component in polymict ureilites, in general, is higher than that in monomict ureilites. The graphite in diamond free ureilite ALH78019, that is almost devoid of primordial noble gases, contains nitrogen with $\delta^{15}N \geq 19$ ‰ while the amorphous carbon that carries most of the primordial noble gases, have relatively light nitrogen with $\delta^{15}N \leq -21$‰. This implies that the nitrogen isotopic compositions of all the three carbon phases present in ureilite are quite different while they contain noble gases with uniform isotopic composition. The large difference in nitrogen isotopic composition between these phases most likely reflects the differences in physicochemical conditions at the formation location of these phases in the solar nebula.

It has been shown that diamonds from both polymict and monomict ureilite have very light nitrogen with $\delta^{15}N \leq -100$‰ that is independent of nitrogen composition of whole rock samples. However, amorphous carbon and graphite have much heavier nitrogen. Therefore, the presence of light nitrogen can be used as an indicator for the presence or absence of diamond. Based on this, the polymict ureilite EET83309 has been suggested to be a diamond free ureilite.

The origin of diamonds in ureilite is a highly debated topic and still not settled. There are two schools of thought for the origin of diamond. One is that the diamonds are in situ produced by the shock conversion of graphite while the other is that diamonds are nebular condensate. The uniform nitrogen isotopic composition shown by diamonds from both monomict and polymict ureilites that have very different bulk nitrogen isotopic compositions argue against the in situ origin of diamonds. The elemental analysis by INAA reveals that most of refractory elements as well as siderophile trace elements in bulk samples of ureilites are accounted for, by carbon rich residues and is suggestive of nebular origin of carbon in ureilites. Nitrogen and noble gas studies along with elemental studies of acid residues suggest that the all the three forms of carbon in ureilites are produced directly from the solar nebula.

Based on the decrease in the elemental ratios of $^{132}Xe/^{36}Ar$ and $^{84}Kr/^{36}Ar$ with increasing temperature of combustion (*i.e.,* with depth from surface of carrier grains *e.g.*, diamond),

it has been suggested that the noble gases (and nitrogen as well) are incorporated into diamonds (or amorphous carbon) by ion implantation from the solar nebula.

Göbel *et al.* (1978) suggested the presence of an unknown carrier 'X', in addition to diamond that contains large amount of noble gases, but having very different noble gas elemental ratios. In this study it has been shown that the unknown carrier 'X' is amorphous carbon phase and the variations in the noble gas elemental composition is caused by mass dependent (diffusion) loss of trapped gases during parent body processes. It has also been suggested that amorphous carbon phase and diamond initially trapped noble gases with similar elemental composition. Being refractory, the diamond has been least affected by the parent body processes while an appreciable amount of these gases are lost from amorphous carbon carrier. During this process, the loss of nitrogen was considerably smaller as compared to noble gases due to its reactivity (capable to form chemical bond with carbon). A minor shift in nitrogen isotopic composition of amorphous carbon carrier could also be due to loss induced fractionation caused by the parent body processes.

It has been shown that the ratios ^{129}Xe/^{132}Xe and ^{36}Ar/^{38}Ar in phase Q are significantly higher than that of diamond from ureilite. The capture of cosmic ray produced secondary neutrons on respective targets, can not account for these excesses, suggesting the presence of live ^{129}I and ^{36}Cl at the time of incorporation of noble gases in phase Q. The comparison of slope of elemental abundance patterns between phase Q from primitive chondrites and diamonds from ureilite suggest that noble gases in diamonds have been implanted at higher plasma temperature than that of phase Q. The low temperature incorporation of noble gases in phase Q can also demonstrate the preferential incorporation of ^{129}I and ^{36}Cl as compared to diamonds from ureilite.

Comparing the nitrogen isotopic compositions and noble gas elemental ratios in various carriers of primordial gases, it has been conjectured that higher plasma temperatures fractionate nitrogen toward lower δ^{15}N (*i.e.*, light nitrogen). Based on this, it has been suggested that nebular nitrogen must be heavier than that shown by phase Q. Laboratory simulation experiments are necessary to further understand this important issue.

Contents

Introduction

Meteorites are pieces of asteroids, the leftover rubbles in the formation of larger solar system objects. They are the first solid objects to form in the solar system and have preserved the records of early solar system processes in them, in the form of physicochemical changes. Meteorites can be generally classified into two broad categories: Primitive and differentiated. Primitive meteorites also called chondrites, are those solid objects, which have been subjected to minimum processing (*viz.* aqueous alteration and thermal metamorphism) since their formation. Carbonaceous and enstatite chondrites formed respectively under oxidizing and reducing conditions and ordinary chondrites formed under normal conditions belong to this category. Differentiated meteorites also called achondrites, are those coming from parent asteroids that have undergone extensive heating, leading to melting and chemical differentiation, thereby obliterating the original features. Achondrites can be silicate rich, metal rich (stony-irons) or almost pure metal (iron meteorites). Study of chondrites helps in understanding the earliest processes in the solar nebula, while study of achondrites helps in deciphering the earliest processes on large planetesimals.

1.1 Ureilites: an enigmatic group of achondrites

Ureilites are an enigmatic group of achondrites, having also some characteristics of primitive chondrites. Ureilites as a group of meteorite got their name from meteorite 'Novo Urei' which fell on Russian territory on 4th September, 1886. They are the second largest group among achondrites (differentiated meteorites) after HED consist more than ninety (unpaired) members. Broadly, ureilites can be classified into two subunits: Polymict and Monomict. Polymict ureilites are characterized by their

brecciated nature and presence of lithic clasts and mineral fragments of rock types other than main group of ureilite (MGUs) called monomict ureilites.

1.1.1 Geochemical features

Ureilites are coarse-grained ultramafic rocks. They are composed mainly of olivine and pigeonite in carbonaceous matrix. It contains carbon comparable to or some times even greater than carbonaceous chondrites. Carbon is mainly present in the form of graphite and diamonds, while in some cases lonsdalite has also been reported to be present. Ureilites are unique group of achondrite because it shows both igneous and primitive features.

In terms of minerology, texture, lithophile element chemistry and some aspect of Sm-Nd systematics they appear to be highly fractionated rock: either magmatic cumulates (Berkley *et al.*, 1976; Berkley 1989; Goodrich *et al.*, 1987) or partial melt residues (Boynton *et al.*, 1976; Scott *et al.*, 1993) and thus the product of planetary differentiation processes.

Ureilites also contain some minor components, which have several primitive characteristics that are unlikely to have survived extensive igneous processing on parent body. These include high abundance of carbon that contains large amount of fractionated primordial noble gases (reside mostly in diamonds), metal with high abundance of trace siderophile elements, both of which are typical of undifferentiated, chondritic material. In addition to these primitive signatures carried by minor components, they contain oxygen isotope signature of primitive chondrites. Oxygen is carried mostly by silicates, a major component of ureilites. In the three isotope plot, the oxygen isotopic data of ureilites fall along slope 'one' line defined by refractory inclusions of C2-C3 chondrites, while most of the differentiated bodies *e.g.*, Moon, Earth, Mars, other achondrites, form slope 'half' mass dependant fractionation line (Clayton and Mayeda, 1988). This has been interpreted to mean that ureilites parent body had not undergone extensive melting, homogenization and differentiation. Ureilites are expected to represent the products of melting of isotopically heterogeneous materials. The correlation between oxygen isotopic composition and the iron content of olivine and pyroxene implied that both the isotopic variation and the major chemical variations were inherited from nebular, not planetary, processes.

The compositions of olivine and the shock states of the ureilites that have been studied for nitrogen and noble gases in the present work are listed in Table 1.1.

Recently another piece of puzzle added to ureilites is the [33]S enrichment relative to carbonaceous, enstatite and ordinary chondrites, and triolite from iron meteorites. In situ production of S by cosmic ray spallation reactions involving Fe is unlikely to cause the enrichment because ureilites have very short cosmic ray exposure ages, low

Table 1.1 The shock state and % Fo (MgO) of ureilites studied in this work.

	Fo	Shock state	References
	Olivine		
Haverö (fall)	79.3	high	1
Kenna (find)	78.9	medium	2
Lahrauli (fall)	79		3, 4
Nilpena (find)	77-81	breccia	5
ALH78019	76.7	Very low	6, 7
ALH82130	94.9	low	8, 9, 10
ALH81101	78.5	High	11,12,13
EET83309	62-98	breccia	14, 15
EET87720	79-87	breccia	16, 17
LEW85328	80	medium	18,19

1. Neuvonen *et al.*(1972). 2. Berkley *et al.* (1976). 3. Malhotra (1962). 4. Bhandari *et al.* (1981). 5. Jaques and Fitzgerald (1982). 6. Berkley and Jones (1982). 7. Takeda *et al.* (1980). 8. Takeda (1987). 9. Takeda *et al.* (1989). 10. Berkley *et al.* (1985). 11. Berkley (1986). 12. Antarctic Meteorite News Letter (1983). 13. Saito and Takeda (1990). 14. Prinz *et al.* (1987). 15. Warren and Kallemeyn (1989). 16. Antarctic Meteorite News Letter (1990). 17. Warren and Kallemeyn (1991). 18. Antarctic Meteorite News Letter (1987). 19. Saito and Takeda (1989).

Fe/S ratio relative to the only documented phase that contains spallogenic sulfur (metal phase in iron meteorites) and no corresponding [36]S, enrichment. It has been argued that the [33]S enrichment has been derived from heterogeneity in solar nebula (Farquhar *et al.*, 2000).

1.1.2 Models for ureilite petrogenesis

Several models have been proposed for the ureilite petrogenesis. The most difficult aspect in constructing a viable model seems to be a consistent explanation for the contradictory nature of 'primitive' and 'igneous' features. The models have been divided into two categories, based on how they attempt to reconcile the apparent

conflict between igneous and primitive characteristics of ureilites. Most workers agree that the cause of primitive nature of ureilites, especially the oxygen isotopic anomaly, is to be attributed to nebular processes. Consequently, most of the models assume two or more O isotopic components representing different parts of solar nebula or initially heterogeneous parent body or collisional processes of multiple planetesimals. The igneous cumulate models (Berkley and Jones, 1982, Goodrich *et al.*, 1987) assume that ureilite fromation occurred essentially in a single object, in a deep part of a rather large (>100 km) asteroid, deep enough to keep the fO$_2$ stabilized by the C-CO buffer high enough to prevent Fe^{2+} in the silicates from being totally reduced to metallic Fe (Walker and Groove, 1993). Scott *et al.* (1993) also assume that ureilites were formed in a large asteroid, but they consider that ureilites were partial melt residues. The planetary collision model (Takeda, 1987, 1989) explains that ureilites are formed by shock heating of carbonaceous chondrite-like material from which a small amount of partially melted liquid was removed. Rubin (1988) explains that ureilites are impact melt product of CV-chondrite-like material. The above models basically assume that the O isotopic anomaly already existed at the onset of heating processes within the ureilite parent body; however it is not always assured that such heterogeneity may last through out the igneous events. Some other models assume that the O isotopic anomaly was produced by mixing of different components carried by different planetesimals: the partially disruptive impact model of Warren and Kallemeyn (1989) explains that the ureilite parent body, originally a largely molten asteroid, was severely disrupted by a C-rich impactor, forming C-rich veins enriched in planetary noble gases.

1.2 Trapped noble gases in meteorites

Noble gases (He, Ne, Ar, Kr, Xe and Rn) are the most inert elements of the periodic table, and known as 'inert gases'. Because of this property, under the pressure and temperature conditions prevalent in the solar nebula they are governed purely by their physical rather than more complex chemical properties. They are also most volatile elements, and the abundance of these elements are several order of magnitude depleted in even the most volatile rich meteorites (CI chondrites). Since they are present in trace quantity in meteorites and planetary objects, any small changes brought about by physicochemical or nebular processes recorded as variations in elemental and isotopic compositions in noble gases, can easily be detected. To decode

these changes in terms of geochemical and cosmochemical changes operational in the past history of the samples, one need to have proper understanding of various noble gas components present in meteorites and planetary objects. Here, various components of noble gases present in meteorites and planetary objects will be describe briefly (For more detail refer to Ozima and Podosek 1983).
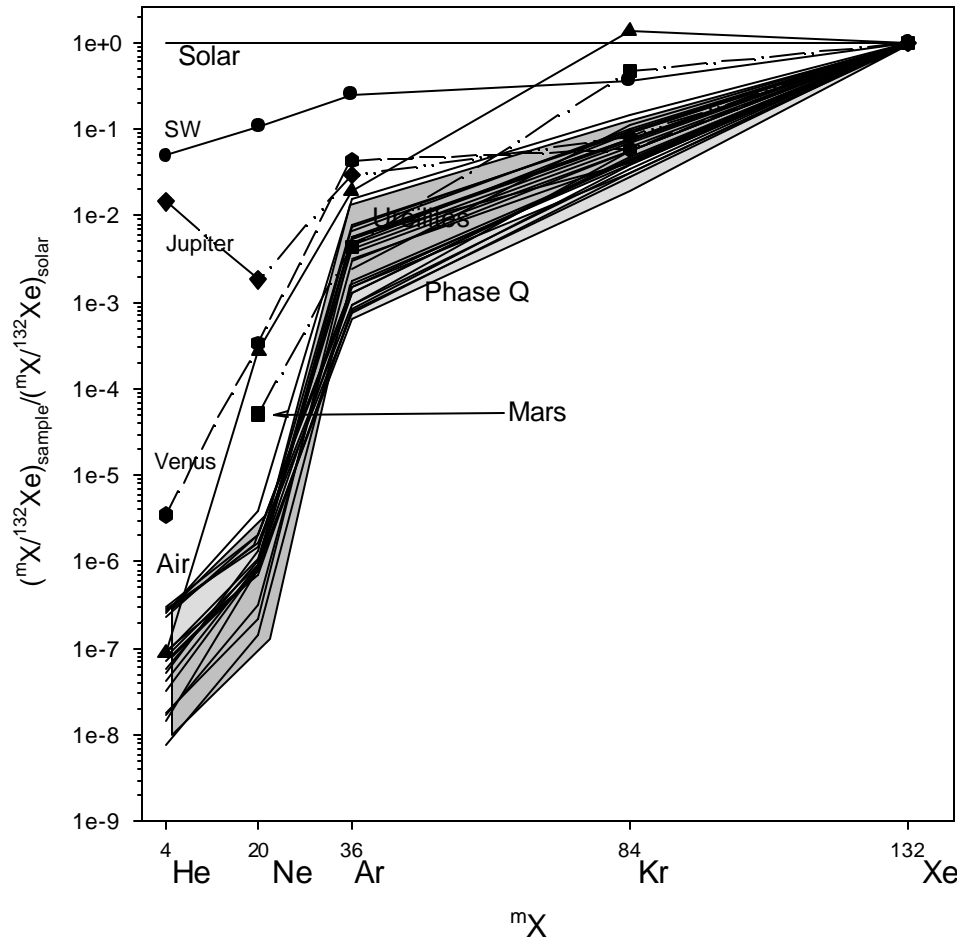
Fig 1.1 *Elemental abundance of noble gas in various reservoirs from the solar system normalized to solar abundances (Anders and Grevesse, 1989) normalized to ^{132}Xe along with ranges shown by ureilites and Phase Q. References: Ureilite: Göbel et al., (1978); Phase Q: Busemann et al., (2000); Jupiter: Niemann et al., (1996); Venus & Mars: Donahue et al., (1981) and Pollack &.Black (1982).*

1.2.1 Elemental abundance patterns

Based on measurements of noble gas elemental abundance patterns from meteorites and planetary objects *e.g.*, Earth, Moon *etc.*, it can be inferred that most of the solar system solids contain two dominant noble gas components having very distinct

elemental compositions (Signer and Suess, 1963). One of these components has elemental composition similar to Sun (Anders and Grevesse, 1989) or in solar wind and known as 'solar' noble gas. The other component is heavily depleted in light noble gases normalized to xenon, compared to 'solar' abundance (Fig 1.1) and known as 'planetary' noble gas, since they roughly resemble those of planetary atmospheres. However the term 'planetary' appears misleading. 'Planetary' noble gas components do not have to originate from planetary atmosphere. In Fig 1.1, it can be seen clearly that both ureilites and phase Q show remarkably similar elemental abundance patterns.

1.2.2 Isotopic compositions

A number of different isotopic components have been discovered in meteoritic noble gases. The isotopic ratios that can be explained as a result of fractionation mechanism with in the solar system or the parent molecular cloud are called 'local'. In meteorites, a number of noble gas components that have been discovered can not be produced by known solar system processes from solar compositions, and most likely have extra-solar origin (from some stellar environment) and are designated as 'exotic' e.g., Ne-E, Xe-S, Xe-HL *etc.* For details refer to Huss and Lewis 1994a and b. Here the isotopic compositions of the various trapped noble gases of 'local' origin are summarized. The ubiquitous cosmogenic component, present in all noble gases, to varying proportions, will not be addressed here.

Neon

Neon has three stable isotopes. To first order neon consists of mixture of two trapped components: a component associated with planetary noble-gas elemental patterns, and a component associated with solar gas. These two components were given designations of Ne-A and Ne-B by Pepin (1967). At least two other components have been identified subsequently (and named) Ne-Q (Smith *et al.*, 1977), and Ne-U (Ott *et al.*, 1985a,b) in the noble gas rich carbon phases from chondrites and ureilites respectively.

Helium

Far fewer isotopic compositions have been identified for He. This may be partly because of the fact that there are only two He isotopes, one of which (^{3}He) is often dominated by spallation, and the other (^{4}He) is often radiogenic, making it difficult to resolve the components. Trapped He components therefore are frequently identified

by their correlation with Ne components. There is definitely a difference between solar He (He-B) and planetary He (He-A). Large (orders of magnitude) variations in He isotopic composition have been observed for solar wind on time scales ranging from hours to billions of years (Geiss and Boschsler 1981). Geiss and Reeves (1972) suggested that modern solar He ratio should be enhanced considerably in ^{3}He over primordial solar He, because the Sun would have converted virtually all of its deuterium to ^{3}He during its premain-sequence evolution. If planetary He (He-A) is assumed to be primordial solar He, the difference between it and modern solar He leads to a calculated primordial D/H ratio of 2×10^{-5} (Geiss and Bochsler, 1981), which is astrophysically reasonable.

Argon

Argon has three stable isotopes, but one of them, ^{40}Ar, is almost always dominated by the contributions from the decay of ^{40}K. Furthermore, the ^{40}Ar/^{36}Ar ratio in terrestrial atmosphere (295.5) is higher than in most suggested meteoritic-trapped components by three orders of magnitudes or more, so that the contamination is a potentially severe problem. In the ureilite Dyalpur, ^{40}Ar/^{36}Ar ratio is $(2.9 \pm 1.7) \times 10^{-4}$ (Göbel *et al.*, 1978), about six orders of magnitude smaller than on Earth. The ratio ^{38}Ar/^{36}Ar for 'planetary' component is 0.188 and is indistinguishable from terrestrial air, while for solar wind, this ratio is 0.182 (Benkert *et al.*, 1993)

Xenon

Xenon has the largest number of stable isotopes, among all the noble gases, which makes it easier to identify the various components but it also has most in situ components. The most prominent is radiogenic ^{129}Xe from the decay of now extinct ^{129}I. Fission (e.g., of ^{244}Pu or U) can produce the heavy isotopes (^{131}Xe to ^{136}Xe) and spallation produced can be significant, particularly at the rare light isotopes. In addition, neutron-capture effects are some times important for ^{128}Xe (from ^{127}I) and ^{131}Xe (from ^{130}Ba).

Xenon in solar wind is not abundant enough to be measured in the foil experiments, but measurements of the surface correlated component in lunar soils and gas rich meteorites are generally consistent with one another. Various calculated components do have differences that could be related by mass dependant fractionation of less than 0.5% per amu.

The isotopic composition of 'planetary' Xe was originally thought to be equal to the 'average value for carbonaceous chondrites' (AVCC) (Eugster *et al.*, 1967). Large variations from this composition are observed in acid residues of chondrites (Lewis *et al.*, 1975), and it is now clear that AVCC is not a distinct component, but rather a mixture of other components. However, whole-rock samples of carbonaceous and ordinary chondrites show only subtle variations from AVCC composition, indicating nearly constant proportions of various components forming AVCC.

Xe-Q and Xe in ureilitic diamonds

The compositions of Q-Xe from several carbonaceous and ordinary chondrites yielded a fairly uniform composition, indicating that a uniform Xe-Q has been incorporated
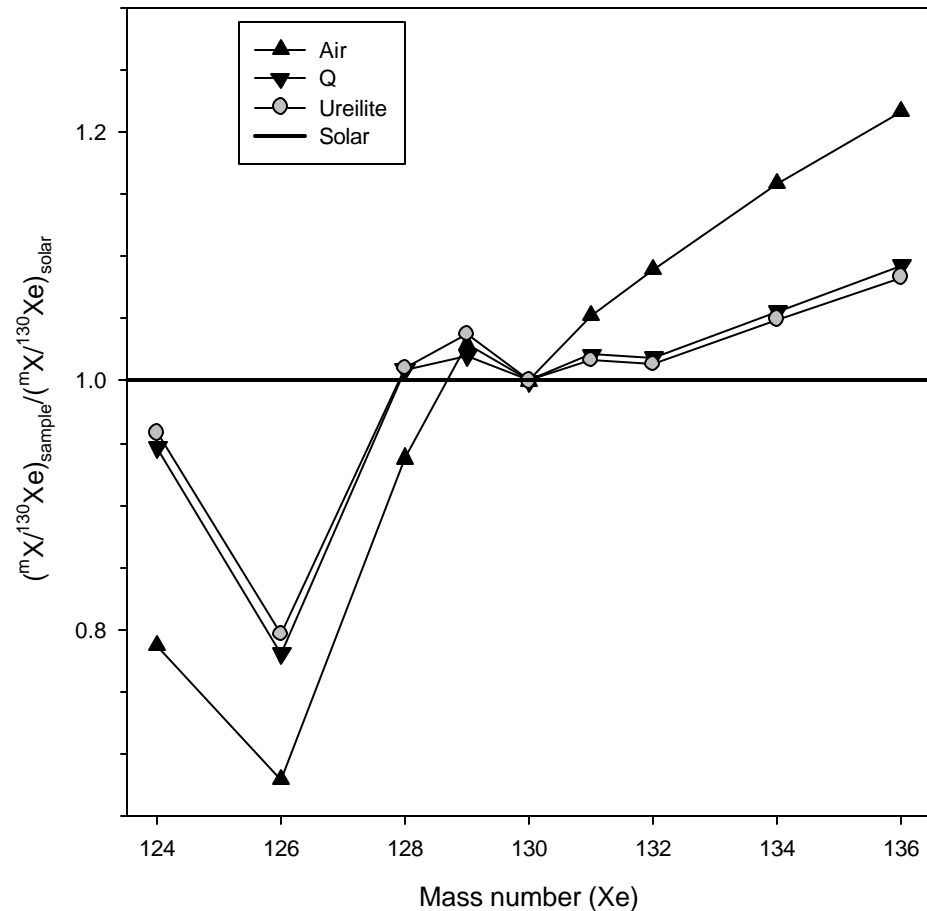
Fig 1.2 *Plot showing the relative isotopic compositions of various xenon components observed in meteorites. References: Air from Basford et. al., (1973); Phase Q from Busemann et al., (2000); Solar from Marti (1969).*

and has not changed its isotopic composition because of thermal metamorphism or aqueous alterations. The mean isotopic composition for diamonds from seven ureilites are identical to that of Q-Xe. As elemental abundances of trapped gases in ureilites are almost identical to those in phase Q, Ott *et al.* (1985a,b) suggested that these ureilitic noble gases must be closely related to the primordial Q noble gases (Fig 1.2), although they reside in achondritic, heavily differentiated and partly shocked meteorites (Goodrich, 1992). Component Xe-Q has also been found in other achondrite classes such as lodranite, acapulcoites, brachinites and even solar gas-rich howardite Kapoeta (Eugster and Weigel, 1993; McCoy *et al.*, 1996; Swindle *et al.*, 1998; Becker *et al.*, 1998).

Krypton

Krypton has seven stable isotopes and has no *in situ* radiogenic component as important as radiogenic ^{129}Xe and observed variations in trapped compositions have been far less dramatic for Kr than for Xe. There are some Kr components that are produced *in situ*, the most prominent being spallation, fission (mainly at ^{86}Kr) and (n,γ) reactions (usually at ^{80}Kr and ^{82}Kr from Br).

Kr-Q and Kr from Ureilites

Few data available for Kr-Q and related components. As for Xe, all Kr compositions are similar to each other, and particularly also to Kr in ureilites (Busemann *et al.*, 2000).

1.3 Nitrogen in Meteorites

Although nitrogen is sixth most abundant element in solar system, and a key element in the terrestrial atmosphere and biosphere, we know surprisingly little about its cosmochemical behavior during the formation of solar system. It is present in trace amounts in meteorites. This is mainly because of high stability of its molecular form N_2 in which it exists in nebula (the second most stable molecule after CO in nebular condition). Nitrogen in its molecular form behaves like inert gases. Therefore, nitrogen along with noble gases can be used as tracer to understand the various physicochemical processes in the early solar nebula.

Nuclei of carbon, oxygen and nitrogen are synthesized in similar astrophysical sites and these elements have interrelated chemistries. Yet nitrogen differs from the carbon
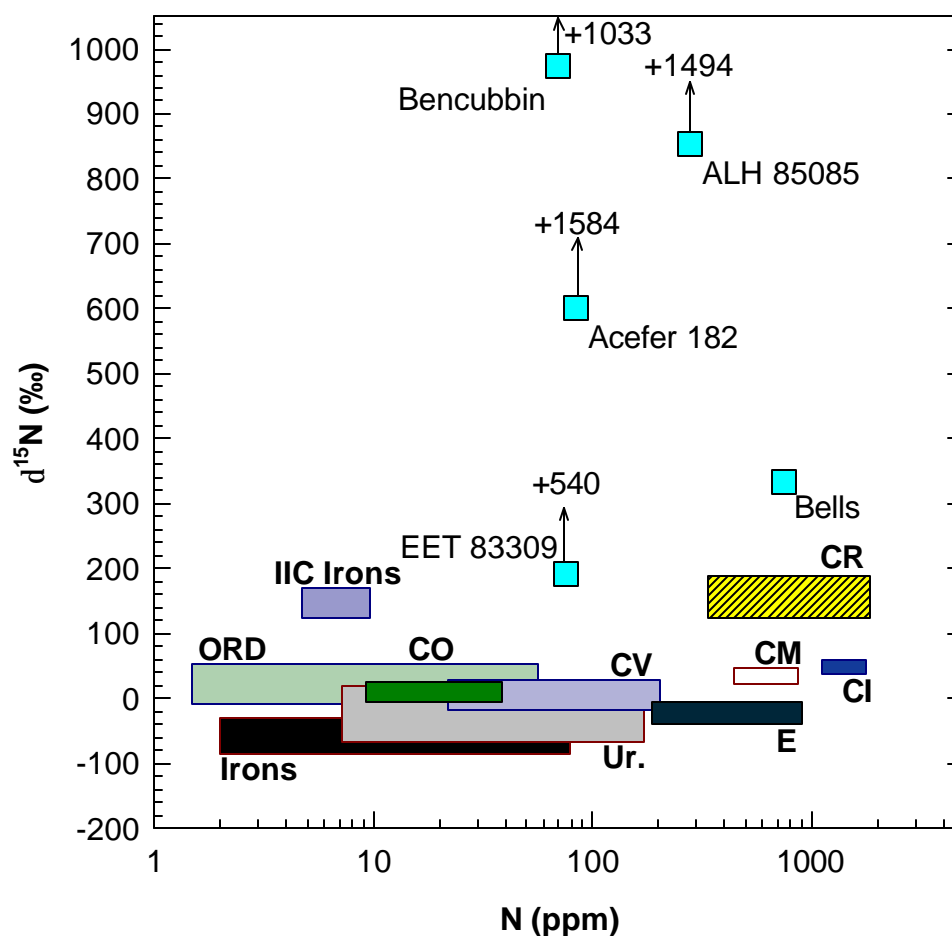
Fig 1.3 *The range of concentrations and isotopic composition of nitrogen shown by various classes of meteorites.* $d^{15}N$ *of some other individual meteorites, which do not belong to any of these classes (known as anomalous), have also being listed. Abbreviations: ORD: Ordinary Chondrite; CI, CV, CM, CO, CR: Carbonaceous Chondrites; E: Enstatite Chondrite; Ur: Ureilites; Irons: Irons.*

and oxygen in exhibiting a range of isotopic composition (varying over 1000‰) in bulk meteorite samples, whereas carbon exhibits a range of only 40‰. These variations may be a result of heterogeneity, as nitrogen isotope nucleosynthesis takes place in two somewhat different astrophysical sites: ^{14}N in the equilibrium CNO cycle and ^{15}N in the explosive CNO cycle.

Nitrogen isotope systematics for the early solar system are complex. The origin of the large range of nitrogen isotopic compositions in extraterrestrial samples is not well understood. Stony meteorites exhibit a range of bulk $\delta^{15}N$ from –45 to +860‰ (Kung and Clayton, 1978; Grady and Pillinger, 1990), and Bencubbin, an unusual stony

breccia, has a bulk $\delta^{15}N$ of about 1000‰ (Prombo and Clayton, 1985; Franchi *et al.*, 1986). Nitrogen measurements from iron meteorite range from −96 to +156 ‰, with most of them having values more negative than −50‰ (Prombo and Clayton, 1993; Franchi *et al.*, 1993). The nitrogen isotopic composition of solar wind as measured in lunar soil samples appears to have undergone a secular change from −278‰ (Carr *et al.*, 1985) to 150‰ (Clayton and Thiemens, 1980; Norris *et al.*, 1983). Fig 1.3 shows the abundance and isotopic composition of nitrogen in various classes of meteorites. It can be seen clearly that the different classes of meteorites exhibit large range of $\delta^{15}N$. Was there once uniform primordial nitrogen composition, which was later modified by chemical, physical, and nuclear processes? Or were primordial inhomogeneities dominant in determining the nitrogen isotopic compositions of solar system objects? The existing database for nitrogen isotopic measurements of chondrites, achondrites, iron meteorites and solar wind does not suggest a uniform 'planetary' nitrogen component analogous to the 'planetary' noble gases.

Interstellar dust grains of diamond and silicon carbide, found in all classes of primitive chondrites, contain nitrogen with large isotopic anomalies of nucleosynthetic origin. The nitrogen in interstellar diamonds typically has $\delta^{15}N = -340‰$ (Arden *et al.*, 1989). The contribution of this component in chondrites is on the order of 1ppm, corresponding to a few percent of the total nitrogen inventory of these meteorites. It is thus a significant contributor of isotopic variability in the bulk chondrites, but can not account for the whole range of observed isotopic compositions. The silicon carbide component is much less abundant, but contains a wider range of isotopic compositions, from −800 to +22,000‰ (Zinner *et al.*, 1989).

1.4 Noble gases in Ureilite

Ureilites contain large amount of noble gases mostly carried by diamonds (Gobel *et al.*, 1978, Wilkening and Marti, 1976) while graphite the other form of carbon present in carbon rich veins is almost free of noble gases. One of the ureilites (ALH78019) that contains carbon mostly in the form of crystalline graphite but no diamonds, also contains comparable amount of noble gases (Ott *et al.*, 1985b, Wacker 1986). Furthermore, Wacker (1986) reported chondritic $^{132}Xe/C$ ratio for ALH78019 and argued that the gas rich carbon trapped its gases in the solar nebula at pressure (P) and Temperature (T) condition similar to that of Phase Q.

Although ureilites are severely depleted in other highly volatile elements, they contain trapped noble gases in abundance similar to those in carbonaceous chondrites. Moreover, the relative abundance pattern of noble gases in ureilites is of the fractionated 'planetary' type as it is in carbonaceous chondrites, as opposed to the 'solar' type. Gas contents vary considerably (for example, Xe contents vary by a factor of ~ 100 in bulk samples), but elemental and isotopic abundance ratios in ureilites are similar. Analysis of separated fractions of the carbonaceous matrix or vein material showed the noble gases to be enriched at least 600 fold relative to the silicates, and demonstrated that the gases are largely contained in carbon (Weber *et al.*, 1971; Göbel *et al.*, 1978). In diamond bearing ureilites, diamond is the principal gas carrier and graphite is virtually free of trapped gases (Göbel *et al.*, 1978) The diamond free ureilite, ALH78019, has trapped noble gas abundances comparable to those of diamond bearing ureilites. Most of the noble gases contained in this ureilite are contained in a fine-grained carbon, whose structural state is unknown. As in diamonds bearing ureilites, most of the graphite in ALH78019 is gas free. Wacker (1986) noted that the fine -grained gas-bearing carbon has a near-chondritic Xe/C ratio.

Most of the ^{3}He in ureilites, is cosmogenic in origin. Most of the ^{4}He appears to be trapped. ^{40}Ar/^{36}Ar ratios in ureilites are extremely low, indicating very little radiogenic Ar and thus very early fractionation of K and Ar. The ^{40}Ar/^{36}Ar ratio in the ureilite Dyalpur [$(2.9\pm1.7) \times 10^{-4}$] is the lowest measured so far and was taken by Göbel *et al.* (1978) as an upper limit for the primordial value. Neon in monomict ureilites appears to be a mixture of a trapped and a cosmogenic component. The composition of the trapped component has been estimated from Hajmah, which contains little cosmogenic Ne (Ott *et al.*, 1985). This component is different from other trapped Ne components recognized in chondrites (Ne-A, B, E, D, A1) and is named as Ne-U. (Ott *et al.*, 1985). The polymict breccia, EET83309 and EET87720, have an order of magnitude more ^{4}He than other ureilites and contains Ne-B, the component of solar wind neon observed in gas-rich meteorites (Ott *et al.*, 1989) indicating that they are rigolith breccia.

1.5 Carbon and nitrogen in ureilite

Carbon isotopic compositions have been measured in 15 ureilites (Grady *et al.*, 1985; Grady and Pillinger 1987 & 1988; Smith *et al.*, 1999). For any particular ureilite δ^{13}C

values are fairly constant over the entire range of C combustion temperatures, indicating that graphite and diamond probably have the same isotopic composition (Grady *et al.*, 1985). Among all ureilites, carbon isotopic compositions fall into two groups, which show some correlation with forsterite (Fo) content: the more FeO-rich group has $\delta^{13}C$ values clustering around $-2‰$ and the more magnesian group has $\delta^{13}C$ values clustering around $-10‰$. However, there is no monotonic relationship of $\delta^{13}C$ value with Fo.

Nitrogen abundance and isotopic compositions have been reported for several bulk samples and six acid residues of ureilites (Grady *et al.,* 1985 & 1986; Grady and Pillinger 1988) Yamamoto *et al.*, 1998; Murty, 1994; Russell *et al.*, 1993). Bulk samples contain a few ppm to tens of ppm of nitrogen, while the acid residues contain several tens of ppm to a few hundred ppm of nitrogen. Monomict ureilites, in general, showed the presence of a light nitrogen with $\delta^{15}N < -100‰$ while the polymict ureilites on the other hand, showed extremely heavy nitrogen with $\delta^{15}N$ up to 540‰.

1.6 Models for origin of planetary gases

More than 25 years after the discovery of planetary gases, the origin of planetary noble gases are still not clear. Though number of models have been proposed for the origin of 'planetary' noble gases that are based on–solution, adsorption, trapping during synthesis and ambipolar diffusion, here only two of these that are more realistic will be discussed: a) Physical adsorption; b) Ambipolar diffusion.

a) Physical adsorption

The important features of adsorption model are that the distribution coefficient can be made arbitrarily high by appropriate stipulation of temperature, and that adsorption easily produces the steep elemental fractionation characteristic of planetary gas. Fanale and Cannon (1972) showed that adsorption on meteoritic material at very low temperature at about 100K would produce the elemental abundance pattern of planetary gases at least for heavy noble gases. The qualitative features of adsorption make it an attractive model for the origin of planetary gas pattern. In details, however, there are qualifications as well as limitations. However, adsorption seems unlikely to result in observed retentive siting of planetary gases (without postulating some effective fixing mechanism) and the required temperature seems to be unreasonably low. If adsorption is indeed involved in producing the heavy planetary gases, it still

needs some other mechanism for the lighter noble gases (Ne and He). The major problem for the adsorption model is the absolute abundance of noble gases. To explain the observed concentrations, several orders of magnitude higher pressure than the standard pressure in the nebula is required.

b) Ambipolar diffusion

A quite different model for the origin of planetary noble gases usually cited as 'ambipolar' diffusion', has been proposed by Jokipii (1964). The premise is that if gas of cosmic composition is partially ionized, strong chemical fractionation can be effected by loss of neutral species from a region in which the ions are held by a magnetic field. The ion composition depends on the mechanism and extent of ionization and on the details of electronic configuration, but for moderate ionization of a coherent chemical faimily such as the noble gases, the dominant factor governing elemental fractionation of ions and the original reservoir is $e^{(\delta E/kT)}$, where T is the relevant temperature and δE is the difference in (first) ionization potential. Since ionization potential decrease monotonically from He to Xe, the ion population is fractionated in favor of heavy gases. A temperature about 10^4 K produces a quite respectable match to planetary composition. In this model, the noble gases are already in planetary proportions. This is an important advantage of this model: since the reservoir already has the right composition, it is easier to understand that the various materials could sample the same composition at a wide variety of concentrations. Still, some trapping mechanism must be invoked to get the gases into solids, presumably without much further elemental fractionation.

In this thesis, a variant of this model has been used to explain the various features observed in elemental abundance pattern of ureilite diamonds as well as Phase Q. *In this model the separation of neutrals from ionized species are not needed. Both the neutrals and ions are present simultaneously but only ions are incorporated into the carrier phases (i.e. solids) by the mechanism like ion implantation.* The fractionation similar to that of planetary gases has already been observed in diamonds and amorphous carbon produced under low pressure plasma atmosphere (Matsuda *et al.*, 1991; Fukanaga and Matsuda, 1997). This also explains the more or less uniform isotopic compositions in spite of large variation in the absolute and relative abundance of noble gases.

1.7 Objectives of the present work

We have seen that ureilites have several unique features and the most important one is the coexistence of igneous and primitive features. Most of the models given for the ureilite petrogenesis tried to deal mainly with igneous features observed and none of them have seriously addressed the primitive features of ureilites, which should have been lost if ureilite were once severely melted and recrystallized as observed in case of other achondrites. One aspect of present study is to understand the origin of carbon (diamonds) in ureilites that might hold the clues to several enigmatic features shown by ureilites and might be helpful in understanding the origin and evolution of ureilite parent body (UPB). The origin of diamonds in ureilite is highly debated topic and still not settled. One group says that diamond is produced by shock conversion of graphite while others argue that diamond is nebular condensate. Irrespective of whether diamond either produced by shock conversion of graphite or condensed directly from solar nebula, there is little doubt that the 'planetary' noble gas carried by carbon must have their origin in solar nebula. If noble gases in carbon from ureilites are nebular, the nitrogen trapped along with it should also be nebular and is least affected by later proccessing (parent body or spallation) because it is trapped in highly refractory phase (diamond). So the study of nitrogen in ureilite diamond provide an opportunity to look for 'planetary nitrogen' or more correctly 'nebular nitrogen' analogous to planetary noble gases.

Earlier work on ureilites has been focussed either on noble gases only or nitrogen and carbon (Göbel *et al.*, 1978; Grady *et al.*, 1985). The present work is first comprehensive simultaneous study of nitrogen and noble gases in ureilites and their various chemically separated phases has been aimed to address the following questions:

- How many nitrogen components are present in ureilites and what are their carriers?

- What is the carrier 'X', that has noble gases with very different elemental composition (Göbel *et al.*, 1978) as compared to the main carrier diamond?

- What is the origin of carbon phases in ureilites, more specifically origin of diamonds and how and when they acquired their gases?

- What is role of shock in evolution of ureilite parent body?

- Is there any relationship existing between ureilite and carbonaceous chondrites or any chondrites?

- To understand the relation between amorphous carbon in ureilites with that of phase Q (the carriers of primordial noble gases in primitive meteorites) and.

- To decipher the nebular nitrogen composition.

Experimental

In the present work, the bulk samples as well as various chemically separated phases from a number of ureilites have been analyzed for nitrogen and noble gases. The objectives are to measure the concentration as well as isotopic compositions of nitrogen and noble gases in various phases of ureilites. This will help us to understand the various geochemical and cosmochemical processes that occurred during the formation of ureilites' parent body that is in turn related to physicochemical condition in the early solar nebula. The trapped gases were extracted from the samples by heating stepwise either under ultra high vacuum by RF (radio frequency) heater (pyrolysis) or in presence of oxygen using resistance heater if the samples are combustible phases (combustion). In this chapter, the sample preparation, characterization and techniques used for measurements of noble gases and nitrogen in bulk sample as well as acid residues will be discussed. To observe the change in the morphological features after acid treatment, SEM photographs of all the acid residues as well as oxidized residues have been taken at various magnifications. Chemical compositions of a few selected bulk samples as well as their acid residues have been determined by INAA (Instrumental Neutron Activation Analysis). These procedures will be described briefly in this chapter.

2.1 Sample Preparation

2.1.1 Bulk Samples: The bulk samples were analyzed after simple cleaning by distilled water (or some times with acetone or alcohol). To remove atmospheric contamination, the samples were heated at $\sim 150^\circ$C using IR lamps under vacuum intermittently for a week prior to analysis. Some of the features (% Fo, shock state and cosmic ray exposure ages) of the samples analyzed have been listed in Table 2.1.

Although the ureilites, in general, show low cosmic ray exposure ages, the samples analyzed here have covered wide range of exposure ages.. The samples analyzed also cover different degrees of shock ranging from very low to highly shocked.

2.1.2 Residue Preparation: The HF-HCl-resistant residues have been prepared by dissolving a few hundreds of mg of the bulk samples in 6N HCl and 10N HF/6N HCl alternatively (for details see Table 2.2). This procedure is repeated several times (4 to six cycles in general). The residues are then washed with water (to remove fluorides), CS_2 (to remove sulfur) and alcohol several times before drying.

The treatment with hydrochloric acid and hydrofluoric acid removes the bulk mass (silicates, metals) that carries major part of cosmogenic (and solar) gases. The 6N HCl removes precipitated fluorides and most sulfides. Elemental sulfur can be removed by solution in CS_2.

In order to avoid the transfer losses, the residue is not weighed at this stage. Roughly, one half of the residue obtained from HF-HCl dissolution, is treated with perchloric

Table 2.1: List of samples studied and some of their important features.

Sample	Fo (%) Olivine	Shock state[*]	Exposure ages (Ma)
Monomict ureilites			
Haverö (fall)	79.3	high	18
ALH81101	78.5	High	9.7
Kenna (find)	78.9	medium	28
Lahrauli (fall)	79	medium	16.8
LEW85328	80	medium	9.6
ALH82130	94.9	low	1.1
ALH78019	76.7	Very low	0.1
Polymict ureilites			
EET83309	62-98	breccia	46
EET87720	79-87	breccia	7.8
Nilpena (find)	77-81	breccia	9.7

[*] Refer to Berkley and Jones (1980)

acid ($HClO_4$). This treatment is supposed to remove non-crystallized (amourphous) form of carbon and fine-grained graphite (coarse-grained graphite can survive).

2.2 Mass spectrometry

2.2.1 The VG Micromass 1200

It is a commercially available gas source mass spectrometer from the Vacuum Generators Ltd. U. K.. Operated in the static mode, this unit is suitable for measuring small samples of inert gases. Gas ionization is achieved in this by a Neir type ion source with a source magnet to increase the ionization efficiency. Subsequent to ionization, the ionized species are accelerated by electrostatic potential of 4KV. The VG Micromass 1200 is a magnetic deflection mass spectrometer, with a 60° electromagnetic sector that acts as a mass analyzer. The different m/e$^-$ signals are measured by varying the magnetic field. A Faraday cup and an electron multiplier for ion detection, enable the measurement of wide range (varying over more than six orders of magnitude) of signals. The mass spectrometer is attached, through all metal ultra high vacuum (UHV) valves, to an oil diffusion pump and ion pump for evacuation, with which a vacuum as low as $<10^{-9}$ torr can be maintained. The mass

Table 2.2: Sample weights and yields of the acid resistant residues.

Sample	Starting weights (mg)	Treatment	Yield (mg)	Number of $HClO_4$ treatment	Designation
Haverö (fall)	1642	HF-H$_2$SO$_4$	23.9		Hv
Kenna (find)	-	-	-	-	Ken
Lahrauli (fall)	-	-	-	-	Lah
LEW85328	463	HF-HCl	13.8	1	L28
ALH78019	229.7	HF-HCl	8.4	4	A19
ALH82130	466.6	HF-HCl	9.9	2	A30
ALH81101	252.2	HF-HCl	5.1	2	A01
EET83309	485.5	HF-HCl	18.6	3	E09
EET87720	604.7	HF-HCl	15.3	4	E20
Nil		HF-HCl	4.6 %		Nil

spectrometer is isolated from these pumps during sample analysis. A SAES^{TM} getter attached to the mass spectrometer through a valve keeps the hydrogen background low and that in turn reduces the hydrocarbon background to a minimum. Since it also acts as a chemical getter for nitrogen, the SAS getter is isolated during the analysis of nitrogen. The mass spectrometer has an external oven that can bake the unit up to 300°C for degassing.

2.2.2 The Extraction system

The mass spectrometer is attached to a gas extraction system through a UHV valve. This system, suitable for separation and cleaning of nitrogen and noble gases extracted from samples for the mass spectrometry, has been fabricated at PRL using commercially available UHV components. Though nitrogen (N_2) behaves like the noble gases under normal conditions of temperature and pressure, in ultra high vacuum, the clean surfaces of certain metals are active to getter nitrogen (Fast, 1965). Stainless steel, aluminum, copper oxide (CuO), molybdenum (Mo), tungsten (W), nickel (Ni) at room temperature are inert to nitrogen, while titanium (Ti), titanium-zirconium (Ti-Zr) alloy, titanium-palladium (Ti-Pd) alloy, SAES getter, some forms of charcoal and hot Ni are some of the materials which scavenge nitrogen very fast. These aspects have been well considered while fabricating the extraction system. Proper isolation valves have been incorporated in the line by which the materials that act as a getter for nitrogen can be isolated from the extraction system while nitrogen is being processed. Fig.2.1 is a schematic diagram of the extraction system. It essentially consists of three parts (excluding the pumps and pressure measuring devices).

1. Gas extraction unit.

2. A standard gas reservoir (Air standard reservoir) that provides standard sample for calibration. This is a reservoir containing standard air, which is connected to the main line through a pipette valve (V11 and V12, *see* Fig. 2.1). Known volumes of the air-standard are pipetted for calibration purposes.

3. The main line used for purification and separation of the gases.

Following is a brief description of these sub units.

2.3. The gas extraction unit
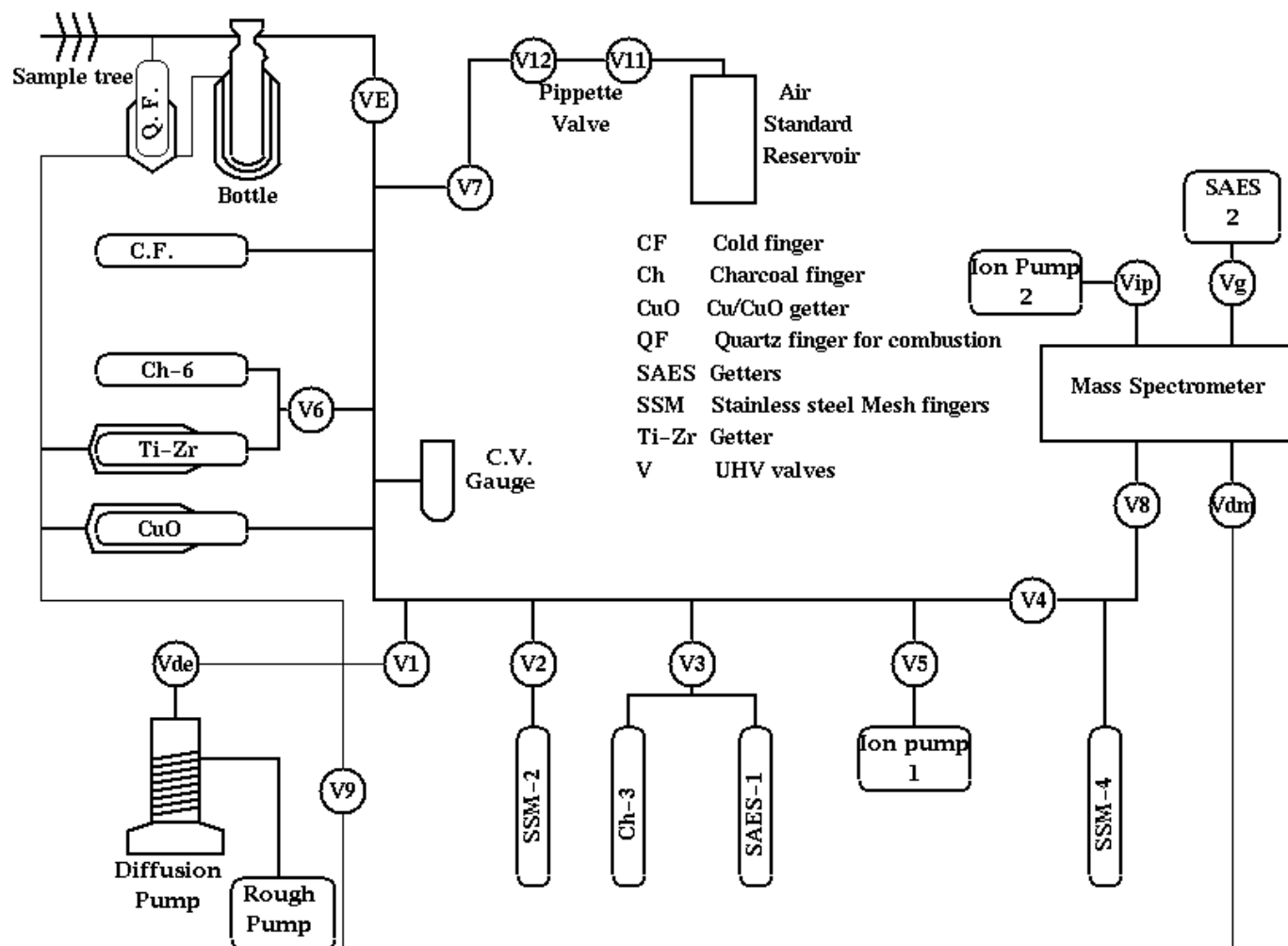
Fig 2.1 *Schematic diagram of the extraction system.*

It consists of a combustion finger and an extraction bottle for the extraction of gases from solid samples. The extraction unit is connected to an online sample tree where the samples are kept prior to their gas extraction. For gas extraction the samples are maneuvered from the sample-tree into the combustion finger and/or the extraction-bottle by an external hand magnet and nickel pieces (which are loaded into the sample tree along with the samples).

2.3.1. Combustion Finger

The extraction system is attached to a double-walled (vacuum jacketed) quartz finger that can be heated up to 1075 °C (the safe limit without collapsing the quartz) by means of an external resistance heater. The outer vacuum line of this finger is connected to the diffusion pump. Sample is introduced into this finger by a quartz boat that can be maneuvered with an external hand magnet. For combustion purposes, samples are heated within this finger in an environment of oxygen generated from an inline Cu/CuO getter.

2.3.2 Extraction bottle

The extraction bottle is used for extracting gases from the solid samples by heating them in temperature steps up to 1850 °C. It is a double-vacuum bottle that is cooled externally by a water jacket (Fig. 2.2). It is partly quartz and partly Pyrex™: quartz is used in regions that are subjected to higher temperatures and rest of the bottle is made of Pyrex. Only the innermost wall of the bottle is made of quartz, while the rest is Pyrex. The extraction bottle contains a Mo crucible (melting point >2500 °C) that is suspended through a funnel shaped quartz tube and is heated inductively by RF power. An outer chilled water jacket provides cooling to the Pyrex layer that is subjected to high temperatures due to the radiation heating from the crucible. The intermediate vacuum layer between the water jacket and the quartz wall is intended to serve two purposes:

a. Once the quartz wall is degassed, it remains clean as it is in vacuum on both sides, and there is no possibility of constant loading of gases into quartz.

b. The diffusion of helium through quartz from outside is minimized as there is no He available to diffuse in, due to vacuum.
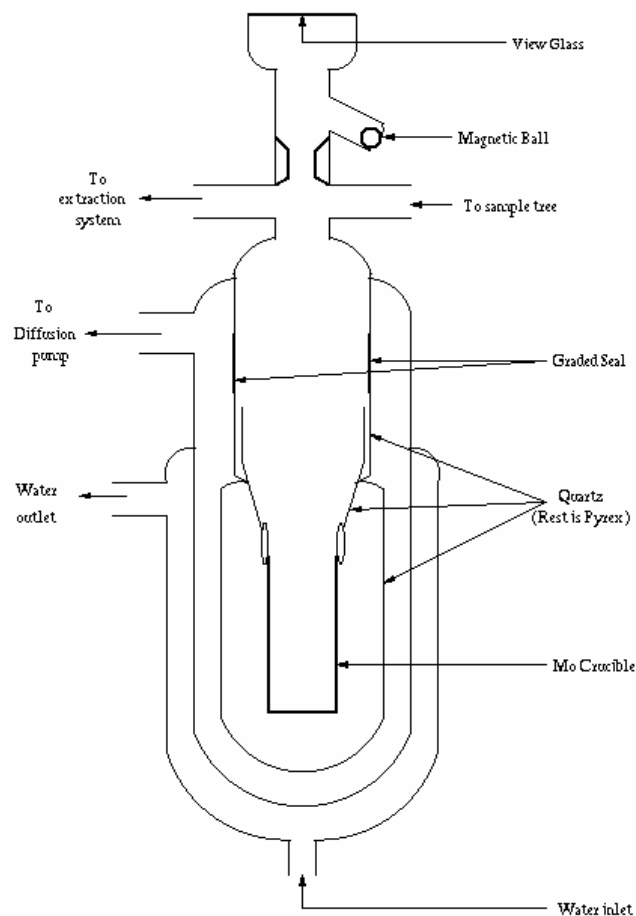
Fig.2.2. *Schematic diagram of the extraction bottle. It is mostly made up of Pyrex, with quartz at places.*

Both of these factors lead to lowering the blank levels to great extent and enable analysis of small samples. The optically flat view glass, at the top of the bottle allows viewing the crucible bottom for temperature calibration using an optical pyrometer, and also to confirm sample melting by visual inspection. A magnetic ball and the seating prevent the vapor deposits on the view glass.

2.3.3. The main line

Subsequent to its extraction, the sample gas passes through a series of cleaning and separation processes in the main line. It consists of a series of fingers (for the adsorption or condensation of gases) and getters (for removing the unwanted gases) many of which can be isolated from the main line by UHV valves. The essential features of this unit are described below.

The line fingers

The gas–separations, in the inert gas mass spectrometry, are based on the differential adsorption and desorption properties of the gases He, Ne, Ar, Kr, Xe and N_2. The main line has two stainless steel meshes (SSM-2 and SSM-4) that contain inside them meshes made up of stainless steel powder of 2 μm size. The adsorption/desorption properties of these meshes are similar to those of the activated charcoal or zeolite, with an added advantage that they can be baked up to 800 °C thus enabling thorough degassing and UHV conditions. The conventional activated charcoal and zeolite, if baked beyond 400°C, undergo structural damages, which affect their adsorption/desorption properties. Additionally in the case of charcoal, there may be a possibility of carbon monoxide (CO) contamination to nitrogen. Thus for processing of nitrogen, only the SSM fingers are used. The main line has also two Pyrex fingers (CH-3 and CH-6) containing activated charcoal inside them for processing the noble gases. The charcoal and SSM fingers have been connected to the main line by UHV valves. Besides these fingers, which can be isolated from the main line when required, the main line contains an online Pyrex cold-finger that is used for separating the unwanted condensable species (H_2O and CO_2, *for example*) from the rest of the gases.

Gases extracted from the samples contain many other species in addition to the noble gases and nitrogen. These species are troublesome, as their signals often interfere with those of interest and it is difficult to resolve them by the usual resolving power of a mass spectrometer. Therefore it is desirable to get rid of these interfering species, prior to the analysis of the sample gas, by adopting suitable cleaning procedures. The extraction line is provided with a Cu/CuO finger and two getters (TiZr and SAES) that are used for cleaning the sample gas.

Cu/Cuo finger

It is often convenient to clean the sample gas by oxidizing the interfering species (CO, H_2 and the hydrocarbons etc., for example), followed by a cryogenic separation of the condensable oxides that form (CO_2, H_2O etc.). For this purpose, the main line is equipped with an online Cu/CuO getter. Essentially it is a double-walled quartz finger that contains wires (~0.65 × 6 mm) of copper oxide (MERCK™) wrapped in Pt-foil. Ultra−pure O_2 can be generated in the main line by heating the quartz finger with an

external heater (usually) at 700 ℃. This oxygen is used for both the combustion of the samples as well as for cleaning of the sample gas (*discussed later*).

The Ti–Zr and SAES getters

These are materials that chemically react with the reactive species such as N_2, carbon dioxide (CO_2), O_2, hydrogen (H_2) and the hydrocarbons to form refractory compounds. Noble gases can be effectively cleaned of these species by exposing them to these getters. The main line has been provided with two getters for this purpose. The Ti-Zr getter is a double-walled quartz tube containing sponges of an alloy of Ti and Zr, which is heated by an external heater. The Ti-Zr getter works in the following way. At temperatures >700 ℃, Ti continuously reacts with N_2, O_2, CO_2, CO and decomposes the hydrocarbons by taking up C from them, and leaving behind the H_2 gas that is sorbed at temperatures below 400 ℃. Zr decomposes H_2O vapor, reacts with O_2 to form refractory oxide and sorbs H_2 at temperatures ~300 °C.

The SAES (AP-10GJ) getter that contains a non-evaporating getter material (ST 101 Zr Al alloy) has a gettering action similar to that of the Ti-Zr getter. It is used for further finer cleaning of the noble gases that have already been cleaned by the Ti-Zr getter, to remove the further traces of the interfering species. For cleaning, the SAES getter is usually heated to 750 °C and then is cooled to 300 ℃ in slow steps.

The Ti-Zr and SAES getters that are very useful for the noble gases are detrimental for nitrogen, as they have a gettering effect on it. Therefore, during the processing of the nitrogen fraction they are isolated from the main line by UHV valves (V3, and V6, *see* Fig. 2.1). After each experiment, the Ti-Zr and SAES getters are degassed at 800 ℃ before further use.

2.4. Standard Procedures

Fig. 2.3 is a flow diagram illustrating the standard procedures adopted for the experiment. The experiment involves the extraction and cleaning of the sample gas, followed by the separation into individual gas fractions and their subsequent analysis in the mass spectrometer and the data acquisition.

2.4.1. Gas extraction

Nitrogen and the noble gases, being inert species, are extracted from the solid samples by heating them in temperature steps. Stepwise heating, as it is called, is a powerful
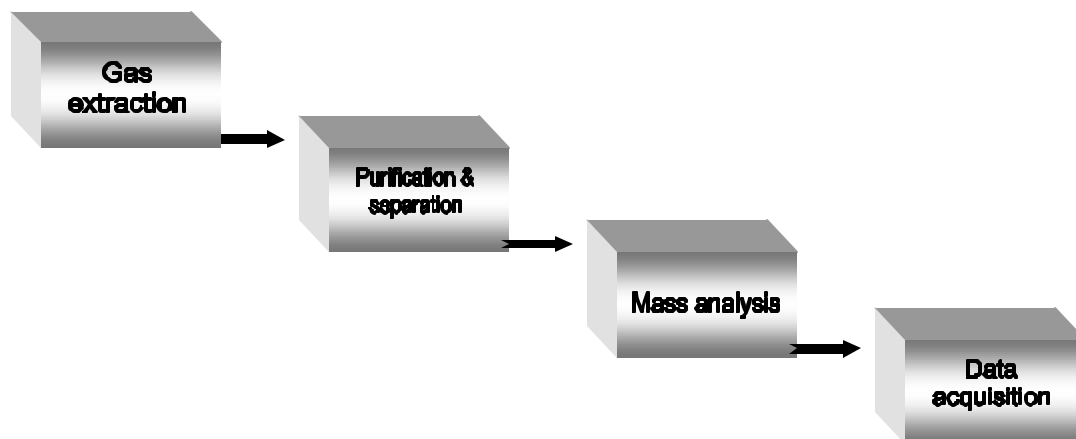
Fig.2.3. *Flow diagram of the standard experimental procedures.*

technique that is commonly followed in the noble gas mass spectrometry (Ozima and Podosek, 1983). A number of components of different origin are often sited in physically different sites in a sample. These components will have different release patterns in stepwise heating. Thus with stepwise heating, it is possible to decouple the various components present in a sample.

Based on whether gas extraction is done by heating the samples in an oxygen atmosphere or in vacuum, the extraction technique is, respectively, termed combustion or pyrolysis. Both of these are useful ways of gas extraction depending on the nature of samples studied.

Stepped Combustion

In this method, the sample is heated inside the combustion finger in an environment of oxygen. The oxygen for combustion is obtained from the on-line Cu/CuO by heating it to ~850 ℃. The temperature steps of heating and the amounts of oxygen vary with the samples of interest. For most of the bulk samples, an initial combustion at 400 ℃ in 2 torr of oxygen is carried out to remove the surficial contaminants. In case of carbon rich residues, heating from 200 to 1050 ℃ in steps in an oxygen pressure of ~2 torr (5 torr oxygen pressure have been used for acid residues of Havero and ALH78019) is done to extract the gases. Heating is usually done for 45 minutes during which the combustion finger is isolated from the main line by an UHV valve. After the heating is over the gas is expanded to the main line and processed for analysis.

Stepped Pyrolysis

The process of stepped pyrolysis involves heating the samples in a pre-degassed Mo crucible (in the extraction bottle) in temperature steps up to 1850 °C, using RF heater. The temperature steps are decided acc ording to the samples under study. The sample is heated at each step for 45 minutes (30 minutes in the melting step), the gases released being simultaneously adsorbed on a stainless steel mesh (SSM), maintained at liquid nitrogen temperature. Subsequent to heating, the main line is isolated from the extraction bottle and the gases from the stainless steel mesh are desorbed for their processing.

2.4.2. Cleaning and separation

As noted earlier, the extracted gas contains many unwanted species, in addition to noble gases and nitrogen that contaminate the mass spectrometer and could cause mass interference. These are removed from or minimized in the sample gas at various stages of cleaning. Initially, the gases are cleaned by exposing them to the Cu/CuO that is heated to 700 °C for 20 minutes followed by cooling to 400 °C in steps. During heating the non-condensable species like C, CO, H_2 are oxidized to condensable species CO_2 and H_2O which are isolated from sample gas by using liquid nitrogen trap. A portion of this clean sample gas (typically 10 %), free from the interfering species, is isolated for the analysis of nitrogen before collecting the rest of the fraction on charcoal finger for exposure to getters for the noble gases study. Cleaning by the Cu/CuO is an essential procedure for processing nitrogen. As this is the only way of cleaning for the nitrogen fraction, the sample gas often is cleaned by the Cu/CuO a number of times. Usually, if the amounts of condensable gases generated are large a second Cu/CuO clean up is done. The fraction for noble gases along with the species condensed on the cold finger is then cleaned by exposing it to the Ti-Zr getter, after which the heavy noble gases (xenon, krypton and argon) are adsorbed on a charcoal finger (CH−6) at liquid nitrogen temperature. The helium-neon fraction that remains in the gas phase is further exposed to the SAES getter, and then introduced into the mass spectrometer via a let-in valve. However, during the analysis of the helium-neon fraction, a liquid nitrogen trap is constantly maintained on the SSM in the let-in volume. This serves two purposes: a) it adsorbs any water, CO_2 or argon that might have escaped from the cleaning stage, b) it also adsorbs the background species built

up in the mass spectrometer during the analysis. Both these reduce the interfering background species for neon. The split of noble fraction trapped in the charcoal finger is now a mixture of xenon, krypton and argon. These are separated in two steps, by allowing selective adsorption of the species on a charcoal finger by at suitable temperature (-108 °C for Xe and -154 °C for Kr) using a variable temperature probe. Each of these is transferred to the let-in volume before introducing them into the mass spectrometer.

2.4.3. Mass analysis

Each of the separated fractions from the extraction line is introduced into the mass spectrometer through an UHV valve, and analyzed for the masses by scanning the peaks manually in a number of cycles. In addition to the masses of interest, peak signals at masses 2 (H_2^+), 18 (H_2O^+), 40 ($^{40}Ar^+$) and 44 (CO_2^+) in the He–Ne fraction, and 40 ($^{40}Ar^+$) in the Kr–fraction are monitored regularly to assess the background contributions (*discussed later*). The noble gases are measured usually on the electron multiplier except for mass 4 and 40 in some samples that are measured on the Faraday cup. Nitrogen is measured in the molecular form on the Faraday cup for mass 28, 29 and 30. For smaller nitrogen samples, the peaks 29 and 30 were run on the multiplier, after scanning on Faraday for mass peaks 28 and 29. Measuring mass 30 in the nitrogen fraction allows a precise estimation and correction for the interference from CO (*discussed later*).

2.4.4. Data acquisition and reduction

The signals from the mass spectrometer are acquired and recorded on an on-line computer by using suitable interface and programs. A parallel XY recorder gives a graphic view of the scan and helps in the identification of the peaks. The digitized 'time vs. signal' data is processed for the time and peak-heights. The time zero (T_0) values for the peak heights and the ratios are found out from this data by offline data reduction. The data thus acquired is corrected for the blank, backgrounds and the instrumental mass discrimination.

a. Blanks

Blanks performed in identical fashion to the sample steps, both precede and follow the samples. The blank contributions are always ≤ 5 % for nitrogen, and seldom exceed 10

% for the noble gases (except helium and neon). Isotopic compositions of the blanks are 5 ± 2 ‰ for nitrogen, and nearly atmospheric for the noble gases.

b. Interference corrections

The measured signals often have a contribution from the interfering species. With the usual resolving powers of the mass spectrometer, it is not always possible to resolve these contributions from the measured signals. In some cases, it is however possible to identify the interfering species and correct for their contributions, which are outlined below.

B1. Interference at mass 3

The molecular ion of hydrogen (H_3^+) is an interfering species for the ^3He mass. The peaks for these two masses cannot be resolved with the resolution of 170 of the mass spectrometer. The contribution of H_3^+ at mass 3, however, can be assessed and corrected for, by measuring the peak at mass 2 (H_2^+) and estimating the corresponding H_3^+ contribution using a predetermined H_3^+/H_2^+ ratio (using pure H_2). As the SAES getter in the mass spectrometer keeps the H_2 background very low, the contribution due to H_3^+ is in general negligible ($<<1\%$).

B2. Interference at masses 20 and 22

Contributions from $H_2^{18}O^+$ and $^{40}Ar^{++}$ at mass 20 and $^{44}CO_2^{++}$ at mass 22 cannot be resolved from the neon peak signals by the mass spectrometer. The neon data is, therefore, corrected for these background contributions from the measured peak signals of the masses 18, 40 and 44 and using the $^{18}O/^{16}O$, $40^{++}/40^+$, and $44^{++}/44^+$ abundance ratios, respectively. The abundance ratios $40^{++}/40^+$, and $44^{++}/44^+$, in the above correction, are periodically determined for the operating conditions of the mass spectrometer from the air standard. The typical values of $40^{++}/40^+$, and $44^{++}/44^+$ are 0.0359 and 0.00703 respectively.

B3. CO correction:

Peak height at mass 30 can have contributions from $^{15}N^{15}N$, $^{12}C^{18}O$ and possibly from the hydrocarbons. Assuming that all the hydrocarbon contribution at masses 30 and 31 would be comparable, and considering the near absence of any 31 peak in the signal, it is considered that the hydrocarbon peak at mass 30 is negligible. Therefore, the excess over $^{15}N^{15}N$ at mass 30 is assigned wholly to CO contribution. The effect

of CO contribution, which shifts the $\delta^{15}N$ to more positive value, is corrected for by routinely measuring mass 30 along with the masses 28 and 29 in the nitrogen-fraction. The correction procedure is as follows.

i. Estimate excess at mass 30:

$30_{excess} = ([30/29]_{meas.} - [30/29]_{expect.}) \times 29_{meas.}$

where $(30/29)_{expct.} = 1/4 \times (29/28)_{meas.}$ (from the abundance of ^{15}N and ^{14}N)

This is assigned, wholly, to the contribution of 30 from CO.

ii. Contribution at mass 29 from CO (^{29}CO) is now estimated from the amount of ^{30}CO derived in the previous step, using the $^{29}CO/^{30}CO$ ratio of 5.711 for normal C, O isotopic compositions. The ^{29}CO, which has a $^{28}CO/^{29}CO$ ratio of 85.939, is subtracted from the measured nitrogen ($29_{meas.}$) to obtain the CO-corrected 28/29. After five iterations, the 28/29 values converge, and this value is used as the CO-corrected 28/29. The ^{29}CO in the last iteration is subtracted from the measured 29 to obtain the CO-corrected nitrogen amount. For deriving the $^{28}CO/^{29}CO$ and $^{30}CO/^{29}CO$ ratios, the terrestrial C, O isotopic compositions are assumed. The CO correction on $\delta^{15}N$ is usually much less than 1‰.

B4. Correction for the contribution of $^{40}Ar_2^+$ at mass 80

$^{40}Ar_2^+$ has an unresolvable contribution at mass 80. This is assessed from the $^{40}Ar^+$ measured in the krypton fraction, and using a ratio of $^{40}Ar_2^+/^{40}Ar^+$ measured in the krypton fraction of an air standard. The Kr fraction of an air standard always has some ^{40}Ar, because of incomplete separation of Ar and Kr. Therefore the ^{40}Ar in the Kr fraction of an air standard is always monitored, and used in estimating the $^{40}Ar_2^+/^{40}Ar^+$ ratio the following way.

i. Estimating the [80/84] ratio corrected for mass discrimination

$[80/84]_{corr.} = [80/84]_{meas.} - (4 \times \text{mass discrimination} \times [80/84]_{meas.})$

ii. Estimating the excess at 80:

$80_{excess} = ([80/84]_{corr.} - [80/84]_{Air}) \times 84_{meas.}$

iii. $^{40}Ar_2^+/^{40}Ar^+ = 80_{excess} / 40_{meas. \text{ in Kr fraction}}.$

Table 2.3. Mass spectrometer calibration parameters.

Species	Detector and Resistance(Ω)used	Sensitivity[A] (ccSTP/Counts)	Yield[A] (%)	M.D. %.amu^{-1}
^{22}Ne	M, 10^8	1.38×10^{-13}		2.2 (.07)
^{28}N$_2$	F, 10^{10}	5.9×10^{-8} (μg/Counts)		2.4 (.03)
^{36}Ar	M, 10^8	1.5×10^{-14}	90	1.01(.15) F 0.98(.01) M
^{40}Ar	F, 10^{10}	5.4×10^{-11}		
^{84}Kr	M, 10^9	1.2×10^{-15}	80	0.86(0.07)
^{132}Xe	M, 10^9	8.9×10^{-16}	73	0.72(.09)

[A] The sensitivities among the Air standards lie within 10%, while the yields vary within 5 %. F= Faraday cup; M= multiplier.

A typical value of this ratio is 4×10^{-7}. This correction is not very significant in case of ureilites, because they have very low ^{40}Ar/^{36}Ar ratio and hence negligible ^{40}Ar$_2^+$ contribution on ^{80}Kr.

2.5. Calibration of the mass spectrometer

Known amounts air standards, processed in a fashion similar to the samples, are run periodically to calibrate the mass spectrometer, for its sensitivity and mass discrimination. An Air standard is also used to find out the separation efficiency of Ar, Kr and Xe in a mixture of these gases. Typical values of the air standard parameters that are used in calibration are given in Table 2.3. The sensitivities lie within 10 % between standards, analyzed over several months. For a particular experiment, the closest air standard parameters are used. The mass discrimination is more reproducible for long periods of time. For most of the analysis, the separation yields of Ar, Kr and Xe have been calculated for individual measurements to get precise elemental abundance values.

2.5.1. Mass Discrimination

The sensitivity of the mass spectrometer for different isotopes of an element are not the same and causes a systematic difference in measured isotopic ratios and actual isotopic ratios. The correction factor for mass discrimination can be calculated using reference gas (air) with known isotopic composition using the following equation:

$$m.d. = \left[\frac{Ratio_{meas.}}{Ratio_{Std.}} - 1\right] \times \frac{100}{m_j - m_i} \qquad (\%/amu)$$

where,

$$Where, \quad Ratio = \frac{[m_i]}{[m_j]}, \quad and \quad if \quad \left[\frac{md}{100} \times (m_j - m_i)\right] \ll 1 \quad then$$

$$R_{true} = R_{meas.}\left[1 - \frac{m\,d}{100}\cdot(m_j - m_i)\right] = R_{meas.} \times mdf$$

where,

$$mdf = \left[1 - \frac{m\,d}{100}\cdot(m_j - m_i)\right]$$

So by multiplying the $R_{meas.}$ by the factor mdf, the true ratio R_{true} is obtained.

Mass discrimination is determined from air standard runs. These are more or less constant for each air standard run for all elements over long periods of time. The mass discrimination and sensitivity remains the same over certain range of total pressure in the mass spectrometer, during the measurement of a certain gas. For the case of Xe, Kr and Ne, in general, the total gas pressure in the mass spectrometer during the
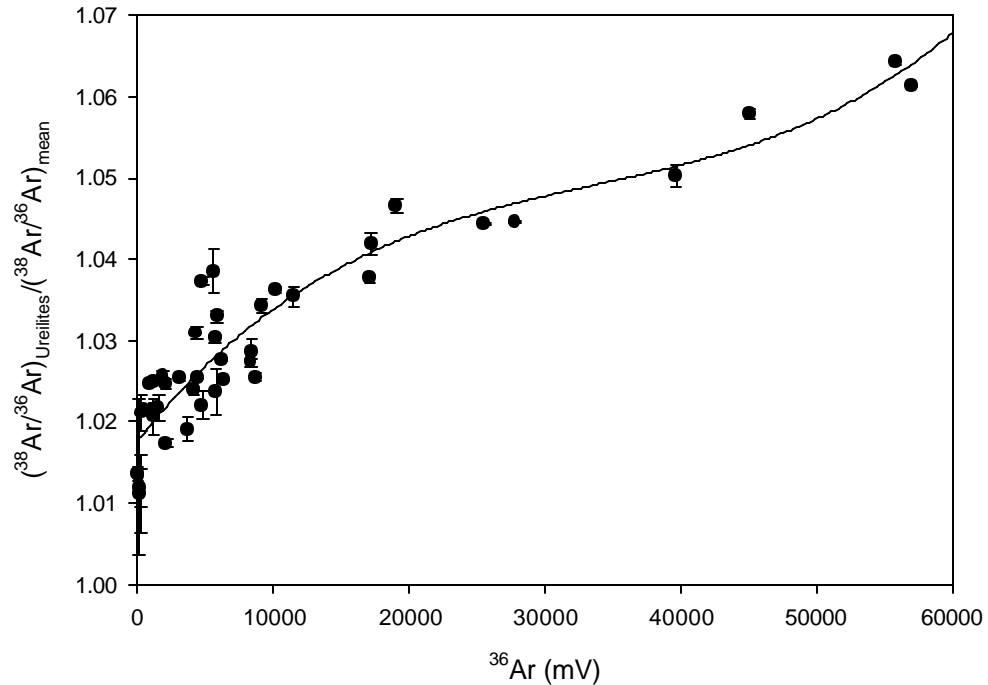
Fig 2.4 *Plot showing the variations of $^{38}Ar/^{36}Ar$ ratios of the acid residues with amount of ^{36}Ar measured. The $(^{38}Ar/^{36}Ar)_{ureilite}$ values used in this plot have been corrected for mass discrimination obtained from air standard. The normalization to the mean value as obtained from seven acid residue measurements by Göbel et al. (1978), is done to make the trend very clear.*

analysis of sample gas falls within this range and we use a fixed value of sensitivity and *mdf*. But in the case of nitrogen and argon in particular cases (like in ureilites) this may not be true, as we deal with samples having a wide range of nitrogen contents and $^{40}Ar/^{36}Ar$ ratios respectively. In Fig 2.4, the ratio of $^{38}Ar/^{36}Ar$ for various carbon rich acid residues from ureilites (with usual air standard based mass discrimination correction) normalized to the mean of $^{38}Ar/^{36}Ar$ of seven residues from Göbel *et al.* (1978) have been plotted as a function of argon amounts. The large increase in the $^{38}Ar/^{36}Ar$ ratios with argon amount in our measurements can be seen clearly. Are these variations real or an artifact due to variations in *mdf* with argon amounts? This needs to be investigated. So, we have investigated the effect of total gas pressure on the *mdf* and sensitivity for N_2 and Ar.

Nitrogen: From the air standard, different aliquots of nitrogen have been introduced into the mass spectrometer and the sensitivity and *mdf* have been determined with respect to standard measurement condition (signal of N_2 ~ 2 volt on F10). In Fig 2.5, the *mdf* have been plotted against the signal of $^{28}N_2$ (on Faraday cup, using 10^{10} Ω
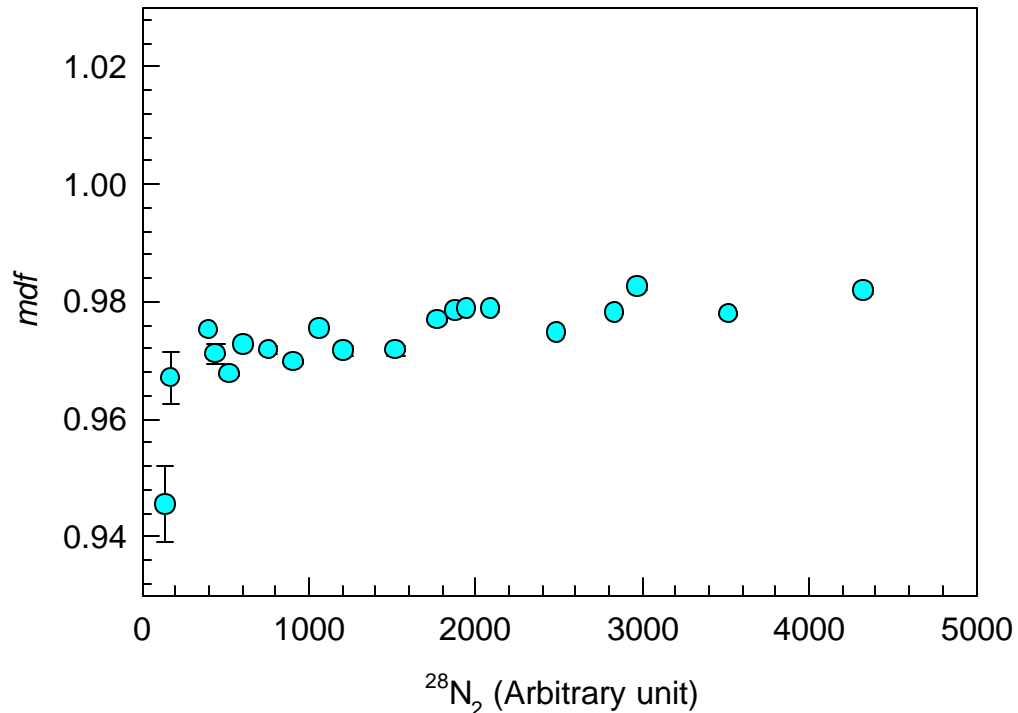
Fig 2.5 *Mass discrimination factor (mdf) of $^{28}N_2/^{29}N_2$ as function of nitrogen amount ($^{28}N_2$). MDF is more or less constant except in cases where the nitrogen amount is very small.*
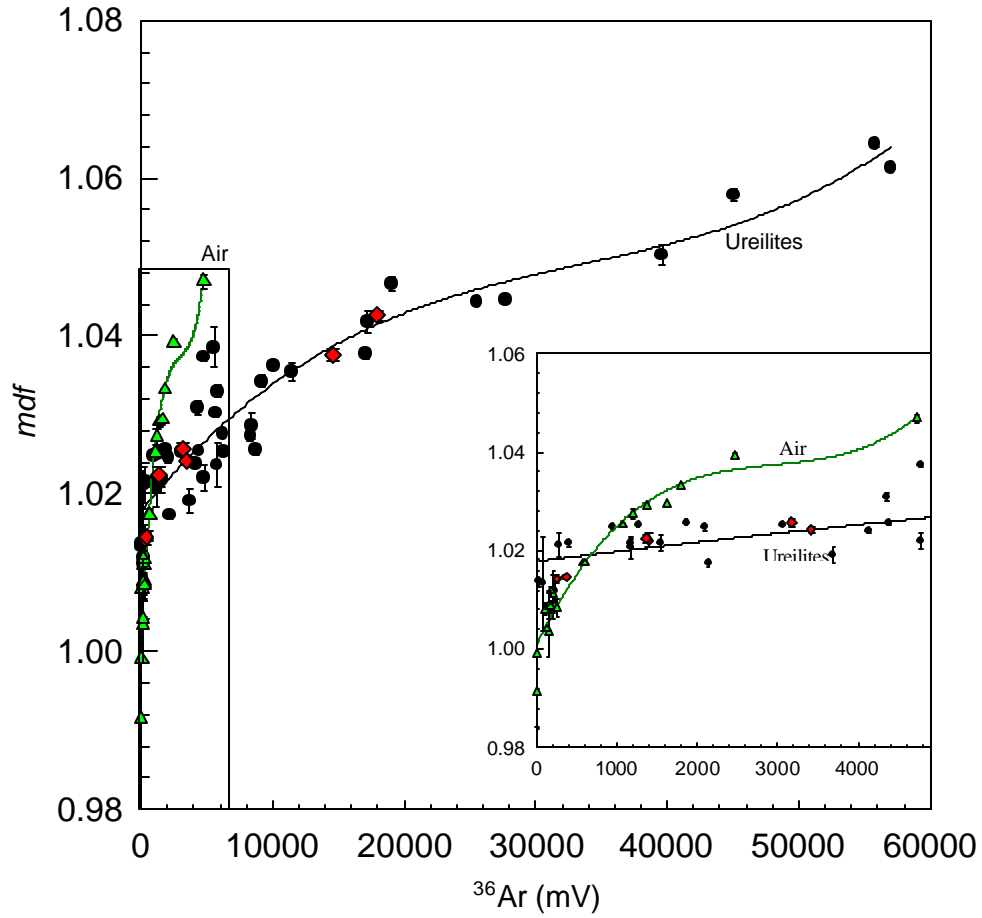
Fig 2.6 *Plot showing the mass discrimination factor for $^{38}Ar/^{36}Ar$ ratio as a function of ^{36}Ar amounts (in mV). The large variations in mdf with argon amount can be seen clearly. Two very distinct mdf patterns can be seen for the two reservoirs with low and high $^{40}Ar/^{36}Ar$ ratios. In the inset, blown-up portion of rectangular box is shown.*

resistor). It can be seen that *mdf* values are almost constant above $^{28}N_2$ signal of >200 mV. The sensitivity plot will be having similar trend, with almost constant sensitivity for signal over >200 mV, but higher sensitivity below a signal size of $^{28}N_2$ < 200 mV. The sample size during analysis corresponded to $^{28}N_2$ signal range of 500 mV to 4000 mV and we used the *mdf* and sensitivity corresponding to the standard conditions ($^{28}N_2 \sim 2000$ mV) for all the cases.

Argon: Argon in most meteorite samples has $(^{40}Ar/^{36}Ar) \geq (^{40}Ar/^{36}Ar)_{Air}$, due to large contributions from radiogenic ^{40}Ar. Hence, the abundance of ^{40}Ar isotope, in general, determines the total pressure of the argon sample of a meteorite (similar to the case of air). But for ureilites (bulk samples as well as acid residues) having the ratio $(^{40}Ar/^{36}Ar)<1$, instead of the ^{40}Ar, isotope ^{36}Ar determines the total pressure of argon.

If there is any pressure effect on the sensitivity and *mdf* for argon, it would be very severe in the case of ureilites. Our initial measurements of ureilite samples have given $^{38}Ar/^{36}Ar$ values that are much lower than 0.188 (the normal value for trapped argon in meteorites) by adopting the *mdf* value corresponding to standard air argon (Fig 2.4). We realized the importance of pressure effect on *mdf* of argon and investigated it using both air argon as well as argon from ureilites. Similar variations in *mdf* for $^{38}Ar/^{36}Ar$ have also been noticed earlier in case of bulk ureilites that have low abundance of ^{40}Ar (Wilkening and Marti, 1976).

In order to understand the cause of variations in *mdf* of argon with pressure inside the mass-spectrometer and to quantify these variations, the *mdf* of ^{38}Ar at various pressures have been measured for a number of aliquots from two reservoirs that have a large difference in ^{40}Ar abundance (air argon and argon collected from acid resistant residues of ureilites). At the end of analysis of Ar fractions of individual temperature fractions of acid residues, it has been collected into a separate volume to build a Ar gas reservoir with uniform $^{38}Ar/^{36}Ar$ ratio but negligible amount of ^{40}Ar. Aliquots from this reservoir have been used to build the curve in Fig 2.6 [symbol (red diamond)]. These points follow the similar trend as obtained for acid residues from different ureilites. The plot shows the variation of mass discrimination factor with amount of ^{36}Ar introduced into mass spectrometer. Though the *mdf* of nitrogen shows more or less constant values with nitrogen amount (i.e. pressure) (*see* Fig 2.5), the *mdf* of argon, on the other hand, show strong pressure dependence. The *mdf* of $^{38}Ar/^{36}Ar$ ratio varies significantly depending on the amount of ^{40}Ar present. Moreover, the *mdf* is also not a simple function of (or linearly dependent on) total Ar pressure ($p^{40}Ar$ $+p^{38}Ar+p^{36}Ar$), and in both the cases (air standard argon and ureilite argon) they define two quite different *mdf* curves i.e., for the similar pressure of argon, the *mdf* of $^{38}Ar/^{36}Ar$ ratio for air standard is significantly higher than that of ureilite argon (with low ^{40}Ar abundance) (Fig 2.7). This implies that the *mdf*, calculated from air standard (or any standard with high $^{40}Ar/^{36}Ar$ ratio) with some fixed amount of Ar, can not be used for a sample having very low $^{40}Ar/^{36}Ar$. The exact mechanism for the variations of sensitivity for different isotopes of argon in reservoirs with high and low abundance of ^{40}Ar, is not yet understood.

In all the measurements of argon in this study, the measured ratios of $^{38}Ar/^{36}Ar$ have been corrected by using different *mdf* values depending on amount of ^{36}Ar, from *mdf*
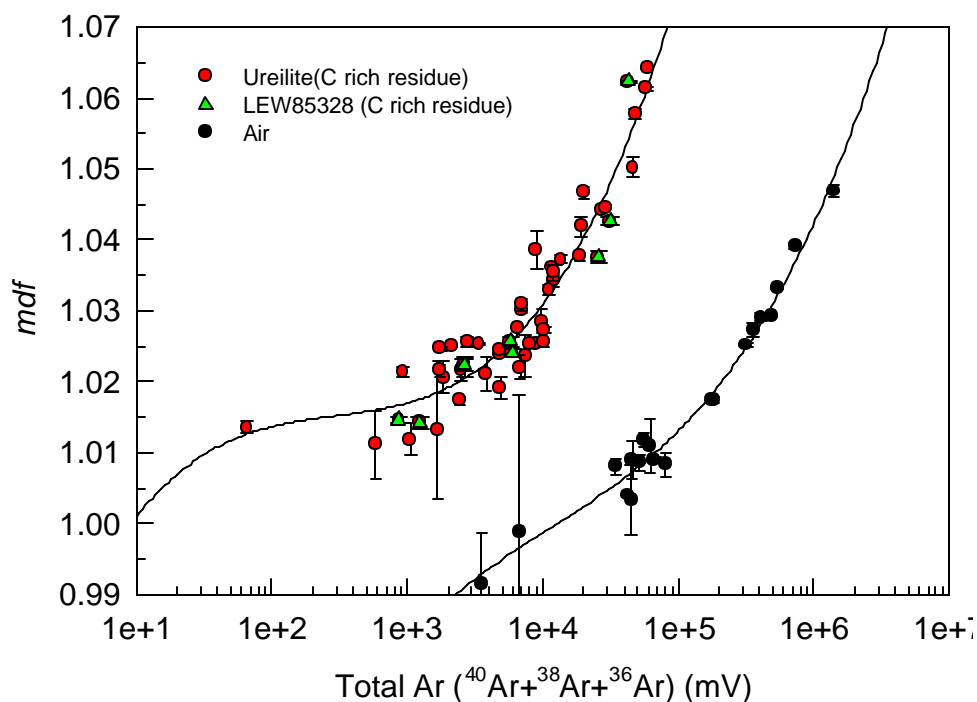
Fig 2.7 *Plot showing the mass discrimination factor for $^{38}Ar/^{36}Ar$ ratio as function of total Ar amounts (in mV). Two quite distinct mdf curves can be seen for 'air argon' and 'argon from C rich residues of ureilites'. The mdf is not simple function of Ar pressure.*

curve obtained for ureilite argon reservoir (inset Fig 2.6) rather than using single *mdf* value from air standard. To calculate the *mdf* of ureilite argon reservoir, the mean $^{38}Ar/^{36}Ar$ ratio from acid residues of seven ureilites (Göbel *et al.*, 1978) has been used as a reference value for the ratio of $^{38}Ar/^{36}Ar$.

2.6. Characterization of residues

2.6.1. SEM photograph: SEM photomicrograph of all the acid residues have been taken by the instrument LEO440-*i* with 25kV and 20kV EHT at various magnifications. Plate like big crystals of graphites (20-500 micron) are seen clearly in all the photographs. No diamond like crystal structures are seen even at the resolution of 1-3 micron, indicating that the diamonds are much smaller in size. The rough surfaces of grains from HF-HCl residue become clear and shiny after perchloric acid treatment indicating removal of the amorphous (non-crystallized) carbon sticking on the large graphite crystals by $HClO_4$ treatment (*discussed later*). *See* chapter 4 for the SEM pictures (Fig 4.1).

2.6.2 INAA analysis: A few selected bulk samples as well as acid residues of both monomict and polymict ureilites have been analyzed for trace elements by Instrumental Neutron Activation Analysis (INAA). The samples packed in Al foil along with USGS standards BCR-1 (Colambia River Basalt) and Allende meteorite, have been transferred to a quartz vial and sealed subsequently. Blank Al foil has also been packed along with the samples and standards to see the contribution from Al foil. The sealed quartz vial subsequently has been irradiated (with a neutron fluence of 10^{18} neutron/cm^2) in DHRUVA reactor at BARC (Bhabha Atomic Research Centre), Mumbai. The irradiated samples were counted on a Hyper Pure Germanium Solid State (HPGE) γ–ray detector (148 cc), which is housed in 10 cm thick lead shield, to asses the intensity of various γ rays emitted by various radioisotope. The counting was repeated after appropriate cooling intervals to determine both short and long lived radioisotopes. The concentration of various elements are measured by comparative method. The results will be discussed in the 4th chapter.

Nitrogen in bulk samples of Ureilites

3.1 Introduction

In this chapter, the nitrogen and argon studies of bulk ureilites are discussed. Out of the following ureilites, Haverö, Kenna, Lahrauli, LEW85328, ALH81101, ALH82130 (monomict), EET87720, EET83309, Nilpena (polymict) and ALH78019 (diamond free) analyzed in the present study, nitrogen data are being reported for the first time for Haverö, Lahrauli, LEW85328, ALH81101, ALH82130, ALH78019 and EET87720. For the ureilites, Haverö, Kenna, LEW85328, ALH78019, EET83309, EET87720, and Nilpena, noble gas data have been reported earlier (Göbel *et al.*, 1978; Wilkening and Marti, 1976; Wacker, 1986, Ott *et al.*, 1986; Waber *et al.*, 1976; Bogard *et al.*, 1973), while for Kenna, EET83309, Nilpena nitrogen data have been reported (Grady *et al.*, 1985; Grady and Pillinger, 1988). The simultaneous study of nitrogen and noble gases, so far exist for ALH77257, Asuka 881931 and Yamato 791538, none of which are included in the present study (Yamamoto *et al.*, 1998). While most of the noble gas studies employed both combustion and pyrolysis for gas extraction, the nitrogen studies are reported so far by combustion only.

While combustion will be a good technique to release gases from separated carbon phases, a complete gas extraction is not assured by combustion of the bulk ureilites for two reasons. The carbon phases which are occluded in silicates and metal may not combust and release gases and the noncombustible phases may not completely release their gases at the temperatures (up to 1100℃) used normally for combustion.

In the present study we employed a combination of combustion and pyrolysis to resolve the different components as well as to identify the carriers.

The data for each bulk meteorite is individually described first, while the general trends for ureilites are dealt with in the discussion at the end of the chapter. The data for the amounts and isotopic ratios of nitrogen and argon, but amounts only for krypton and xenon are compiled in Table 3.1 for monomict ureilites and the diamond free ureilites and in Table 3.2 for polymict ureilites.

3.2 Results

3.2.1 Nitrogen in monomict ureilites

Lewis Cliff 85328 (L28-B1 & L28-B2) ……

This is a monomict ureilite from Antarctic collection with typical ureilitic texture. It is a medium shocked ureilite (Goodrich, 1992).
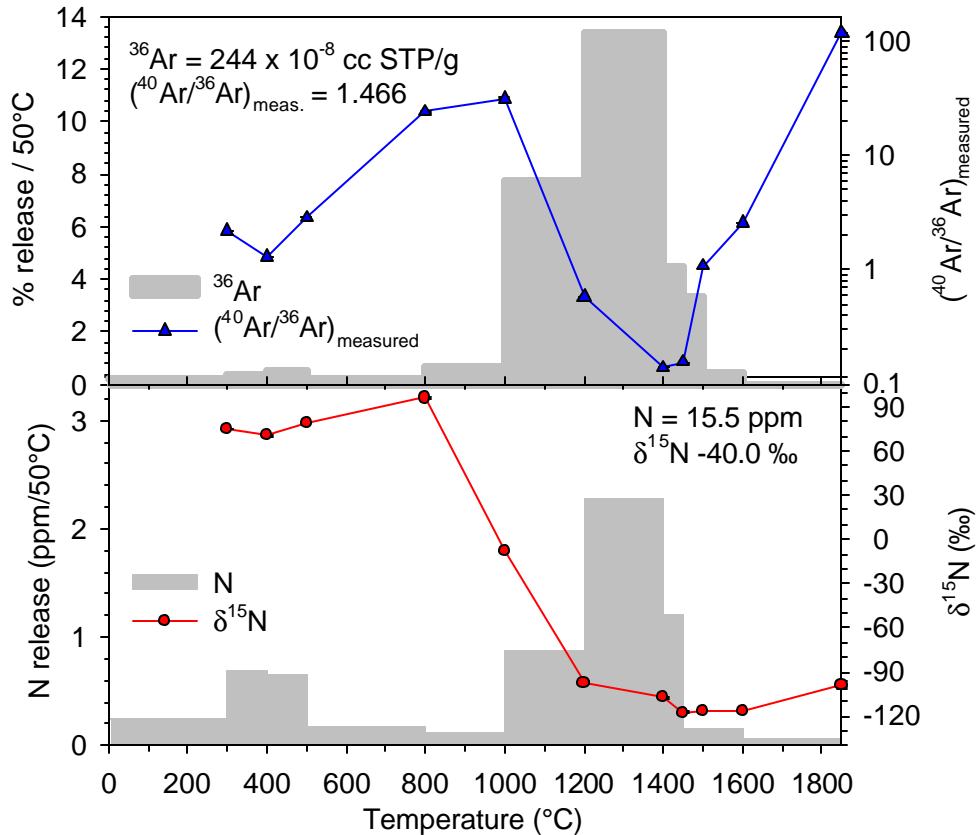
Fig 3.1 *Nitrogen, argon release pattern as well as isotopic ratios determined by stepped pyrolysis of the whole rock sample of LEW85328 (L28-B1).*

Fig 3.1 shows the release pattern of nitrogen, ^{36}Ar and corresponding δ^{15}N and ^{40}Ar/^{36}Ar on pyrolysis [except the initial three steps (up to 500°C) that are combustion steps at 2 torr oxygen]. Argon release and ^{40}Ar/^{36}Ar ratio have been plotted together
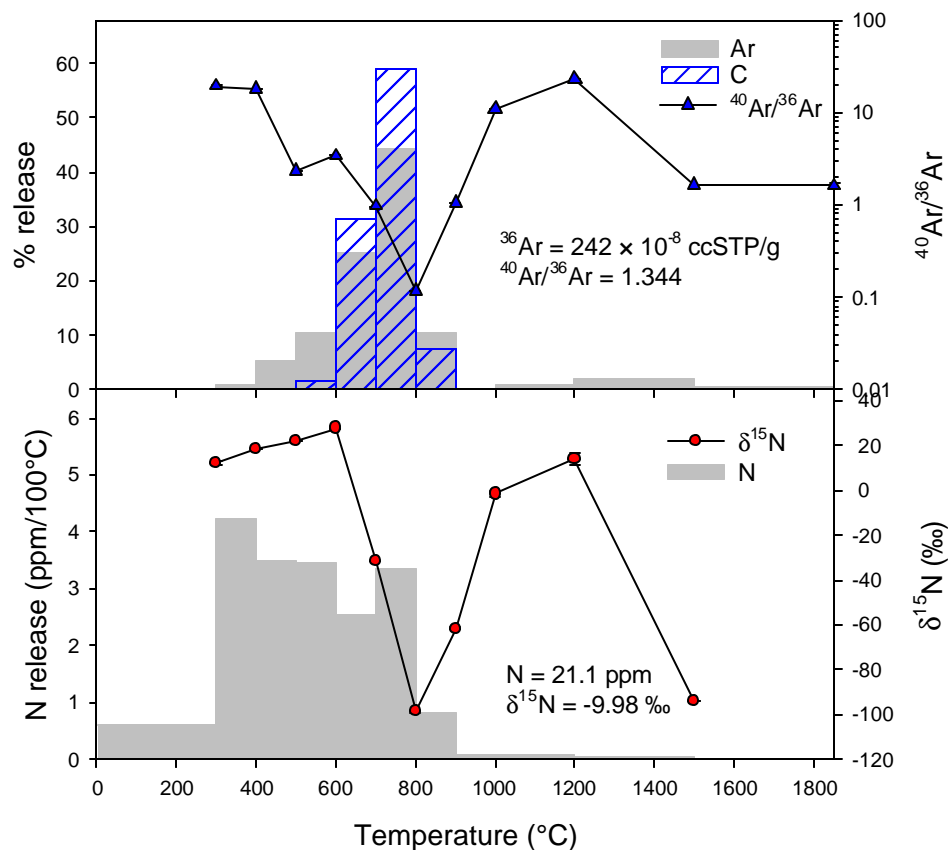
Fig 3.2 *Nitrogen and argon release patterns as well as isotopic composition on stepped combustion at 2 torr O_2 for whole rock sample of LEW85328 (L28-B2). The CO_2 liberated during combustion has also been plotted. After 1000°C, the gases are extracted by stepped pyrolysis.*

with nitrogen release and isotopic compositions because it can be used as indicator of 'primordial' noble gas release. The bulk sample L28-B1 yields 15.5 ppm of nitrogen with bulk $\delta^{15}N$ of –40‰. Two nitrogen components can clearly be resolved with very distinct $\delta^{15}N$. The low temperature release nitrogen component is enriched in ^{15}N up to 96‰. This nitrogen is not associated with noble gas release while the release behavior of this component in initial steps of combustion reveals that the carrier must be a low temperature combustible phase. Though the peak in $\delta^{15}N$ is observed at 800°C, the release of this N component can be felt up to 1400°C. The other nitrogen component is released above 1000°C with minimum $\delta^{15}N$ of –118‰ (at 1450°C) and is associated with 'primordial' noble gas release. Though the peak release of this nitrogen component is at 1400°C, the light nitrogen yields very constant value $\delta^{15}N$ of ≤-110‰ only after 1425°C. This nitrogen component is associated with lowest value of $^{40}Ar/^{36}Ar$.

Table 3.1 Nitrogen and noble gases in bulk samples of monomict and diamond free ureilites.

Temp. (°C)	N (ppm)	δ^{15}N (‰)	^{36}Ar (10^8 ccSTP/g)	^{38}Ar/^{36}Ar	^{40}Ar/^{36}Ar	^{84}Kr (10^{-10} ccSTP/g)	^{132}Xe (10^{-10} ccSTP/g)	P_{CO2+CO}
LEW85328-Bulk, L28-B1, Pyrolysis, 77.4mg								
300c[‡]	1.5	74.96	2.9	0.1896	1.632	1.8	1.3	
		±0.39		0.0003	0.002			
400c	1.4	70.52	1.9	0.1875	0.2860	12.0	8.4	
		0.86		0.0003	0.0041			
500c	1.3	79.01	2.4	0.1862	2.012	13.7	12.9	
		0.63		0.0002	0.004			
800	1.0	95.95	3.1	0.1883	24.22	1.6	2.5	
		0.38		0.0002	0.02			
1000	0.4	-8.07	6.2	0.1874	31.67	6.4	12.6	
		0.42		0.0003	0.52			
1200	3.5	-97.12	75.2	0.1907	0.5456	41.4	43.5	
		0.66		0.0001	0.0012			
1400	3.1	-106.2	108.1	0.1922	0.1327	98.8	90.1	
		0.4		0.0001	0.0002			
1425	1.5	-109.8	22.4	0.1916	0.0103	27.7	19.2	
		0.8		0.0001	0.0004			
1450	1.2	-117.6	10.9	0.1926	0.0068	16.6	14.2	
		0.6		0.0002	0.0003			
1500	0.1		8.1	0.1916	0.3288	12.0	10.8	
				0.0001	0.0018			
1600	0.3	-116.4	2.3	0.2216	0.3271	1.4	0.6	
		0.5		0.0001	0.0075			

[‡] combustion at 2 torr O$_2$.

1850	0.18	-94.77	0.1	0.2065	94.35			
		2.13		0.0009	0.09			
Total	15.4	-40.22	243.6	0.1914	1.446	233.3	216.0	
		0.59		0.0001	0.014			

LEW85328‑Bulk, L28‑B2, Combustion and Pyrolysis, 26.33mg

300	1.8	12.33	0.3	0.1914	19.24	0.2	0.2	2
		0.85		0.0007	0.12			
400	4.2	18.70	1.9	0.1891	17.77	1.1	1.1	0
		0.16		0.0005	0.03			
450	0.5	15.21	0.4	0.1907	9.587	0.3	0.2	0
		0.51		0.0002	0.068			
500	3.0	23.18	12.3	0.1899	2.059	7.4	6.5	0
		0.23		0.0001	0.003			
600	3.4	27.77	24.8	0.1893	3.432	14.2	15.3	21
		0.07		0.0001	0.001			
700	2.5	-31.58	60.4	0.1910	0.965	62.6	66.7	398
		0.17		0.0001	0.001			
800	3.3	-98.79	107.4	0.1915	0.116	94.7	75.0	750
		0.26		0.0001	0.001			
900	0.8	-61.76	24.8	0.1902	1.064	13.1	10.2	95
		0.49		0.0001	0.001			
1000	0.1	-1.58	0.7	0.1910	11.017	0.5	0.4	0
		1.28		0.0004	0.032			
1200	0.1	14.12	2.4	0.1994	22.93	1.3	0.7	
		2.33		0.0012	0.03			
1500	0.2	-93.74	5.0	0.2245	1.659	1.6	0.7	
		0.13		0.0002	0.011			
1850			1.2	0.2481	1.606	0.6	0.1	

				0.0008	0.102		
Total	20.1	-9.98	241.5	0.1920	1.344	197.6	177.0
		0.28		0.0001	0.002		

Kenna-Bulk, KNA-B, Pyrolysis, 49.49mg

400c	1.2	18.76	8.2	0.1894	0.3084	2.8	-
		1.41		0.0003	0.0014		
800	2.0	24.48	8.9	0.1908	0.3429	5.1	6.2
		1.04		0.0001	0.0014		
1000	2.3	-75.78	3.8	0.1927	0.0917	3.5	6.2
		0.37		0.0001	0.0063		
1200	4.7	-79.20	15.9	0.1925	0.0063	15.5	13.6
		0.48		0.0002	0.0011		
1300	4.2	-96.70	19.8	0.1958	0.0358	16.8	11.0
		1.12		0.0001	0.0003		
1350	0.8	-123.4	5.3	0.1941	0.2782	6.6	6.3
		2.6		0.0002	0.0462		
1400	0.4	-103.0	5.4	0.1913	0.1409	6.4	5.3
		0.8		0.0003	0.0015		
1450	0.7	-117.0	3.9	0.1930	0.3506	21.9	17.1
		1.0		0.0001	0.0052		
1500	0.5	-137.5	3.4	0.1953	0.5887	5.1	5.1
		1.5		0.0001	0.0024		
1600	0.4	-99.84	0.4	0.3702	23.73	0.4	0.2
		1.52		0.0006	0.06		
1850	0.3	-75.62	0.02	0.1756	28.30	0.9	0.2
		3.58		0.0007	0.39		
Total	17.5	-70.37	75.0	0.1930	0.2969	82.2	71.2
		0.99		0.0001	0.0050		

Lahrauli-bulk, LAH-B, 29.89mg, Pyrolysis and combustion

300	8.7	8.66	0.9	0.1891	8.685	-	-	7
		0.20		0.0006	0.084			
400	11.1	8.95	1.8	0.1937	8.473	0.6	0.5	13
		0.20		0.0001	0.113			
500	11.6	12.96	5.0	0.1959	16.23	1.7	2.2	10
		0.12		0.0009	0.03			
600	9.3	3.62	9.7	0.1991	2.488	5.3	10.8	66
		0.45		0.0005	0.006			
700	7.8	-32.23	31.2	0.1941	0.540	18.0	22.5	225
		0.10		0.0001	0.001			
800	5.3	-23.83	7.3	0.2053	9.764	4.9	8.5	144
		0.14		0.0004	0.007			
900	1.4	-5.55	0.4	0.3038	23.75	0.5	0.3	2
		0.29		0.0002	0.01			
1200	1.4	-2.83	0.8	0.3570	48.46	0.6	0.2	
		0.07		0.0004	0.19			
1500	1.0	-80.89	3.6	0.2696	1.647	1.1	0.4	
		0.29		0.0003	0.015			
1850			0.9	0.2815	17.67	0.6	0.1	
				0.0001	0.11			
Total	52.2	-2.28	77.3	0.2045	4.701	33.4	45.4	
		0.21		0.0002	0.014			

Havero-bulk, HAV-B, Pyrolysis, 76.53mg

400	8.5	16.49	0.2	0.1918	9.558		0.3	
		0.38		0.0010	0.25			
1000	4.1	54.30	0.8	0.2258	12.20	0.8	0.6	
		0.37		0.0001	0.02			

1200	1.0	19.63	2.2	0.1945	0.1123	1.5	1.6
		0.61		0.0001	0.0056		
1400	3.9	-38.39	20.6	0.1941	0.4800	4.5	8.9
		0.21		0.0001	0.0024		
1600	3.9	-77.79	57.2	0.1921	0.3326	17.5	28.8
		0.27		0.0003	0.0013		
1800	0.8	-22.89	0.3	0.2205	187.8		
		0.29		0.0002	1.1		
Total	22.1	-4.01	81.4	0.1929	1.202	24.3	39.6
		0.34		0.0002	0.007		

ALH81101-Bulk, A01-B, Pyrolysis, 42.34mg

400c	23.4	4.42	0.2	0.2127	54.17	0.6	0.8
		0.37		0.0007	0.06		
500	7.4	6.39	0.5	0.2027	16.09	0.7	2.0
		0.44		0.0001	0.03		
800	11.8	4.02	0.2	0.2365	59.48	0.4	1.1
		0.38		0.0013	0.06		
1000	2.6	-15.64	0.2	0.2255	15.49	0.5	3.2
		0.42		0.0010	0.22		
1200	3.0	-59.60	7.6	0.1942	1.329	5.1	7.2
		0.40		0.0001	0.001		
1400	2.4	-85.90	21.1	0.1900	0.031	18.8	19.3
		0.476		0.0001	0.005		
1600	2.8	-84.73	9.8	0.1949	3.224	10.7	15.2
		0.42		0.0001	0.005		
1850	-						
Total	53.2	-8.58	39.7	0.1922	1.965	36.6	48.8
		0.39		0.0001	0.004		

ALH82130 -Bulk, A30 -B, Pyrolysis, 50.24mg

400	30.4	0.80	0.3	0.1899	35.69	0.4	1.3
		0.43		0.0003	0.03		
500	12.0	6.73	0.7	0.1948	15.64	0.6	2.9
		0.43		0.0007	0.03		
800	4.03	-3.68	0.3	0.1880	18.72	0.2	1.9
		0.96		0.0007	0.09		
1000	1.4	-45.40	0.6	0.1906	2.775	0.6	13.3
		0.40		0.0004	0.032		
1200	2.0	-93.44	5.9	0.1952	0.3552	2.6	25.3
		0.69		0.0003	0.0020		
1400	0.9	-76.29	10.8	0.1951	0.4214	9.1	63.7
		0.82		0.0001	0.0008		
1600	2.9	-100.3	2.1	0.1903	1.788	1.6	1.9
		0.49		0.0001	0.015		
1800	0.5	-93.33	0.1	0.2033	165.3		
		0.43		0.0012	0.4		
1850	0.7	-28.46					
		0.77					
Total	54.9	-10.65	20.6	0.1943	2.513	15	110.1
		0.49		0.0002	0.008		
Total[*]	24.3	-25.03					
		0.56					

ALH78019 -bulk, A19 -B, pyrolysis, 42.20mg (Diamond free ureilite)

400	0.9	-16.02	4.1	0.1906	1.370	2.1	0.2
		0.45		0.0004	0.021		
1000	2.8	-9.30	11.7	0.1884	1.344	5.6	3.8
		1.82		0.0001	0.003		

1200	0.4	-19.54	12.9	0.1893	0.0966	6.7	3.4
		0.43		0.0001	0.0020		
1400	1.6	-3.54	46.1	0.1955	0.0123	16.7	10.4
		0.35		0.0001	0.0019		
1600	0.4	-47.47	34.7	0.1899	0.0887	8.5	8.7
		2.927		0.0001	0.0035		
1800	0.1	-45.71	0.6	0.1903	23.44	0.3	0.2
		3.23		0.0001	0.2353		
Total	6.3	-13.54	110.1	0.1937	0.3603	40.0	26.7
		1.30		0.0001	0.0045		

*Excluding 400°C step.

Another aliquot of the bulk sample of LEW85328 (L28-B2) has been analyzed by combination of combustion and pyrolysis to have better understanding of the carriers of trapped gases. Up to 1000°C the sample is combusted at 2 torr oxygen pressure, and is later pyrolyzed at 1200, 1500 and 1850°C (Fig. 3.2). The sample L28-B2 yields 20.1 ppm of nitrogen with $\delta^{15}N$ of –10‰. On combustion, most of the noble gases are released between 500°C to 800°C with peak release at 800°C. A small amount (1-5 %) of primordial gases (as indicated by lower values of $^{40}Ar/^{36}Ar$ and light nitrogen) release at higher temperature pyrolysis steps of the combusted sample which released negligible amount of trapped gases even at 1000°C combustion step. This indicates that either appreciable amount of primordial gases are trapped in non combustible refractory phases like silicates and metal or gases are trapped in combustible phases protected by silicates or metal that make them inaccessible to oxygen. Nitrogen in L28-B2 also shows two nitrogen components like L28-B1 but the heaviest nitrogen observed here is not as heavy ($\delta^{15}N$ =28‰ as compared to 96‰) as seen in the previous aliquot. This could be because of either mixing of heavy nitrogen component with lighter nitrogen component dominated at higher temperature steps or heavy nitrogen is distributed heterogeneously on centimeter scale. The light nitrogen component also seems to be affected by tailing of heavy nitrogen component, as the minimum $\delta^{15}N$ value observed here is –99‰ compared to –118‰ in L28-B1. An

excursion in $\delta^{15}N$ (=14‰) is seen at 1200°C pyrolysis and is followed by light nitrogen with $\delta^{15}N$ = -94‰. The light nitrogen could most likely be coming either from refractory non-combustible phases or protected combustible phases. The heavy nitrogen on the other hand, could either be attributed to cosmic ray produced nitrogen or it could be due to adsorbed atmospheric nitrogen because the sample was accidentally exposed to atmosphere after combustion (though it is re-combusted at 900°C in order to remove atmospheric contamination). Considering the relatively higher value of $^{40}Ar/^{36}Ar$ and the nitrogen, heavier than expected for atmospheric nitrogen (14‰ as compared to ±5‰), indicates that the excursion is due to the mixing of both atmospheric and cosmogenic nitrogen.

Kenna (KNA-B)……

This is a medium shocked monomict ureilite which has been studied earlier for noble

Fig 3.3 *Nitrogen and argon release patterns as well as isotopic compositions during stepped heating (pyrolysis) of whole rock sample of monomict ureilite Kenna (KNA-B).*

gases in detail (Wilkening and Marti, 1976; Göbel *et al.*, 1978; Wacker, 1986). The cosmic ray exposure age of Kenna is 23 Ma (Wilkening and Marti, 1976. Earlier measurement of nitrogen in bulk sample of Kenna yielded 37.5 ppm of nitrogen with bulk $\delta^{15}N$ of $-24.8‰$ (analyzed by combustion). The variation of $\delta^{15}N$ with combustion temperature reveals the presence of a light nitrogen component released between 700°-900°C and seems to be associated with peak carbon combustion with $\delta^{13}C$ of $-2‰$ PDB (Grady *et al.*, 1985).

Release patterns as well as isotopic compositions of nitrogen and argon in various temperature steps are depicted in Fig 3.3 and the corresponding data are listed in Table 3.1. The bulk Kenna sample is pyrolyzed stepwise up to 1850°C with initial step of combustion at 400°C. The bulk sample contains 17.5 ppm of nitrogen with bulk $\delta^{15}N$ of $-71‰$. It also contains large amount of primordial noble gases (^{36}Ar concentration is 75 x 10^{-8} ccSTP/g and also other noble gases, Table 3.1). Like LEW85328, Kenna also shows two nitrogen components with very distinct isotopic composition and release temperatures. The first nitrogen component with $\delta^{15}N_{max} = 25‰$ starts to be released right from initial combustion at 400°C and continues up to temperatures as high as 1400°C or more until the nitrogen composition is dominated by the release of light nitrogen component with $\delta^{15}N \leq -100‰$. The lowest value of $\delta^{15}N = -126‰$ is observed at 1500°C. The light nitrogen component is accompanied by noble gas peak release while only a minor amount of noble gases are released along with heavier nitrogen.

Lahrauli (LAH-B) ……

Lahrauli is a monomict ureilite with medium shock level (Goodrich 1992, Bhandari *et al.*, 1981). The cosmic ray exposure age was calculated to be 16 Ma based on ^{21}Ne. Earlier measurement of nitrogen in the bulk Lahrauli yielded 11.3 ppm of nitrogen with $\delta^{15}N$ of $-72‰$ (Murty and Bhandari 1992). The diamonds from Lahrauli showed large enrichment of nitrogen (by the factor of 70) and the isotopic composition of N in diamonds is depleted in ^{15}N with $\delta^{15}N$ value down to $-111‰$. In the present study another aliquot of bulk sample has been analyzed for nitrogen and noble gases by combination of combustion and pyrolysis (combustion up to 900°C and latter pyrolyzed in three steps at 1200, 1500 and 1850°C) in order to understand the association of light nitrogen and noble gases with carbon.
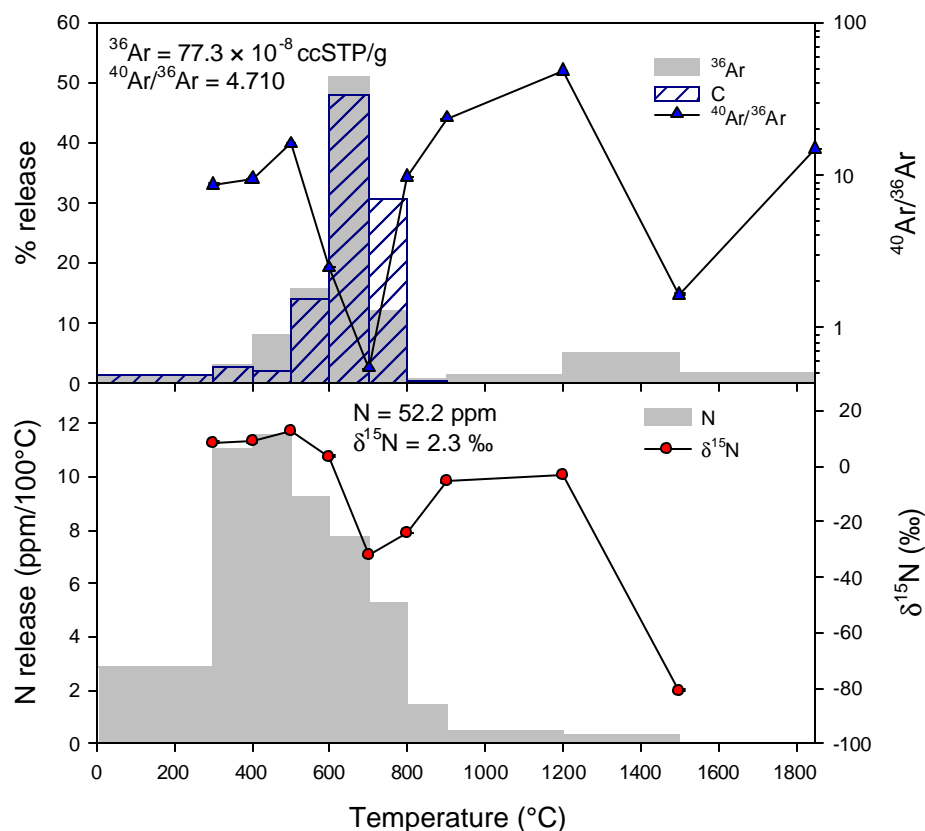
Fig 3.4 *Nitrogen and argon release patterns as well as isotopic composition on stepped combustion at 2 torr O_2 for whole rock sample of Lahrauli (LAH-B). The CO_2 liberated during combustion has also been plotted. After 1000°C, the gases are extracted by stepped pyrolysis.*

Nitrogen concentration (52.2 ppm) in Lahrauli bulk is five times higher than that of earlier measurement (11.3 ppm). More than 75 % of the nitrogen released before 600°C are relatively heavy with $\delta^{15}N$ of 13‰. Also the light nitrogen $\delta^{15}N_{min}$= − 32‰) observed here is not as light as observed in earlier measurement for the same ureilite ($\delta^{15}N_{min}$= −107‰) (Fig.3.4 and Table 3.1). The reason for this discrepancy could most likely be due to the heterogeneous distribution of the carriers of heavy and light nitrogen within same meteorite. The overlap of release temperatures of the carriers of heavy and light nitrogen on combustion could also be responsible for masking the isotopic composition of light nitrogen. Nearly 1 ppm of light nitrogen is released at 1500°C with $\delta^{15}N$ of –81‰ (release from protected phase) revealing that the higher proportion of heavier nitrogen in this aliquot might be responsible for not observing the light nitrogen with $\delta^{15}N \leq$-100‰ during combustion. Like other ureilites, the dip in $\delta^{15}N$ between 600°-800°C is accompanied by trapped noble gases and carbon combustion.

Haverö (HAV-B)……

Haverö is most widely studied ureilite, which is highly shocked. It has been extensively studied for noble gases by Göbel *et al.* (1978). Based on bimodal release pattern of ^{3}He and the association of only the high temperature ^{3}He peak with primordial noble gases, Göbel *et al.* (1978) proposed that the graphite is free of

Fig 3.5 *Nitrogen and argon release patterns as well as isotopic compositions during stepped heating (pyrolysis) of whole rock sample of monomict ureilite Haverö (HAV-B).*

trapped gases. The noble gas systematics will be discussed latter in detail. This sample has cosmic ray exposure age ~30 Ma. Based on noble gas studies, Göbel *et al.* (1978) proposed two carriers of trapped gases with very distinct elemental abundance ratios present in this meteorite.

Haverö bulk sample contains 22.1 ppm of nitrogen with δ^{15}N of –4‰ along with large amount of primordial noble gases (81.4 $\times$ 10^{-8} ccSTP/g of ^{36}Ar) (see Table 3.1). The release pattern as well as isotopic composition of nitrogen and argon are depicted in

Fig 3.5. It shows two major nitrogen components with deference in $\delta^{15}N$ of more than 100‰. More than 60% of nitrogen released at temperatures $\leq 1200°C$ is isotopically heavy with maximum $\delta^{15}N$ of +54‰ and seem to be carried by combustible phase as indicated by large release at 400°C combustion step. The second nitrogen component released at >1200°C is lighter with minimum $\delta^{15}N$ of –78‰. The isotopic composition of light nitrogen seems to be obscured by co-release of small amount of heavy nitrogen. To further confirm this, nitrogen in various phases need to be analyzed. Haverö too has major noble gas release associated only with light nitrogen.

ALH81101 (A01-B)……

ALH81101 is a highly shocked monomict ureilite with cosmic ray exposure age of ~10 Ma. The stepwise temperature release pattern of nitrogen and noble gases as well as corresponding isotopic compositions are depicted in Fig 3.6. The gases are extracted in stepwise pyrolysis up to 1850°C with initial two steps of combustion at
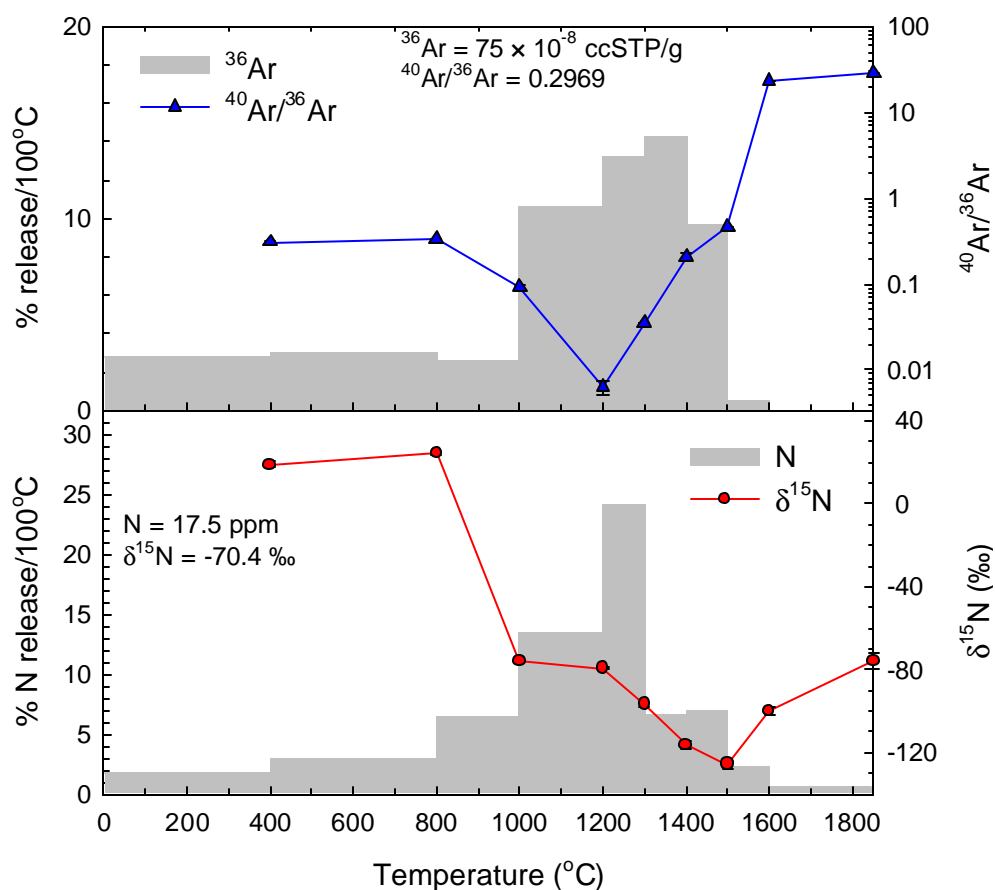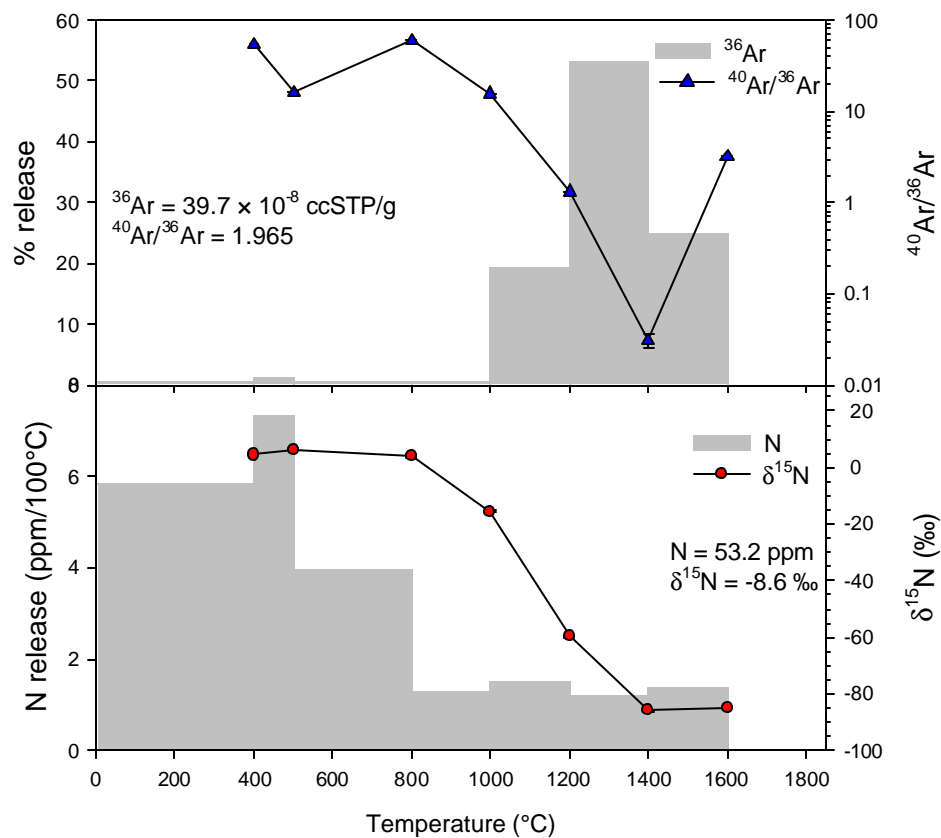

Fig 3.6 *Nitrogen and argon release patterns as well as isotopic compositions during stepped heating (pyrolysis) of whole rock sample of monomict ureilite ALH81101 (A01-B).*

400° and 500°C. The bulk sample yields 53 ppm of nitrogen with δ^{15}N of -8.6 ‰ (Table. 3.1). As in other ureilites, A01-B also shows two major nitrogen components with very distinct isotopic compositions. More than three-fourth of the total nitrogen, is released at initial three temperature steps (up to 800°C), including two combustion steps at 400° and 500°C. This nitrogen component is having δ^{15}N close to the atmospheric and is most likely due to an admixture of indigenous heavier nitrogen and adsorbed atmospheric nitrogen or due to some terrestrial weathering product formed during its Antarctic residence. A small amount (~8 ppm) of nitrogen release at higher temperatures, ≥ 1200°C is isotopically light and is accompanied by most of the primordial noble gas release and lowest value of ^{40}Ar/^{36}Ar. The lowest value of δ^{15}N observed in A01-B is -86‰.

ALH82130 (A30-B)……

ALH82130 ureilite is unusual in several respects. Its mineral compositions are significantly different from other ureilites. It is the most reduced ureilite so far identified (Berkley *et al.*, 1985) and is a low shocked ureilite. It has 2.63 wt % carbon with δ^{13}C of -9.8 ‰ PDB. The combustion analysis of this meteorite yields 129 ppm of nitrogen with δ^{15}N of -19.3‰ with minimum δ^{15}N value of -83.1‰ (4ppm) observed at 800°C (Grady and Pillinger, 1986).

The nitrogen and argon release patterns as well as isotopic composition are depicted in Fig 3.7. The bulk sample of ALH82130 yields 55 ppm of nitrogen with δ^{15}N of -10.6‰ (Table. 3.1). Nearly 80 % of the total nitrogen is released in three initial steps including two combustion steps of 400 and 500°C. A major portion of this nitrogen is most likely due to terrestrial contamination (Antarctic weathering?) (as indicated by their isotopic composition) released on the shoulder of small amount of indigenous nitrogen. A small amount (<20%) of light nitrogen is released at higher temperature steps with minimum δ^{15}N of -100‰. On combustion, light nitrogen is released at 800°C and is most likely carried by graphite-diamond intergrowth (Grady and Pillinger, 1986). As in other ureilites, discussed above, the light nitrogen in ALH82130 too is accompanied by primordial noble gases while only a minor fraction of noble gases are released along with low temperature released nitrogen. The most unusual feature of ALH82130 is its high xenon abundance as compared to argon and krypton and will be discussed in subsequent chapter.

Fig 3.7 *Nitrogen and argon release patterns as well as isotopic compositions during stepped heating (pyrolysis) of whole rock sample of monomict ureilite ALH82130 (A30-B).*

3.2.2 Nitrogen in diamond free ureilite

ALH78019 (A19-B)……

ALH78019 is a very lightly shocked, diamond free monomict ureilite. It has very low cosmic ray exposure age (0.1 Ma). This has been studied extensively for noble gas analysis and reported to contain trapped gases comparable to diamond bearing ureilites. The fine-grained amorphous type of carbon has been suggested to be the carrier of noble gases (Wacker, 1986; Ott *et al.*, 1986).

The stepwise release pattern as well as isotopic composition of nitrogen and argon for bulk sample of A19-b is shown in Fig. 3.8. This sample yields 6.3 ppm of nitrogen with $\delta^{15}N$ of -13.5‰ (Table 3.1). The heavier nitrogen ($\delta^{15}N \geq 0$ ‰) that is usually observed at low temperatures in the bulk sample measurements of all the ureilites, is not seen in A19-b. A large amount of nitrogen is released at 1000°C with $\delta^{15}N \leq -9.3$‰. The nitrogen accompanied by noble gas peak release is much heavier with
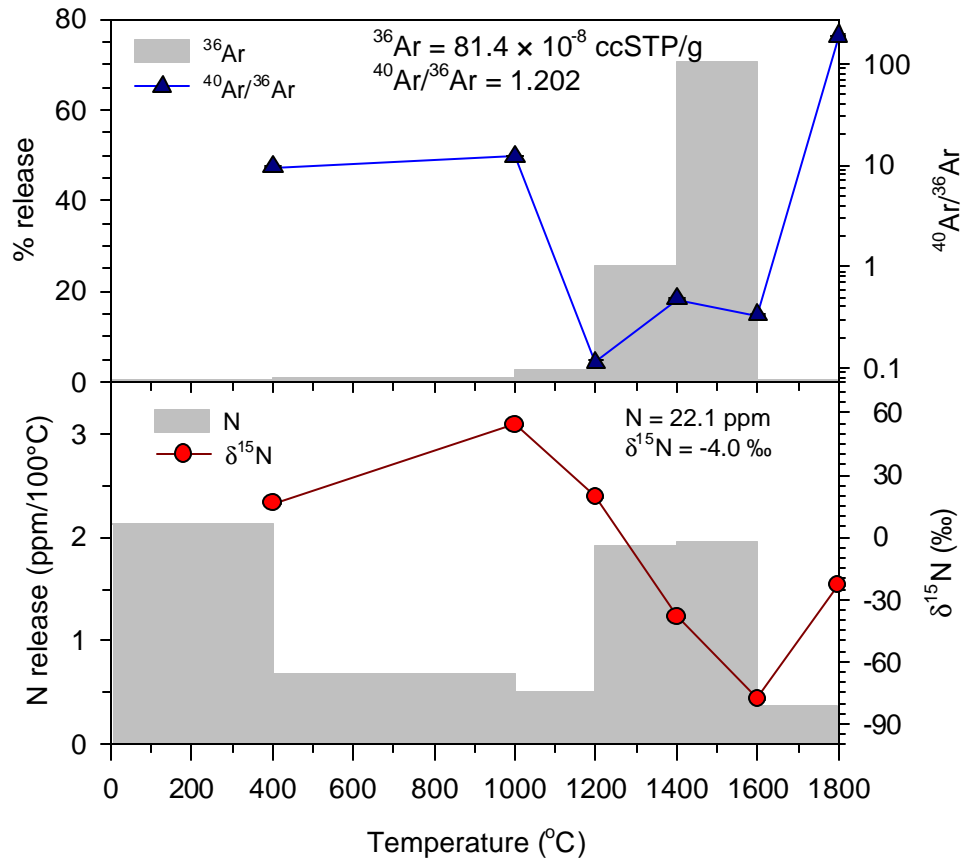
Fig 3.8 *Nitrogen and argon release patterns as well as isotopic compositions during stepped heating (pyrolysis) of whole rock sample of diamond free ureilite ALH78019 (A19-B).*

$\delta^{15}N$ of $-3.5‰$ as compared to $\leq-100‰$ for the other diamond bearing monomict ureilites. A small amount of nitrogen (0.6 ppm, <10% of total N) is released at $1600°$ and $1800°C$ and is relatively light with $\delta^{15}N$ of -47 and $-46‰$ respectively. It could be due to presence of small amount of diamonds but needs further investigation to ascertain this.

3.2.3 Nitrogen in polymict ureilites

In addition to normal ureilitic material, polymict ureilites contain some foreign clasts and mineral fragments amounting up to a few weight percent. The clasts of several types of meteorites have been identified in all the polymict ureilites (Berkley and Prinz, 1992; Warren and Kallemeyn, 1989). Nitrogen isotopic studies in bulk samples of polymict ureilites showed the presence of extremely heavy nitrogen (Grady *et al.*, 1985, Grady and Pillinger, 1988; Rooke *et al.*, 1998; Rai *et al.*, 2000). In addition to

heavy nitrogen, most of them have been shown to contain solar He and Ne in variable proportion (Ott *et al.*, 1993)

Table. 3.2: Nitrogen and Noble gases in bulk samples of polymict ureilites

Temp (°C)	N (ppm)	δ^{15}N (‰)	^{36}Ar (10^8 ccSTP/g)	^{38}Ar/^{36}Ar	^{40}Ar/^{36}Ar	^{84}Kr (10^{-10} ccSTP/g)	^{132}Xe	$P_{\Sigma(CO2+CO)}$
Nilpena -bulk, (Nil-B), 49.15mg (combustion and pyrolysis)								
300c	1.4	18.39	0.03	0.1918	212.9	-	-	2
		0.21		0.0022	0.82			
400c	4.9	26.69	0.1	0.1931	47.50	0.1	0.02	10
		0.11		0.0008	0.080			
500c	5.0	31.16	8.2	0.1950	15.08	0.7	0.4	30
		016		0.0009	0.02			
600c	3.5	0.61	13.5	0.1901	2.530	9.7	5.5	537
		0.18		0.0002	0.001			
700c	4.7	-88.97	18.7	0.1902	1.029	12.2	8.7	1050
		2.007		0.0002	0.001			
800c	3.8	-79.51	15.0	0.1890	1.257	10.4	7.4	856
		0.29		0.0001	0.001			
900c	3.7	-93.54	8.9	0.1899	4.823	8.0	5.7	605
		0.25		0.0002	0.009			
1000c	3.1	-92.36	8.9	0.1897	3.720	5.8	3.7	450
		0.21		0.0001	0.003			
1050c	1.1	-104.3	6.1	0.1896	3.087	2.4	1.3	184
		0.3		0.0001	0.005			
1200	0.7	-15.21	0.9	0.2259	21.26	0.7	0.3	
		1.21		0.0002	0.02			
1500	1.0	-69.10	1.4	0.2839	0.354	0.8	0.4	
		0.77		0.0004	0.020			

1850	0.1	-69.43	0.4	0.2943	7.156	0.4	0.4
		1.01		0.0001	0.151		
Total	32.9	-37.57	82.0	0.1931	3.934	51.2	33.4
		0.50		0.0002	0.006		

EET87720-bulk, (E20-B), pyrolysis, 71.41mg

300c	0.1	107.3	0.4	0.2274	21.97	0.1	0.1
		0.6		0.0024	0.52		
400c	5.7	118.8	0.4	0.1917	17.30	0.8	1.8
		0.4		0.0004	0.02		
500c	11.6	155.5	2.0	0.1900	11.44	1.4	5.3
		0.36		0.0001	0.01		
800	7.9	172.7	1.2	0.1936	16.12	1.2	3.3
		0.4		0.0003	0.01		
1000	3.9	194.5	3.3	0.1919	0.7901	3.1	4.8
		0.4		0.0002	0.0045		
1200	1.7	31.89	7.1	0.1946	0.2917	3.9	3.4
		0.49		0.0001	0.0009		
1400	1.7	-55.45	15.1	0.1920	0.0125	10.2	8.8
		0.39		0.0001	0.0002		
1500	0.7	-84.87	5.2	0.1911	0.0771	5.3	4.9
		0.64		0.0002	0.0008		
1600	0.6	-99.93	0.6	0.1960	7.706	0.6	0.4
		1.08		0.0002	0.034		
1850	0.2	-91.28	0.1	0.2238	31.67		
		0.85		0.0001	0.26		
Total	34.1	130.4	35.0	0.1929	1.76	26.6	32.6
		0.4		0.0001	0.01		

EET83309-bulk, (E09-B), Pyrolysis, 45.90mg

300c	0.4	69.02	0.3	0.2000	18.08	0.3	0.2
		2.86		0.0459	0.04		
400c	2.7	69.88	5.1	0.1916	0.4460	5.0	3.2
		0.46		0.0004	0.0029		
500c	2.2	66.14	22.5	0.1904	0.3759	29.5	24.7
		0.37		0.0001	0.0008		
800	1.1	49.33	7.1	0.1914	1.225	18.1	10.5
		0.78		0.0001	0.002		
1000	1.3	107.3	15.5	0.1928	0.5186	42.5	18.1
		0.4		0.0001	0.0015		
1200	1.1	49.39	33.6	0.1945	0.0794	64.4	40.8
		0.67		0.0001	0.0005		
1400	1.5	-9.31	40.6	0.1964	0.2044	82.1	83.8
		0.50		0.0001	0.0002		
1600	0.7	-6.33	12.9	0.2093	0.4463	31.4	45.6
		0.52		0.0001	0.0023		
1850		-	0.1	0.2237	15.15	0.1	0.1
				0.0017	0.23		
Total	10.8	54.05	137.7	0.1954	0.3724	273.3	226.8
		0.58		0.0002	0.0011		

EET87720 (E20-B)……

The release pattern as well as isotopic composition of nitrogen and argon is shown in Fig 3.9. The gases are extracted by combustion at 2 torr oxygen pressure in the initial three temperature steps up to 500℃ and latter by stepwise pyrolysis up to 1850℃. The sample E20-B yields 34.1 ppm of nitrogen with bulk $\delta^{15}N$ of 130‰. Like monomict ureilites, E20-B also exhibits two isotopically very distinct major nitrogen components. The nitrogen released at low temperature is highly enriched in ^{15}N up to 195‰ or more (at 1000℃), and not accompanied by much of the noble gas release
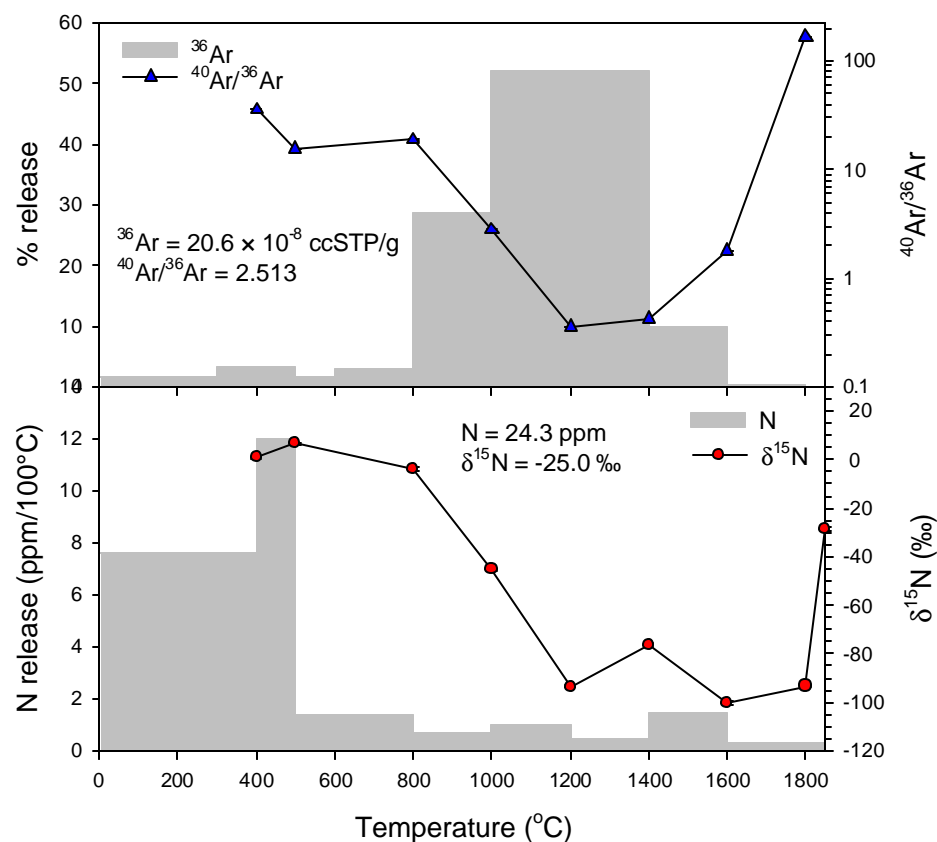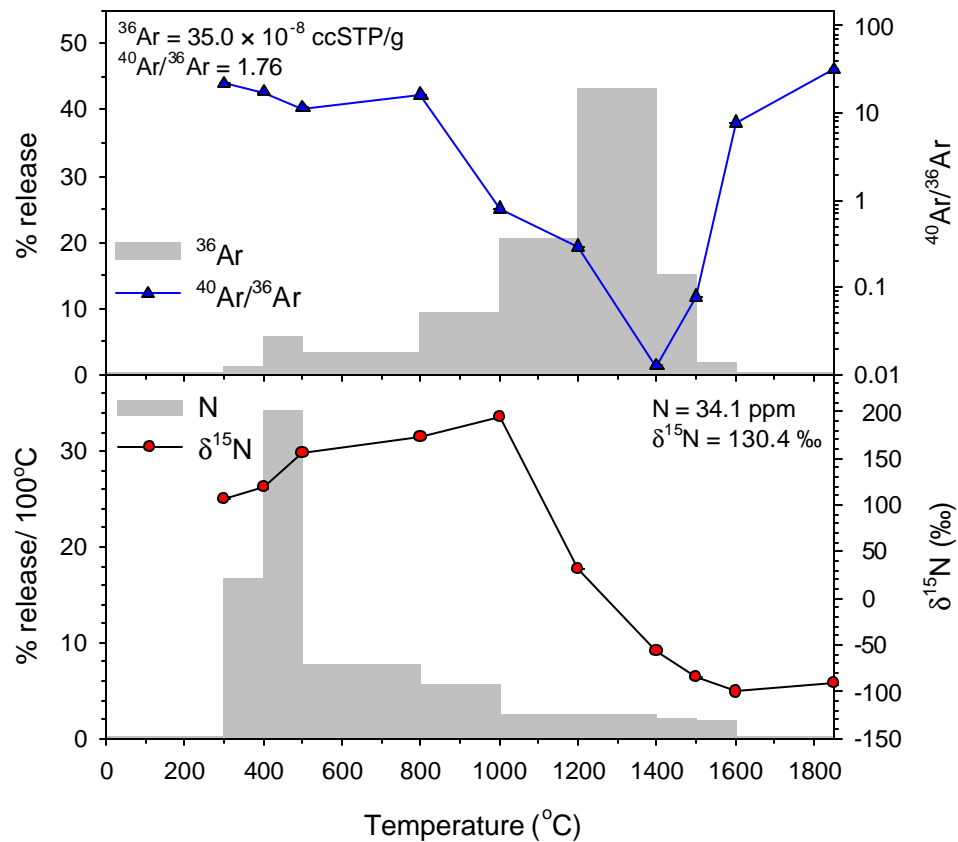
Fig 3.9 *Nitrogen and argon release patterns as well as isotopic compositions during stepped heating (pyrolysis) of whole rock sample of polymict urelite EET87720 (E20-B).*

(Table 3.2). The δ^{15}N starts from 107‰ at 300°C, reaching peak value of 195‰ at 1000°C, while the peak nitrogen release is observed only at 500°C. This could be because of mixing of two nitrogen components: the first one is isotopically normal (δ^{15}N ~20‰, present in all the monomict ureilites) with decreasing amounts released at higher temperatures than that of the second component with isotopic composition of $\geq$195‰. Another nitrogen component released at higher temperature ($\geq$1200°C) is isotopically lighter with δ^{15}N value of $\leq$-100‰. Release of this nitrogen component is accompanied by primordial noble gas release. More than 50% of the total nitrogen released between the two temperature steps of 400° and 500°C on combustion indicating that the heavy nitrogen resides in highly combustible phase. Earlier measurement of nitrogen from the in EET87720 also revealed the presence of heavy nitrogen but the observed enrichment of ^{15}N was only up to 75‰, released at temperature $\leq$550°C on combustion (Rooke *et al.*, 1998).
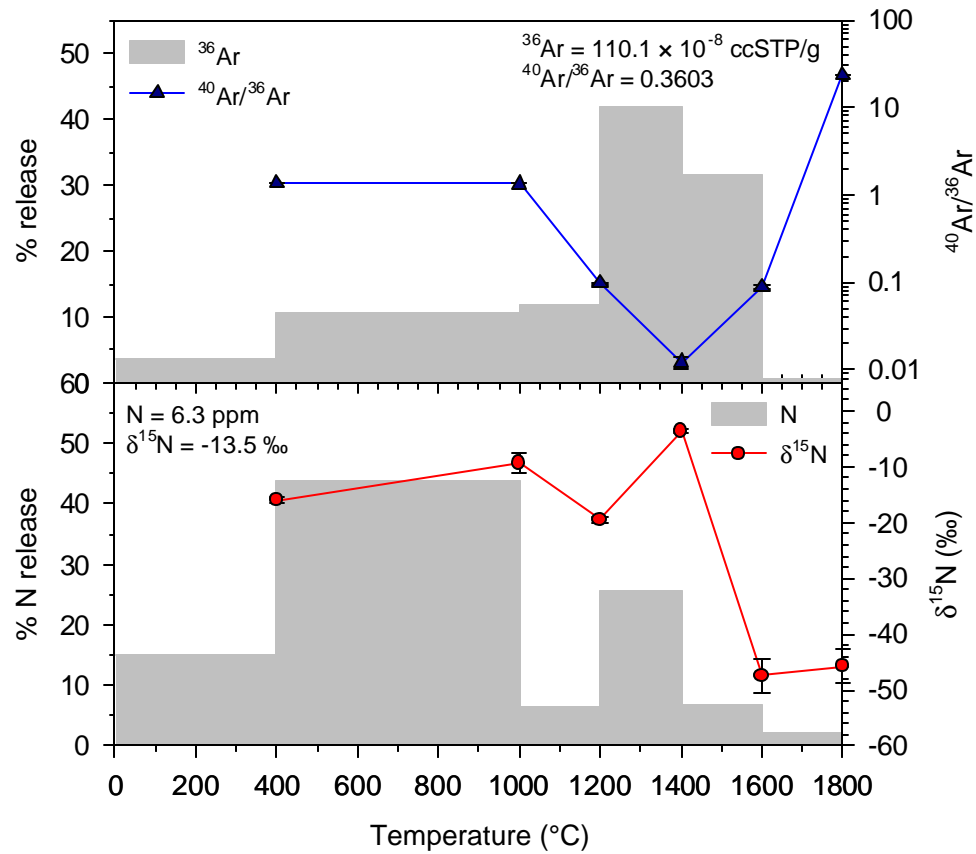
Nilpena (NIL-B)......
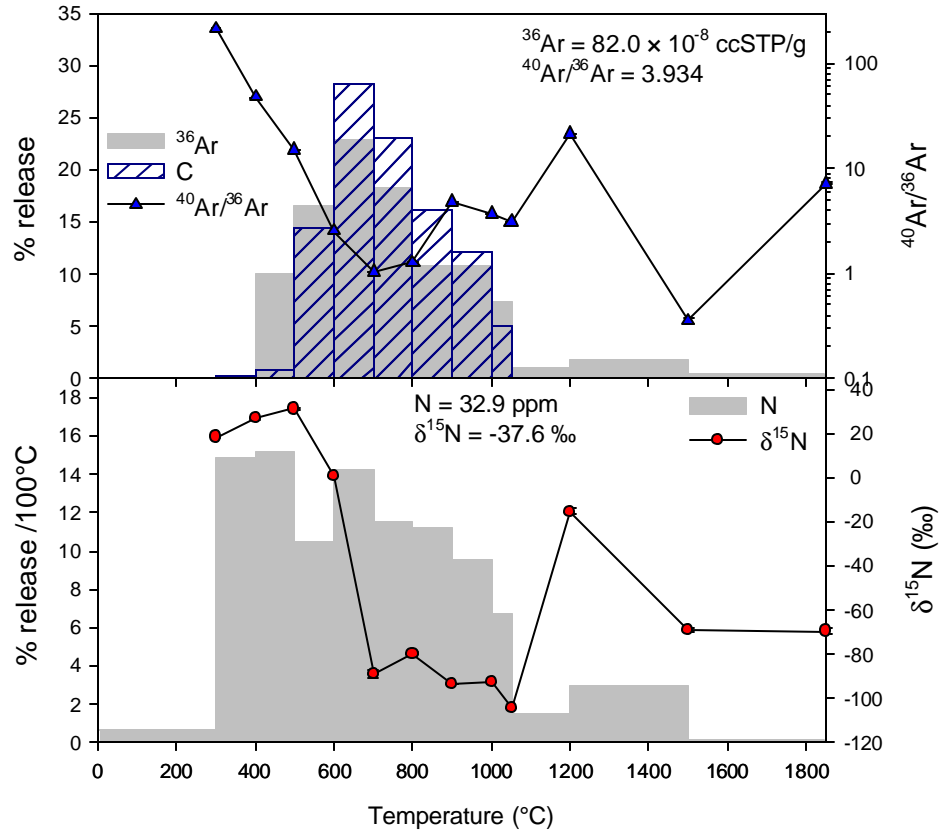
Fig 3.10 *Nitrogen and argon release patterns as well as isotopic compositions during stepped heating (pyrolysis) of whole rock sample of polymict ureilite Nilpena (NIL-B).*

Nilpena is a polymict breccia with cosmic ray exposure age of 9.7 Ma. It contains large amount of noble gases similar to that of other monomict and polymict ureilites. Earlier nitrogen study showed the presence of heavy nitrogen with $\delta^{15}N$ up to 153‰ (Grady and Pillinger, 1988).

The release pattern as well as isotopic composition of nitrogen and argon is shown in Fig 3.10. The gases were extracted by combustion at 2 torr oxygen pressure up to 1050°C and latter by pyrolysis at 1200, 1500 and 1850°C. The bulk Nilpena yields 32 ppm of nitrogen with $\delta^{15}N$ of –38‰. Like other ureilites, Nilpena also shows two nitrogen components. The nitrogen released at lower temperature is isotopically heavy with maximum $\delta^{15}N$ of 31‰ at 500°C. A light nitrogen is released at temperatures between 700°-1050°C with $\delta^{15}N \leq$-104‰. The bulk $\delta^{15}N$ measured here, is much lighter than that reported earlier, that is +32‰ (Grady and Pillinger, 1988). This discrepancy could most likely be due to heterogeneous distribution of heavy nitrogen carrier in Nilpena.

EET83309 (E09-B)……

The bulk sample of EET83309 (E09-B) yields 10.8 ppm of nitrogen with $\delta^{15}N$ of 54‰. (Fig 3.11). The maximum $\delta^{15}N$ is observed at 1000°C and is immediately followed by relatively light nitrogen with $\delta^{15}N$ of –9‰ (the lightest nitrogen observed
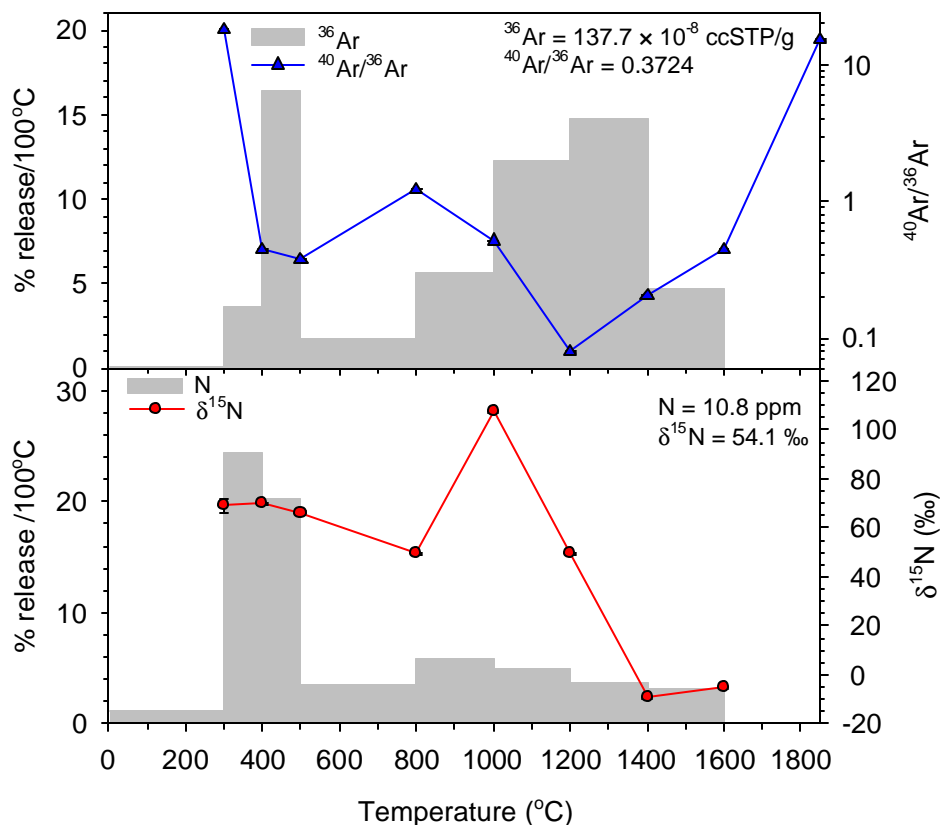
Fig 3.11 *Nitrogen and argon release patterns as well as isotopic compositions during stepped heating (pyrolysis) of whole rock sample of polymict ureilite EET83309 (E09-B).*

for this ureilite). Large amount of relatively heavy nitrogen is released at 400°C and 500°C combustion steps indicating that the carrier of heavy nitrogen in E09-B is also a combustible phase. The carrier of the heavy nitrogen in E09-B contains large amount of noble gases unlike their counterparts in other ureilites. The light nitrogen with $\delta^{15}N$ of ~-100‰ is not observed for this ureilite. The other peak of noble gases is observed at 1400°C and is accompanied by relatively lighter nitrogen. Further investigation is needed to ascertain the carrier of this light nitrogen.

3.3 Discussion

3.3.1 General release patterns of nitrogen and Noble gases

Excluding ALH78019 and EET83309 (will be discussed separately), rest of the monomict and polymict ureilites seem to have two major nitrogen components. At least three other minor nitrogen components are required to explain isotopic trends in all the bulk samples of ureilites. The nitrogen released at higher temperatures ≥1400°C on pyrolysis and between 600°C-900°C on combustion, is isotopically light with $\delta^{15}N$ of ≤-100‰, and is present ubiquitously in both monomict and polymict ureilites. The lowest value of $\delta^{15}N$ observed is −126‰ for Kenna and this is the lowest value observed for any bulk samples of ureilites so far. Though the light nitrogen seems to be present in all these ureilites (except ALH78019 and EET83309), sometimes, it is not resolved completely due to mixing with the other major nitrogen component present in all the ureilites, and is relatively heavy. The heavy nitrogen component shows large variations in isotopic composition with $\delta^{15}N$ varying from 5‰ to nearly 200‰ (for E20-B). Irrespective of 'find' or 'fall' a nitrogen component with $\delta^{15}N$ of 5‰ to 30‰ is always present in all the monomict ureilites in significant amount and therefore may not be attributed solely to terrestrial contamination, though a substantial contribution of atmospheric gases that affect the measured isotopic composition, cannot be ruled out. In some monomict ureilites, the highest $\delta^{15}N$ values of heavy nitrogen reach more than 50‰ e.g., Haverö, LEW85328 (96‰) (present work), ALH77257 and Asuka881931 (Yamamoto *et al.*, 1998). The heavy nitrogen present in polymict ureilites is, in general, heavier than that in monomict ureilites. ^{15}N enrichment up to 540‰ has been reported for EET83309 (Grady and Pillinger 1988). However, this study reveals $\delta^{15}N$ only up to 107‰ for the same meteorite. But in the case of EET87720, the maximum $\delta^{15}N$ observed in this study is 196‰, much heavier than 75‰, reported by Rooke *et al.* (1998a and b).

In ALH78019 and EET83309, the release patterns as well as trends in isotopic compositions are distinctly different from other ureilites. Unlike other ureilites, in A19-B, no heavy nitrogen is observed at lower temperatures and also only, a minor amount of nitrogen is released at 1600°C and above, which is not as light as observed for other monomict ureilites though the noble gas release patterns are similar to the others. Though the noble gas release pattern does not show much difference on

pyrolysis between this and other ureilites, on combustion this difference is quite significant. On combustion, most of the noble gases were released at lower temperatures than that of diamond bearing ureilites. This indicates that the carrier is some highly combustible phase (Ott *et al.*, 1986). It could either be a very fine-grained diamond or amorphous carbon because both presolar nano-diamonds and amorphous carbon (ill defined carbonaceous phase) are shown to combust at lower temperatures (Frick and Pepin, 1981; Schelhaas *et al.*, 1990). Though the latter was suggested by Wacker (1986) as a carrier of noble gases in ALH78019, the former is more favorable due to the presence of small amount of light nitrogen at higher temperature steps, provided the light nitrogen is assumed to be the indicator for presence of diamonds. But the presence of light nitrogen does not rule out the possibility that the amorphous carbon is not the carrier of trapped gases because the nitrogen composition of amorphous carbon is not, a priory, known. To further understand this the study of trapped gases in various chemically separated phases are required.

The release pattern for the bulk sample of EET83309 is also quite different than shown by other ureilites in two respects: firstly, the heavy nitrogen that is released largely at initial two combustion temperature steps, is accompanied by primordial noble gases (in other cases, not much of the noble gases are accompanied by heavy nitrogen), secondly the light nitrogen with $\delta^{15}N$ of $\leq$-100‰ is not seen though a dip in $\delta^{15}N$ is observed at 1400°C. It seems that the small amount of light nitrogen is released on the shoulder of heavy nitrogen and the true signature of nitrogen is obscured due to admixture of heavy and light nitrogen.

3.3.2 Number of nitrogen components

In addition to the two major nitrogen components (light and heavy nitrogen) discussed above, three other minor nitrogen components are required to explain the observed isotopic trends. The third component, released predominantly at lower temperatures with $\delta^{15}N$ close to 0‰, is most likely the adsorbed atmospheric component as it is accompanied by argon with high $^{40}Ar/^{36}Ar$ ratio (~295). The fourth nitrogen component is a minor one, but needed to explain the excursion in $\delta^{15}N$ and $^{40}Ar/^{36}Ar$ at higher temperatures. Superimposed on these N components, some times spallation nitrogen is seen (in case of ureilites with high cosmic ray exposure age) as excursion

in $\delta^{15}N$, as they are accompanied by cosmogenic noble gas components specifically observed in cases of light noble gases (^{21}Ne and ^{38}Ar).

3.3.3 Identification of carriers

Based on extensive noble gases analysis it has been argued that the carrier of primordail noble gases are diamonds that release their gases at very high temperature (Gobel et al., 1978). In the present study as well as in the earlier studies, it has been shown that light nitrogen is always accompanied by release of primordial noble gases. Based on these, it can be inferred that the carrier of light nitrogen is diamond. Though Göbel et al. (1978) showed that the graphite in ureilites is almost free of noble gases, it is not clear from the study of bulk ureilites whether it contains some nitrogen, which needs further investigations. The heavy nitrogen on the other hand resides in highly combustible phase as inferred from the large release at low temperature combustion steps. This phase is most likely a fine grained amorphous carbon as proposed for the carrier of noble gases in diamond free ureilite ALH78019 (Ott et al 1986 ; Wacker 1986). The major difference between amorphous carbon carriers in diamond free ureilite and from diamond bearing ureilites is that the former contains large amount of noble gases while the latter is depleted in them. To understand the relation between these two amorphous carriers further analysis in separated phases is needed.

3.3.4 Heterogeneity in carrier distribution

A close look on the noble gas data from earlier measurement of two aliquots of the same ureilite measured in the same laboratory as well as in different laboratories showed substantial variations in gas contents (Wilkening and Marti, 1976; Göbel *et al.*, 1978; Weber *et al.*, 1976; Bogard *et al.,* 1973; Vdovykin 1976). The repeat analysis of two aliquots of the same ureilite in this study showed the variations in nitrogen contents as well as bulk isotopic compositions and noble gas contents though their general release patterns are more or less similar. Also, the maximum and minimum values of $\delta^{15}N$ measured vary substantially between the two aliquots. The similar variations in the repeat analysis have also been observed in the data from the literature (Grady *et al.*, 1985; Grady and Pillinger, 1987 & 1988; Rooke *et al.*, 1998; Yamamoto *et al.*, 1998) and this is beyond the analytical uncertainty and most likely to be the intrinsic nature of ureilites. To explain the variation in maximum $\delta^{15}N$ of heavy nitrogen, two alternatives could be possible. Heavy nitrogen with homogeneous

Table 3.3 Summary of the results of nitrogen study on bulk ureilites.

Sample	$N_2/^{36}Ar$	N (ppm)	$d^{15}N$ (‰) total	max.	min.	Type
L28-B1	5057	15.4	-40.2	96.0	-117.6	Monomict
L28-B2	6658	20.1	-10.0	27.8	-98.8	'
KNA-B	18667	17.5	-70.4	24.5	-117.0	'
HAV-B	21720	22.1	-4.4	54.3	-77.8	'
A01-B	107204	53.2	-8.6	6.4	-85.9	"
A30-B	213204	54.9	-10.7	6.7	-100.3	"
LAH-B	54023	52.2	-2.3	13.0	-32.2	'
A19-B	4578	6.3	-13.5	-3.5	-47.5	Diamond free
E09-B	15985	10.8	54.1	107.3	-9.3	Polymict
E20-B	77943	34.1	130.4	194.5	-99.9	"
Nil-B	32098	32.9	-37.6	31.2	-104.3	'

isotopic composition (extremely heavy $\geq 540‰$) is present and distributed heterogeneously within ureilite parent body on centimeter scale. The other alternative is the isotopic composition of heavy nitrogen itself is heterogeneous *i.e.*, the mechanism by which, the heavy nitrogen is formed itself fractionate nitrogen to variable extent. Any one of the above or the combination of both might be responsible for the variable composition of heavy nitrogen component. The light nitrogen on the other hand, shows comparatively narrow range of variations. Variable proportion of the carriers of heavy nitrogen, light nitrogen and other components that might be present in silicates and metals *etc.* (most probably gas poor) as well as heterogeneous distribution of gases between these phases, might be responsible for the observed variations in content as well as isotopic composition of nitrogen and noble gases.

3.4 Summary

Table 3.3 summarizes the results of nitrogen study of bulk ureilites. At least two major nitrogen components are present in bulk samples of both monomict and polymict ureilites. The one released at temperature higher than 1400°C, is light with $\delta^{15}N \leq -100‰$ (accompanied by primordial noble gases). The other one is heavier with highly variable $\delta^{15}N$, and is released at a temperature at least 200°C lower than the light nitrogen, and could be a mixture of indigenous heavy nitrogen and cosmogenic nitrogen. Both light and heavy nitrogen (noble gases as well) are heterogeneously distributed within ureilites. To constraint the carriers of these two nitrogen components, separated phases need to be analyzed.

Nitrogen in Acid Residues of Ureilites

4.1 Introduction

It has been shown in the previous chapter (Chapter 3) that the bulk samples of both monomict and polymict ureilites, in general, contain two major nitrogen components. One of them is a light nitrogen component having $\delta^{15}N$ in the range of $-100‰$ to $-130‰$ and released at temperature $\geq 1400°C$. The second major nitrogen component is released at lower temperatures of $\leq 1400°C$ on pyrolysis and $\leq 500°C$ on combustion is having variable nitrogen composition between $20‰$ to $196‰$. Whether the variations in $\delta^{15}N$ of heavy nitrogen released at lower temperatures is due to an admixture of two or more nitrogen components (two end members) or is produced by a processes like fractional loss from single uniform reservoir with uniform nitrogen composition, is not yet clear and requires further investigations. Superimposed on this, two or three minor N components are required to explain the isotopic trends. In order to understand the exact nature and behavior of these carriers of heavy and light nitrogen components and their relationship if any, with the primordial noble gases, simultaneous study of nitrogen and noble gases in various chemically separated phases of ureilites has been planned. The details of chemical treatment for preparation of residues have been discussed in Chapter 2. Since the residues are mostly carbon (either graphite or diamond) combustion in presence of oxygen has been used to extract the trapped gases in these samples. To further understand the nature of the carriers of heavy and light nitrogen, a few selected samples have also been pyrolyzed. One of the advantages of acid resistant residue is that the gases released from them are free from spallation component except in He (due to absence of target elements). The removal of silicates, metals and sulfides by acid dissolution most likely make the release trends of nitrogen and noble gases less complex as compared to bulk samples.

Within the SEM panels, the following labels and instrument readings appear:

a: Haverö -A
EHT=20.00 kV WD= 26 mm Mag= 2.35 K X
10µm Photo No.=4408 Detector= SE1

b: ALH81101 -A
EHT=20.00 kV WD= 32 mm Mag= 4.30 K X
3µm Photo No.=4386 Detector= SE1

c: ALH81101 -O1
EHT=20.00 kV WD= 33 mm Mag= 757 X
30µm Photo No.=4388 Detector= SE1

d: ALH81101 -O2
EHT=20.00 kV WD= 33 mm Mag= 4.46 K X
3µm Photo No.=4390 Detector= SE1

e: ALH81101 -O3
EHT=20.00 kV WD= 33 mm Mag= 1.64 K X
3µm Photo No.=4391 Detector= SE1

f: ALH81101 -O4
EHT=20.00 kV WD= 33 mm Mag= 1.64 K X
3µm Photo No.=4391 Detector= SE1

Fig 4.1 (a,b,c,d,e,f) *SEM photomicrographs of acid resistant residues (HF-HCl) and oxidized residues (HF-HCl-HClO$_4$) of Haverö and ALH81101 (both monomict ureilites).*
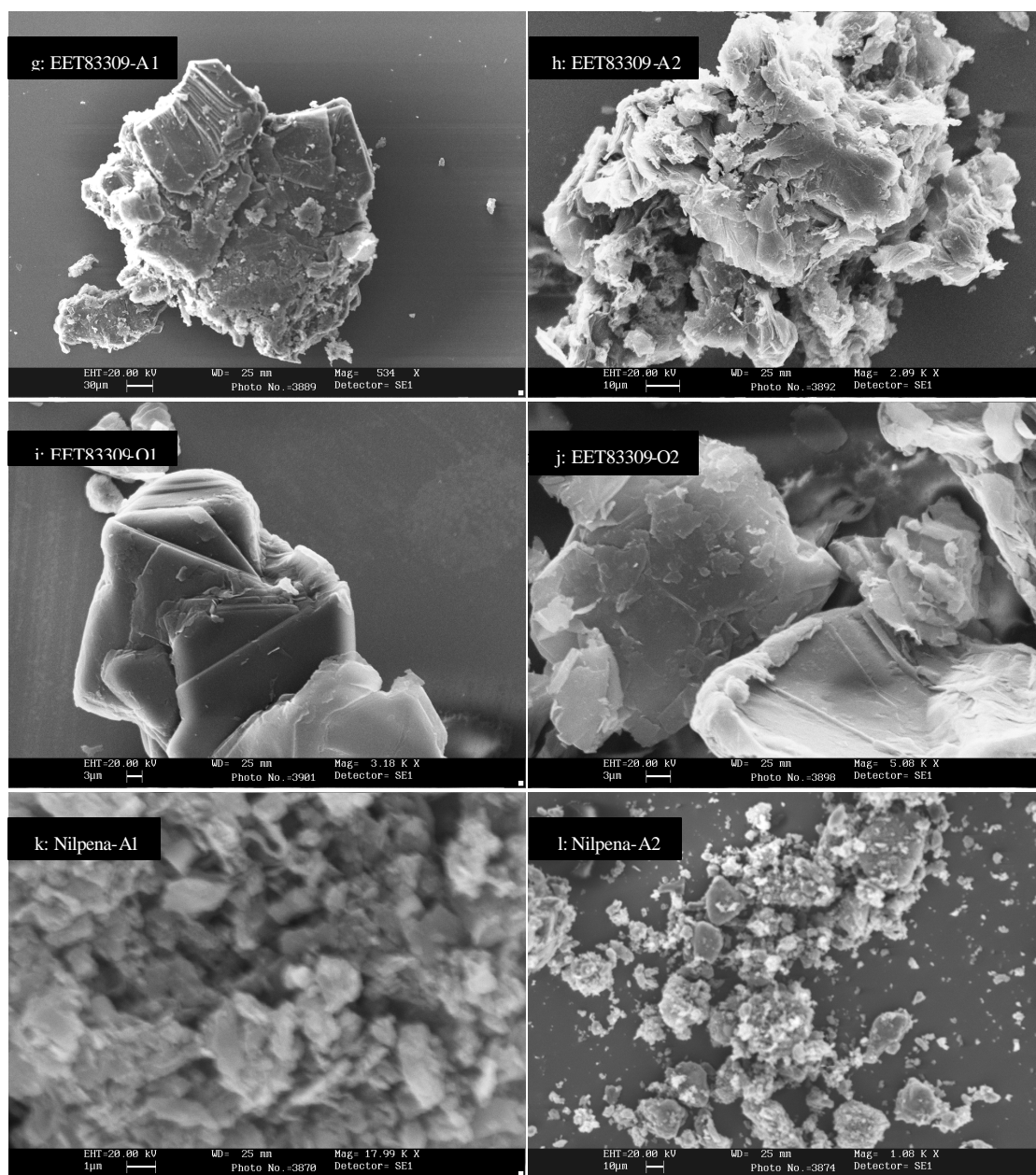
Fig 4.1(g,h,I,j,k,l) *(contd.) SEM photomicrographs of acid resistant residues (HF-HCl)
and oxidized residues (HF-HCl-HClO₄) of EET83309 and Nilpena (both polymict
ureilites).*
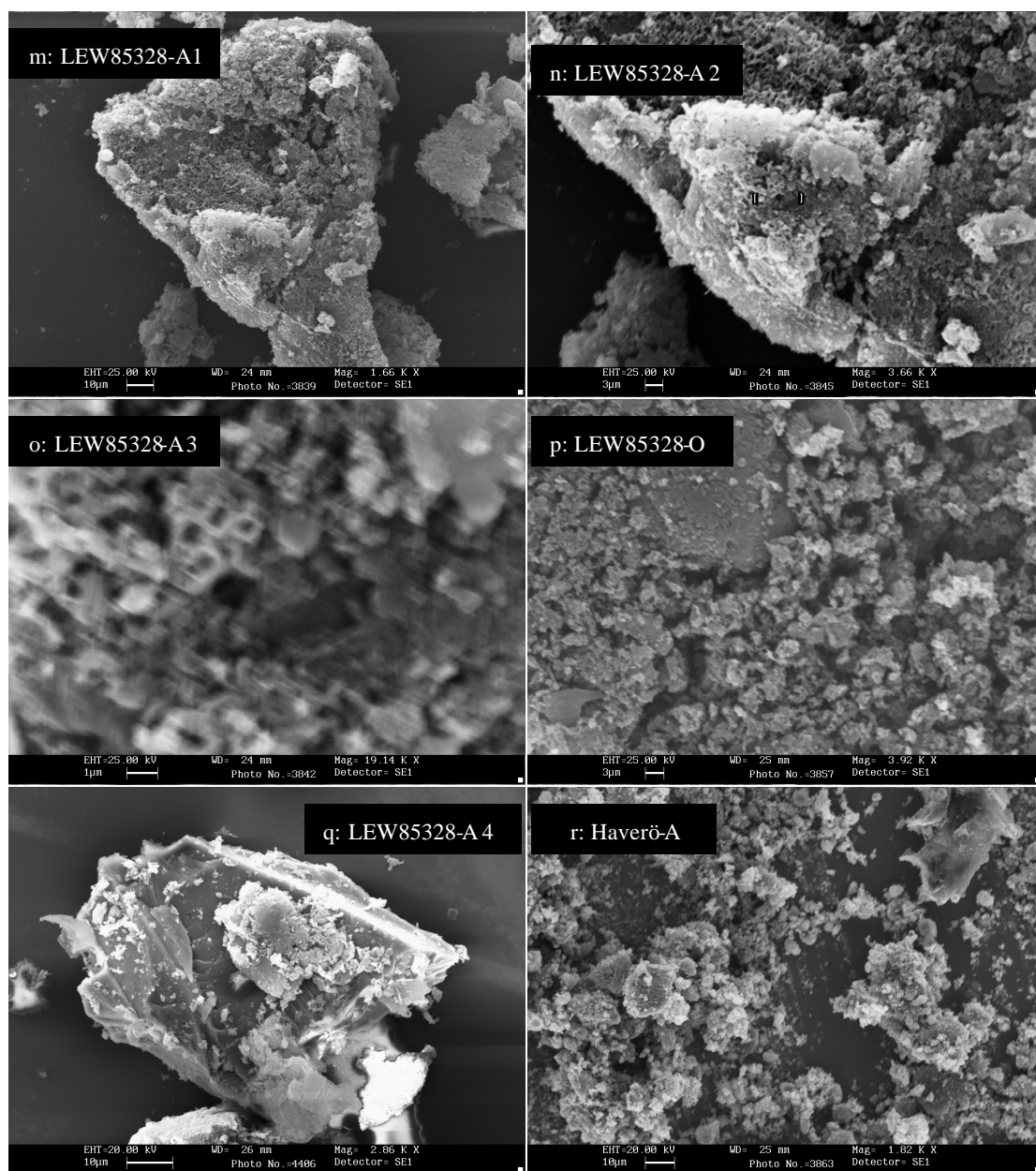
Fig 4.1 *(m,n,o,p,q,r) (contd.) SEM photomicrographs of acid resistant residues (HF-HCl) and oxidized residues (HF-HCl-HClO$_4$) of LEW85328 and HF-H$_2$SO$_4$ residue of Haverö (both monomict ureilites).*
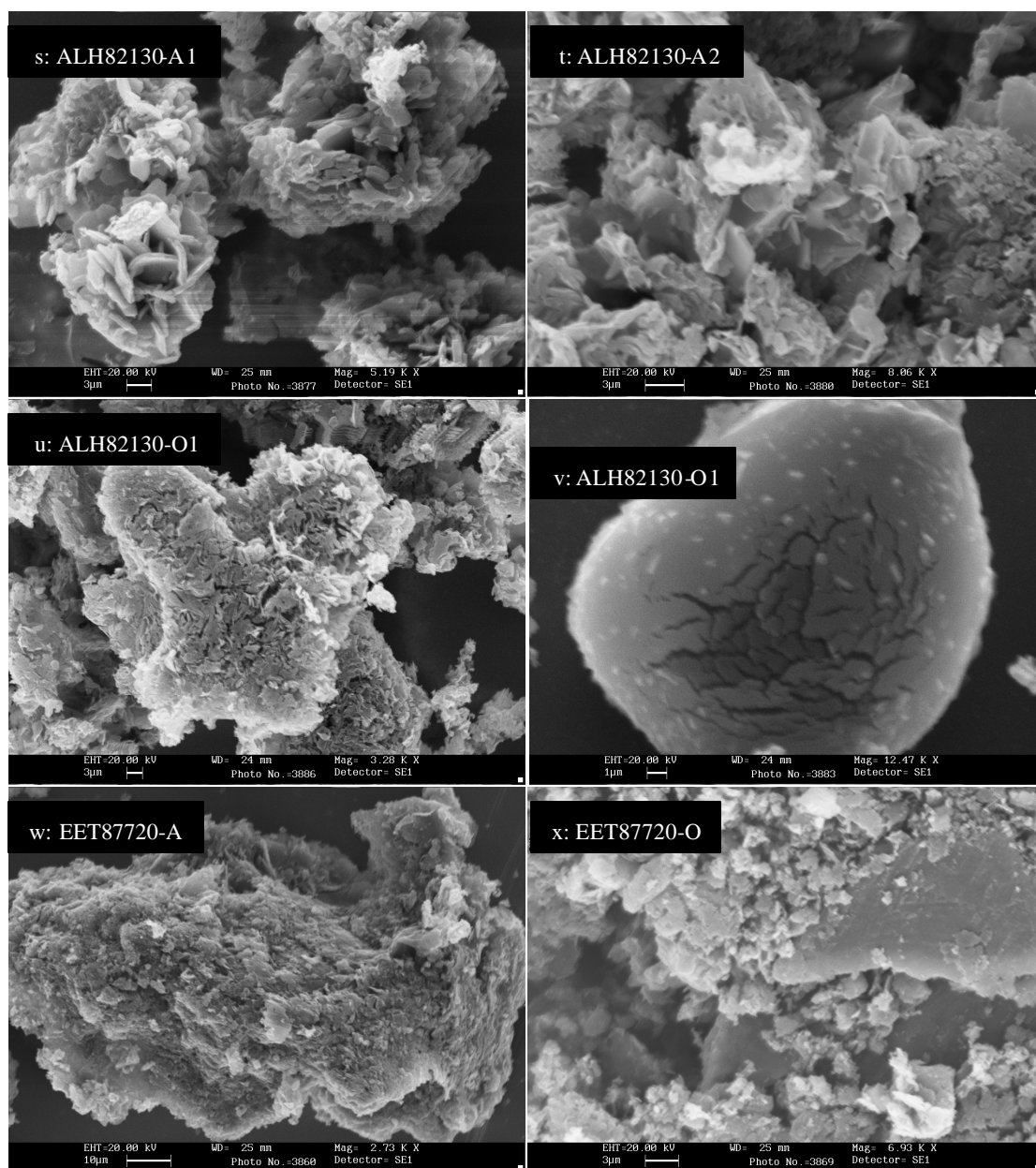
Fig 4.1 (s,t,u,v,w,x) *(contd.) SEM photomicrographs of acid resistant residues (HF-HCl) and oxidized residues (HF-HCl-HClO₄) residues of ALH82130 (monomict ureilite) and EET87720 (Polymict ureilite).*
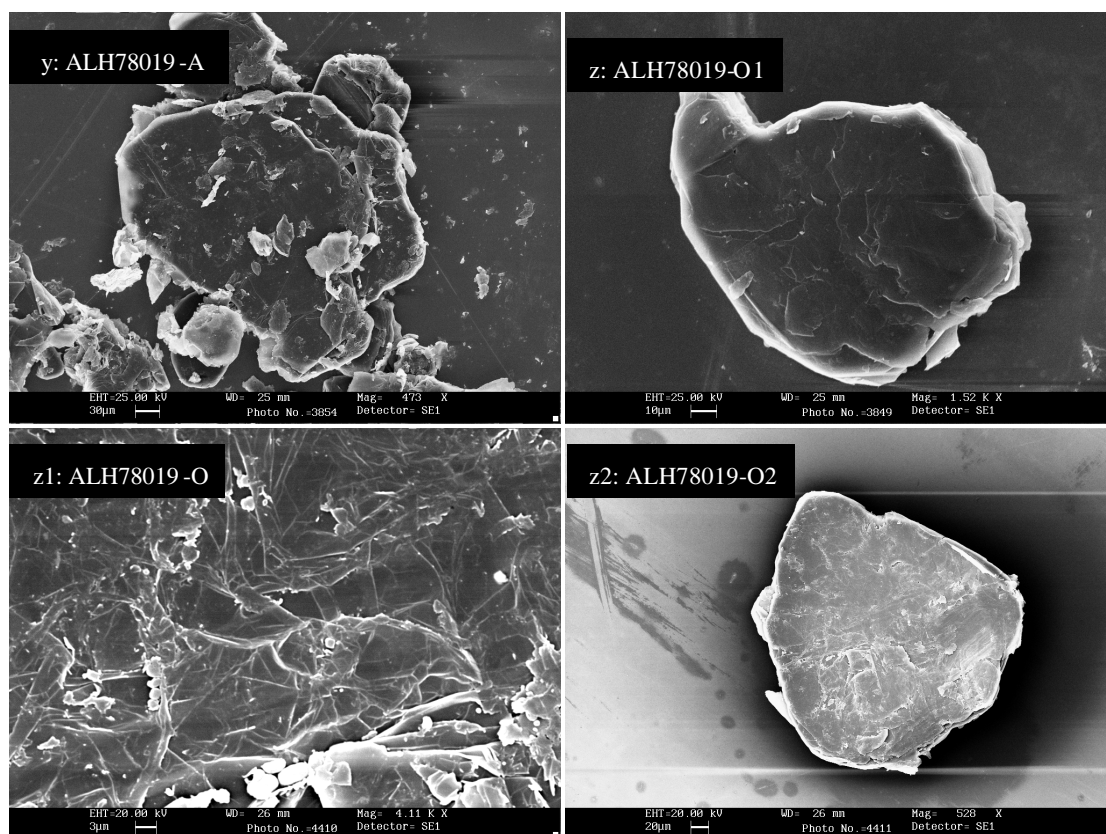
Fig 4.1(y, z, z1, z2) *(contd.) SEM photomicrographs of acid resistant residues (HF-HCl) and oxidized residues (HF-HCl-HClO$_4$) of ALH78019 (diamond free ureilites).*

Table 4.1 Chemical composition of bulk sample as well as acid residues of a few selected ureilites determined by INAA.

Elements	ALH78019		Haverö		LEW85328			EET87720			Nilpena		Blank
	Bulk	HClO$_4$	Bulk	HF-HCl	Bulk	HF-HCl	HClO$_4$	Bulk	HF-HCl	HClO$_4$	Bulk	HF-HCl	Al foil
Ir (ng/g)	53.9	101	19.2	1403	66.7	548	412	72.6	1184	147	285	2779	
Os(ng/g)			142			400			656	321	654	268	
Fe (%)	14.2	0.09	15.9	9.11	13.5	1.57	2.68	14.1	1.68	1.92	13.9	3.79	
Ni (µg/g)	566	366	926	5775	1300	684	662	1845	849	924	3027	1478	7.39
Co	80	1.6	97.5	6917	93.2	21.9	50.0	119	35.7	39.8	227	186	0.01
Cr	4003	108	4413	8143	4321	2444	1461	4820	784	759	4927	14019	0.28
Au	487	25439	1103	6321	255	13328	3158	729	17890	15960	397	6101	
Ag	186	8192	235	3632	112	3986	1939	106	6342	3736	137	2885	63
Zn	388	102	216	154	323	65.1	45.6	138	58.8	72.7	326	236	0.59
Ta	0.19			549						5.52	13.9		
Sc	5.78	10.8	5.10	4.43	8.70	4.71	3.02	7.22	8.39	6.39	9.92	4.58	0.09
Ce	1.18	40.00	2.01	14.20	0.88	17.4	10.5	1.13	32.3	20.8	3.12	18.3	0.33
Eu											0.09		
Gd		4.30				2.27							
Tb		0.73				0.25			0.41	0.41		0.35	
Yb									1.91	1.91	0.26		
Lu		1.47				0.67			0.66	0.66			0.01

Note: The values reported here are having statistical error of <10%

Out of the ten bulk samples analyzed for nitrogen and noble gases, acid resistant residues have been prepared for eight of them (Haverö, LEW85328, ALH81101, ALH82130, ALH78019, EET83309, EET87720 & Nilpena) by dissolving a few hundred mg of bulk samples in concentrated HF-HCl. Seven of these (all HF-HCl residues except Nilpena) acid resistant residues have been further treated with perchloric acid ($HClO_4$), to obtain oxidized residues. $HClO_4$ treatment is supposed to remove amorphous carbon and graphite (if it is fine grained) and leave the residue enriched in diamonds. The morphological features of acid resistant residues are shown in SEM photomicrographs (Fig 4.1).

4.2 Results

We have attempted to characterize the acid residue by physical (SEM) and chemical (INAA) studies. These results will be summarized before discussing the isotopic systematics of nitrogen and noble gases in them.

4.2.1. Physical and chemical characterization of acid residues

A. Physical characterization: Morphology of acid resistant residues

The SEM (Scanning Electron Microscope) pictures of acid resistant residues and oxidized residues of all the ureilites analyzed for noble gases and nitrogen, are taken by LEO440*i* with 25KV and 20KV EHT and are shown in Fig 4.1. In all the acid residues but one, no clear diamonds crystals are seen even with resolutions of micron level. This indicates that in most of the cases diamonds are less than a micron in size. Clear crystal structure is only seen for the HF-HCl residue of LEW85328 (LEW85328-A1 of Fig 4.22). The graphite seems to be dominated in all the residues and recognized easily by their platy structures (EET83309-A1 and O1, ALH78019-O1 and others). In some cases the graphite plates are deformed and the reason is most likely the shock stress which most of the ureilites suffered in their parent body(ies) (most clearly seen in EET83309-O1). The most striking features of acid resistant residues are their rough surfaces that became clean and smooth after perchloric acid treatment (see ALH81101-A, ALH81101-O1). The diamonds are most probably intergrown with graphite and the rough surface seen over graphite are the amorphous layer of carbon, which is removed almost completely by perchloric acid treatment. The coarse grained graphite flakes are clearly seen in most of the oxidized residues indicating that the graphite is only partially removed (unaffecting the coarse grained

graphite) by perchloric acid treatment though the etching effect of acid on the surface is clearly visible (EET83309-O1, ALH81101-O1, ALH78019-O1,O2 & O3). In addition to these carbonaceous phases, two very strange grains are seen in ALH81101 and ALH82130. In Fig ALH81101-O4, silicon (inferred from X-ray spectrum) rich very smooth and shiny grains are seen whose survival is difficult to understand after acid treatment. The second one is having spherule like structure with smooth surface (ALH82130-O1) with inter connected cracks and seemed to be an igneous product. It is also enriched in Si, Ca, Na and K. Its survival through acid dissolution is also puzzling.

B. Chemical characterization: INAA analysis

A few selected bulk samples as well as their acid residues have been analyzed for trace element composition by INAA (Instrumental Neutron Activation Analysis). Because of smaller sample sizes, only a few elements could be measured with good precision. The data are reported in Table 4.1 and plotted in Fig 4.2a and Fig 4.2b. In Fig 4.2a, the relative abundances of various elements with respect to bulk samples normalized to Fe (Iron) are plotted for the five ureilites. In Fig 4.2b, the same data sets are plotted in a different manner where the abundance of elements in both bulk and residues are normalized to solar abundance that is close to CI abundance (Anders and Grevesse, 1989). In both the figures, elements are divided into two sub groups of refractory and siderophile and are plotted in order of increasing volatility in both the groups. The abundance distribution of the elements in carbon rich acid residue shows two main features; the enrichment of refractory elements (Lu, Sc, Ir, Tb, Gd, Ce and Ta) by factors of 10 to 1000 and the high enrichment of Cr Au and Ag (again by the two to three orders of magnitude (Fig 4.2a).

Refractory Elements: The earlier measurement of siderophile trace elements in bulk samples as well as carbon rich vein materials from several ureilites are reported by Goodrich 1992; Boynton *et al.*, 1976; Goodrich *et al.*, 1987; Higuchi *et al.*, 1976; Janssens *et al.*, 1987; Spitz, 1992; Spitz and Boynton, 1991; Wänke *et al.*, 1972; Warren and Kallemeyn, 1989; Wasson *et al.*, 1976. Within each ureilite abundances of refractory siderophiles, Re, Os, W and Ir are similar, and range from $\sim 0.1\text{-}2.2 \times$ CI values. Abundances of more volatile siderophiles, Ni, Au, Ga, Co, and Ge, are lower, ranging from $\sim 0.07\text{-}0.7 \times$ CI values. These siderophile elements are high in comparison to ultramafic rocks from other differentiated planets, for example, Earth,
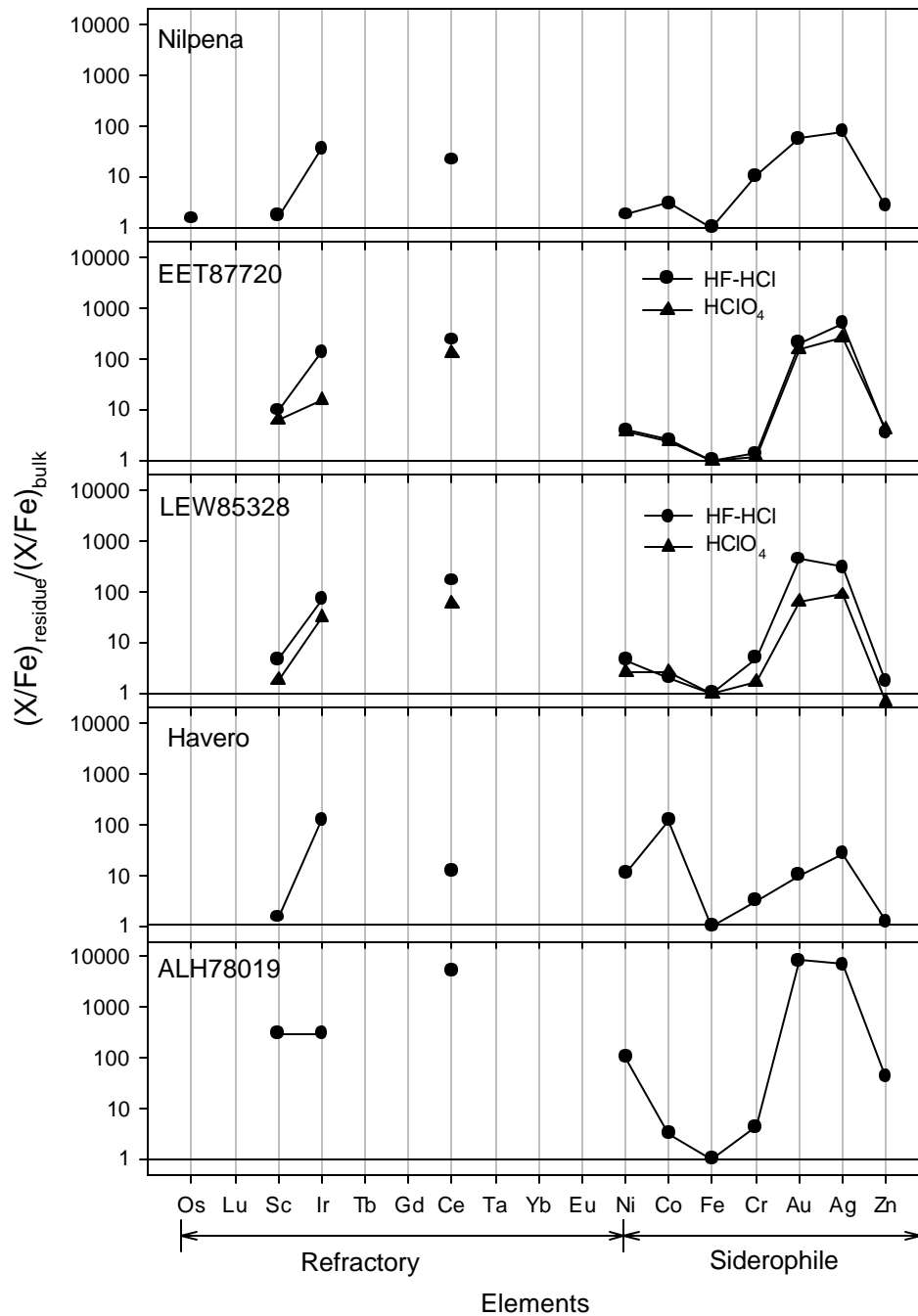
Fig 4.2 a. *Relative abundance of various elements in acid residues of ureilites with respect to bulk samples, normalized to Fe (Iron) is plotted for the five ureilites. The elements are divided into two subgroups refractory and siderophile and within these subgroups the elements are arranged in increasing order of volatility.*

Moon and the SNC parent body (Goodrich 1992). Element-element plots show good linear correlations among all the refractory siderophiles in ureilites (Goodrich 1992) suggesting that the refractory siderophiles are contained in a common component. Further more they also concluded that the ureilite siderophile elements could be a

mixture of refractory rich and refractory poor component. Carbonaceous vein separates seemed to be the refractory rich end member. Though the carbon rich interstitial material (consisting of carbon, metal, sulfides and minor silicates) was established to be the carrier of trace refractory siderophile, the carrier of these trace
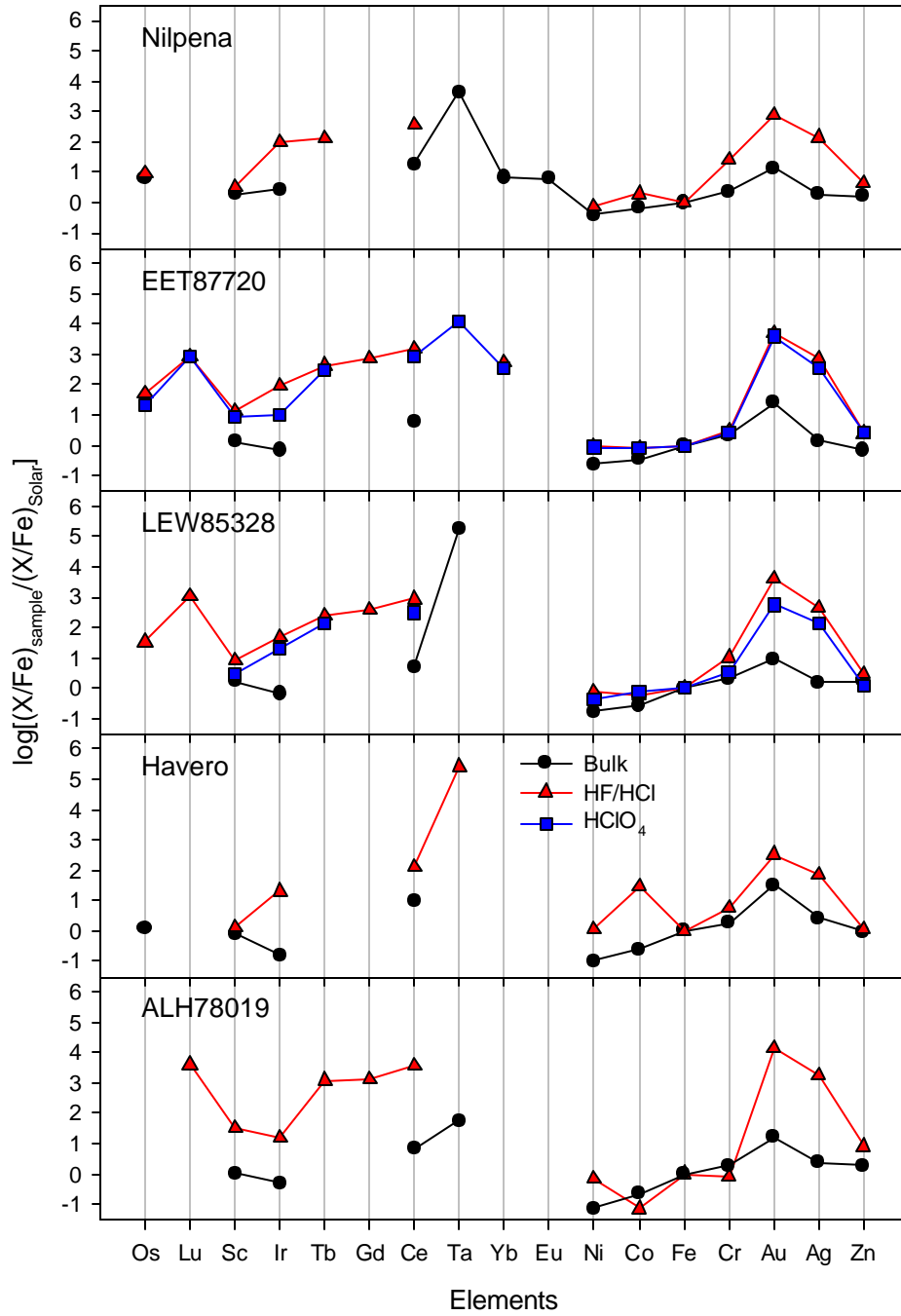
Fig 4.2 contd. b. *The (same) elemental abundance data for acid residues as well as bulk samples of ureilites, normalized to the solar abundance (that is taken as CI abundance) relative to iron (Fe) (Anders and Grevesse (1989).*

elements within the interstitial material is not clear. From Fig 4.2a and Fig 4.2b, it can be seen that the carbon rich acid residues are highly enriched in refractory elements and account for nearly all the refractory elements carried by the bulk samples. This implies that the silicates, which account for more than 90% of total mass of the ureilite, are depleted in refractory siderophile elements as well as refractory elements. Since ureilites are highly differentiated meteorite, these elements have tendency to go with metals (present also in vein material) rather than carbon. If carbon would have been a part of the magma from which ureilites are formed, one should not expect such a high enrichment of refractory elements in carbon (mainly present in the form of graphite and diamond). This implies that the carbon in ureilites is having different origin than that of silicates and argues against magmatic crystallization of graphite. Based on the above observation we propose that the carbon phases in ureilites have their origin in solar nebula where refractory elements served as nuclei over which the graphite and diamonds had condensed by non-equilibrium process.

Siderophile elements: From Fig 4.2a & 4.2b, it is clearly seen that the elements Au and Ag are highly enriched in acid residues (both HF-HCl and HClO$_4$ residues). Mass balance calculation reveals that nearly all inventory of Au and Ag in the bulk samples of ureilites are accounted for by the acid residues only. It seems that their high abundance in acid residues are more likely established by cosmochemical behavior (nebular processes) rather than geochmical behavior (parent body processes) because the geochmical property of Ni, Au and Ag can not explain the high abundance of these elements in carbon phase. The condensation temperature of Au and Ag are lower than that of Fe, Co and Ni (Wasson 1985), implying that these elements were incorporated into diamonds, graphite and amorphous carbon during or after their condensation, by chemically non-selective process (*e.g.*, ion implantation), at temperatures less than 1225K (50% condensation) when most part of the Fe, Ni and Co has already been condensed (and isolated).

The high enrichment of refractory and refractory trace siderophile elements in the carbon in ureilites argues against the *in situ* origin of carbon in ureilites. The carbon in ureilites that is present mostly in the form of graphite, diamond and amorphous carbon are most likely formed in solar nebula by non-equilibrium condensation process.

4.2.2. Nitrogen in acid residues of monomict ureilites

In this section nitrogen and argon release patterns will be discussed individually for each of the acid resistant residues as well as oxidized residues of four monomict ureilites. Out of these four ureilites, three are from Antarctic collection and none of them have previously been studied for nitrogen. The yield of the residues after acid treatment is given in Chapter 2.

LEW85328 (HF-HCl residue), L28-A1 & L28-A2……

The release patterns of the amounts as well as isotopic compositions of nitrogen and argon by combustion are shown in Fig 4.3 and the corresponding data are shown in
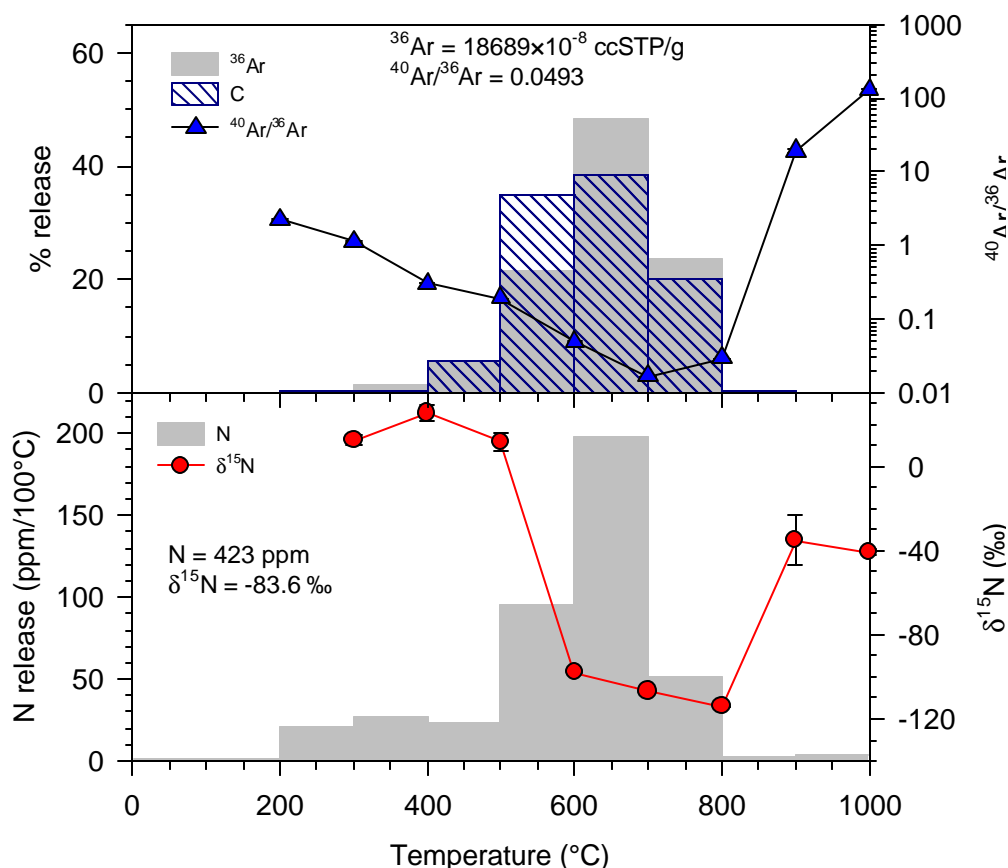
Fig 4.3 *Stepwise combustion release profile for nitrogen, argon and CO$_2$ for HF-HCl residue of monomict ureilite LEW85328 (L28-A1) (Weight =1.21mg).*

Table 4.1. L28-A1 contains 424 ppm of N (δ^{15}N= -82 ‰) and 18689 ×10^8 ccSTP/g of argon. Mass balance calculation reveals that L28-A1 contains nearly 80 % of the total nitrogen carried by the bulk sample L28-b1. In other words, nearly 20 % of the nitrogen is carried by acid soluble phase, while the residue L28-A1 accounts for

almost all the noble gases. Like bulk sample, L28-A1 also shows two nitrogen components. More than 80% of the total nitrogen released is light with minimum $\delta^{15}N$ value of –114‰, and is released between 600° and 800°C. This is also accompanied by peak noble gas release and peak carbon combustion and lowest value of $^{40}Ar/^{36}Ar$ (an indicator of primordial noble gas release). The second nitrogen
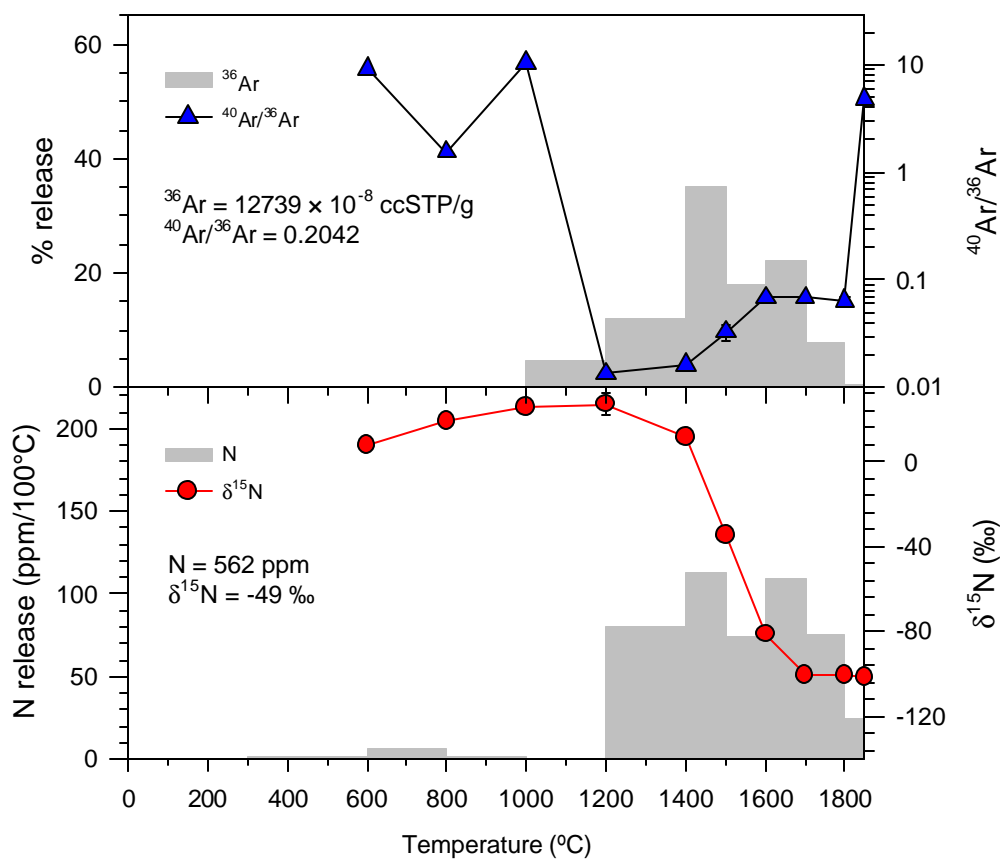
Fig 4.4 *Stepwise pyrolysis release profile for nitrogen and argon for HF-HCl residue of monomict ureilite LEW85328 (L28-A2) (Weight =1.00mg).*

component is isotopically heavier, released at temperatures ≤500°C, and having maximum $\delta^{15}N$ value of 25‰. It is not associated with either appreciable carbon combustion or noble gas release. A very minor amount of relatively heavier nitrogen is also released at temperature >800°C.

Another aliquot (L28-A2) of this HF-HCl residue has been analyzed by pyrolysis to understand the behavior of heavy and light nitrogen carriers during pyrolysis. The release patterns as well as isotopic composition of nitrogen and noble gases depicted in Fig 4.4 and the data is compiled in Table 4.2. The sample L28-A2 yields 562 ppm of nitrogen with bulk $\delta^{15}N$ of -49 ‰ (-82‰ for L28-A1) and 12739 × 10^{-8} ccSTP/g

of Ar. As compared to L28-A1, the proportion of light nitrogen is smaller (<50% against >80% in L28-A1). The signature of light nitrogen seems to be modified by the contribution of a small amount of heavy nitrogen. The higher nitrogen concentration in L28-A2 with higher $\delta^{15}N$ and lower noble gas content indicate that the carrier of heavy nitrogen is enriched in nitrogen as compared to that of light nitrogen carrier but poor in noble gases concentration. The signature of heavy nitrogen is similar to that observed for L28-A1 with maximum $\delta^{15}N$ of 27‰. But in both cases the maximum $\delta^{15}N$ of heavy nitrogen is much lower than that observed for bulk sample L28-B1 (Fig 3.1). The partial removal of heavy nitrogen carriers superimposed on a small amount of adsorbed atmospheric nitrogen during acid dissolution could most likely be the cause for obscuring the true heavy nitrogen signatures in these samples.

LEW85328 (HClO$_4$ residue), L28-O1, L28-O2 ......

The release patterns as well as isotopic composition of nitrogen and argon of L28-O1 and L28-O2 are shown in Fig 4.5 and 4.6 respectively. The release patterns of nitrogen and argon (also Kr and Xe) in L28-O1 and L28A1 are almost similar except
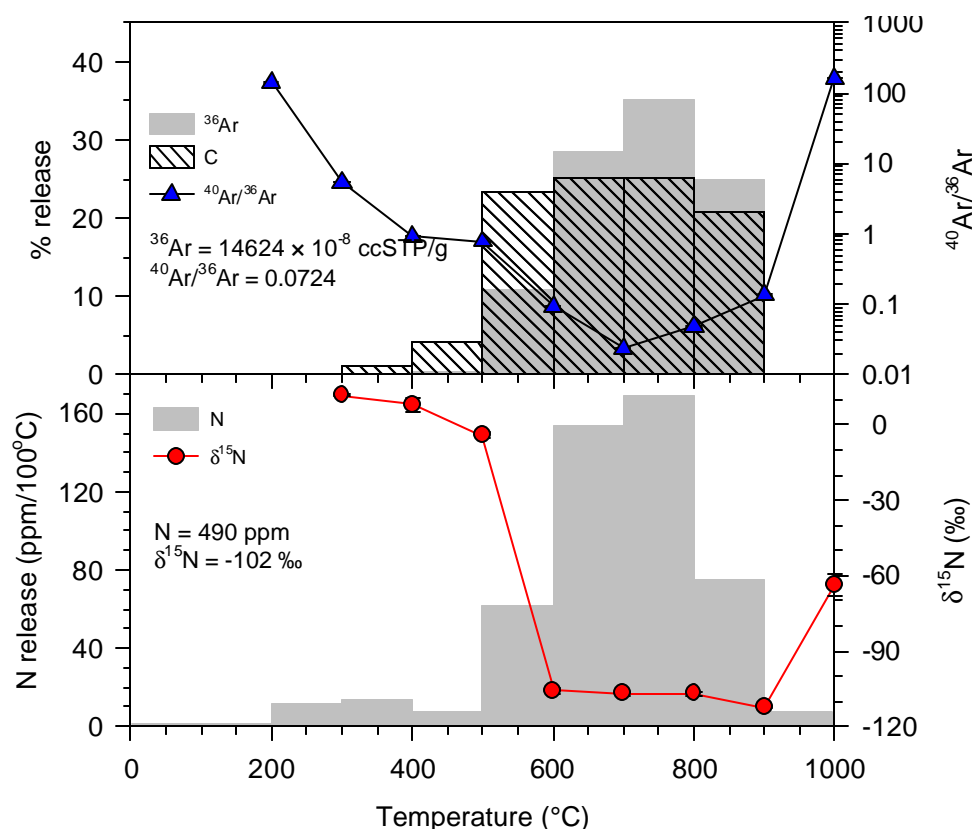
Fig 4.5 *Stepwise combustion (at 2 torr O$_2$) release pattern of nitrogen, argon and CO$_2$ of oxidized residue of LEW85328 (L28-O1) (Wt. =2.07mg).*
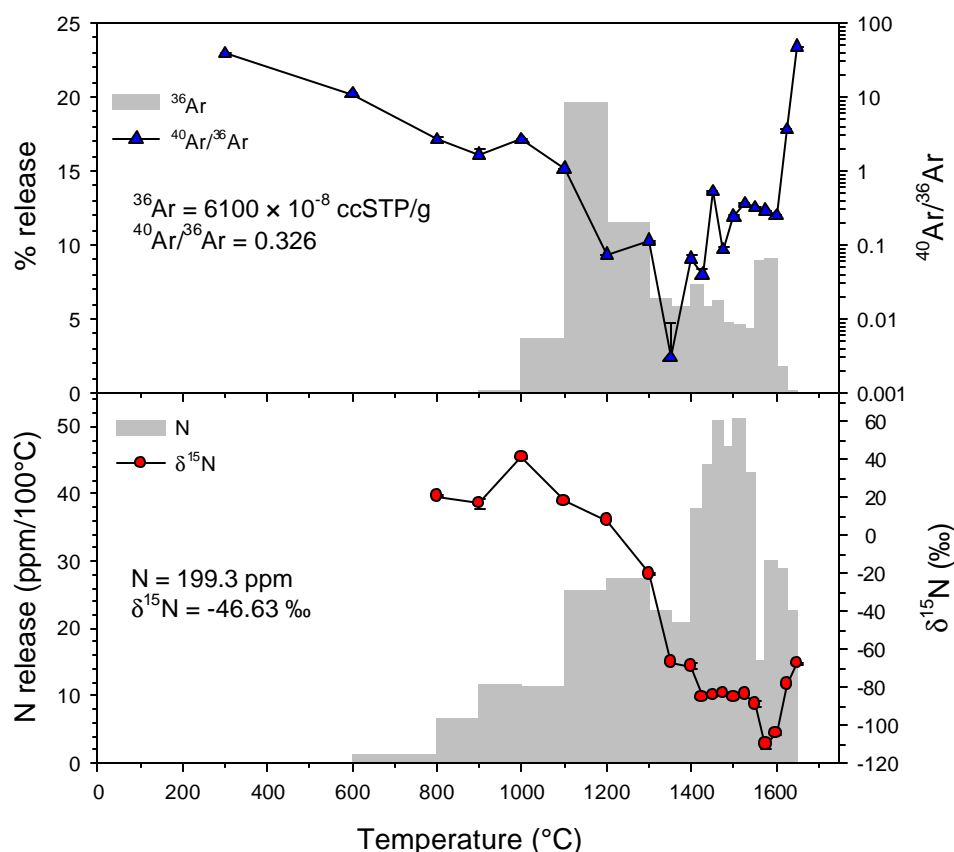
Fig 4.6 *Stepwise release pattern of nitrogen and argon on pyrolysis of oxidized residue of LEW85328 (L28-O2) (Wt. =1.40mg).*

one difference that the proportion of heavy nitrogen is even smaller (<5%) in L28-O1. The L28-O1 yields 590 ppm of nitrogen with bulk $\delta^{15}N$ of -102‰. Most of the light nitrogen is released between 600° and 900°C along with primordial noble gases and peak carbon combustion and shows uniform $\delta^{15}N$ between -106 to -113 ‰. Since the perchloric acid treatment is supposed to remove amorphous carbon and fine-grained graphite, the release of light nitrogen can be attributed to diamonds, the carbon phase that is resistant to $HClO_4$ attack. The relatively heavy nitrogen released at ≤500°C is much lighter ($\delta^{15}N = 12$‰) than that observed in L28-A1 and L28-B implying almost complete removal of carriers of heavy nitrogen.

Another aliquot of this sample (L28-O2) is analyzed by pyrolysis and the release patterns are shown in Fig 4.6. The gas release might not be complete for the sample, as the maximum temperature attainable by the RF heating during this period is only about 1700°C, due to a technical problem. This sample yielded 199 ppm of nitrogen with bulk $\delta^{15}N$ of -46‰ along with 6010×10^{-8} ccSTP/g of Ar. The light nitrogen was released only from 1500°C.

In all the analyses of the acid residue from LEW85328, it has been observed that the higher nitrogen concentration in analysis of one of the two or more aliquots of the same sample studied is always associated with higher $\delta^{15}N$ and lower noble gas content. This is indicating the presence of a nitrogen carrier other than diamonds (carrier of light nitrogen) that is more enriched in nitrogen than light nitrogen carrier and depleted in noble gases.

Haverö (HF-H$_2$SO$_4$ residue) Hav-A1 & Hav -A2……

The release patterns as well as isotopic compositions of nitrogen and Ar of acid resistant residue of Haverö (Hav-A1) are shown in Fig 4.7 and data are listed in Table 4.2. The Hav-A1 yields 372 ppm of nitrogen with bulk $\delta^{15}N$ of –8‰. Mass balance calculation reveals that nearly 25 % of the nitrogen in bulk sample is carried by acid resistant residue while residues account for almost all the noble gases (Table 4.6) (this work; Göbel *et al.*, 1978). Similar to L28-A1, two major nitrogen components can
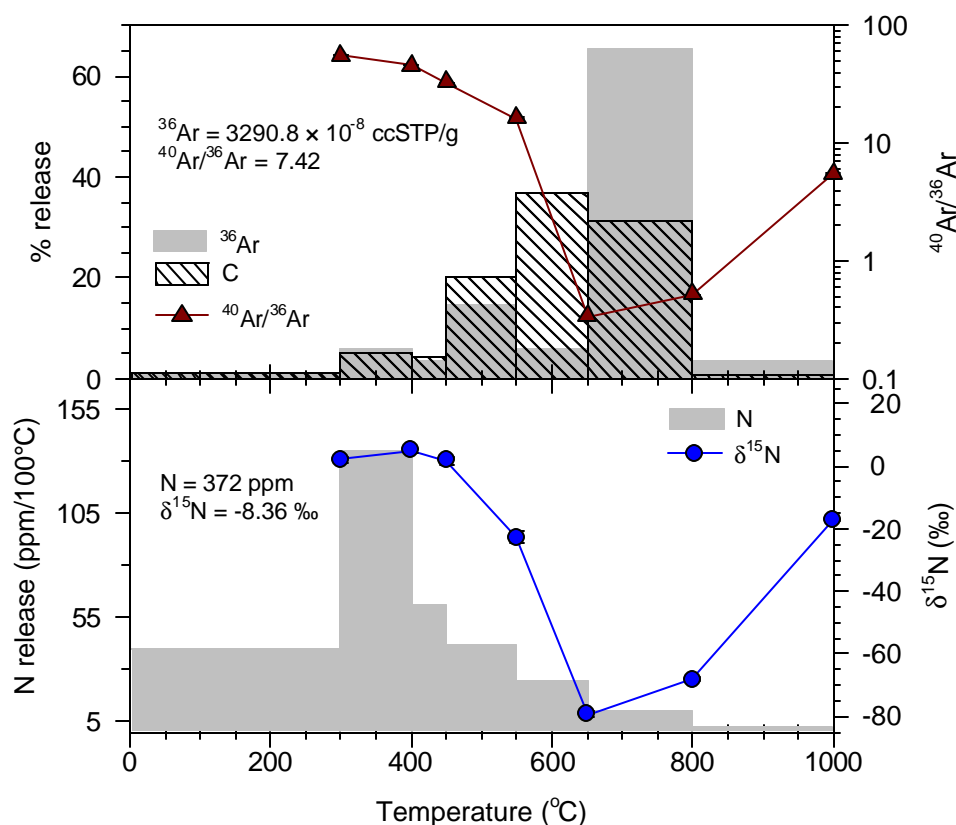
Fig 4.7 *Stepwise combustion (at 5 torr O$_2$) release pattern of nitrogen, argon and CO$_2$ of HF-HCl residue of Haverö (Hav-A1) (Wt. =1.18mg).*
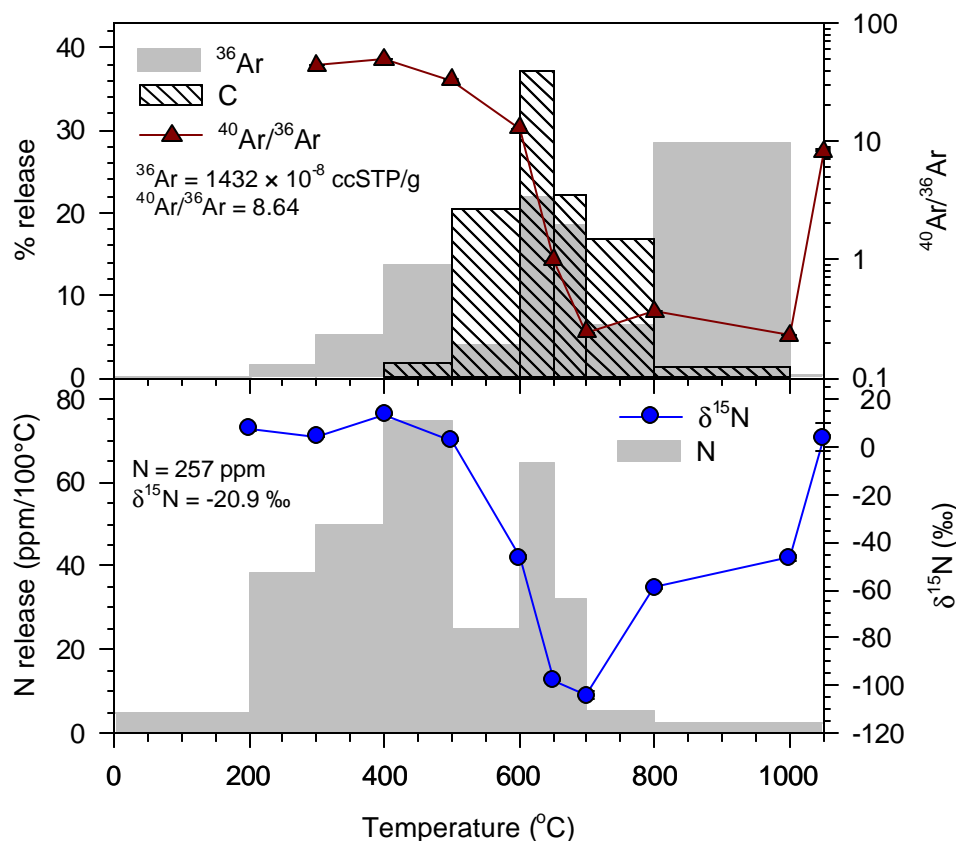
Fig 4.8 *Stepwise combustion (at 2 torr O_2) release pattern of nitrogen, argon and CO_2 of HF -HCl residue of Haverö (Hav-A2) (Wt. =3.28mg).*

clearly be seen based on isotopic composition. The light nitrogen released (~11%) at 650°C and 800°C with minimum $\delta^{15}N$ value of –79‰ is close to observed minimum $\delta^{15}N$ for the bulk sample analysis (-78‰, Fig 3.5). More than 75% of the total nitrogen is released at initial three temperature steps and is relatively heavy with maximum $\delta^{15}N$ of 5‰. This heavy nitrogen in Hav-A1 is much lighter than maximum $\delta^{15}N$ observed for bulk Haverö (Hav-B) and could most likely be caused by admixture of small amount of indigenous nitrogen ($\delta^{15}N$ of ≥ 50‰) with adsorbed atmospheric nitrogen ($\delta^{15}N$ of close to 0‰). Like the acid resistant residue from LEW85328, only the light nitrogen component is accompanied by primordial noble gas (and lowest value of $^{40}Ar/^{36}Ar$) release and peak carbon combustion. In addition to these two nitrogen components, a minor nitrogen component is needed to explain the excursion in $\delta^{15}N$ at 1000°C.

Another aliquot (Hav-A2) of the above sample is again analyzed by combustion at 2 torr O_2 pressure instead of 5 torr used for Hav-A1 and with more closely spaced
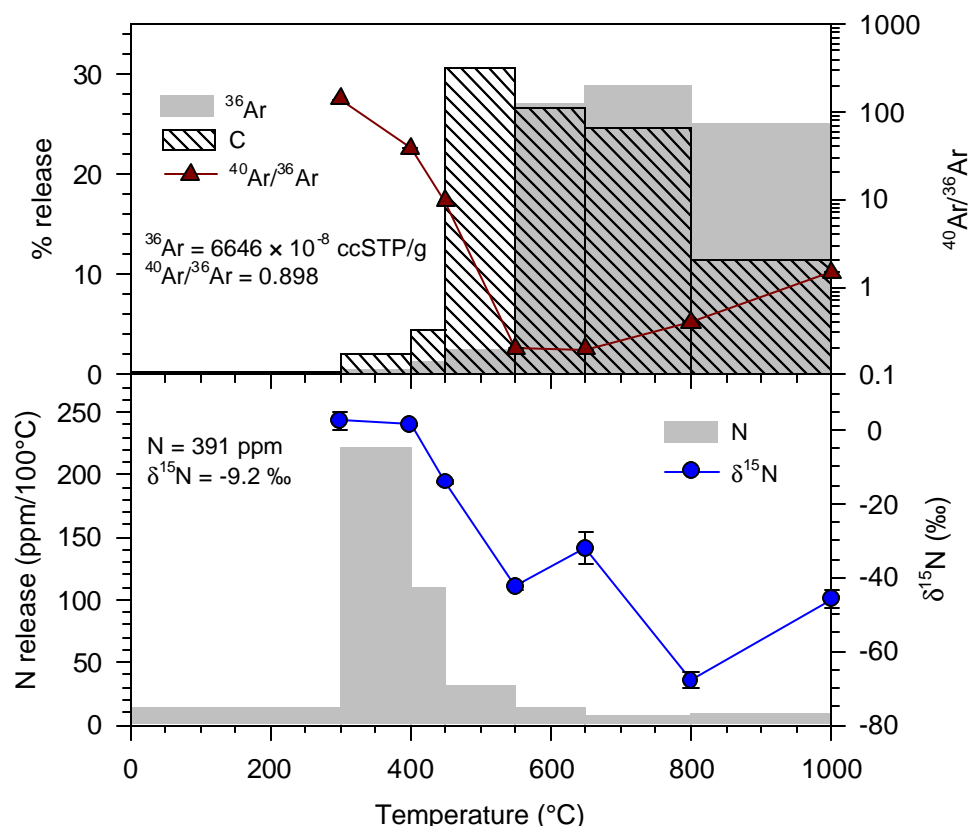
Fig 4.9 *Stepwise combustion (at 5 torr O$_2$) release pattern of nitrogen, argon and CO$_2$ of oxidized residue of Haverö (Hav-O) (Wt. = 0.56 mg).*

temperature intervals. The purpose of this study is two folds. The first one is to get better resolution between heavy and light nitrogen components and the second is to check reproducibility. The release patterns and isotopic compositions of nitrogen and argon are depicted in Fig 4.8 and data is listed in Table 4.2. The sample yields 257 ppm of nitrogen with bulk $\delta^{15}N$ of -21‰. Though the nitrogen yield in Hav-A2 is only 70‰ of that of Hav-A1, the nitrogen composition is better resolved. The minimum $\delta^{15}N$ observed in this case is much smaller (with $\delta^{15}N$ of $-104‰$) than in the previous sample ($-79‰$). The large amount ($>65\%$) of heavy nitrogen is released at temperature less than $500°C$ with maximum $\delta^{15}N$ of 14‰, and it is higher than observed for Hav-A1. The noble gas concentration is also lower than that of previous sample (Hav-A1). ^{36}Ar concentration is less than 50% of the concentration observed in Hav-A1 and this is very much beyond the experimental uncertainty. This discrepancy is most likely due to sample heterogeneity. Such heterogeneity has been reported for bulk as well as acid residues for the noble gases also (Göbel *et al.*, 1978).

If the proportion of graphite [a carrier of relatively heavy nitrogen (will be discussed in later section), but devoid of noble gases] is different in both the aliquots, the observed discrepancy is explainable.

Haverö (HClO$_4$ residue) Hav-O......

Nitrogen and noble gases are extracted by stepwise combustion at 5 torr O$_2$ pressure. The release patterns as well as isotopic compositions are shown in Fig 4.9 and data are listed in Table 4.2. Sample Hav-O yields 391 ppm of nitrogen with δ^{15}N of -9 ‰ and 6646×10^{-8} ccSTP/g of ^{36}Ar. The release pattern of nitrogen in Hav-O is dominated by release of relatively heavy nitrogen (close to atmospheric composition). The light nitrogen starts releasing at 550°C along with primordial noble gases and peak carbon combustion but its composition seems to be obscured by release of heavier nitrogen component alongside. The minimum value of δ^{15}N here is only $-$ 68‰, much heavier than lowest values observed for bulk sample and acid resistant residues of Haverö. More than 60% of nitrogen released at initial two temperature steps showing δ^{15}N close to air value and most likely dominated by adsorbed atmospheric nitrogen on the shoulder of small amount of indigenous heavy nitrogen (δ^{15}N ≥ 20‰) release.

ALH81101 (HF-HCl residue), A01-A......

The release patterns and isotopic compositions of nitrogen and Ar of HF-HCl residue of ALH81101 (A01-A) are shown in Fig 4.10 and the data are listed in Table 4.2. The gases are extracted by stepwise combustion at 2 torr O$_2$ pressure. The sample A01-A yields 140 ppm of nitrogen and 1233×10^{-8} ccSTP/g of ^{36}Ar. This contributes less than 5% of the total nitrogen release while more than 60 % of Ar (noble gases) carried by this (Table 4.6). The lower contribution of nitrogen to that of bulk sample is most probably not due to lower concentration of nitrogen in acid residue but because of higher amount of nitrogen of terrestrial origin in the bulk sample probably due to Antarctic weathering processes (Fig 3.6). Like other acid residues, A01-A also contains two nitrogen components based on their isotopic composition. The light nitrogen (~50%) is released between 600°C to 800°C with minimum δ^{15}N value of $-$ 94% and accompanied by peak carbon combustion and primordial noble gas release. Large amount of heavy nitrogen is released at temperatures lower than 500°C wherein only minor amount of noble gases and carbon are released, with maximum δ^{15}N value
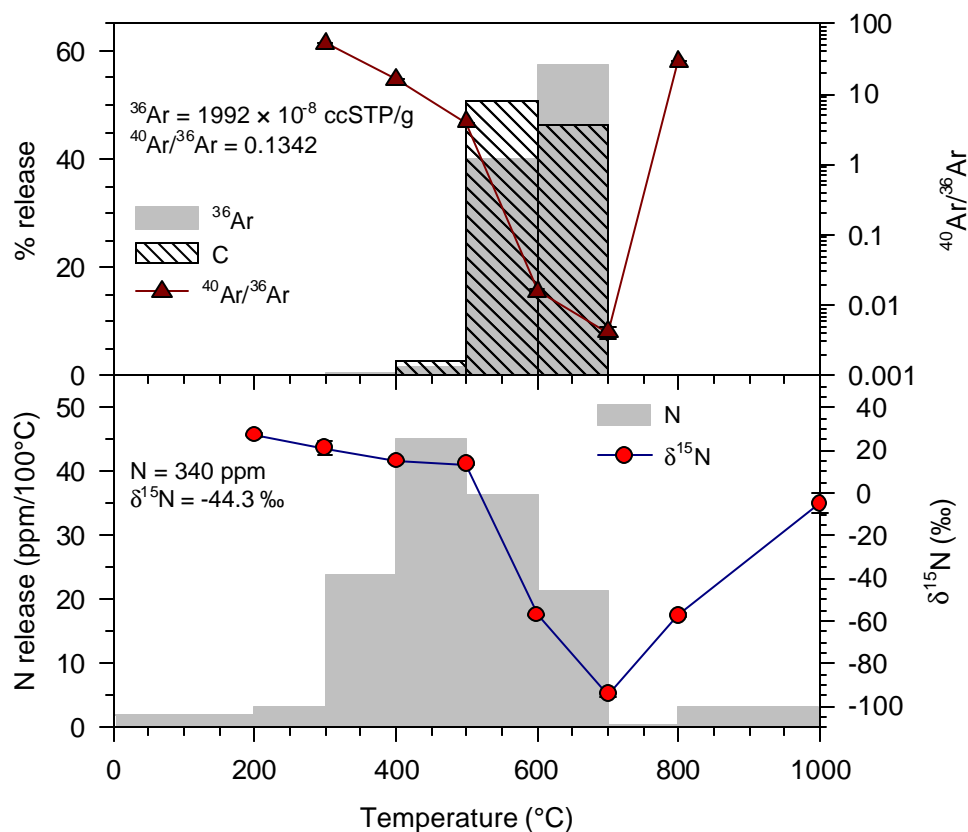
Fig 4.10 *Stepwise combustion (at 2 torr O$_2$) release pattern of nitrogen, argon and CO$_2$ of HF-HCl residue of ALH81101 (A01-A) (Wt. =1.06 mg).*

of 27‰. Another minor nitrogen component is needed to explain excursion in δ^{15}N at 1000°C.

ALH81101 (HClO$_4$ residue), A01-O……

The release patterns and isotopic compositions of nitrogen and Ar are shown in Fig 4.12 and data are listed in Table 4.2. The gases are extracted by stepwise combustion at 2 torr O$_2$. The sample A01-O yields 340 ppm of nitrogen with bulk δ^{15}N value of –44‰ and 1992 ×10^{-8} ccSTP/g of ^{36}Ar. The relative proportion of heavy nitrogen is reduced by HClO$_4$ treatment indicating the carrier of heavy nitrogen is soluble in oxidizing acid and require more harsh condition for complete removal. Like A01-A, the heavy nitrogen in this sample also is released at lower temperature (≤500ºC) and accompanied by a minor amount of noble gases and C. The maximum δ^{15}N of heavy nitrogen observed is 24‰, close to that observed for A01-A (Fig 4.9). The light nitrogen on the other hand is better resolved due to partial removal of heavy nitrogen carrier and yields a minimum δ^{15}N value of -108‰ at 700°C. Release of this
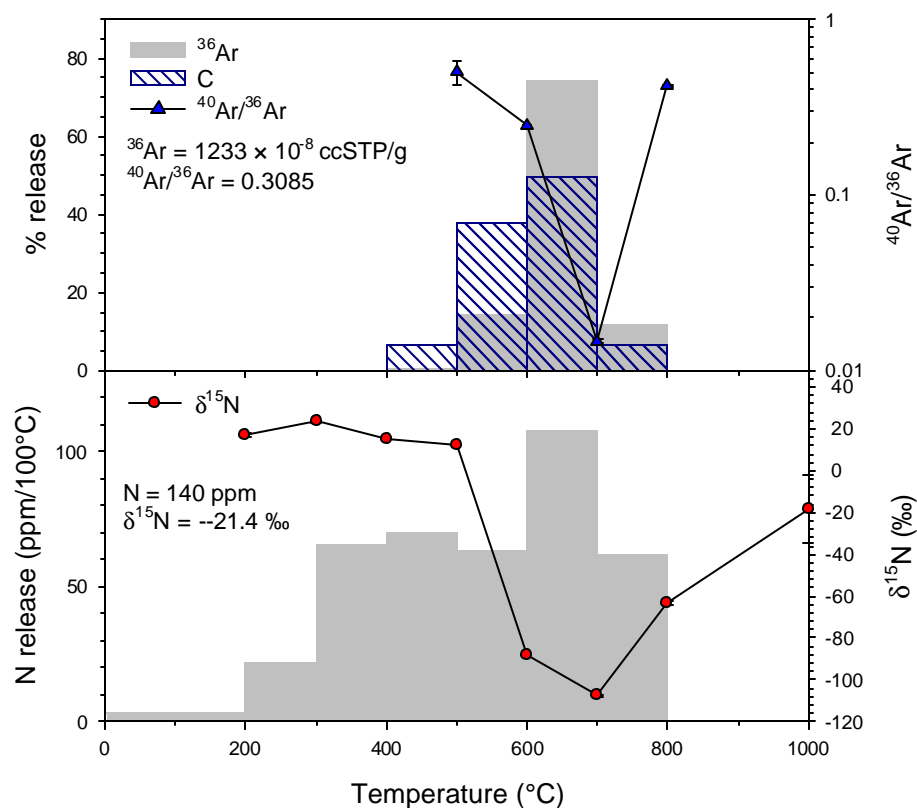
Fig 4.11 *Stepwise combustion at (2 torr O$_2$) release pattern of nitrogen, argon and CO$_2$ of oxidized residue of ALH81101 (A01-O) (Wt. = 1.06 mg).*

component is accompanied by release of large amount of primordial noble gases and carbon combustion.

ALH82130 (HF-HCl residue), A30-A……

This is the most reduced specimen among all the known ureilites (Berkley *et al.*, 1985) and showed unusually high $^{132}Xe/^{36}Ar$ ratio in the bulk sample analysis (A30-B in Table 3.1). The A30-A is analyzed by combination of combustion and pyrolysis. The gas extraction was started with 800°C pyrolysis followed by combustion at 2 torr O$_2$ pressure up to 1000°C and subsequently pyrolyzed at 1850°C in the final step of gas extraction. The purpose of this gas extraction protocol is to understand the nature of heavy nitrogen carrier, which combusted at ≥800°C in most of the acid residues after diamond-graphite combustion and caused excursion in $\delta^{15}N$. The release patterns as well as isotopic composition of nitrogen and argon are shown in Fig 4.12 and the data are listed in Table 4.2. The sample A30-A yields 108 ppm of nitrogen with bulk $\delta^{15}N$ value of -37.7 ‰ and 643×10^{-8} ccSTP/g of ^{36}Ar. Mass balance calculation reveals that A30-A accounts for only ~4% of the total nitrogen contained by the bulk

sample (A30-B) (Table 4.6). The low yield of nitrogen and noble gases in this residue as compared to bulk can be attributed to terrestrial contamination of the bulk sample due to Antarctic weathering processes. The first pyrolysis step yields very heavy nitrogen with $\delta^{15}N$ of 87‰ (shown by open circle) indicating that the indigenous
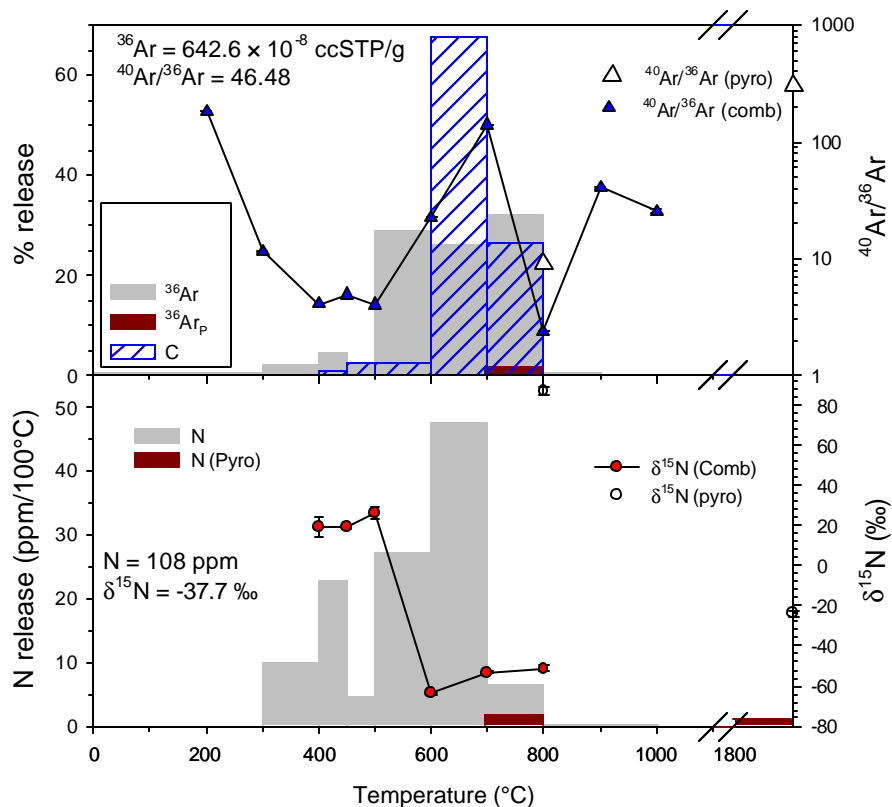
Fig 4.12 *Stepwise combustion release pattern of nitrogen, argon and CO_2 of HF - HCl residue of ALH82130 (A30-A) (Wt. =1.32 mg). Sample is combusted at 2 torr O_2 up to 1000° C, afterward, the sample is pyrolyzed at 1850°C.*

heavy nitrogen should have even higher $\delta^{15}N$ because it must be diluted by some contribution from adsorbed atmospheric nitrogen. Like other samples, the heavy nitrogen in A30-A too is associated with only minor amount of noble gases and C combustion. The light nitrogen is released between 600°C and 800°C with lowest $\delta^{15}N$ value of −64‰ and also accompanied by large amount of primordial noble gas release and carbon combustion. A small amount of nitrogen (<1%) released at 1800 pyrolysis step is having $\delta^{15}N$ of −24‰ along with almost atmospheric argon as indicated by air like $^{40}Ar/^{36}Ar$.

The two important points to be noticed in this sample are its $^{40}Ar/^{36}Ar$ ratio and $^{132}Xe/^{36}Ar$ ratio. These are higher compared to the residues from other ureilites and will be discussed in details in next chapter.

ALH82130 (HClO$_4$ residue), A30-O……

The release patterns and isotopic composition of nitrogen and argon are shown in Fig 4.13 and data is listed in Table 4.2. Similar to A30-A, A30-O is also analyzed by
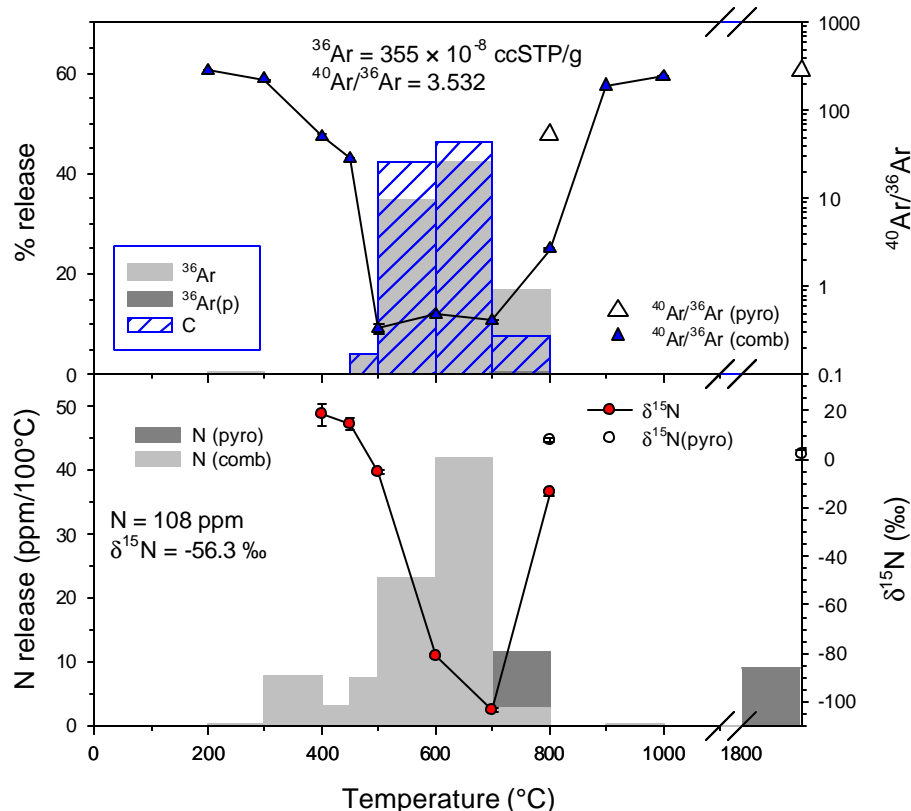
Fig 4.13 *Stepwise combustion release pattern of nitrogen, argon and CO$_2$ of oxidized residue of ALH82130 (A30-O) (Wt. =1.82 mg). Sample is combusted at 2 torr O$_2$ up to 1000°C, afterward, the sample is pyrolyzed at 1850°C.*

combination of combustion and pyrolysis. The gas extraction was started with 800°C pyrolysis and later on combusted at 2 torr O$_2$ pressure up to 1000°C and subsequently pyrolyzed at 1850°C in the final step of gas extraction. The oxidized residue of ALH82130 (hereafter A30-O) yields 108 ppm of nitrogen with bulk $\delta^{15}N$ value of $-$56‰ and 355 $\times$ 10^{-8} ccSTP/g of ^{36}Ar. Nearly 10% of nitrogen is released at initial 800°C pyrolysis step with $\delta^{15}N$ value of only 8‰ and is much lighter than nitrogen release in corresponding temperature step of A30-A. A similar amount of nitrogen is

also released in the final step of 1800°C but with $\delta^{15}N$ close to atmospheric value (2‰) (most likely air nitrogen as indicated by high $^{40}Ar/^{36}Ar$ ratio). The light nitrogen released between 600°C-800°C with lowest value of $\delta^{15}N$ of –103‰ is accompanied by large amount of noble gases and carbon combustion. The heavy nitrogen released at lower temperatures of less than 500°C is accompanied by only a minor amount of noble gases and carbon and having highest $\delta^{15}N$ value of 19‰. Though the argon (Kr and Xe also) amount in A30-O is about half of that shown by A30-A, the $^{40}Ar/^{36}Ar$ ratio is much lower in the former. The Xe/Ar ratio in A30-O is quite normal and falls within the range shown by other ureilites. The excess xenon seen in bulk (A30-B) as well as A30-A, is also removed by perchloric acid treatment indicating that the diamond from most reduced specimen of ureilites is similar to that of other ureilites. This could be the because of high proportion of carrier enriched in xenon as compared to other lighter noble gases. The xenon-enriched carrier most likely is the amorphous carbon, lost most of the Kr and Ar during parent body processing. The other alternative explanation could be the xenon-enriched carrier trapped their gases at lower nebular temperature under nebular plasma.

4.2.3 Nitrogen in acid residue of diamond free ureilite

The bulk sample of the only known diamond free ureilite ALH78019 (A19-B) shows a complex nitrogen release pattern on pyrolysis while the noble gas release pattern is quite normal (Fig 3.8). X ray-diffraction does not show the presence of diamond in this ureilite (Berkley and Jones, 1982, Ott *et al.*, 1984; Wacker, 1984 & 1986). But the detection of diamonds by XRD has two limitations: the size limitation and concentration limitation. Below certain critical size the diamonds cannot be detected and very low concentration of diamond can also lead to similar result. We have seen that all the monomict ureilites contain light nitrogen and its carrier is a carbon phase unaffected by mineral acid and oxidizing acid treatments, indicating that this carrier is diamonds. Therefore, the presence of light nitrogen can be used as an indicator for the presence of diamond in ureilites. In the present section, the nitrogen and noble gas results of acid residues of diamond free ureilite will be discussed. Visually the residues of ALH78019 are coarse grained and look very different from residues of other ureilites (Fig 4.1).

ALH78019 (HF-HCl residue), A19-A……

The bulk sample A19-B, showed a small amount of light nitrogen after 1600°C step with $\delta^{15}N$ value of -45‰. It is important to ascertain, if this light nitrogen signature is an indication for the presence of diamonds in this meteorite. Release patterns and isotopic composition of acid resistant residue of ALH78019 (hereafter A19-A) are
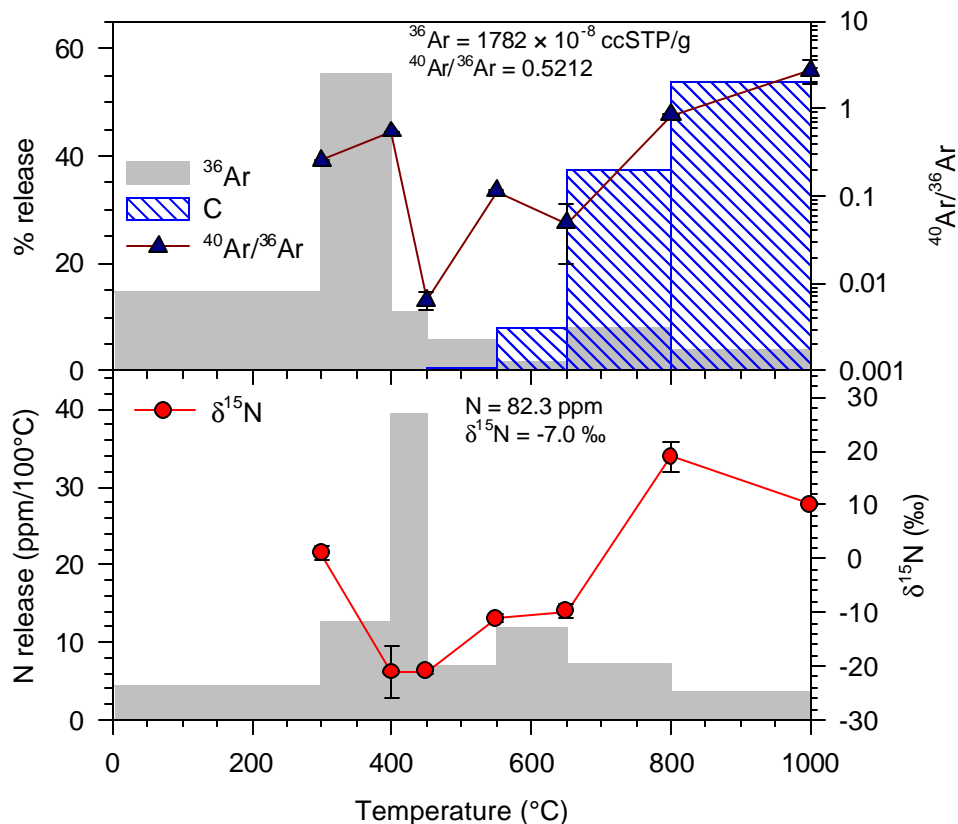
Fig 4.14 *Stepwise combustion release pattern of nitrogen, argon and CO_2 of HF-HCl residue of ALH78019 (A19-A; diamond free ureilite) (Wt. =1.35mg). Sample is combusted at 5 torr O_2*

shown in Fig 4.14 and data are listed in Table 4.2. The gases are extracted by combustion at 5 torr O_2 pressure. The sample yields 82 ppm of nitrogen with bulk $\delta^{15}N$ value of -7‰ and 1782×10^{-8} ccSTP/g of ^{36}Ar. This accounts for nearly 50% of total nitrogen present in bulk sample. Based on $\delta^{15}N$, two nitrogen components can clearly be seen. This trend is opposite to the trend observed in residues of other monomict ureilites. A large amount (.60%) of the nitrogen with $\delta^{15}N$ value of ~-21‰ is released at temperature lower than 550ºC wherein less than 1% carbon combusts

and is accompanied by most of the primordial noble gases ($\geq 85\%$). Most of the carbon combusts only after $650°C$ where only minor amount of noble gases are released. The nitrogen released along with peak carbon combustion is having highest value of $\delta^{15}N$ of 19‰. The nitrogen released along with primordial noble gas peak is having $\delta^{15}N$ of -21‰ indicating that the nitrogen accompanied by primordial noble gases in diamond free ureilite is much heavier than those of diamond bearing ureilites ($\delta^{15}N \leq -100$‰). The low combustion temperature and high temperature release on pyrolysis indicates that the carrier is most likely an amorphous carbon phase.

ALH78019 (HClO$_4$ residue), A19-O……

The release patterns as well as isotopic composition of nitrogen and Ar are shown in Fig 4.15 and data are listed in Table 4.2. The gases are extracted in identical fashion like A19-A. This sample yields 156 ppm of nitrogen with bulk $\delta^{15}N$ value of -5‰ and 60×10^{-8} ccSTP/g of ^{36}Ar. A large amount of carbon combust at higher temperature
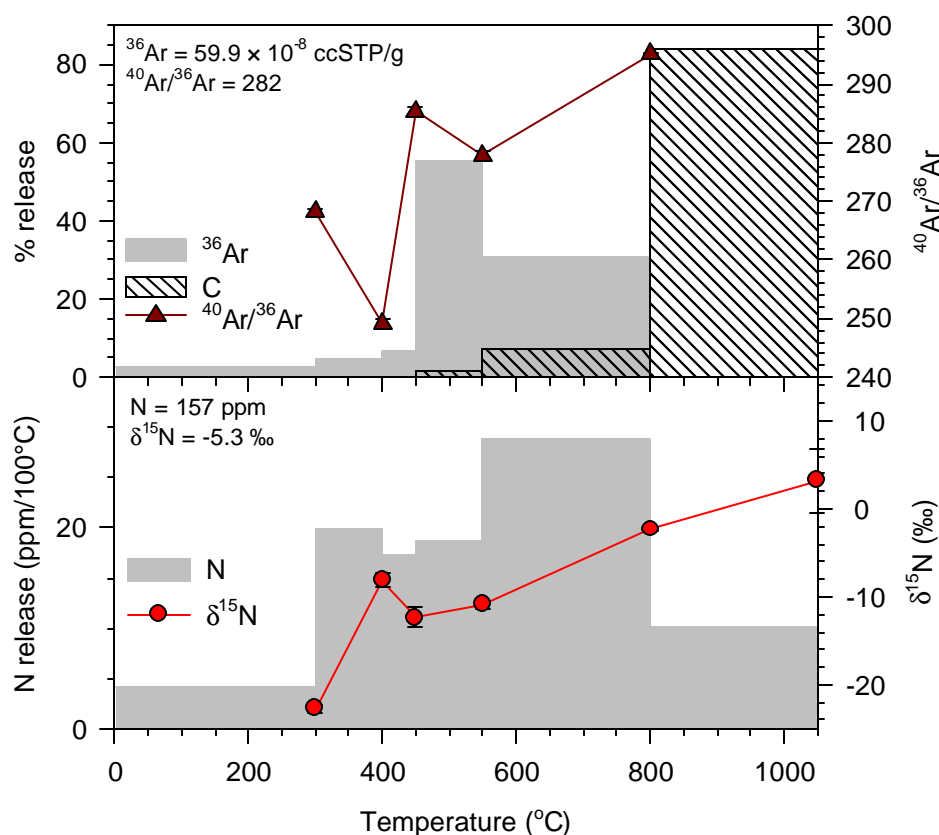
Fig 4.15 *Stepwise combustion release pattern of nitrogen, argon and CO$_2$ of oxidized residue of ALH78019 (A19-O; diamond free ureilite) (Wt. =1.00 mg). Sample is combusted at 5 torr O$_2$.*

($\geq$800°C) but contained negligible amounts of noble gases. The ^{36}Ar released here is only 5% of that from A19-A and with mostly atmospheric ^{40}Ar/^{36}Ar ratio. Though the nitrogen released is almost double that of HF-HCl residue, it seems to be dominated by the atmospheric nitrogen released on the shoulder of small amount of N of indigenous origin. The loss of noble gases upon perchloric acid treatment is indicative of the absence of diamonds and hence the carrier of trapped primordial noble gases is most likely the amorphous carbon. Because the bulk sample (A19-B) showed the presence of small amount of light nitrogen at temperatures higher than 1600°C, it could be an indicator for the presence of a small amounts of very fine grained diamonds that might have been lost subsequently into the acid solution during sample dissolution. Furthermore, the behavior of the carrier of trapped gases in ALH78019 and Q phase from primitive chondrites towards oxidized acid treatment is similar suggesting that these phases most likely share similar origin. This will be discussed in details in later section.

Table 4.2: Nitrogen and noble gases in acid residues of monomict and diamond free ureilites.

Temp.	N	δ^{15}N	^{36}Ar	^{38}Ar/^{36}Ar	^{40}Ar/^{36}Ar	^{84}Kr	^{132}Xe	P_{CO2+CO}
	(ppm)	(‰)	(10^{-8} ccSTP/g)			(10^{-10} ccSTP/g)		
Haverö (HF/HCl residue), HAV-A1, combustion, 5 torr O$_2$, 1.18 mg								
300	118.9	2.30	36.7	0.1887	55.44	72.4	8.67	16
		0.93		0.0001	0.11			
400	135.1	5.01	193.7	0.1861	46.32	271. 3	396.3	66
		0.47		0.0001	0.01			
450	30.5	1.86	110.1	0.1883	33.09	160.1	201.6	58
		1.36		0.0001	0.02			
550	42.3	-22.82	484.7	0.1878	16.35	483.4	540.2	264
		1.97		0.0001	0.05			
650	25.0	-79.35	196.8	0.1871	0.3378	1099.4	1582.9	477
		1.03		0.0001	0.0029			
800	15.86	-68.87	2150.1	0.1881	0.5194	946.9	2878.1	408

	0.80			0.0004	0.0016			
1000	4.7	-16.90	117.9	0.1896	5.522	30.8	220.7	9
	0.37			0.0001	0.058			
Total	372.3	-8.36	3290.8	0.1878	7.420	3064.2	5906.6	1298
	0.91			0.0003	0.013			

Haverö (HF/HCl residue), HAV-A2, Combustion, 2 torr O $_2$, 3.28 mg

200	9.8	7.69	0.8	0.2012	58.32	-	-	0
	0.59			0.0010	0.62			
300	38.4	4.37	23.6	0.1893	44.38	47.7	15.1	0
	0.17			0.0003	0.09			
400	49.9	13.71	74.2	0.1874	49.62	133.2	65.0	0
	0.66			0.0003	0.10			
500	74.8	2.63	195.4	0.1871	32.90	325.3	176.6	44
	0.26			0.0002	0.08			
600	25.1	-46.20	55.9	0.1890	12.86	263.7	57.1	510
	1.19			0.0002	0.03			
650	32.2	-97.80	313.5	0.1901	0.9842	762.6	120.7	924
	0.35			0.0002	0.0040			
700	16.0	-104.2	264.2	0.1909	0.2422	520.2	105.6	553
	1.9			0.0003	0.0008			
800	5.2	-59.02	90.4	0.1888	0.3628	165.5	35.0	418
	0.89			0.0002	0.0014			
1000	4.7	-46.35	408.3	0.1896	0.2283[1]	221.0	88.1	35
	1.16			0.0002	0.0001			
1050	1.1	4.18	5.8	0.1881	8.288	2.5	1.0	0
	5.69			0.0013	0.149			
Total	257.2	-20.87	1432. 0	0.1894	8.644	2441.7	664.0[2]	2484.0
	0.60			0.0002	0.020			

---

[1] as measured.
[2] a fraction of Xe is pumped off.

Haverö (HClO$_4$ residue), Combustion, 5 torr O$_2$, HAV-O 0.56 mg

300	42.4	2.56 ±2.45	2.2	0.1865 0.0005	139.5833 0.8526			2
400	221.2	1.53 0.31	28.1	0.1912 0.0004	38.1744 0.0309	35.7	15.7	12
450	54.7	-14.13 0.39	82.8	0.1878 0.0006	9.8456 0.0412	29.9	30.1	27
550	31. 6	-42.47 1.17	162.9	0.1847 0.0002	0.2001 0.0060	269.9	233.2	184
650	13.7	-32.18 4.42	2789.5	0.1902 0.0001	0.1938 0.0006	1073.7	553.5	160
800	10.8	-67.91 2.30	1911.9	0.1881 0.0004	0.3933 0.0094	747.1	466.7	148
1000	16.7	-45.95 2.47	1668.3	0.1887 0.0001	1.4657 0.0087	974.1	391.0	69
Total	391.1	-9.22 0.91	6645.9	0.1891 0.0002	0.8981 0.0062	3130.4	1690.2	602

LEW85328(HF/HCl residue), L28-A1, Combustion, 2 torr O$_2$, 1.21mg

200	1.4	174.0 23.9	0.91	0.1912 0.0025	2.2193[*] 0.0992	-	-	0
300	21.1	12.43 2.07	29.5	0.1902 0.0009	1.1135 0.0115	-	-	4
400	27.5	25.48 3.76	243.9	0.1897 0.0002	0.3057 0.0010	134.6	161.8	10
500	23.3	11.63 4.00	998.6	0.1906 0.0002	0.1915 0.0005	495.7	934.1	134
600	95.7	-97.87 0.45	4030.0	0.1907 0.0002	0.0488 0.0002	2759.3	3572.9	845

[*] Measured ratio.

700	197.4	-106.7	8994.4	0.1901	0.0167	2376.2	4546.8	924
		0.3		0.0002	0.0001			
800	51.7	-114.1	4383.3	0.1908	0.0292	572.2	1618.9	488
		0.3		0.0002	0.0001			
900	2.3	-35.19	7.7	0.1864	19.19	-	-	8
		12.02		0.0082	0.82			
1000	4.0	-40.68	0.5	0.2028	128.9[*]	-	-	2
		1.82		0.0013	0.4			
Total	424.4	-82.70	18689	0.1904	0.0493	6337.9	10835	2415
		1.01		0.0002	0.0005			
Total	423.0[3]	-83.55	18687[4]	0.1904	0.0493			
		0.94		0.0002	0.0005			

LEW 85328(HF/HCl residue),L28-A2, Pyrolysis, 1.00 mg

300			4.4	0.2019	0.6367	3.5	1.4
				0.0013	0.2093		
600	3.0	8.16	25.4	0.1931	9.245	202.1	25.7
		1.88		0.0009	0.044		
800	12.4	19.42	23.0	0.1930	1.541	14.9	12.1
		0.27		0.0003	0.015		
1000	2.2	25.85	15.8	0.1844	10.47	72.5	48.1
		0.91		0.0003	0.02		
1200	0.3	27.04	572.5	0.1906	0.0135	356.7	282.0
		4.93		0.0020	0.0007		
1400	160.3	11.96	1527.1	0.1907	0.0161	921.8	791.5
		0.30		0.0032	0.0003		
1500	112.9	-34.41	4456.0	0.1913	0.0325	1657.5	1086.5
		0.45		0.0002	0.0053		

---

[*] measured ratio
[3] Neglecting 200 °C step.
[4] Neglecting 200 °C and 1000°C steps

Temp								
1600	74.0	-81.25	2267.4	0.1914	0.0679	1556.7	1008.3	
		0.08		0.0001	0.0010			
1700	108.9	-100.5	2837.0	0.1906	0.2499	1958.7	1623.5	
		0.4		0.0001	0.0021			
1800	75.9	-100.5	800.3	0.1892	0.0641	725.1	981.6	
		0.6		0.0001	0.0040			
1801	Added to 1800 °C fraction		168.2	0.1890	2.007	161.2	554.2	
				0.0001	0.020			
1850	12.1	-101.1	37.8	0.1905	4.783	337.5	234.2	
		2.0		0.0006	0.077			
1851			4.1	0.2106	135.3	9.4	7.0	
				0.0002	0.7			
Total	561.8	-48.82	12739	0.1903	0.2042	7977.3	6656.9	
		0.41		0.0006	0.0384			

LEW85328($HClO_4$ residue), L28-O1, combustion, 2 torr O_2, 2.07 mg

Temp								
200	2.6		0.1	0.2949	140.7	0.9	-	0
				0.0048	4.2			
300	11.8	11.86	3.3	0.1943	5.409	3.1	4.3	6
		0.62		0.0002	0.081			
400	1.3	1.26	26.0	0.1872	0.914	28.6	56.3	44
		2.90		0.0002	0.004			
500	7.1	-4.12	50.4	0.1879	0.7708	61.6	128.8	156
		1.21		0.0003	0.0025			
600	61.4	-105.6	1586.3	0.1900	0.0920	1543.7	1459.1	890
		1.3		0.0003	0.0002			
700	154.2	-106.9	4156.7	0.1897	0.0234	3026.5	2481.5	960
		0.9		0.0002	0.0001			
800	168.7	-107.0	5145.1	0.1896	0.0475	2656.1	2163.9	954
		0.5		0.0002	0.0001			

900	75.0	-112.7	3656.0	0.1905	0.1344	1583.3	1504.1	790
		0.3		0.0003	0.0014			
1000	7.4	-63.88	0.3	0.1843	-	3.5	2.3	0
		4.40		0.0009				
Total	489.5	-102.1	14624	0.1899	0.0724	8908.2	7793.8	3800
		0.8		0.0002	0.0005			
Total			14624	0.1899	0.0724			
				0.0002	0.0005			

LEW85328(HClO$_4$ residue), L28-O2, pyrolysis, 1.40 mg

300			0.3	0.2791	38.29		
				0.0100	1.61		
600			0.5	0.2960	10.93		
				0.0041	0.46		
800	2.4	20.57	2.6	0.1960	2.641	5.2	7.7
		0.85		0.0020	0.244		
900	6.6	16.68	3.6	0.2028	1.675	5.4	5.9
		2.50		0.0011	0.249		
1000	11.7	10.93	10.5	0.1985	2.664	8.8	8.2
		0.34		0.0007	0.076		
1100	11.4	18.02	219.8	0.1873	1.068	148.1	109.4
		1.35		0.0021	0.010		
1200	25.6	7.98	1180.5	0.1864	0.073	665.7	534.9
		0.32		0.0002	0.001		
1300	27.3	-20.27	687.2	0.1867	0.112	533.2	394.2
		0.37		0.0001	0.004		
1350	11.3	-66.73	379.4	0.1879	0.003	320.6	250.6
		0.84		0.0001	0.006		
1400	10.4	-68.84	349.7	0.1878	0.065	312.6	263.0
		1.25		0.0001	0.007		

1425	9.4	-85.08	435.6	0.1874	0.040	364.1	312.0
		0.48		0.0001	0.006		
1450	11.1	-84.06	353.1	0.1877	0.521	336.9	287.9
		0.82		0.0001	0.007		
1475	12.7	-83.27	372.5	0.1878	0.085	337.5	329.4
		0.40		0.0001	0.007		
1500	11.7	-85.06	281.8	0.1879	0.242	290.3	257.1
		0.44		0.0001	0.006		
1525	12.8	-83.75	273.8	0.1880	0.359	286.6	266.2
		0.35		0.0178	0.020		
1550	10.8	-88.80	261.6	0.1878	0.318	287.9	271.3
		1.42		0.0132	0.007		
1575	3.8	-110.0	537.2	0.1872	0.290	625.5	543.0
		2.3		0.0072	0.004		
1600	7.5	-104.3	546.5	0.1871	0.249	613.8	514.4
		0.8		0.0001	0.005		
1625	7.2	-78.38	106.9	0.1885	3.624	99.7	83.1
		0.67		0.0256	0.029		
1650	5.6	-67.49	6.7	0.1925	47.295		
		0.40		0.0745	0.233		
Total	199.3	-46.63	6009.9	0.1873	0.326	5242.0	4438.2
		0.77		0.0027	0.007		

LEW85328(HClO$_4$ residue), L28-O3, pyrolysis, 0.69 mg

300	0.3	-	-	-			
600	0.3	-49.36	2.9	0.2095	10.81	11.1	10.2
		9.69		0.0023	0.23		
800	2.5	68.74	6.3	0.1963	0.5959	8.3	8.6
		3.98		0.0011	0.0654		
1000	1.5	7.20	18.4	0.1904	0.5970	10.8	7.5

Temp								
		4.58		0.0004	0.0359			
1200	0.03	-	83.9	0.1912	0.1506	58.3	27.2	
				0.0001	0.0089			
1400	95.9	-2.18	605.9	0.1903	0.1327	414.0	180.5	
		0.12		0.0002	0.0030			
1600	86.1	-68.11	4331.3	0.1912	0.1425	2014.3	797.0	
		0.14		0.0001	0.0008			
1850	454.9	-28.33	3746.7	0.1903	0.2293	2604.5	2332.3	
		0.28		0.0001	0.0019			
1851	40.6	-67.75	33.6	0.1899	12.57	44.5	322.3	
		0.77		0.0005	0.12			
1852	16.4	-42.31	-			22.0	125.4	
		0.14						
Total	695.8	-31.99	8829.1	0.1908	0.2609	5187.7	3810.9	
		0.29		0.0001	0.0021			

ALH81101(HF/HCl residue), A01-A, 2 torr O$_2$, 1.06mg

Temp								
200	3.8	27.09	0.2	0.2104	294.2			0
		1.07		0.0029	0.6			
300	3.1	20.98	1.2	0.2027	53.13	3.8	2.7	0
		3.11		0.0019	0.24			
400	23.9	14.90	5.8	0.1906	16.39	12.6	14.7	0
		0.28		0.0004	0.04			
500	45.2	13.52	20.4	0.1922	3.957	41.1	159.3	36
		0.11		0.0002	0.023			
600	36.3	-57.32	492.5	0.1908	0.0159	783.2	1232.1	685
		0.10		0.0002	0.0010			
700	21.2	-94.50	708.6	0.1895	0.0041	845.2	877.4	627
		0.90		0.0002	0.0007			
800	0.5	-57.67	3.5	0.2117	29.51	31.3	7.2	2

		1.03		0.0024	0.13			
1000	6.3	-4.87	0.8	0.1813	37.50	-	-	0
		4.63		0.0009	1.81			
Total	140.3	-21.42	1232.9	0.1902	0.3635	1717.1	2293.3	1350
		0.56		0.0002	0.0031			
Total			1232.7[5]	0.1902	0.3085			
				0.0002	0.0030			

ALH81101(HClO$_4$ residue), A01-O, 2 torr O$_2$, 1.06 mg

200	5.6	16.88	0.2	0.2767	197.1	-	-	0
		1.01		0.0040	0.9			
300	21.4	23.57	0.3	0.2778	89.28	-	-	0
		0.28		0.0028	0.58			
400	65.4	15.41	0.3	0.2041	53.35[6]	2.2	4.8	0
		0.56		0.0019	0.65			
500	70.1	12.37	5.8	0.1895	0.5018	40.5	152.7	85
		0.21		0.0014	0.0733			
600	63.4	-88.12	280.9	0.1895	0.2492	607.5	1030.2	503
		0.46		0.0002	0.0021			
700	107. 3	-107.7	1474.8	0.1902	0.0146	1457.4	1113.5	663
		0.2		0.0002	0.0021			
800	61.7	-63.15	228.2	0.1890	0.4185	154.5	143.5	86
		1.26		0.0002	0.0021			
1000	1.0	-17.96	1.2	0.1890	3.445	-	-	0
		16.15		0.0002	1.286			
Total	340.4	-44.26	1991.7	0.1894	0.1342	2262.0	2444.7	1337.0
		0.42		0.0002	0.0019			

ALH82130 (HF/HCl res.), A30-A, 2 torr O$_2$, 1.32mg

800p	1.7	87.29	10.7	0.2026	9.174	10.7	59.5	

---

[5] Neglecting 200 °C step
[6] measured ratio

		2.44		0.0004	0.027			
200	-		2.4	0.2365	181.948			
				0.0004	0.644			
300	0.1		3.1	0.2386	11.464			
				0.0002	0.298			
400	9.9	19.24	14.3	0.1965	4.091	9.8	10.7	
		4.82		0.0001	0.059			
450	11.4	19.54	28.3	0.1955	4.898	20.4	46.5	12
		0.71		0.0003	0.017			
500	2.3	26.02	17.3	0.1987	4.035	15.1	129.6	27
		3.07		0.0005	0.047			
600	27.2	-63.59	186.6	0.1877	22.75	168.3	1629.6	27
		0.58		0.0002	0.01			
700	47.6	-53.30	168.0	0.1894	140.99	275.2	2310.2	745
		0.68		0.0001	0.01			
800	6.5	-51.18	206.9	0.1894	2.389	125.1	625.8	290
		1.35		0.0001	0.007			
900	0.2	-	2.5	0.2072	40.402			
				0.0019	0.147			
1000	0.3	-	0.8	0.3305	25.546			
				0.0001	1.015			
1800p	1.1	-23.92	1.6	0.1943	303.5			
				0.0018	0.45			
Total	108.3	-37.66	642.6	0.1905	46.48	624.6	4811.9	
		1.21		0.0002	0.02			

ALH82130 (HClO$_4$ res.), A30-O, 2 torr O$_2$, 1.82mg

800p	11.6	8.06	1.5	0.1989	52.57	6.3	12.6	
		0.55		0.0005	0.05			
200	-		0.1	0.2440	285.1			

				0.0037	0.4			
300	0.2		1.3	0.2303	226.7			
				0.0007	1.0			
400	8.0	18.52	0.3	0.2944	51.13			
		4.39		0.0027	2.06			
450	3.3	14.42	0.9	0.2475	28.46	1.8	3.2	90
		2.42		0.0025	0.29			
500	7.5	-5.33	15.1	0.1916	0.3309	12.5	45.6	924
		0.98		0.0001	0.0418			
600	23.1	-80.67	123.2	0.1903	0.4870	158.5	282.0	1010
		0.52		0.0002	0.0053			
700	42.0	-103.3	150.6	0.1898	0.4160	236.2	208.0	168
		0.4		0.0003	0.0079			
800	3.0	-13.87	59.4	0.1909	2.659	55.1	32.6	
		0.90		0.0001	0.018			
900	-		0.3	0.1932	192.8	-	-	
				0.0014	1.2			
1000	-		1.1	0.2113	246.5	-	-	
				0.0014	0.1			
1800p	9.0	2.00	0.7	0.1783	278.6		-	
		2.17		0.0001	0.7			
Total	108.1	-56.34	354.6	0.1907	3.532	470.5	583.7	
		1.06		0.0002	0.019			

ALH 78019 (HF/HCl residue), A19-A, 1.35mg, combustion at 5 torr O$_2$

300	13.3	1.03	261.0	0.1888	0.2535	63.4	60.0	1
		1.42		0.0001	0.0010			
400	12.5	-21.09	987.3	0.1889	0.5468	577.1	130.2	1
		4.69		0.0001	0.0004			
450	19.7	-20.97	197.7	0.1858	0.0064	167.8	77.1	1

		0.55		0.0001	0.0015			
550	6.9	-11.14	98.8	0.1861	0.1141	120.2	90.0	14
		0.78		0.0001	0.0038			
650	11.8	-9.88	27.9	0.1916	0.0486	5.5	57.3	172
		1.26		0.0005	0.0324			
800	10.8	18.94	140.8	0.1893	0.8437	83.0	66.3	795
		2.62		0.0001	0.0176			
1000	7.3	10.06	68.1	0.1892	2.790	18.7	30.4	1020+
		0.39		0.0001	0.087			117[7]
Total	82.3	-7.02	1781.6	0.1885	0.5212	1035.7	511.1	2121
		1.70		0.0001	0.0060			

ALH 78019 (HClO$_4$ residue), A19-O, 1.00 mg, combustion at 5 torr O$_2$

300	12.2	-22.65	1.5	0.2184	268.1			0
		0.45		0.0003	0.5			
400	19.8	-8.16	2.7	0.1919	249.4	27.7		0
		0.83		0.0034	0.8			
450	8.7	-12.32	4.1	0.1887	285.4	7.9		0
		1.22		0.0001	0.8			
550	18.7	-10.88	33.2	0.1890	277.9	60.2	5.7	27
		0.41		0.0012	0.7			
800	72.2	-2.29	18.4	0.1885	295.1	25.8	30.2	206
		0.32		0.0010	0.3			
1050	25.3	3.24	n.d.	-	-	34.0	11.3	1240
		3.62						
Total	157.0	-5.30	59.9	0.1897	282.2	155.6	47.3	1473
		0.99		0.0005	0.6			

---

[7] CO$_2$ pressure at 1050 °C step.

4.2.4. Nitrogen in acid residue of polymict ureilites

The bulk sample of polymict ureilites showed two major nitrogen components. Though both monomict and polymict ureilites contain a heavy nitrogen released at lower temperature, this nitrogen in polymict ureilites is in general, more heavier than that found in monomict ureilites. The heavy nitrogen is volumetrically a major component and resides in a low temperature combustible phase. Except EET83309 (E09-B), both EET87720 and Nilpena show the presence of light nitrogen that is released at very high temperature on pyrolysis. In order to understand the nature of heavy and light nitrogen carriers towards acid treatment, acid residues of three polymict ureilites are analyzed and the data are compiled in Table 4.3.

EET87720(HF-HCl residues), E20-A1 & E20-A2……

The release patterns as well as the isotopic composition of nitrogen and noble gases are depicted in Fig 4.16. The E20-A1 yields 533 ppm of nitrogen with $\delta^{15}N$ of 21‰

Fig 4.16 *Stepwise combustion release pattern of nitrogen, argon and CO$_2$ of HF-HCl residue of EET87720 (E20-A1; polymict ureilite) (Wt. =1.76 mg). Sample is combusted at 2 torr O$_2$.*

and 4471×10^{-8} ccSTP/g of ^{36}Ar. Mass balance calculation reveals that nearly 40% of nitrogen in the bulk sample is carried by acid resistant residue E20-A1 (Table 4.6). Two nitrogen components are clearly seen as in residues from other ureilites. The bulk sample E20-B showed large proportion of heavy nitrogen with highest δ^{15}N of 196‰ while E20-A1 also yields large amount (>55%) of relatively heavy nitrogen with maximum δ^{15}N of 108‰ at temperature below 500°C. Nearly 40% of the total nitrogen released between 600-800°C is light with lowest value of δ^{15}N of −60‰ and is accompanied by primordial noble gas release and peak carbon combustion. The lowest observed δ^{15}N in bulk sample (E20-B) is much lower (-100‰) than that observed for E20-A1 (could have been obscured by mixing of small amount of heavier nitrogen). The heavy nitrogen too is not as heavy as observed in case of bulk sample and could most likely be modified by co-release of adsorbed atmospheric nitrogen that is acquired during acid dissolution. The reduction in the relative proportion of heavy nitrogen as compared to light nitrogen indicates that the heavy nitrogen carrier is partially removed by mineral acid (HF-HCl) treatment.

Another aliquot of acid resistant residue of EET87720 (E20-A2) has been analyzed by pyrolysis to understand the nature of heavy and light nitrogen present in this meteorite. The release patterns of nitrogen and argon are shown in Fig 4.17. The gases are extracted by stepwise pyrolysis from 300°C to 1850°C in 13 steps. The sample yields 646 ppm of nitrogen with bulk δ^{15}N value 54‰ and 2640×10^{-8} ccSTP/g of ^{36}Ar. Like E20-A1, two nitrogen peaks can clearly be seen with very distinct δ^{15}N. The nitrogen released at lower temperature steps is heavy, peaking at 1400°C along with peak in δ^{15}N of 106‰ which is very close to highest δ^{15}N measured for E20A1. At higher temperatures, the release is dominated by light nitrogen (with $\delta^{15}N_{min} = −24$ ‰) but the composition of this component is not completely resolved because of co-release of small amount of heavy nitrogen. Though the maximum δ^{15}N measured yields similar values for both the aliquots done by combustion and pyrolysis, this is quite lower than that measured for bulk sample E20-B (196‰). This indicates that either corelease of air nitrogen trapped during acid dissolution or early release of light nitrogen along with indigenous heavy nitrogen is responsible for lowering the δ^{15}N measured for the heavy nitrogen. Though the nitrogen yield in E20-A2 is 20% higher than that of E20-A1, the noble gas concentrations are lower (Ar is 60% of E20-A1).

Fig 4.17 *Stepwise release pattern of nitrogen and argon on pyrolysis of HF-HCl residue of EET87720 (E20-A2; polymict ureilite) (Wt. =1.07mg).*

This is an indication of heterogeneous distribution of heavy and light nitrogen carriers and that the carrier of heavy nitrogen is depleted in noble gas concentration and enriched in nitrogen as compared to the carrier of light nitrogen.

EET87720 (HClO₄ residues), E20-O……

The release patterns as well as isotopic composition of nitrogen and noble gases are shown in Fig 4.17 and data are compiled in Table 3.2. The sample E20-O yields 182 ppm of nitrogen with bulk $\delta^{15}N$ of –52‰ and 4156 $\times 10^{-8}$ ccSTP/g of ^{36}Ar. Most of the heavy nitrogen released at lower temperatures in E20-B, E20-A1 and E20-A2 is removed by perchloric acid treatment. The small amount of residual heavy nitrogen left is released at temperature ≤500°C and shows the maximum $\delta^{15}N$ value of 19‰ that is much lighter than observed for other residues of the EET87720 discussed above. Nearly 70% of nitrogen released at temperature higher than 600°C is light with lowest $\delta^{15}N$ value of -99‰ and is accompanied by primordial noble gas release and CO_2 release. Excursion in $\delta^{15}N$ at 900°C and 1000°C requires another minor nitrogen component.
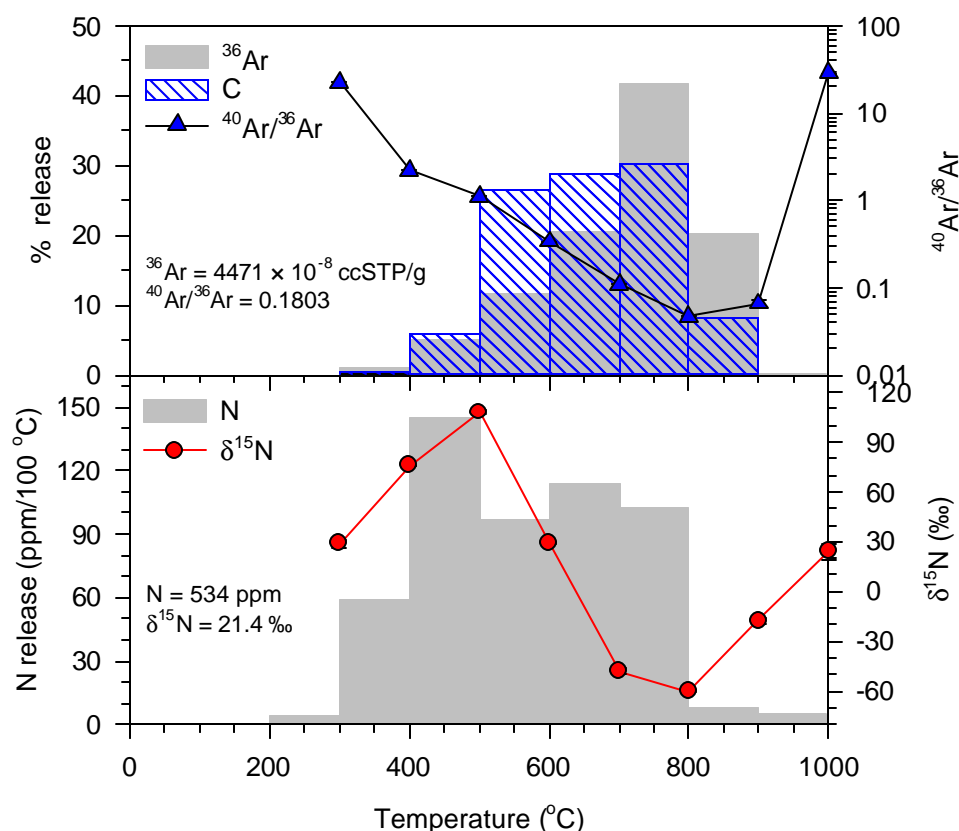
Fig 4.18 *Stepwise combustion release pattern of nitrogen, argon and CO₂ of oxidized residue of EET87720 (polymict ureilite) (Wt. = 1.89 mg). The sample is combusted at 2 torr O₂.*

Nilpena (HF-HCl residue) Nil-A1 & Nil-A2……

Release patterns and isotopic composition of nitrogen and noble gases are shown in Fig 4.19 and data are listed in Table 4.2. The sample Nil-A yields 274 ppm of nitrogen with bulk $\delta^{15}N$ value of -42‰ and 3756×10^{-8} ccSTP/g of ^{36}Ar. Nil-A accounts for nearly 40% of the total nitrogen carried by the sample Nil-B (Table 4.6). Two nitrogen components are clearly visible from the release pattern as well as isotopic composition. A heavy nitrogen release at lower temperatures of <500°C with highest value of $\delta^{15}N$ of 77‰ and accompanied by only minor amount of noble gases and CO_2 release. The light nitrogen on the other hand is released at higher temperature of >600°C with lowest value of $\delta^{15}N$ of –110‰ and is accompanied by peak noble gases release and CO_2 release. Another minor nitrogen component is required to explain the excursion in $\delta^{15}N$ at 800°C onward.
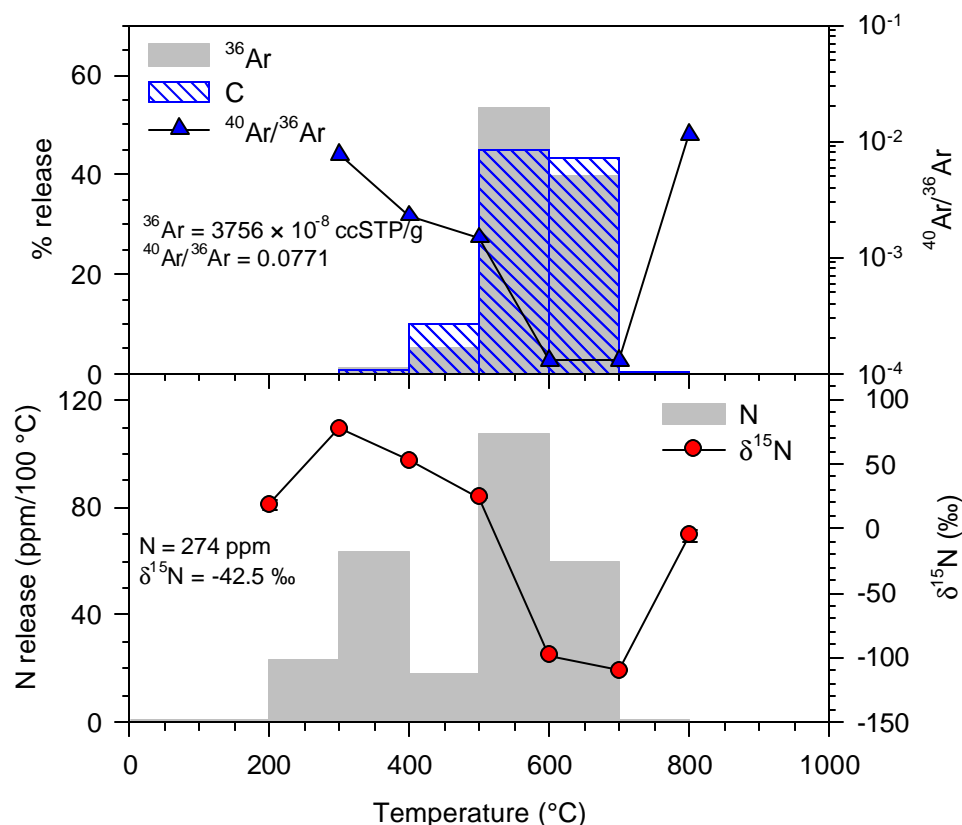
Fig 4.19 *Stepwise combustion release pattern of nitrogen, argon and CO_2 of HF - HCl residue of Nilpena (Nil-A1; polymict ureilite) (Wt. = 2.57 mg). Sample is combusted at 2 torr O_2.*

The second aliquot of this sample (Nil-A2) has been pyrolyzed stepwise from 300°C to 1850°C in thirteen steps. The release patterns as well as isotopic composition of nitrogen and argon are shown in Fig 4.20. Nil-A2 contains 517 ppm of nitrogen with bulk $\delta^{15}N$ value of 7‰ and 3337 $\times 10^{-8}$ ccSTP/g of ^{36}Ar. Similar to Nil-A1, this sample also shows two nitrogen components. The heavy nitrogen released at relatively lower temperature with peak at 1400°C has the highest $\delta^{15}N$ value of 50‰. This is quite lower than that observed for Nil-A1 (77‰). The second nitrogen component is light with lowest $\delta^{15}N$ of –73 ‰ and is also much heavier than that measured for Nil-A1. This is most likely due to overlap of release temperature of heavy and light nitrogen components on pyrolysis. The nitrogen released from Nil-A2 is almost double of that observed for Nil-A1. The bulk $\delta^{15}N$ is also higher than that measured for previous aliquot. That is due to release of higher proportion of heavy nitrogen relative to light nitrogen. The higher amount of total nitrogen release with

relatively high $\delta^{15}N$ and lower amount of noble gases is due to heterogeneous distribution of heavy nitrogen carrier, which is depleted, in primordial noble gases.
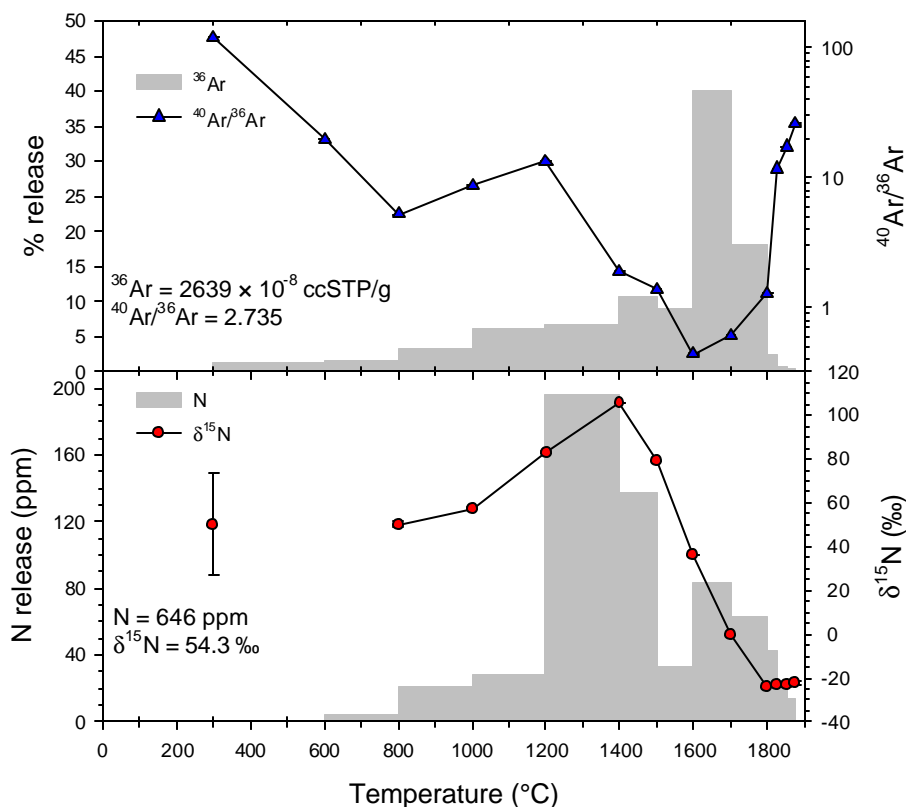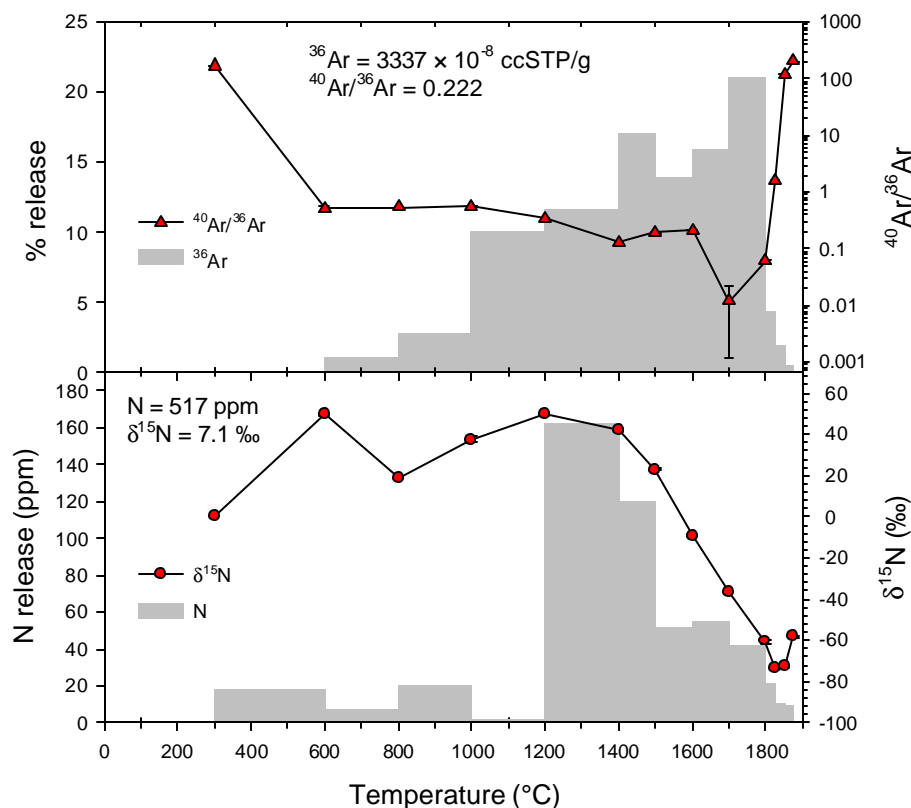

Fig 4.20 *Stepwise release pattern of nitrogen and argon on pyrolysis of HF-HCl residue of Nilpena (Nil-A2; polymict ureilite) (Wt. = 1.07 mg).*

EET83309(HF-HCl residue), E09-A……

The release patterns as well as isotopic compositions of nitrogen and argon are shown in Fig 4.21 and data are listed in Table 4.3. The gases are extracted by combustion at 2 torr O_2 pressure from 200°C to 1000°C in steps of 100°C. The sample yields 126 ppm of nitrogen with bulk $\delta^{15}N$ of 52‰ and 5229×10^{-8} ccSTP/g of ^{36}Ar. The acid resistant residue of EET83309 (E09-A) contributes nearly 45% of nitrogen contained by the bulk sample (E09-B) (Table 4.6). The nitrogen release peaks at 500°C while the heaviest nitrogen is observed at 700°C with highest $\delta^{15}N$ value of 153‰ and immediately followed by lightest nitrogen measured that is having $\delta^{15}N$ value of only –22‰. Though the light nitrogen composition measured here is much heavier than that observed for other monomict as well as polymict ureilites, it might be an indication of the presence of small amount of diamond (carrier of light nitrogen) with
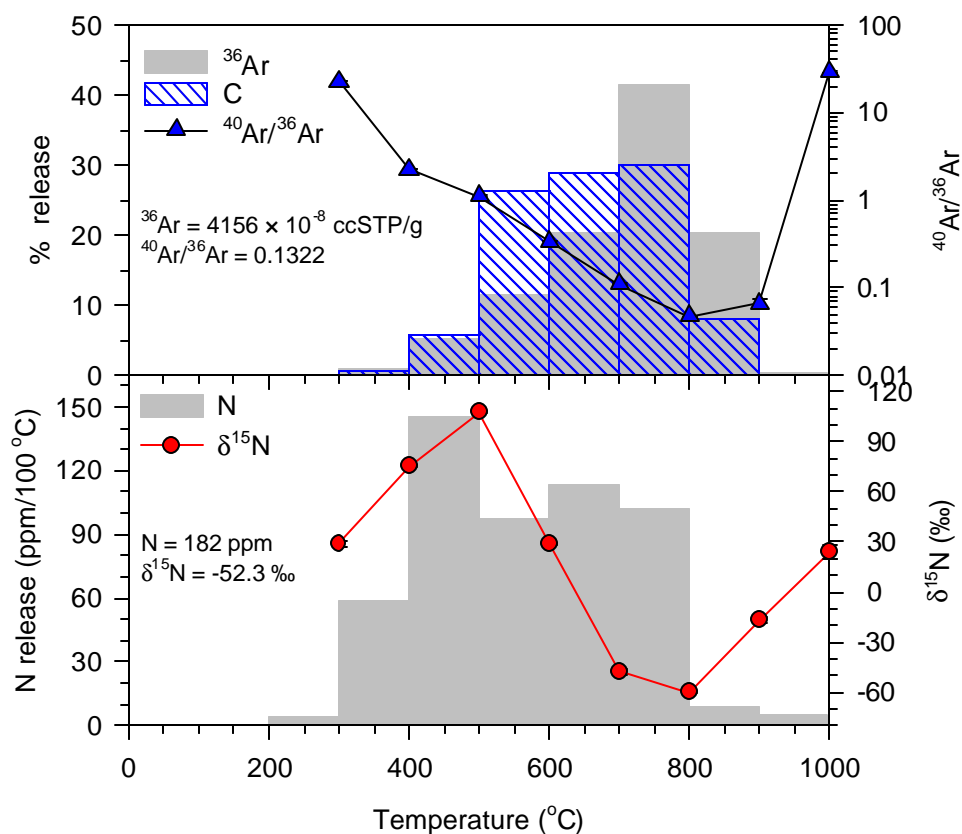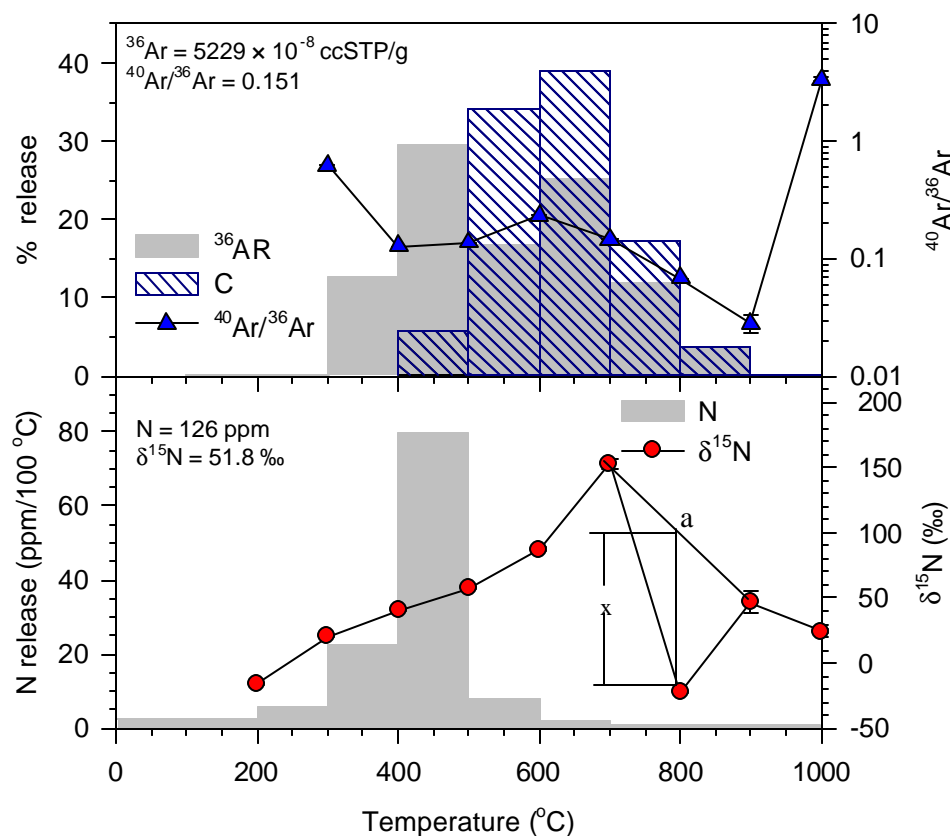
Fig 4.21 *Stepwise combustion release pattern of nitrogen, argon and CO₂ of HF-HCl residue of EET83309 (E09-A; polymict ureilite) (Wt. =1.63 mg). Sample is combusted at 2 torr O₂. The negative excursion of d¹⁵N at 800°C, is due to a admixture of a (hypothetical) heavy component (indicated by 'a') and a light component whose d¹⁵N £−120‰, can be derived.*

$\delta^{15}N$ of ≤ -100‰ and the signature is not completely resolved due to simultaneous release of heavy nitrogen (as shown by the arrow in the Fig 4.21 at 800°C). **The noble gases on the other hand show bimodal release (peaks at 500°C and 700°C) indicating that the heavy nitrogen in E09-A is accompanied by primordial noble gases unlike in other ureilites where the heavy nitrogen carrier is depleted in noble gases.** This has already been observed from bulk sample analysis where large amounts of noble gases are released at lower temperatures (Fig 3.10). The heaviest nitrogen measured here is much lighter than that reported for acid resistant residue of the same meteorite by Grady & Pillinger (1988) who reported a $\delta^{15}N$ value of 211‰ at 400°C combustion. They have observed light nitrogen (<15% of total) with lowest $\delta^{15}N$ value of -94‰ at 1000°C on combustion. The inconsistency between the nitrogen amounts and $\delta^{15}N$ is most likely due to heterogeneous distribution of heavy
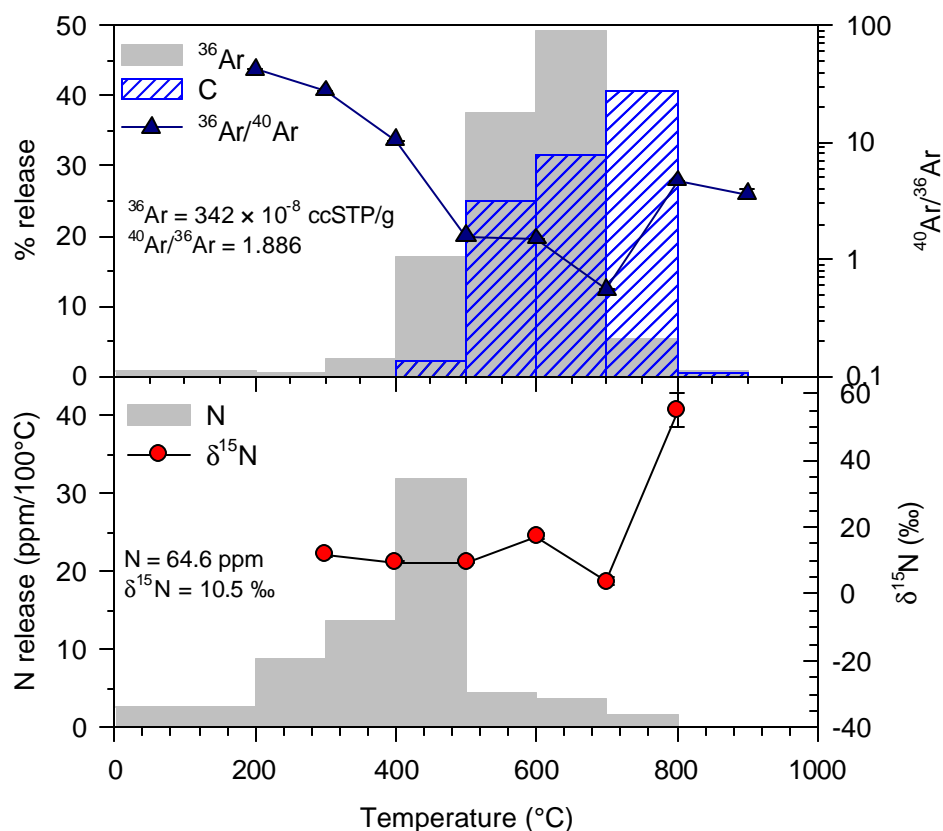
Fig 4.22 *Stepwise combustion release pattern of nitrogen, argon and CO₂ of oxidized residue of EET83309 (E09-O; polymict ureilite) (Wt. = 1.61 mg). Sample is combusted at 2 torr O₂.*

and light nitrogen carriers. A minor amount of adsorbed atmospheric nitrogen and could also be responsible for the poor resolution of heavy and light nitrogen.

EET83309(HClO₄ residue), E09-O……

The release patterns of nitrogen and argon of E09-O are shown in Fig 4.22 and the data are listed in Table 4.2. The sample yields 65 ppm of nitrogen with bulk $\delta^{15}N$ value of 10.5‰ and 342×10^{-8} ccSTP/g of ^{36}Ar. Nearly half of the nitrogen and more than 90% of the noble gases are removed by perchloric acid treatment. The release of nitrogen peaks at 500°C while the isotopic composition yields plateau in $\delta^{15}N$ of between 0 to 20‰ except slight increase in $\delta^{15}N$ at 800°C where less than 3% of nitrogen is released. The loss of noble gases by perchloric acid treatment and absence of light nitrogen (with $\delta^{15}N$ of $\leq -100‰$) indicates the absence of diamonds in this sample. But the presence of a small amount of light nitrogen in E09-B and E09-A but not in E09-O could also be possible by the presence of small amount of very fine

grained diamonds which would have been lost by perchloric acid treatment through colloidal solution (Amari *et al.*, 1994).

Table 4.3 Nitrogen and noble gas in acid residues of polymict ureilites.

Temp (°C)	N (ppm)	$\delta^{15}N$ (‰)	^{36}Ar 10^{-8} ccSTP/g	$^{38}Ar/^{36}Ar$	$^{40}Ar/^{36}Ar$	^{84}Kr 10^{-10} ccSTP/g	^{132}Xe	$P_{\Sigma(CO2+CO)}$
EET83309 (HF/HCl residue), E09-A, combustion, 2 torr O$_2$, 1.63mg								
200	5.6	-15.59						0
		0.70						
300	5.9	20.27	5.7	0.1877	0.6240[8]	25.7	13.2	0
		0.86		0.0002	0.0003			
400	22.7	40.48	662.0	0.1891	0.0944	433.4	233.8	0
		0.59		0.0002	0.0002			
500	79.5	57.29	1542.9	0.1898	0.1367	1845.91	1798.6	120
		0.39		0.0002	0.0004			
600	7.7	87.38	878.2	0.1908	0.2347	2841.50	2986.3	715
		2.11		0.0006	0.0006			
700	2.1	152.68	1320.4	0.1912	0.1435	3088.4	2747.3	815
		3.62		0.0002	0.0004			
800	1.1	-22.26	628.5	0.1902	0.0674	978.3	740.8	360
		1.36		0.0002	0.0005			
900	1.0	46.51	178.6	0.1898	0.0253	167.4	92.9	80
		8.32		0.0004	0.0051			
1000	0.9	24.43	12.1	0.1889	3.378	3.9	2.1	4
		1.26		0.0018	0.132			
Total	126.4	51.79	5228.9	0.1903	0.151	9384.4	8117.9	2094
		0.69		0.0003	0.001			

EET83309 (HClO$_4$ residue), E09-O, combustion, 2 torr O$_2$, 1.61mg

---

[8] As measured (without blank correction)

200	5.4		2.8	0.2063	42.06	4.5	4.7	0
				0.0020	0.25			
300	8.7	11.68	1.2	0.1998	27.68	6.9	2.4	0
		0.36		0.0032	0.06			
400	13.6	9.38	7.3	0.1913	10.41	12.9	4.6	0
		0.32		0.0002	0.04			
500	31.8	9.46	51.6	0.1899	1.579	57.0	28.6	44
		0.27		0.0003	0.007			
600	4.4	16.98	112.9	0.1896	1.506	112.1	71.2	530
		0.71		0.0002	0.004			
700	3.9	-0.71	148.0	0.1878	0.5607	267.1	88.1	667
		1.07		0.0003	0.0028			
800	1.9	40.62	16.1	0.1904	4.712	18.8	8.9	862
		5.25		0.0007	0.016			
900			2.5	0.1945	3.619			12
				0.0009	0.313			
1000								0
Total	64.6	10.54	342.3	0.1892	1.886	479.3	208.5	2115
		0.54		0.0003	0.010			

Nilpena(HF/HCl residue), Nil-A1, combustion, 2 torr O_2, 2.57mg

200	1.3	18.80						0
		3.78						
300	23.1	77.22	5.0	0.1924	2.745	6.5	4.6	2
		0.41		0.0006	0.008			
400	62.5	52.61	43.0	0.1891	0.9704	31.7	28.8	23
		0.37		0.0002	0.0023			
500	18.1	24.36	195.4	0.1891	0.3466	108.5	109.4	270
		0.46		0.0002	0.0015			
600	107.9	-98.12	1999.3	0.1895	0.0463	834.9	385.1	1200

		0.42		0.0002	0.0001			
700	59.9	-109.9	1492.5	0.1901	0.0164	750.5	294.8	1150
		0.2		0.0002	0.0001			
800	1.0	-5.21	20.7	0.1904	1.806	17.3	12.4	13
		4.60		0.0005	0.012			
1000	0.1							0
Total	273.9[9]	-42.47	3755.9	0.1897	0.0771	1749.5	835.0	2658
		0.39		0.0003	0.0003			

Nilpena(HF/HCl residue), Nil-A2, pyrolysis, 1.07mg

300	-	-	2.8	0.2142	168.6		
				0.0026	0.3		
600	17.9	49.43	2.6	0.1856	0.5227	26.3	22.6
		0.36		0.0001	0.0611		
800	6.9	18.79	36.2	0.1918	0.5376	21.7	10.9
		0.28		0.0007	0.0081		
1000	20.1	37.44	91.5	0.1917	0.5621	53.6	33.0
		1.31		0.0005	0.0040		
1200	1.8	49.88	332.2	0.1902	0.3453	205.6	146.8
		0.65		0.0001	0.0012		
1400	162.5	42.35	387.4	0.1902	0.1286	182.1	129.8
		0.10		0.0001	0.0055		
1500	119.6	22.89	568.7	0.1902	0.1915	198.7	165.9
		0.44		0.0001	0.0056		
1600	51.1	-8.89	463.9	0.1906	0.2131	164.6	93.0
		0.26		0.0002	0.0047		
1700	55.2	-36.66	530.0	0.1893	0.0118	282.0	140.9
		0.23		0.0001	0.0106		
1850	41.7	-60.34	699.9	0.1887	0.0603	268.9	186.3
		0.98		0.0001	0.0047		

[9] Neglecting 1000° C step

1851	21.5	-73.44	146.0	0.1889	1.575	66.2	88.8	
		0.73		0.0001	0.048			
1852	10.1	-72.84	62.5	0.1837	119.9	44.3	42.8	
		0.20		0.0005	0.1			
1853	8.6	-58.14	13.3	0.1888	204.1	14.2	23.4	
		0.48		0.0004	0.1			
Total	517.0	7.14	3337.1	0.1897	0.222	1528.2	1084.3	
		0.37		0.0001	0.007			

Total

EET87720(HF/HCl residue), E20-A1, combustion, 2 torr O$_2$, 1.76mg

200	0.1		0.2	0.2242	64.50			0
				0.0012	0.13			
300	3.9	28.94	1.6	0.1957	22.66	2.7	2.4	1
		2.13		0.0011	0.08			
400	58.8	75.56	40.9	0.1893	2.243	34.3	63.3	17
		0.25		0.0072	0.006			
500	145.0	107.9	228.0	0.1894	1.116	148.2	275.9	172
		0.8		0.0002	0.003			
600	97.0	29.05	518.3	0.1907	0.3381	265.0	435.0	775
		0.39		0.0004	0.0007			
700	113.7	-47.81	911.7	0.1906	0.1099	306.0	507.6	850
		1.43		0.0002	0.0004			
800	101.9	-60.12	1856.6	0.1908	0.0470	751.0	548.6	885
		0.51		0.0002	0.0002			
900	8.2	-17.17	903.3	0.1908	0.0663	280.6[10]	204.9	237
		1.85		0.0002	0.0063			
1000	4.9	23.93	10.3	0.1935	[11]28.69	6.6	2.8	1
		0.81		0.0003	0.037			

---

[10] calculated based on previous step Kr/Xe ratio (lost due to defective MS valves)
[11] measured value, without blank correction.

Total	533.5	21.44	4470.8	0.1907	0.1826	1794.4	2039.9	2938
		0.81		0.0003	0.0018			
Total [12]	533.4	21.45	[13]4470.7	0.1907	0.1803			
		0.81		0.0003	0.0018			

EET87720(HClO$_4$ residue), E20-O, combustion, 2 torr O$_2$, 1.89mg

200	0.2		0.1			n.d.	n.d.	0
300	5.5	10.11	0.2	0.2216	86.62	n.d.	n.d.	1
		1.91		0.0019	1.14			
400	28.3	19.22	3.3	0.1902	12.62	3.1	3.3	20
		2.56		0.0003	0.07			
500	20.3	8.03	26.0	0.1899	0.8784	9.4	16.0	104
		0.38		0.0004	0.0045			
600	37.2	-55.04	583.7	0.1909	0.4056	67.7	219.5	830
		0.27		0.0002	0.0009			
700	61.0	-93.96	2487.8	0.1911	0.0706	586.7	580.1	1090
		0.55		0.0002	0.0001			
800	22.1	-99.26	1054.4	0.1906	0.0647	243.6	246.4	740
		0.24		0.0002	0.0073			
900	4.4	-43.52	0.8			2.8	1.1	3
		1.01						
1000	2.5	-34.35	-.	-	-			0
		1.90						
Total	181.6	-52.33	4156.2	0.1909	0.1322	907.7	1066.3	2788
		0.82		0.0002	0.0026			

EET87720(HF/HCl residue), E20-a2, pyrolysis, 1.07mg

300	0.8	50.22	1.4	0.1945	120.1			
		23.00		0.0034	0.1			
600	0.3	-	31.2	0.1896	19.60	30.6	33.2	

---

[12] neglecting 200 °C temperature step.
[13] neglecting 200 °C temperature step.

				0.0003	0.02		
800	3.8	50.09	37.6	0.1900	5.194	27.4	23.5
		1.41		0.0003	0.026		
1000	21.0	57.55	88.6	0.1897	8.638	51.8	46.9
		0.26		0.0075	0.034		
1200	28.1	82.95	159.4	0.1888	13.310	126.8	104.9
		0.43		0.0004	0.013		
1400	195.4	105.9	175.0	0.1906	1.882	136.7	156.2
		0.1		0.0001	0.007		
1500	137.4	79.09	281.9	0.1910	1.373	140.4	154.3
		0.12		0.0001	0.005		
1600	33.1	36.08	236.9	0.1899	0.4360	115.3	80.2
		0.28		0.0001	0.0090		
1700	82.8	-0.01	1058.0	0.1902	0.6087	397.9	235.9
		0.120		0.0001	0.0036		
1850	63.4	-24.17	480.3	0.1890	1.288	190.0	153.0
		0.31		0.0001	0.010		
1851	42.0	-23.15	64.5	0.1888	11.73	29.9	49.6
		0.74		0.0001	0.09		
1852	23.9	-23.19	15.0	0.1900	17.23	10.1	14.8
		0.95		0.0002	0.19		
1853	14.1	-22.45	10.2	0.1911	25.67	8.0	11.0
		0.83		0.0001	0.19		
Total	646.0	54.33	2639.8	0.1894	2.735	1264.7	1063.5
		0.28		0.0004	0.012		

4.3 Discussion

4.3.1 Comparison to literature data

Most of the acid residues of ureilites have been analyzed for the first time for nitrogen. For the cases of the few residues where literature data is available for comparison, the match is not exact, though the trends are similar. For the HF/HCl residue of EET83309, Grady and Pillinger (1988) have reported the extreme $\delta^{15}N$ of 540‰, which is not found in the present study. The earlier measurement of acid residue of Nilpena, yielded $\delta^{15}N$ value of -74‰ with lowest value of -83‰(Russell *et al.*, 1993). Acid resistant residue analyzed in this study yielded bulk $\delta^{15}N$ of –42 ‰ with the lowest value of –110‰. The lowest value of $\delta^{15}N$ for acid resistant residue of any ureilites is for –118.1 ‰ for Novo Urei (Russell *et al.*, 1993) which is close to the lowest value of -114.1‰ measured for L28-A1. These differences are due to heterogeneity of the residues in terms of the proportion of different carbon phases in a given aliquot.

4.3.2 Heterogeneity of acid resistant residues

The repeat analysis of the acid resistant residues from several ureilites did not reproduce the results and the discrepancy is beyond the analytical uncertainty. In most of the cases, the second aliquot has been analyzed by pyrolysis if the first one is done by combustion. The reason for this discrepancy is either incomplete release of gases in pyrolysis at the temperature achieved by RF heater (1850°C) or the residue itself is heterogeneous. The former is less likely because the repeat analysis at 1850°C did not yield appreciable amount of gases in the final steps (except for one sample L28-O2) and this is also favored by more nitrogen concentration (in some of the cases) than the aliquot done by combustion. The only option that remains is the heterogeneity of acid residue. SEM pictures (Fig 4.1), XRD (from literature) and noble gas and nitrogen isotopic studies of the acid residues from ureilite give clear indication of three major carriers of nitrogen present in residues; graphite, diamond and amorphous carbon. It should be noted here that ureilites contain two types of amorphous carbon, the first one contained by diamond bearing ureilites and most likely lost a major part of their noble gases, while the second one is enriched in noble gases as well as nitrogen. Apart from these three major carbonaceous components, a small amounts of refractory oxides, chromites and some other components (Wacker, 1986) are also present in acid

residues but these are of little importance for noble gas and nitrogen systematics because they are supposed to be poor in volatiles as well as contribute very small fraction of bulk mass of acid residues. The diamond is highly enriched in nitrogen and noble gases, while the amorphous carbon contain nitrogen in all the ureilites except two, in concentrations comparable to or higher than diamond but depleted in noble gases. In A19-A and E09-A, most of the noble gases and nitrogen are carried by amorphous carbon. Graphite, which is present as coarse-grained crystal (Fig 4.1), contains significant amounts of nitrogen but no noble gases. The isotopic compositions of nitrogen are also quite different in these three phases *e.g.*, the diamond has very light nitrogen ($\delta^{15}N \leq -100$ ‰), nitrogen from graphite has $\delta^{15}N$ ≥ 19‰ (in A19-A) while the amorphous C exhibit very large range of nitrogen composition from $\delta^{15}N \geq 20$‰ to 540‰ (Murty *et al.*, 1999; Grady and Pillinger, 1988). Heterogeneous contributions of these three phases in sample analyzed for noble gases and nitrogen may cause the observed discrepancy in gas concentrations *e.g.*, higher proportion of amorphous carbon relative to diamond and graphite can lead to high concentration of nitrogen but low concentration of noble gases. The higher proportion of graphite in the sample can result in lowering of both nitrogen and noble gas concentrations. Also, most of the residues are of mixed grain size, with coarse-grained graphite most abundant (Fig 4.1). When the samples of size ~1 mg are taken from the total residue, it is not ensured to be representative of total with respect to grain size distribution. A couple of coarse graphite grains in the ~1mg sample size can increase the relative proportion of graphite and the consequent change in nitrogen noble gas amounts and the $\delta^{15}N$. In almost all the cases of repeat analysis of two aliquots, where higher nitrogen concentrations are observed, they are accompanied by low noble gas concentration, implying relatively more amorphous C phase present that in turn led to high $\delta^{15}N$ (amorphous carbon from diamond bearing ureilites have largest concentration of nitrogen among all the three phases because of their negligible mass). The noble gas measurements from the literature also showed large variations (up to 50% or more) in concentration of trapped primordial gases from measurement of two aliquots (see Table 4 in Göbel *et al.*,1978), though they showed uniform isotopic composition.

4.3.3 Carriers of heavy and light nitrogen

The acid residues from monomict ureilites as well as polymict ureilites show two isotopically very distinct major nitrogen components, a heavy nitrogen and a light nitrogen. The heavy nitrogen in monomict ureilites, in general, has lower $\delta^{15}N$ than in polymict ureilites. In acid resistant residues of monomict ureilites, the $\delta^{15}N$ of heavy nitrogen lies between 0 to +87‰ (for A30-A) while in polymict ureilites the $\delta^{15}N$ ranges from 77‰ to 153‰. The carrier of heavy nitrogen is a highly combustible phase and combusts at lower than 500°C in most cases but some times its release can be felt at temperatures of >600°C on combustion. On pyrolysis, the heavy nitrogen is released up to 1400°C or even higher temperatures affecting the resolution of the $\delta^{15}N$ of light nitrogen significantly. In most cases, the heavy nitrogen is not accompanied by primordial noble gases and CO_2 release (during combustion). In E09-A, most of the nitrogen released is heavier with only a minor release of light nitrogen at 800°C.

The light nitrogen on the other hand showed relatively narrow range of $\delta^{15}N$, between -100 to -125 ‰ (KNA-B) unless it is obscured by small amount of heavy nitrogen (Fig 4.7 & 4.8). The peak release of light nitrogen, in general, is observed between 600°-800°C on combustion and ≥ 1400°C on pyrolysis. The release of light nitrogen is always accompanied by peak noble gas release and peak carbon combustion. The peak carbon combustion in acid resistant residues of all the ureilites but one is lying between 600°-800°C that is similar to the combustion characteristics reported for graphite/diamond (Grady *et al.*, 1985). Therefore based on only combustion it is difficult to ascertain whether the gases are released from diamond or graphite. But using both combustion and pyrolysis, this task can be achieved easily because the diamonds release their gases at higher temperature as compared to graphite (Table 4.5) (Göbel *et al.*, 1978). The very high release temperature on pyrolysis together with combustion release profile of acid resistant residues indicates that the carrier of noble gases and light nitrogen is diamond and not graphite. The light nitrogen and primordial noble gases are unaffected by the perchloric acid treatment further confirming that the carrier is diamond. If the light nitrogen is presumed to be the indicator for presence of diamond, the very high release temperature of light nitrogen on pyrolysis of diamond rich residues also support that the graphite is not the carrier

of trapped noble gases. That graphite is not a noble gas carrier is more clear from the ALH78019 residue.

In ALH19-A, most of nitrogen and noble gases are released at temperatures less than 550°C where less than one percent of carbon combusts. Most of the carbon that combusted at further higher temperatures is almost free of primordial noble gases but contained some nitrogen ($\delta^{15}N_{max}$ =19‰). The acid resistant residue of Dhajala [a chondrite of petrologic class H3.8, which does not contain presolar diamonds as
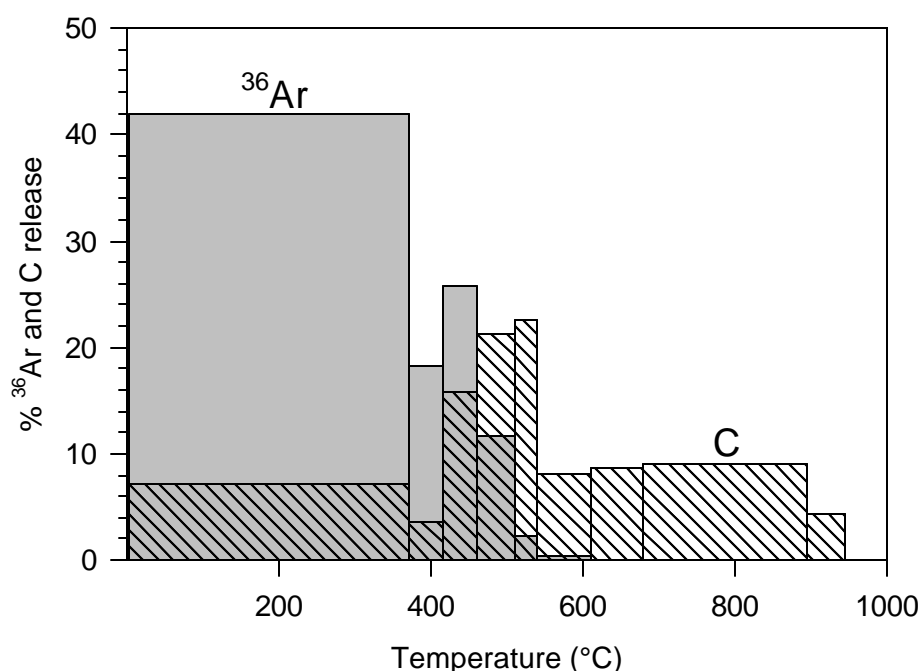
Fig 4.23 *Stepwise combustion release pattern for argon and carbon (CO$_2$) of HF-HCl resistant residue (Phase Q) from Dhajala (H3.8) chondrite (reproduced from Schelhaas et al., 1990). Most of the primordial noble gases trapped in only minor portion of carbon.*

inferred from absence of Xe-HL (Schelhaas *et al.*, 1990)] also showed a very similar release pattern of noble gases (Q-gases) and CO$_2$ on combustion (Fig 4.23). In both the cases, the gases are lost by oxidizing acid treatment without loosing appreciable mass, indicating that the noble gases in ALH78019 also reside in some ill defined carbon phases similar to Q-phase, the carrier of primordial trapped noble gases in primitive chondrites. It has already been established that the carrier of Q gases is an ill-defined carbon phase (Frick & Chang, 1978, Ott *et al.*, 1981; Frick and Pepin, 1981). Wacker (1986) showed that the primordial noble gases in ALH78019 are

highly concentrated in fine-grained phase (≤10 micron) that is acid resistant (HF-HCl). XRD of the HF-HCl residue reveals only graphite lines (Ott *et al.*, 1984) and the combustion experiment clearly established that graphite, combusting at higher temperature is noble gas free. This supports the observation of Göbel *et al.* (1978) that the graphite in ureilite is gas free. This implies that any model for the origin of diamonds in ureilites, which assume that the graphite is the precursor of diamond can be ruled out. The low temperature combustion characteristics of the noble gas carrier in ALH78019 are consistent with amorphous carbon (any crystalline phase of carbon or refractory silicate should have revealed itself in XRD). By combining all the above observations we inferred that the trapped primordial gases in ALH78019 are carried by a fine grained carbon phase similar to Q phase. In later discussion, we refer this phase as amorphous carbon.

From the SEM picture of ALH78019, it is clearly seen that the acid residue contains large (>100 microns and visually quite different from other ureilites) crystals of graphite over which some amorphous type of material is coated. Perchloric acid treatment removes this amorphous material resulting in a clean and shiny graphite crystal surface (Fig 4.1 y, z, z1 & z2). Combining these informations with nitrogen and noble gases results in acid resistant as well as oxidized residues, it can be inferred that almost all the noble gases reside in fine grained amorphous carbon material that comprises only < 1 wt % of total carbon. If we normalized the concentration of noble gases to the weight of amorphous carbon rather than weight of total carbon (mostly gas free graphite), we infer 100-fold increase in gas concentration in amorphous carbon phase. This is at least 10 times higher gas concentration than observed for the diamonds from any ureilites. This implies that the amorphous carbon can trap very high amount of gases as compared to that of diamonds. It is also supported by the laboratory simulation experiment where the trapping efficiency of amorphous carbon (produced by CVD process) is shown to be orders of magnitude higher than that of CVD produced diamond (Fukunaga *et al.*, 1997). The amorphous C is less refractory as compared to diamonds and very prone to loose their trapped gases during parent body processing. This might be the cause for lower noble gas concentration in amorphous C in diamond bearing ureilites. Nitrogen on the other hand can form chemical bonding with carbon and this could be the cause for survival of a significant fraction of nitrogen.

Unlike noble gases which are depleted in graphite as indicated by the negligible release of argon along with peak carbon combustion (Fig 4.14), graphite contains appreciable amount of nitrogen with $\delta^{15}N$ of 19‰. This is a very important information because it is difficult to measure the nitrogen composition of graphite in other ureilites in the presence of diamonds that are not only highly enriched in nitrogen but also have very light nitrogen. In absence of any reliable measurement of nitrogen composition in graphite from diamond bearing ureilite, it can be assumed that graphite from other ureilites should also have $\delta^{15}N$ similar to graphite from diamond free ureilite ALH78019, as it is least shocked and hence subjected to minimal alteration. Diamonds from various ureilites show light nitrogen with vary narrow range of variations in $\delta^{15}N$. Therefore, it can be assumed that the graphite from different ureilites would also show a narrow range of $\delta^{15}N$ with nitrogen composition close to that shown by graphite from ALH78019.

The release patterns of EET83309 also show number of similarities to diamond free ureilites: (i) low temperature release of noble gases where only minor amount of C combusts (ii) loss of noble gases by oxidizing acid treatment (iii) presence of smooth coarse-grained crystals of graphite in SEM picture and (iv) no indication for the presence of diamond in preliminary XRD study (Grady & Pillinger, 1987). The major differences between these two are their nitrogen composition and bimodal noble gas release. The nitrogen in E09-A is highly enriched in ^{15}N as compared to A19-A (Tables 4.2 & 4.3). E09-A has another peak of noble gases that is accompanied by peak CO_2 release. Though not much of the light nitrogen is associated with it but a decrease in $\delta^{15}N$ can be observed at 800°C. By looking at the $\delta^{15}N$ release profile in 700°-900°C temperature interval (Fig 4.21), we can arrive at a reasonable estimate of $\delta^{15}N$ for the lightest nitrogen release at 800°C. By assuming $\delta^{15}N$ of the nitrogen released at 700°C and 900°C as a base composition over which the light nitrogen is released at 800°C, the $\delta^{15}N$ of the nitrogen releases at 800°C has been calculated. The $\delta^{15}N$ of light nitrogen released at 800°C comes out to be at least –120‰. *Could it be an indication for presence of diamonds?* But the loss of most of the trapped gases by perchloric acid treatment along with absence of light nitrogen argues against it. But one possibility exists that the diamonds in this residue are very fine grained (consequently less dense) and could have been lost in perchloric acid solution. The loss of presolar diamonds during alkali permanganate oxidation ($KMnO_4$) solution as

a colloid has been reported by Amari *et al.*, (1994). Since the bulk sample of ALH78019 also showed small amounts of light nitrogen on pyrolysis at 1600°C onward, (but this light nitrogen signature is not seen in acid residues) a similar mechanism can be construed to be responsible for loss of diamonds (if present) for this sample as well.

Table 4.5 summarizes the characteristics of various carriers of trapped gases inferred from acid residues and bulk samples of ureilites. The $\delta^{15}N$ of the acid soluble phases have been calculated based on simple mass balance calculations. The $\delta^{15}N$ of the

Table 4.4 : Characteristics of different nitrogen carriers in ureilites.

Carriers	$\delta^{15}N$	$N_2/^{36}Ar$	Release temperature (°C)	
	(‰)		Combustion	Pyrolysis
Diamonds	≤-100	1000-20000	600-800	≥1600
Graphite	≥+19	6000-9000	600-800	≥1400
Amorphous Carbon in				
Diamond free ureilite	-21	1000-2000	≤500	1000-1400
Polyomict ureilites	+50 to +195	100-4000	300-800	1000-1400
Monomict ureilites	+20 to +95	80000-10^6	≤500	1000-1400
Acid soluble Phase[*]	-35 to +155	-	≥800	≥800

[*] Estimated from mass balance

graphite is the composition of nitrogen released along with peak C combustion in acid resistant residue of ALH78019 (A19-A).

Table 4.6 compiles the mass balance calculation for all the noble gases and nitrogen from present work and literature data as well. The mass balance calculation, in most of the acid residues accounts for more than 100% of noble gases contained by bulk sample. Two explanations could be possible for this. The first one is the bias in sample selection for the acid dissolution, where the carbon rich vein materials has been taken preferentially to obtain the acid residue while the second one is that the bulk samples of ureilites are heterogeneous. This is the case for not only for our samples but data from literature also exhibit similar values. Though the numbers greater than 100% do not have meaning in strict sense, it gives a strong indication that most of the noble gases in bulk ureilites are carried by acid (HF-HCl) insoluble phase *i.e.*, acid soluble phase does not carry significant amount of noble gases. Similar calculations for nitrogen, on the other hand, reveal that a significant part of nitrogen is

carried by acid soluble phases though it is highly enriched in acid insoluble phase. In two cases (ALH81101 and ALH82130), the nitrogen accounted for less than 10% of

Table 4.5 Mass Balance calculation for noble gases and nitrogen and $\delta^{15}N$ for acid soluble phase.

Sample	^{36}Ar (%)	^{84}Kr (%)	^{132}Xe (%)	N_2 (%)	$\delta^{15}N$ (‰) of acid soluble phase	References
Monomict ureilites						
Havero (HF/H$_2$SO$_4$)	58.9	113	354	25	-3	1
Havero (HF/H$_2$SO$_4$)	191	181	165			2
LEW85328 (HF/HCl)	227	81	149	82	155	1
ALH81101 (HF/HCl)	63	95	95	5	-8	1
ALH82130 (HF/HCl)	66	89	92	4	-25	1
Dyalpur (HF/HClO$_4$)	595	208	214			2
DPD (HF/HClO$_4$)	598	858	1063			2
Diamond Free ureilite						
ALH78019 (HF/HCl)	59	95	70	48	-19	1
Polymict ureilites						
EET83309 (HF/HCl)	146	132	137	45	56	1
EET83309 (HF/HCl)				25	600	3
EET87720 (HF/HCl)	323	171	158	40	201	1
Nilpena (HF/HCl)	210	157	114	38	-35	1

[1]This work; [2] Göbel *et al*., 1978; [3] Grady & Pillinger 1988.

the total nitrogen carried by the bulk sample. This could be because of large amount of nitrogen release in the bulk samples (A01-B & A30-B) at initial temperature steps that is most likely due to the terrestrial weathering as both are 'finds' from Antarctica.

4.3.4 Nitrogen to Argon ratio

It has been clearly seen in all the release patterns from acid resistant residues and oxidized residues that the carriers of heavy nitrogen and light nitrogen have very different nitrogen to argon ratio. Except for two cases, the heavy nitrogen (released at $\leq 500°C$) in both monomict and polymict ureilites is, in general, depleted in noble gases relative to nitrogen. Most of the trapped noble gases are released along with light nitrogen above 600°C. In Fig 4.24a & Fig 4.24b, the $N_2/^{36}Ar$ ratios for heavy and light nitrogen are plotted against $\delta^{15}N$ for acid resistant residues of both monomict (Fig 4.24a) and polymict (Fig 4.24b) ureilites. The $N_2/^{36}Ar$ and $\delta^{15}N$ are partitioned

into low temperature (heavy nitrogen) and high temperature (light nitrogen) fractions. These are calculated using the abundance (by nitrogen amount) weighted average of $N_2/^{36}Ar$ and $\delta^{15}N$ released at $\leq 500°C$ (low temperature: LT) and above $500°C$ (high

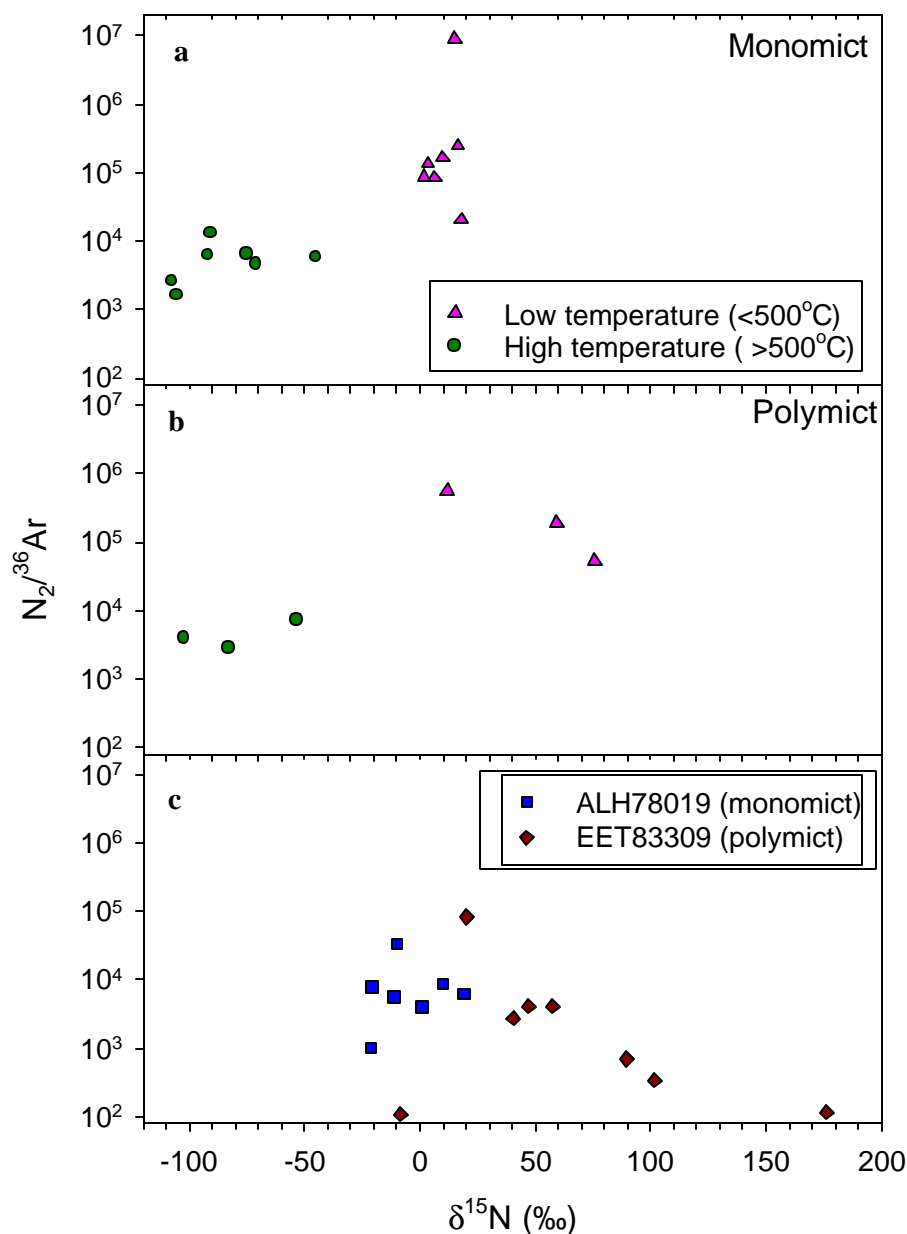**Fig 4.24** *a & b: Nitrogen to argon ($^{28}N_2/^{36}Ar$) ratios for low temperature and high temperature released components (see text for definition) from the acid residues (HF-HCl as well as HClO$_4$) of both monomict (a: top) and polymict (b: middle) ureilites is plotted vs **d**^{15}N. c) $^{28}N_2/^{36}Ar$ ratios for individual temperature steps are plotted against **d**^{15}N for the diamond free ureilites.*

temperature: HT) respectively (in most of the cases). It can be seen clearly that the $N_2/^{36}Ar$ ratios in heavy nitrogen carrier is an order of magnitude higher than that of light nitrogen carrier for both monomict and polymict ureilites. This is most likely due to selective loss of noble gases as compared to nitrogen from amorphous carbon carrier during parent body processes. Relatively smaller loss of nitrogen occurs as compared to noble gases, due to higher reactivity of nitrogen (may form chemical bond unlike noble gas). Diamonds being more refractory could most probably have retained their primordial $N_2/^{36}Ar$ ratio. Two ureilites ALH78019 (monomict) and EET83309 (polymict) do not fit in this scenario and their $N_2/^{36}Ar$ ratios fall within the range shown by carrier of primordial noble gases and light nitrogen (diamond) in diamond bearing monomict and polymict ureilites. Since these ureilites do not contain the low temperature heavy and high temperature light nitrogen as shown by the residues from other ureilites, for these two meteorites $N_2/^{36}Ar$ of individual temperature steps have been plotted in Fig 4.24c. The similar ranges of $N_2/^{36}Ar$ ratios in diamonds and amorphous carbon from diamond free ureilites indicate that amorphous carbon and diamonds initially trapped uniform $N_2/^{36}Ar$ ratios. Furthermore, this also indicates that the amorphous carbon in these two diamond free ureilites is least altered.

4.4 Summary

Eight HF-HCl resistant residues and seven oxidized residues from ten ureilites (6 monomict, 3 polymict and 1 diamond free, ureilites) have been studied for abundance as well as isotopic compositions of nitrogen and noble gases. The results on nitrogen are summarized in Table 4.6. This study reveals that diamonds from both monomict and polymict ureilites show very light nitrogen with narrow range of $\delta^{15}N$ of ≤-100‰ and independent of the $\delta^{15}N$ of their respective bulk ureilites. The release of light nitrogen is always accompanied by primordial noble gas release. In addition to diamonds, most ureilites also contain another major nitrogen carrier that has relatively heavier nitrogen but is poor in noble gas amounts, and released at temperatures lower than 500°C on combustion. The carrier of this nitrogen is amorphous carbon and seems to be affected by parent body processing (heating) during which it has lost most of its noble gases. The amorphous C in polymict ureilites, in general, has heavier nitrogen than that of monomict ureilites. Based on the absence of light nitrogen, EET83309, seems to be a diamond free ureilite. The amorphous carbon in these two

Table 4.6 Summary of the results of nitrogen study on acid residues of ureilites.

Sample	$N_2/^{36}Ar$	N (ppm)	$d^{15}N$ (‰) total	max.	min.	Type
L28-A1	1811	423	-83.55	25.48	-114.1	Monomict
Hav-A1	9051	257	-20.9	2.6	-104.2	'
A01-A	9105	140	-21.4	27.1	-94.5	'
A30-A	13483	108.3	-37.7	87.3	-53.3	'
A19-A	3696	82.3	-7.0	18.9	-21.1	Diamond free
Nil-A	5834	273.9	-42.5	77.2	-109.9	Polymict
E20-A	9545	533.4	21.5	107.9	-60.1	'
E09-A	1934	126.4	51.8	152.7	-22.3	'
L28-O1	2677	490	-102.1	11.86	-112.7	Monomict
Hav-O1	4708	391	-9.2	2.6	67.9	'
A01-O	13673	340.4	-44.3	23.6	-107.7	'
A30-O	24388	108.1	-56.3	18.5	-103.3	'
A19-O	209683	157.0	-5.3	3.3	-22.7	Diamond free
E20-O	3495	181.6	-52.33	19.2	-99.3	Polymict
E09-O	15097	64.6	10.5	11.7	-0.7	"

diamond free ureilites (EET83309 and ALH78019) is quite different from that of other ureilites, in terms of noble gas content. The amorphous C in these two ureilites seems to be least altered carbon phase of ureilites. The origin of various carbon phases, origin of heavy and light nitrogen, mechanism of incorporation of noble gases *etc.* will be discussed in the later chapters.

Noble Gases in Ureilites

5.1 Introduction

Ureilites have been studied for noble gases extensively in 70s and mid 80s by various workers and most of the conclusions drawn by them are mostly valid till date (Vdovykin, 1972 and 1976; Wänke *et al.*, 1972; Waber *et al.*, 1971 & 1976; Wilkening and Marti, 1976; Ott *et al.*, 1985a & b, Wacker *et al.*, 1986). Most of our results on noble gases are in agreement with observations made by earlier workers and will not be discussed here. In this chapter, I mainly focus on the elemental ratios involving radiogenic inputs due to both long-lived and extinct radioisotopes. While elemental ratios might help in understanding the physicochemical conditions in the solar nebula, isotopic ratios like $^{40}Ar/^{36}Ar$, $^{129}Xe/^{132}Xe$ and $^{36}Ar/^{38}Ar$ might provide clues to the time of gas trapping into the ureilite carbon phases. Also the extensive study of Q phase from various types of chondrites have been carried out recently by closed system stepwise etching (CSSE) technique (Wieler *et al.*, 1991 and 1992; Busemann *et al.*, 2000). A comparative study of noble gases in phase Q and diamonds from ureilite would provide a lot of information which can help in understanding the origin of 'planetary' (primordial) noble gases. The elemental composition of noble gases can also be used to identify the imprints of parent body processing and may provide clues to the origin of diamonds. The source of carbon in ureilites, whether magmatic or injected by impactor, is not yet clear and in this chapter I will try to address this problem too. The relation of ureilites with chondrites will also be discussed at the end.

5.2 Neon and Argon isotopic composition

Because of low concentration of neon in acid residues, only bulk samples of ureilite have been studied for neon isotopic composition. Neon and argon isotopic
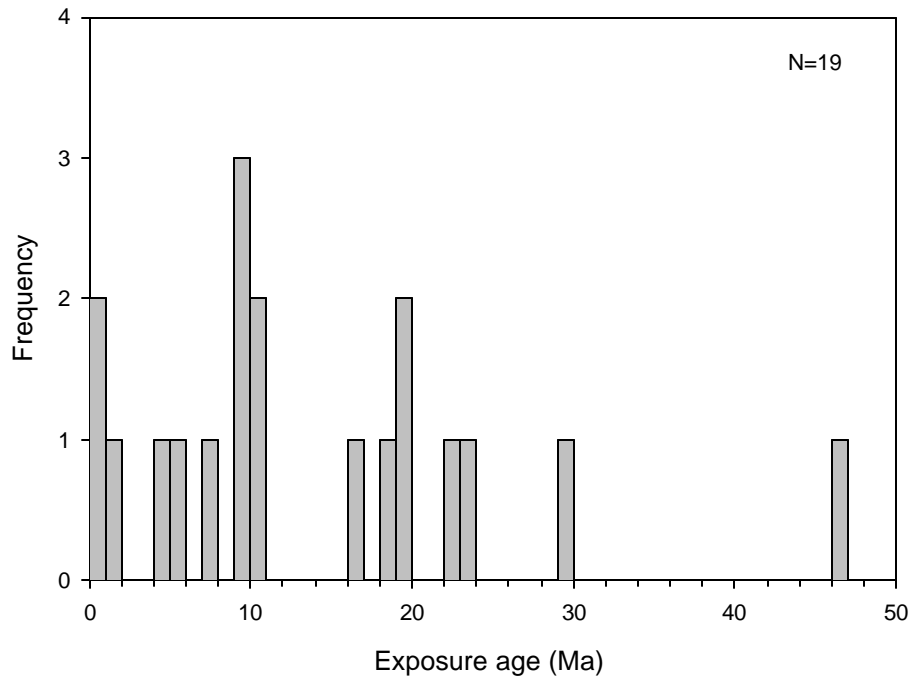
Fig 5.1 *Histogram showing cosmic ray exposure ages of 19 ureilites. A cluster at 10±1 Ma can be seen.*

compositions of various temperature steps and totals for bulk as well as acid residues of ureilites are listed in appendix and chapter 3 respectively. The cosmogenic ^{21}Ne of bulk samples have been used to calculate the exposure ages. The production rate for ^{21}Ne is calculated using empirical equation derived by Schultz and Freundel (1985). Wherever the composition of target is not available, the mean value from 8 ureilites have been used as average ureilite composition (Vdovykin 1976 and references therein). The cosmic ray exposure ages of 19 ureilites are plotted as a histogram (Fig 5.1). Except for a small cluster at 10±1Ma (N=5), the rest of the exposure ages are distributed between 1 Ma to 46 Ma, indicating that no single conspicuous event ejected all the ureilites from their parent bodies. While ALH78019 has the lowest exposure age (0.1 Ma), EET83309 has by far the largest exposure age of 46 Ma. The exposure age data are useful in assessing cosmogenic effects in certain noble gases isotopic ratios, as discussed later.

5.3 Elemental abundances of noble gases

Göbel *et al.*, (1978) have reported a linear correlation of ionization energy and xenon normalized depletion factor, D_x [defined as $D_x=log\{(^mX/^{132}Xe)_{ureilite}/(^mX/^{132}Xe)_{solar}]$ for noble gases from ureilites. The depletion factor yielded a smooth curve from Xe to Ne, only He being anomalous. In Fig 5.2, the xenon normalized elemental abundance
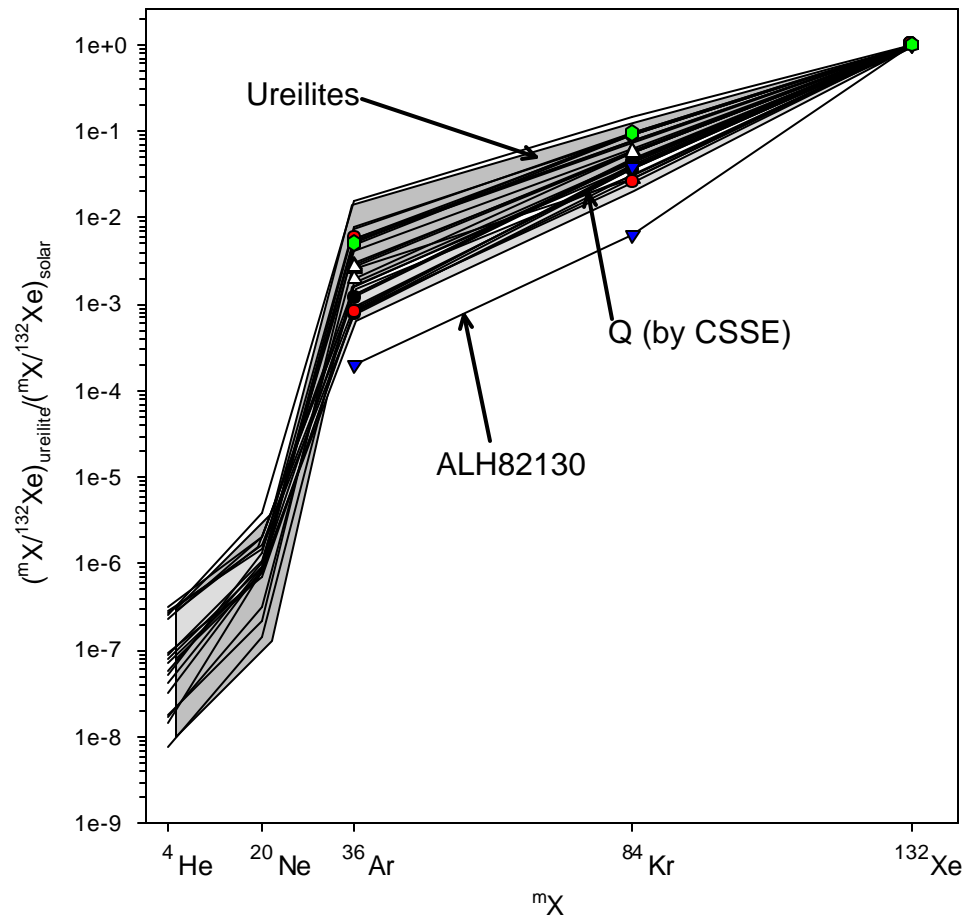
Fig 5.2 *The elemental abundance patterns of noble gases for monomict ureilites (polymict ureilite also showed similar patterns but are not plotted here to avoid cluttering) plotted against mass number. The shaded regions are the ranges shown by earlier measurements of ureilites (Göbel et al., 1978) and Phase Q (Busemann et al., 2000). One of the ureilite ALH82130 falls out side of the ranges shown by phase Q and ureilites.*

pattern of noble gases for the acid residues from ureilite and phase Q have been plotted against mass number. Both of them showed highly fractionated elemental abundance pattern with respect to solar abundance. The elemental abundance pattern of noble gases is relatively more severely fractionated in phase Q as compared to acid residues from ureilite with one exception (ALH82130). In spite of orders of magnitude difference in absolute concentrations of noble gases in carbon rich vein materials, the isotopic compositions and relative differences in elemental ratios are almost similar (Göbel *et al.*, 1978). This implies that the relative elemental abundance pattern is established by trapping process rather than by diffusion loss.

5.3.1 Release pattern of noble gases
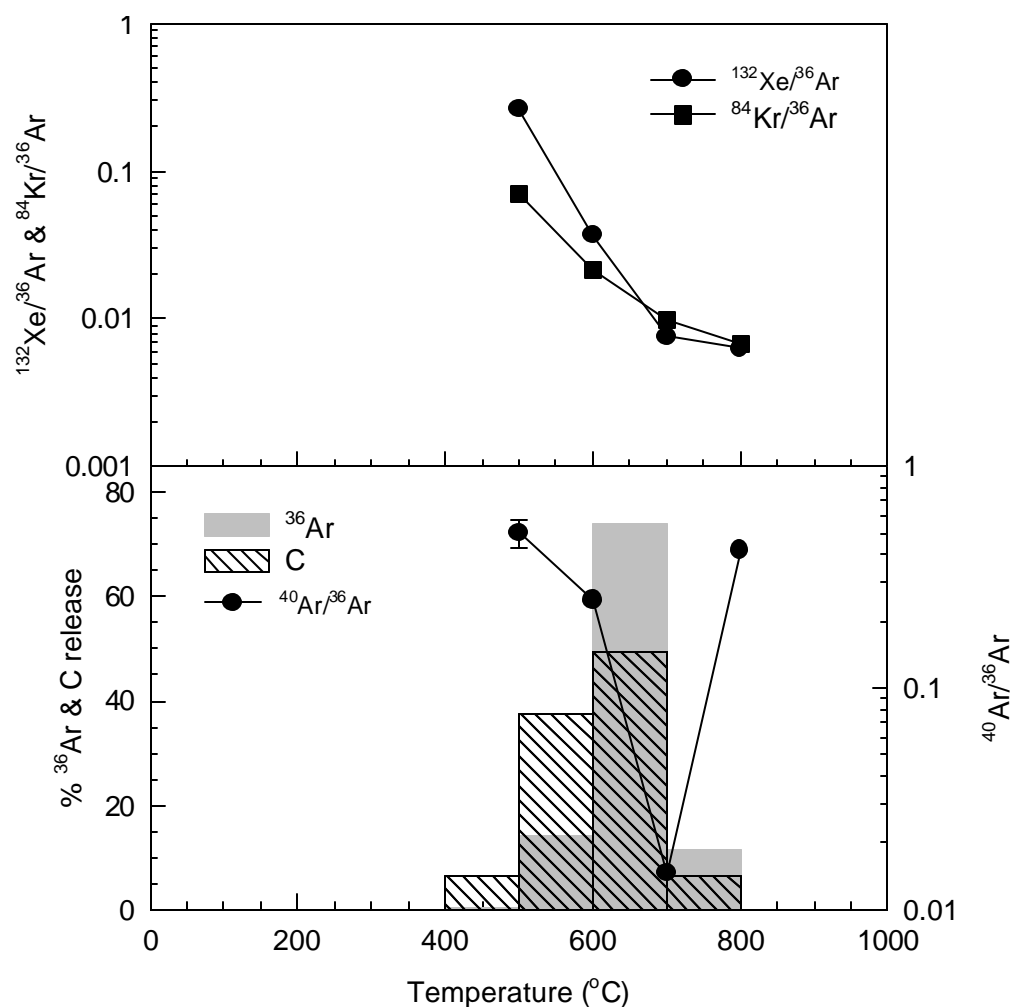
Fig 5.3 *The elemental ratios, $^{132}Xe/^{36}Ar$ and $^{84}Kr/^{36}Ar$ plotted as a function of release temperature on combustion for oxidized residue of ALH81101 and the corresponding ^{36}Ar and CO_2 release as a function of temperature have also been shown in the lower plot.*

The release patterns of argon for all the bulk as well as acid residues have been depicted for each individual sample in the previous two chapters. The release of all the other noble gases ^{84}Kr and ^{132}Xe follow the argon release. Most of the noble gases are released between 600º-900ºC and are accompanied by peak carbon combustion while on pyrolysis, most of the noble gases are released at >1200ºC with peak at 1400ºC. For the acid residues as well as oxidized residues, the noble gas release is between 600º-800ºC on combustion and is accompanied by peak CO_2 release. On pyrolysis, acid residues release most of the noble gases at temperature 200ºC higher than that of bulk samples. In general, the elemental ratios of $^{132}Xe/^{36}Ar$ and $^{84}Kr/^{36}Ar$ show decrement with temperature on combustion, implying that these ratios decrease with depth in diamonds (Fig 5.3). The release of noble gases in acid residues of two

samples, EET83309 and ALH78019, are quite different from others and have already been discussed in previous chapter.

5.3.2 Trapping and incorporation of noble gases

Understanding the processes by which primordial noble gases (hereafter Q gases) get incorporated into their carriers (phase Q, diamonds and amorphous carbon) may provide clues to the origin of 'planetary' gases and *vise versa*. One of the most striking features of Q gases is their more or less uniform isotopic composition that is also similar to those of solar gases (except for ^{3}He/^{4}He) in spite of large elemental fractionation relative to solar gases, with progressively greater depletions of lighter noble gases (Fig 5.3). Wide verities of models have been advanced to account for production of Q gases (or planetary noble gases) in context of processes operating in solar system on nebular gases. In some cases appeal is made to equilibrium physical-chemical processes such as solution or adsorption, in others disequilibrium effects such as ion implantation or trapping of adsorbed gases by mineral growth or pore closure are invoked (Wacker *et al.*, 1985; Zadnic *et al.*, 1985; Wacker, 1989). Such models are essentially microscopic, in that each specimen of the carrier must acquire its own gases through interaction with the nebula. There are also some mega-scopic models, in which the Q component is generated by capture or escape processes in planetary or planetesimal atmosphere (Ozima and Nakazawa,1980; Zahnle *et al.*, 1990; Pepin, 1991; Ozima and Zahnle, 1993). Each of these models has its own strengths and weaknesses and no consensus has been reached so far on any of these models. The similarity of Q gases in wide variety of materials of solar system leads us to think of models in which Q is a truly global component whose basic character is established independently of incorporation in planetary objects, *e.g.*, in the gas phase in the solar nebula. We know that the noble gases are highly volatile elements and got into solid objects in solar nebula very late when the nebula cools below 300K.

5.3.3 Laboratory simulation of diamond formation

A number of attempts have been made to simulate the production of diamonds as well as amorphous C in artificial noble gas atmosphere (Fukunaga *et al.*, 1987; Matsuda *et al.*, 1995; Matsuda *et al.* 1991; Matsuda and Maekawa 1992). Broadly these can be classified into three groups; conversion of graphite to diamond by shock pressure, condensation of diamond on scratched silicon wafer substrate (to serve as nuclei for

condensation) under low pressure plasma by chemical vapor deposition (CVD) process and noble gas implantation in diamonds and graphite by glow discharge. The fractionation patterns shown by the CVD diamond and amorphous carbon is very similar to that of ureilite diamonds or phase Q. In phase Q as well as in the carrier of noble gases in diamond free ureilite, gases are trapped in negligible mass of the carbon phase *i.e.* the carriers must have very high trapping efficienc y as compared to diamonds. It has also been shown that the trapping efficiency of carbonaceous material (amorphous carbon) produced by MHFCVD (Modified Hot Filament C.V.D) were highest among all the synthetic material produced in the laboratory (Fukunaga and Matsuda, 1997). The fractionation pattern from neon to xenon observed in this study is similar to that shown by the carbon phases in ureilites and phase Q (Fukunaga and Matsuda, 1997). Based on the above results it has been proposed that the noble gase s have been incorporated into diamond by ion implantation during or after the growth of diamond (amorphous carbon). A similar process has already been proposed for the trapping of Xe-HL in presolar diamond (Ott 1996; Lewis and Anders 1981).

5.3.4 Simulation of ion implantation
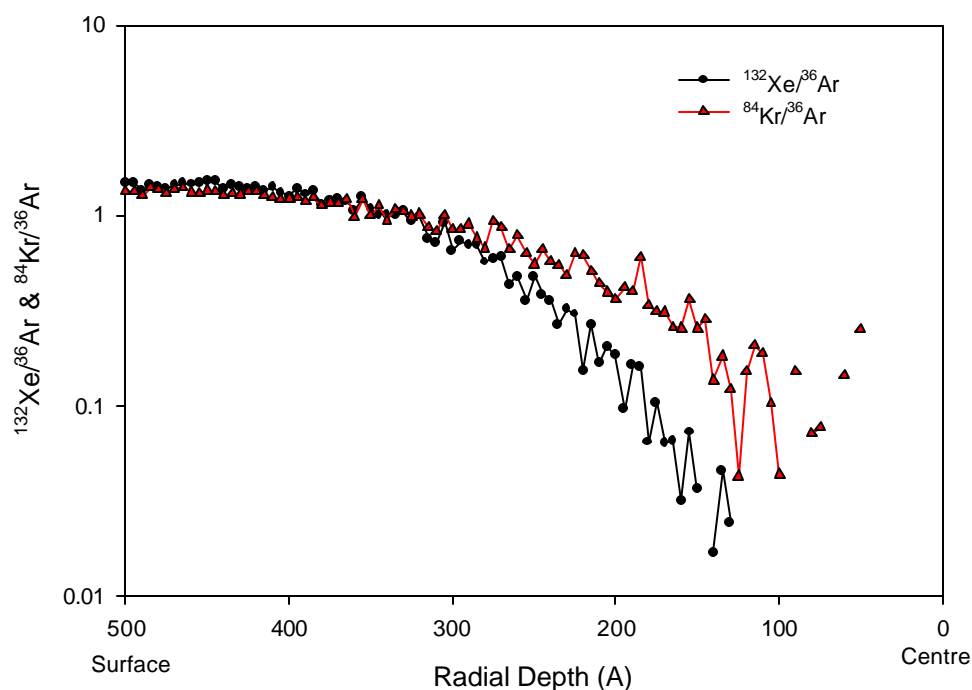
Fig 5.4 *Plot showing the variations of $^{132}Xe/^{36}Ar$ and $^{84}Kr/^{36}Ar$ with radial depth from the surface of diamond grain with radius 0.05 μm. For details see the text. The ratios are decreasing with the depth from the surface.*

Göbel *et al.*, (1978) reported a linear correlation of ionization energy and xenon normalized depletion factor, D_x expressed as $\log\{(^mX/^{132}Xe)_{ureilite}/(^mX/^{132}Xe)_{solar}$. Based on this, it can be suggested that the noble gases in ureilite diamonds were trapped in ionized state. On combustion, the $^{132}Xe/^{36}Ar$ and $^{84}Kr/^{36}Ar$ ratios show decreasing trend with increasing combustion temperatures (Fig 5.3). In other words these ratios decrease with increasing depths in the diamonds, most likely as a result of ion implantation where the heavy elements because of their larger ionic sizes, remain more or less closer to the surface relative to the lighter ones with smaller ionic radius. To verify these, ion implantation in diamond grains with different radius has been simulated using SRIM code (The Stopping and Range of Ions in Matter) (Ziegler
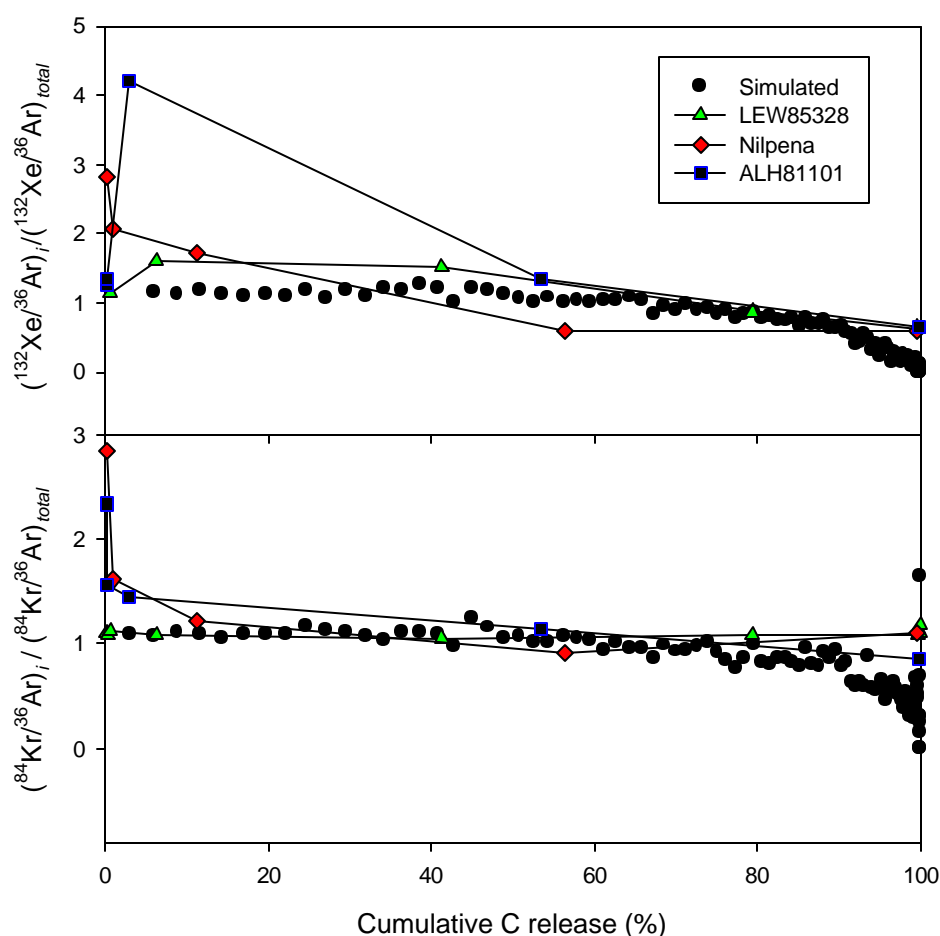
Fig 5.5 $^{132}Xe/^{36}Ar$ and $^{84}Kr/^{36}Ar$ ratios of acid residues from three ureilites (LEW85328-A, Nilpena-A, ALH81101-A) and ratio obtained by simulated ion implantation on diamond grain with 0.04 mm radius and with ions of energy between 5-100 KeV as function of cumulative carbon release.

Home page, 2000, http://www.research.ibm.com/ionbeams/SRIM/SRIMINTR.HTM). The calculations have been carried out for implantation of 1 million ions with energy ranging from 5 to 100 KeV (randomly distributed between the specified range) of heavy and light noble gas elements for the various grain sizes but the results are presented for only 0.08 μm diameter. The ions are implanted with different angles from various positions (both chosen randomly) on the surface of grains. The results are shown in Fig 5.4 & 5.5. From this study, it can be inferred that the trend in elemental ratios (i.e., depth distribution of elements) sensitively depends on energy of incident ion, ionic size of incident ion, radius of the grains (diamonds), angle of incidence, duration of implantation as well as physical properties of the material. The depth dependence of ratios $^{132}Xe/^{36}Ar$ and $^{84}Kr/^{36}Ar$ are depicted in the Fig 5.4. In the Fig 5.5, the same ratios are plotted against the percentage of carbon combustion based on experiment on three residues from ureilites Nilpena (HF/HCl), LEW85328 (HF/HCl) and ALH81101 (HF/HCl). Despite the fact that several parameters are different between the residues and the simulation, the comparison looks reasonably good. The result obtained from simulation is calculated for the single grain size while in reality the residues are ensembles of grains with large difference in grain sizes (with most probably log normal distribution). In addition to this the residues also contain other form of carbon than diamonds that also played important role in deviation from exact matching. This simple ion implantation simulation study clearly indicates that ion implantation is the most plausible mode for the incorporation of noble gases into ureilitic carbon phases.

5.3.5 Elemental abundance of noble gases in Ureilite and Phase Q

In the previous section, we have shown that the 'planetary' (or primordial) noble gas patterns are most likely due to ion implantation under plasma. This mechanism not only explains the elemental fractionation pattern, but also substantiate uniform isotopic compositions (minor differences can be explained either by parent body processes or by *in situ* production). In the plasma, the ionic abundance of a particular element depends on its ionization energy that is same for all the isotopes of an element, therefore ion implantation does not differentiate between the isotopes but differentiate between elements. The noble gases are most volatile elements in the solar nebula, they would have condensed (or adsorbed) very late in solids when the nebula cooled to very low temperature. But the presence of short-lived extinct

radionuclide (will be discussed later) argue in favor of early incorporation of the gases into carriers that is most likely possible by ion implantation (or trapping in ionic condition).

Noble gases in both ureilite diamonds (amorphous carbon as well) and phase Q exhibit highly fractionated elemental abundance trends. The close observation of fractionation patterns reveals significant variations in the general trend for elements while the isotopic compositions are more or less uniform (Fig 5.2). Noble gases in phase Q are relatively more fractionated as compared to ureilite diamonds. Though this difference has never been taken seriously in literatures, it could most probably hold important clues in understanding the origin of 'planetary' noble gases. If noble gases would have been incorporated into their carrier phases by ion implantation process from nebular plasma, the fractionation pattern of noble gases are to be governed by the ionization energy of element and electron temperature of plasma by equation (1) (Elwert, 1952).

$$\frac{H_1^+}{H_2^+} = \frac{H_1^0}{H_2^0} \cdot \frac{n_2}{n_1} \cdot \frac{q_1}{q_2} \cdot \left(\frac{E_2}{E_1}\right)^3 \exp\left[-\left(E_1 - E_2\right)/kT\right] \qquad \cdots\cdots (1)$$

Where H_1^+, H_2^+ are the ionic abundances in plasma at electron temperature T (K) for two elements whose initial abundance ratio is given by H_1^0/H_2^0. E_1 and E_2 are the ionization energy of the two elements, n is principal quantum number and q is the number of electrons in the outermost valence shell of the neutral atoms, k is 'Boltzmann' constant. From the above equation, it is implied that the higher plasma temperatures lead to relatively lower fractionation of noble gas elements. In other words, the noble gases in phase Q have been incorporated at lower temperature as compared to diamonds from ureilite. The difference in the temperatures for the incorporation of noble gases in these two carrier phases could be due to either spatial or temporal differences. Fig 5.6 shows fractionation patterns for different electron temperatures (calculated by using equation 1) along with the ranges of fractionation patterns shown by ureilite diamond and phase Q. It can be seen clearly that the diamond from ureilites must have trapped their noble gases at electron temperatures 1000-2000K higher than phase Q.
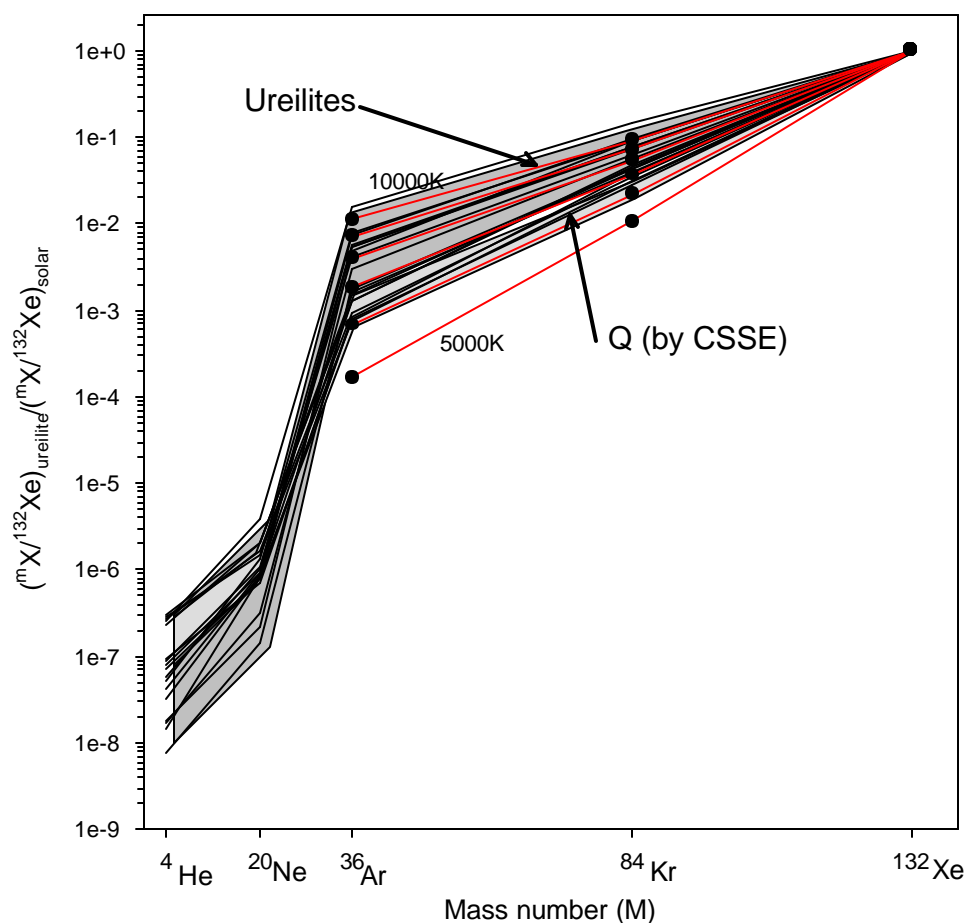
Fig 5.6 *The calculated ionic abundance pattern of noble gases at various electron temperatures in plasma. The shaded region is the range of elemental abundance patterns of noble gases shown by diamonds from ureilites and phase Q from primitive chondrites. Good matches are obtained for the diamonds at 8000 - 10000K while for Q phase at 6000-7000K.*

5.4 Physicochemical settings of gas incorporation into phase Q and diamonds

5.4.1 Live ^{129}I in Ureilite diamonds and Phase Q

The Q phase is the major carrier of primordial gases in primitive chondrites while these gases are carried mostly by the diamonds in ureilites. Whether the gases in phase Q and diamonds from ureilites have been trapped at the same time or at different times can address several important questions regarding the early solar system processes. The noble gases from both ureilites and Q phase show essentially similar isotopic compositions. Though the $^{40}Ar/^{36}Ar$ ratios in both the carriers of 'planetary' gases exhibits very low values, ureilite showed the lowest value measured
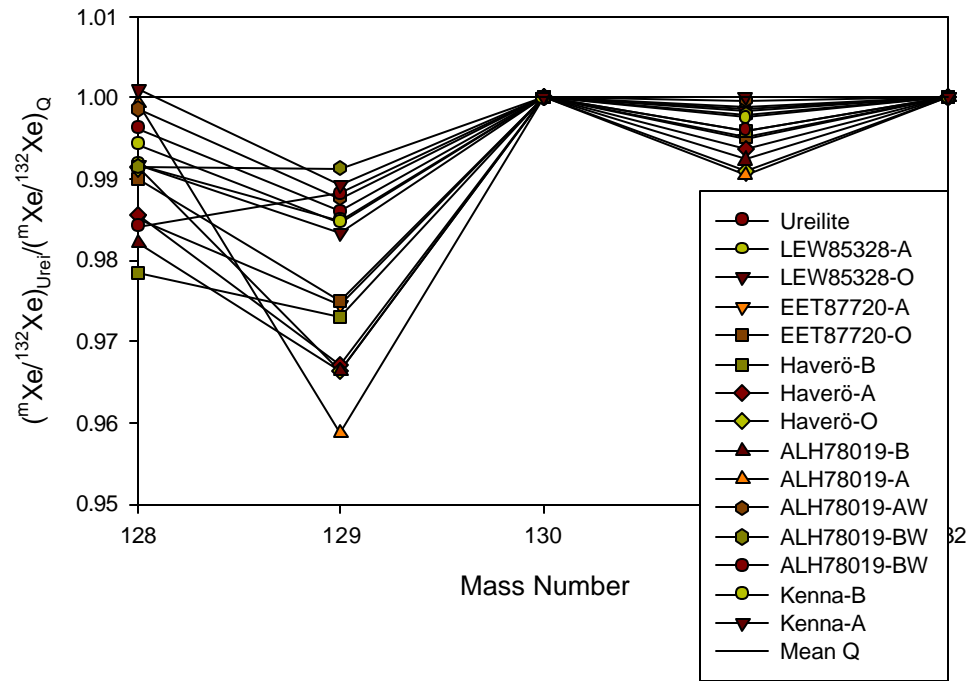
Fig 5.7 *Xenon isotopic composition of ureilites normalized to mean value of phase Q and ^{130}Xe and ^{132}Xe. To compare data from various laboratories, a linear correction has been applied to the data in order to compensate for variations due to MD correction so that all the measurements yield constant $^{130}Xe/^{132}Xe$ ratio (For more detail see text). The phase Q data from Wieler et al., 1991,1992); Busemann et al., (2000); Average ureilite data is average of eight measurements of HF/HCl residue from Göbel et al., (1978); Wacker et al., (1986); Wilkening and Marti (1976).*

(Gobel *et al.*, 1978; Begemann *et al.*, 1976) so far, which is very close to the estimated primordial $^{40}Ar/^{36}Ar$ ratio (Cameron, 1973). This indicates that they both trapped their gases very early in the solar system. A close look of $^{40}Ar/^{36}Ar$ ratio reveals that this value is quite lower in ureilites than that of phase Q. Does it reflect that the noble gases are trapped in diamonds earlier than in Phase Q? In most of the meteorites and planetary objects, the higher ^{40}Ar is mainly due to radiogenic argon produced by the decay of ^{40}K (mean life 1.8×10^9 years). One of the reasons for the lower value of $^{40}Ar/^{36}Ar$ in ureilite than that of phase Q could be the very low abundance of potassium (*i.e.*, ^{40}K) in ureilite as compared to primitive chondrites. A small contamination of radiogenic ^{40}Ar in phase Q (acid resistant residue) can lead to orders of magnitude increase in $^{40}Ar/^{36}Ar$ ratio and hence it is not safe to use the ratio of $^{40}Ar/^{36}Ar$ to infer the relative trapping time of primordial noble gases in phase Q and diamonds from ureilites. Another important isotope of noble gases that can

provide useful information regarding the trapping of noble gases is ^{129}Xe. This isotope is produced by the decay of short lived and now extinct radionuclide ^{129}I (mainly produced by the r process nucleosynthesis in supernova with half-life of 16.4 Ma). Apart from explosive nucleosynthesis, ^{129}Xe can also be produced by the interaction of cosmic ray produced thermal neutron with ^{128}Te if the size of meteorite parent body is large enough and is having higher cosmic ray exposure age. After close inspection of xenon isotopic composition of ureilite and Q phase reveals that the Q phase shows clear excess of ^{129}Xe/^{132}Xe ratio over diamonds from ureilite (Busemann *et al.*, 2000) (Fig 5.7 & Table 5.1). In some cases the radiogenic ^{129}Xe is quite significant (Wieler *et al.*, 1991). Though the majority of the radiogenic ^{129}Xe in primitive chondrites are contained in a carrier other than Q phase as indicated by different release patterns of ^{129}Xe and 'planetary' Xe (Frick and Pepin, 1981), a constant higher value of ^{129}Xe/^{132}Xe (1.073) has been obtained in CSSE in Allende HF-HCl residue, advocating the presence of radiogenic ^{129}Xe in phase Q (Wieler *et al.*, 1991). Though none of the other measurements of xenon isotopic composition of HF-HCl residues from carbonaceous chondrites as well as ordinary chondrites yielded value of ^{129}Xe/^{132}Xe as high as Allende, the mean values of all the CSSE runs is (excluding Allende) ~1.042 ($\pm$0.002) (Busemann *et al.*, 2000) that is distinctly higher than corresponding average value for 11 ureilites 1.035 ($\pm$0.001) (from 21 measurements) (this work, Göbel *et al.* 1978 and Wacker 1986). *Is this small difference in the values of ^{129}Xe/^{132}Xe between ureilite diamonds and phase Q significant?* By assuming solar abundance of noble gases and iodine and canonical value of ^{129}I/^{127}I $=10^{-4}$ (Podosek and Swindle 1988), the mixing of radiogenic ^{129}Xe produced by the complete decay of ^{129}I with solar system xenon, can produce insignificant changes in the ratio of ^{129}Xe/^{132}Xe. To get enhanced ratio of ^{129}Xe/^{132}Xe that can be easily detected, a very early and preferential incorporation of ^{129}I into the noble gas carrier (*i.e.*, ^{127}I over Xe) is required. Therefore the difference between the values 1.042($\pm$0.002) and 1.035($\pm$0.001) are quite significant if one is looking for presence of radiogenic ^{129}Xe.

What is the trapped value of ^{129}Xe/^{132}Xe for the 'planetary' noble gases?: To determine the radiogenic ^{129}Xe, the true-trapped ratio (non-radiogenic) for the ^{129}Xe/^{132}Xe is needed that can be used as base value to calculate the radiogenic ^{129}Xe. In the selection of the trapped value, one need to be very careful because to change the ^{129}Xe/^{132}Xe ratio by one percent, three orders of magnitude enrichment of iodine

over xenon is required and that too when $^{129}I/^{127}I \sim 10^{-4}$. Wieler *et al.*, (1991) assumed the non-radiogenic value of $^{129}Xe/^{132}Xe$ about 1.04 based on the value of 1.036-1.045 from the Kenna ureilite (Wilkening and Marti, 1976; Wacker, 1986). The measurement of xenon isotopic compositions from the different laboratories yielded very different values even for the same sample and this is most probably due to uncertainty in instrumental mass discrimination correction. To remove the inter-laboratory biases, we adopt the following procedure. For the xenon isotopic compositions measured in various laboratories, we assume that the $^{130}Xe/^{132}Xe$ in phase Q and diamonds from ureilites are the same and similar to the mean value for the 21 measurements on carbon rich residues from 11 ureilites [constant value of $^{130}Xe/^{132}Xe$ ratio (= 16.33 $\pm$ 0.03)] (Göbel *et al.*, 1978, Wacker, 1986 and this work). The difference between various measurements for this ratio can be used to calculate a correction factor (per amu) and is multiplied with the ratios of $^{128}Xe/^{132}Xe$, $^{129}Xe/^{132}Xe$, $^{130}Xe/^{132}Xe$ & $^{131}Xe/^{132}Xe$ by assuming linear extrapolation with mass number (or interpolation). In other words, a linear mass dependent correction factor is being applied to remove inter-laboratory biases (assuming them to be due to instrumental mass discrimination correction). The ratios calculated this way, are plotted in Fig 5.7. The data are normalized to mean isotopic composition of ureilite. The excess of ^{129}Xe in phase Q can be seen clearly.

5.4.2 Is the excess ^{129}Xe due to ^{128}Te(n,γ) reaction?

The excess ^{129}Xe in meteorites can be produced by two ways, firstly by the decay of live ^{129}I and secondly by the interaction of cosmogenic neutrons with ^{128}Te but the later is possible only for meteorites with long cosmic ray exposure ages, large size and sufficient Te contents. In order to calculate the excess ^{129}Xe due to decay of primordial ^{129}I, contribution from neutron capture on ^{128}Te should be subtracted from total excess. This can be done with help of other neutron capture products. There are three isotopes of xenon that can be produced by neutron capture by the following reactions.

$$^{128}Te\ (n,\gamma\beta^-)\ ^{129}I\ (T_{1/2}=16.4Ma) \Rightarrow\ ^{129}Xe \tag{2}$$

$$^{130}Te\ (n,\gamma\beta^-)\ ^{131}I\ (T_{1/2}=8.04d) \Rightarrow\ ^{131}Xe \tag{3}$$

$$^{127}I\ (n,\gamma\beta^-)\ ^{128}Xe \tag{4}$$

$$^{130}Ba(n, \gamma\beta^+, \gamma\beta^+)\ldots^{131}Xe \qquad\qquad (5)$$
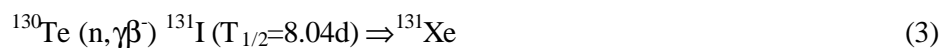
The relative production of ^{129}Xe and ^{131}Xe by the neutron capture of ^{128}Te and ^{130}Te depends on cross section that is a function of neutron energy and relative abundance of ^{128}Te and ^{130}Te. The calculation reveals that the neutron produced ratio of $^{129}Xe/^{131}Xe$ is equal to 0.69 unless the intermediate products ^{129}I (and ^{130}I) are separated before the lifetime of ^{129}I. The separation of ^{129}I during its lifetime always lead to values smaller than 0.69 i.e., this value is the upper limit of the thermal neutron produced $^{129}Xe/^{131}Xe$. ^{128}Xe can be produced by neutron capture on ^{127}I and its production relative to neutron produced ^{131}Xe is a function of $^{127}I/^{130}Te$ ratio in the carrier phase. Assuming the solar ratio of $^{127}I/^{130}Te$, the inferred relative proportion of neutron produced Xe isotopes are $^{128}Xe:^{129}Xe:^{131}Xe \equiv 37:0.69:1$. But I and Te have different cosmochemical behavior and are expected to condensed in different proportion. The concentration of Te and Br in acid residues of Allnede (CV3) has

Table 5.1 Neutron capture ^{131}Xe and $^{129}Xe_{Extinct}$ in phase Q (data from Busemann *et al.* 2000).

Sample	$^{129}Xe_{Ex}/^{132}Xe^{\maltese}$	$^{129}Xe_E$ $^{128}Xe_n$ 10^{-10} ccSTP/g		$^{129}I_{Ext}/^{132}Xe$	$^{127}I/^{132}Xe^{*}$	CREA Ma
Cold Bokkeveld	1.057	33.81	1.637	0.0221	221.0	0.40
Murchison	1.045	33.93	2.346	0.0010	99.8	2.4
Gronaja	1.060	21.50	0.4128	0.0250	250.0	2.1
Allende	1.074	70.07	-	0.0389	389.3	6.8
Lance	1.030	-	-	--	-	5.0
Isna	1.067	62.71	1.917	0.0324	323.9	0.13
Chainpur	1.062	6.874	0.2509	0.0269	268.5	24.6
Dimmitt	1.063	4.363	0.1068	0.0278	277.9	4.9
Mean -Q	1.054					

*Calculated by using connonical value of $^{129}I/^{127}I$ equal to 10^{-4}.
$^{\maltese}$ Corrected for neutron capture effects assuming production ratio for $^{129}Xe/^{131}Xe=0.7$, Xenon isotopic composition are applied a linear correction factor to make all the $^{130}Xe/^{132}Xe$ values equal and equal to the mean value of 21 measurements from 11 ureilites.

been reported but not for the iodine (Anders *et al.*, 1975). The iodine concentration can be inferred from bromine concentration, by assuming I/Br ratio in the phase Q is similar to solar ratio though this will be an upper limit. By taking these values for Te and I, and assuming that all these elements are carried by phase Q, the neutron produced isotopes of xenon are derived to be $^{128}Xe:^{129}Xe:^{131}Xe \equiv 13.6:0.69:1$. The
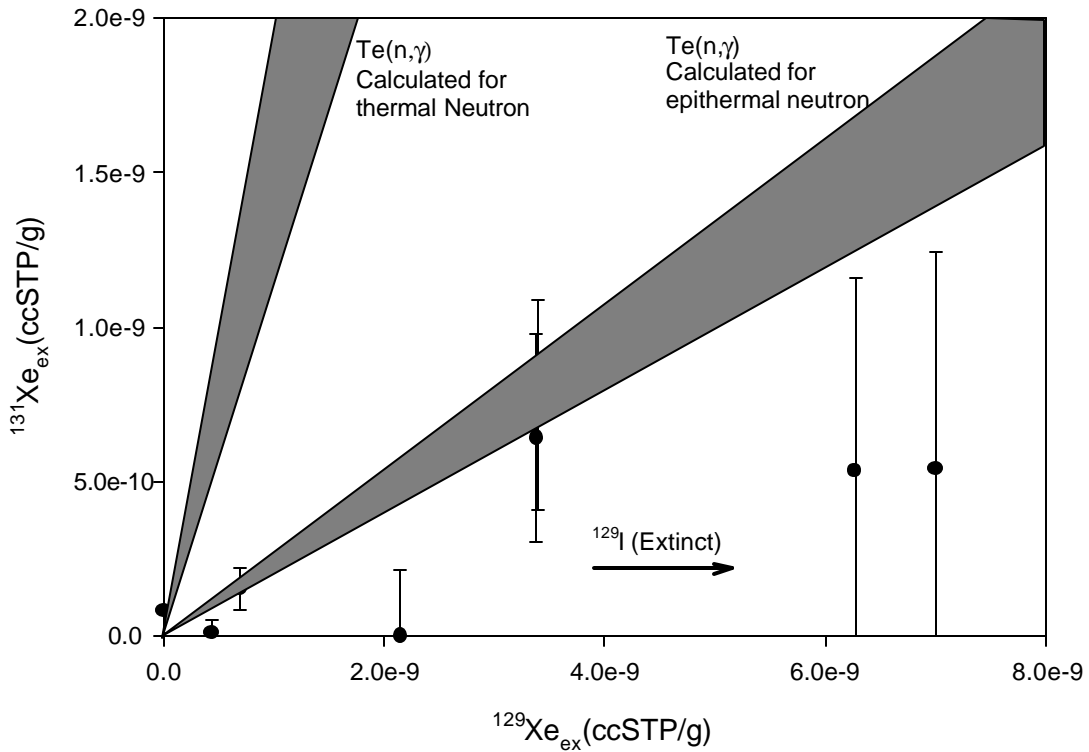
Fig 5.8 *Plot of excesses at ^{129}Xe and ^{131}Xe from phase Q of chondrites listed in Table 5.1.*

calculated ratio of $^{128}Xe/^{131}Xe$ (=13.6) is a lower limit, because the I/Br ratio in condensed phase in solar nebula should always be greater than solar value that in turn lead to increase in the proportion of ^{128}Xe relative to ^{131}Xe. Since lot of uncertainty is involved in the calculation of neutron produced $^{128}Xe/^{131}Xe$, we shall use only neutron produced $^{129}Xe/^{131}Xe$ in the correction *i.e.* the contribution of neutron capture ^{129}Xe produced by ^{128}Te is always 0.7 times of the excess ^{131}Xe (produced by ^{130}Te). In addition to neutron capture of ^{130}Te, ^{131}Xe can also be produced by the interaction of thermal neutron with ^{130}Ba, i.e., the excess ^{131}Xe in phase Q can be due to ^{130}Te and ^{130}Ba while only ^{128}Te can produce ^{129}Xe by neutron capture. In the calculation of ^{129}Xe produced by extinct ^{129}I, we assume all the excess ^{131}Xe is produced by neutron capture by ^{130}Te ($^{131}Xe_n$), and ^{129}Xe contributed by neutron reaction is given by 0.7 times of $^{131}Xe_n$. The $^{129}Xe_n$ calculated this way is an overestimation. Subtraction of this value from the total excess ^{129}Xe will provide lower value of ^{129}Xe that is supported by the extinct ^{129}I. In Table 5.1 the excess ^{129}Xe supported by extinct primordial ^{129}I for the Q phases from various chondrites have been listed. The maximum contribution of neutron produced ^{131}Xe (form ^{130}Te and ^{130}Ba) is very small and is never more than 0.07%. From the calculation, it is clear that at least two to

three orders of magnitude enrichment of iodine over xenon is needed to account for the ^{129}Xe excess. In spite of the presence of very high amount of ^{129}Xe due to decay of extinct ^{129}I (up to 7.0 $\times 10^{-9}$ ccSTP/g), the observed difference in measured and trapped ratios of ^{129}Xe/^{132}Xe is small. This is due to large amount of trapped xenon (other noble gases too), resulting in dilution of excess ^{129}Xe. Since most of the meteorites that were studied for Q gases are having low cosmic ray exposure ages and of smaller in size, significant neutron effects are unlikely. This is further substantiated by poor correlation of cosmic ray exposure age and excess ^{128}Xe/^{132}Xe, ^{129}Xe/^{130}Xe and ^{131}Xe/^{132}Xe (Fig 5.9a).

In the above calculations, we assume the production of ^{129}Xe and ^{131}Xe by the thermal neutron with energy range (<0.025eV). The ratios of ^{129}Xe/^{131}Xe produced by neutron capture vary significantly with the energy of neutron because the capture cross section of neutron for any element is function of energy of neutron (Browne and Berman, 1973). The reaction of epithermal neutron with ^{128}Te and ^{130}Te can produce higher ratio of ^{129}Xe/^{131}Xe between 3.7-5.0. In Fig 5.8, the ^{129}Xe$_{ex}$ and ^{131}Xe$_{ex}$ for bulk phase Q from primitive chondrites (Busemann *et al.*, 2000) have been plotted along with predicted production ratios for thermal and epithermal neutron reactions. Most of the data falls outside the production region of thermal and epithermal neutron and the shift toward positive x-direction clearly indicating a significant component of ^{129}Xe is due to decay of extinct ^{129}I.

The excess ^{129}Xe in phase Q over diamonds (as well as amorphous carbon) from ureilites, implies that the Q phase not only trapped their gases very early in the solar system when ^{129}I was alive but also trapped by a mechanism that enriches iodine over xenon by two to three orders of magnitude. Though, diamonds showed lower ratio of ^{129}Xe/^{132}Xe as compared to phase Q that is more close to the non-radiogenic trapped ratio, some contribution of radiogenic ^{129}Xe in diamonds can not be ruled out. The lower ^{129}Xe/^{132}Xe ratio in diamonds is indicative of two possibilities, either the diamonds have been formed latter than phase Q when most of the ^{129}I has already been decayed or the diamonds have been contemporary to the Q phase but the physicochemical condition in which the primordial noble gases are trapped in diamonds could not enrich iodine as much as in the case of phase Q. Considering the lower values of ^{40}Ar/^{36}Ar in ureilites than that of phase Q, the later one seem to be
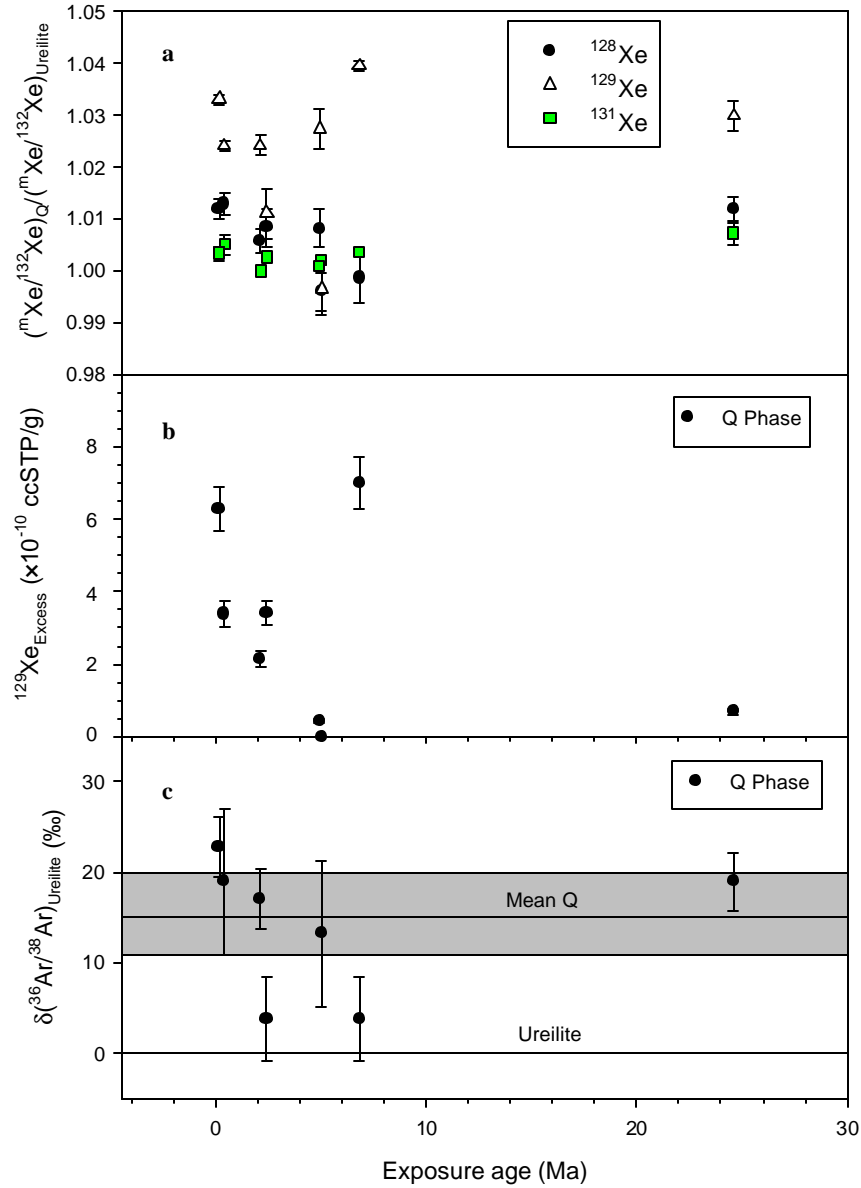
Fig 5.9 *The isotopes of noble gases (in phase Q) prone to be affected by the secondary thermal neutron reaction products are plotted against the cosmic ray exposure ages. No positive correlation can be seen with exposure ages, indicating that the thermal neutrons played very insignificant role in producing these excesses. The clear excesses of ^{129}Xe (top & middle) and ^{36}Ar (lower) seen are most likely be supported by their extinct parents ^{129}I and ^{36}Cl. (For more details, see text).*

more likely. The various scenarios for the noble gas incorporation into diamonds and phase Q will be discussed later.

5.4.3 Live ^{36}Cl in Phase Q

In the last section, we tried to establish the presence of extinct ^{129}I in the phase Q from primitive chondrites by subtracting the contribution due to thermal neutron production by assuming all the excess ^{131}Xe is produced by secondary thermal neutron. But the poor correlation of excess ^{129}Xe (& ^{131}Xe, ^{128}Xe as well) with exposure ages (Fig 5.9a and 5.9b), will not be consistent if thermal neutrons really played an important role in these excesses, as for most of the meteorites, the preatmospheric sizes and cosmic ray exposure ages are too small to have thermal neutron and hence neutron-capture effects.

In Table 5.2, ^{36}Ar/^{38}Ar ratio of phase Q from primitive chondrites (Wieler *et al.*, 1991; Wieler *et al.*, 1990; Busemann *et al.*, 2000) and acid residues from various ureilites have been listed. The ratios in phase Q are, in general, higher than that of ureilite diamonds. We feel that this higher ratio of ^{36}Ar/^{38}Ar in phase Q over ureilite diamond (assumed as base value) is due to excess ^{36}Ar supported by live ^{36}Cl present in early solar system. But to prove this, one has to rule out that it is not produced during cosmic ray exposure in interplanetary space. The spallogenic contribution will tend to reduce this ratio but the secondary neutron induced components will increase this ratio in required direction. Indirect estimation of thermal neutron produced ^{36}Ar excess can be done using ^{131}Xe$_{excess}$, but this will introduce a large uncertainty due to a number of assumptions involved. In the following discussion, I will try to rationalize the higher ^{36}Ar/^{38}Ar ratio in phase Q qualitatively with following assumptions:

a. To produce thermal neutron and hence the neutron capture effects, larger body as well as long cosmic ray exposure ages are needed.

b. The excess of nuclide produced by thermal neutron capture should correlate with each other and also correlates with cosmic ray exposure ages.

Table 5.2 Argon isotopic composition of ureilites and other reservoirs.

Sample	^{36}Ar/^{38}Ar	^{40}Ar/^{36}Ar	Source
Ureilites			
Haverö-A	5.32(1)	7.420(13)	This work
Haverö-A1	5.28((1)	8.664(20)	This work
Haverö-O	5.29(1)	0.8981(62)	This work

Haverö-B-4	5.31(11)	0.0011(1)	Göbel *et al*, (1978)
Haverö-(B-3-1)	5.28(13)	0.0012(1)	Göbel *et al*, (1978)
LEW85328-A1	5.25(2)	0.2042(384)	This work
LEW85328-O1	5.27(1)	0.0724(5)	This work
ALH81101-A	5.26(1)	0.3085(30)	This work
ALH81101-O	5.28((1)	0.1342(19)	This work
ALH82130-A	5.25(1)	46.48(2)	This work
ALH82130-O	5.24(1)	0.5212(60)	This work
ALH78019-A	5.31(1)	0.5212(60)	This work
ALH78019-AC3	5.29(3)	1.0(8)	Wacker (1986)
Kenna-AA1	5.30(5)	0.1(-0.1,+2.6)	Wacker (1986)
Kenna-AB2	5.29(5)	0.3(-0.3,+3.6)	Wacker (1986)
Kenna (B-1)	5.22(9)	0.0017(3)	Göbel *et al*, (1978)
EET83309-A	5.25(1)	0.151(1)	This work
EET83309-O	5.28(1)	1.886(10)	This work
Nilpena-A	5.27(1)	0.0771(3)	This work
EET87720-A	5.24(1)	0.1803(18)	This work
EET87720-O	5.24(1)	0.1322(26)	This work
Dingo pup Donga (B-1)	5.29(7)	0.0023(9)	Göbel *et al*, (1978)
Dingo pup Donga (B-2)	5.21(9)	0.0152(35)	
Dyalpur (B-2-1)	5.28(10)	0.00029(17)	Göbel *et al*, (1978)
North Haig (B-1)	5.22(12)	0.0025(4)	Göbel *et al*, (1978)
Novo Urei (B-1)	5.18(13)	0.0074(40)	Göbel *et al*, (1978)
Novo Urei (B-2)	5.24(9)	0.0024(2)	
Mean Ureilite[§]	**5.27(0.01)**		

Phase Q

Cold Bokkeveld	5.37(4)	1.05(2)	Busemann *et al.*, 2000
Murchison	5.29(2)	0.12(2)	Wieler *et al.*, 1992

Grosnaja	5.36(1)	0.90(2)	Busemann *et al.*, 2000
Allende	5.29(2)	0.43(5)	Wieler *et al.*, 1991
Lance	5.34(4)	1.57(1)	Busemann *et al.*, 2000
Isna	5.39(1)	0.78(1)	Busemann *et al.*, 2000
Chainpur	5.37(1)	3.18(1)	Busemann *et al.*, 2000
Mean Q	5.34(2)		
P1(≡Q)	5.33(3)		Huss *et al*., 1996
OC	5.29(13)		Schelhass *et al.*, 1990
Other reservoirs			
Air	5.32(1)		Neir, 1950
SW	5.48(5)		Benkert *et al.*, 1993
SEP	4.87(5)		Benkert *et al.*, 1993
A	5.3(1)		Reynolds *et al.*, 1978
HL	4.41(6)		Huss and Lewis. 1994
P3	5.26(3)		Huss and Lewis. 1994
Cosmogenic	0.65		Alaerts *et al.,* 1979
Neutron Capture (thermal)	315		(calculated)[*]

[§] Mean value of 27 measurements from acid residues of ureilites.

In Fig 5.9 c, $\delta(^{36}Ar/^{38}Ar)_{Ureilite}$ (*see* appendix) of phase Q (Wieler *et al.*, 1990; Wieler *et al.*, 1991; Busemann *et al.*, 2000) have been plotted verses cosmic ray exposure age. The $\delta(^{36}Ar/^{38}Ar)$ for Q phase have been calculated by assuming the mean value of the 27 measurements from acid residues of ureilites as a reference value. Apparently, no positive correlation is being seen with exposure ages. In fact, a negative correlation can be seen if we exclude the last point with highest exposure age (Chainpur). The same is also true for $^{128}Xe/^{132}Xe$, $^{129}Xe/^{132}Xe$ and $^{131}Xe/^{132}Xe$ (Fig 5.9 a), the ratios normalized to corresponding mean ratio from acid residues of ureilites does not show any systematic correlation with exposure ages. The increase in the ratio of $^{129}Xe/^{132}Xe$ for the phase Q due to the contribution from ^{129}I (*in situ* decay) is very much dependent on the proportion of trapped ^{132}Xe present. So to clearly see the effect of cosmic ray exposure on the excess ^{129}Xe, it is more

appropriate to plot the absolute $^{129}Xe_{exc} = [\{(^{129}Xe/^{132}Xe) - 1.035\} \times {}^{132}Xe]$ against cosmic ray exposure ages (Fig 5.9b). This plot almost parallels Fig 5.9a, and infact shows anticorrelation of $^{129}Xe_{exc}$ with CREA, demonstrating that $^{129}Xe_{exc}$ is independent of CREA and hence confirming the ^{129}I (extinct) parentage. All these imply that noble gas isotopic composition of phase Q is unaffected by the thermal neutron capture effects (on their target) inside their parent body during cosmic ray exposure. Therefore, the excess ^{129}Xe present in phase Q is certainly due to the decay of their short-lived parent ^{129}I, while excess ^{36}Ar is most likely due to extinct ^{36}Cl present in phase Q.

Presence of excess ^{36}Ar has already been reported earlier in Efremovka matrix material (Murty *et al.*, 1997) but not in a Cl rich chondrule of Allende (Murty and Wasserberg 1996). Q phase from Allende shows very little excess of ^{36}Ar and supporting the earlier observations for the absence of extinct ^{36}Cl in this meteorite (Jorden and Pernicka 1981; Göbel *et al.*, 1982). The absence of neutron effect *i.e.*, excess ^{36}Ar in Allende Q, with large meteorite body also support that the secondary neutron did not play any role in excess ^{36}Ar in phase Q.

The Cl (*i.e.,* $^{35}Cl/^{36}Ar$) content as well as the initial trapped ratio of $^{36}Ar/^{38}Ar$ in phase Q are required to calculate the initial ratio of $^{36}Cl/^{35}Cl$. Since ^{36}Cl has very short life ($\tau = 0.43$ Ma), the amount of excess ^{36}Ar observed also depends on how early the ^{36}Cl got incorporated in to phase Q. The chlorine content of phase Q is not reported so far and also its determination is further complicated by contamination of chlorine from HCl used during acid dissolution. Nevertheless the enrichment of Cl over Ar can be calculated by assuming the initial $^{36}Cl/^{35}Cl$ value $= (1.4\pm0.2)\times10^{-6}$, estimated for Efremovka by Murty *et al.* (1997) and the trapped initial $^{36}Ar/^{38}Ar$ ratio in phase Q and ureilite diamonds were equal and also equal to the mean value $^{36}Ar/^{38}Ar$ of ureilite diamonds (=5.27) (Table 1). Taking these values, on the average, five orders of magnitude enrichment of Cl over Ar relative to solar ratio (Anders and Grevesse, 1989) should be required to explain the observed excess of ^{36}Ar in phase Q. Late incorporation of chlorine (and argon) in phase Q can also lead to enhancement of the required enrichment factor.

5.4.4 Can ^{129}I and ^{36}Cl be enriched over Xe and Ar respectively, by ion implantation?
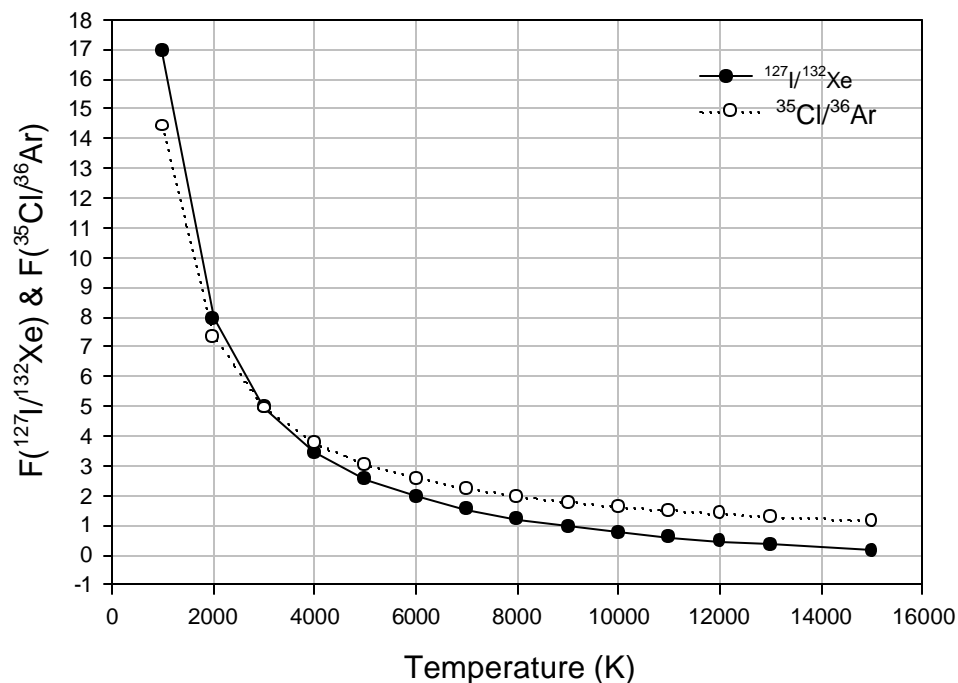
Fig 5.10 *The plot showing the calculated $^{127}I/^{132}Xe$ and $^{35}Cl/^{36}Ar$ (or ionic abundance) normalized to solar system abundance in plasma at different electron temperatures. The lower temperatures favor the enrichment of I and Cl over Xe and Ar respectively. Where, F(A/B) is defined as log[(A^{+}/B^{+}) / (A/B)].*

In section 5.3.5, the mechanism for the incorporation of noble gases has been discussed. Based on several parameters, we argued that the noble gases in phase Q and diamonds from ureilites (amorphous C in ALH78019 as well) have been incorporated by the chemically non-selective processes like ion implantation in nebular plasma. The mechanism for the incorporation of noble gases should also explain the predicted enrichment of ^{127}I and ^{35}Cl (also ^{129}I and ^{36}Cl as well if it is very early) to explain the observed excess in ^{129}Xe and ^{36}Ar. Though there is no direct measurement of iodine and chlorine in phase Q (or acid insoluble phase) so far, high enrichment of bromine has been reported in literature (Anders *et al.*, 1975). If noble gases in diamonds and phase Q would have been incorporated in their carrier by chemically selective process like condensation in cooling solar nebula, enrichment of iodine over xenon upto five order of magnitude can be expected and that will increase the excess ^{129}Xe by at least two orders than what is observed (Lewis and Anders, 1981).

In ion implantation, the proportion of elements incorporated into the carrier, are proportional to ionic abundance that, in turn, depends on ionization energy of the

element. The ionic abundance of elements in plasma is given by the equation 1. In Fig 5.6, the fractionation patterns of noble gases in diamonds from ureilites and phase Q have been plotted with mass number. The theoretically predicted ionic abundance at various temperatures (electron) are also shown in the Fig 5.6. It can be seen clearly that the noble gases in phase Q have been incorporated at temperatures lower than that of ureilite diamonds. The fractionation factors [defined as $F(^{127}I/^{132}Xe)$ = $(^{127}I/^{132}Xe)_{plasma}/ (^{127}I/^{132}Xe)_{solar}$] of iodine relative to xenon, and chlorine relative to argon, have been calculated at various temperatures using equation (1). The results are plotted in Fig 5.10. It can be seen clearly that at lower temperatures, relatively more iodine and chlorine are expected to be implanted in the carriers. This is consistent with the observation that the phase Q that formed at lower temperature than that of ureilite diamonds is expected to have more iodine and chlorine as compared to ureilite diamonds. In equilibrium condensation model for the 'planetary' noble gas formation, we expect very late condensation of noble gases (halogen as well) because of their volatile nature and require much cooler temperature to condense. The presence of live ^{41}Ca (Srinivasan *et al.*, 1996) in CAI that have formed in very hot solar nebula is indicative of high temperature condition prevailed in solar nebula in the first few million year. Because of comparable half-life of ^{36}Cl and ^{41}Ca, the live ^{36}Cl must also have been trapped into their carrier in a few Ma. This indicates that the noble gases must have been trapped in phase Q, when solar nebula was very hot. The large concentration of noble gases by equilibrium condensation in hot epoch of solar nebula is highly unlikely. However, ion implantation that is independent of volatility, could have been active very early when the solar nebula was still hot. We have seen that the trapping of noble gases by ion implantation in solar plasma not only explains the fractionated elemental abundance of noble gases but also explains the presence/absence of live ^{129}I and ^{36}Cl (or high $^{35}Cl/^{36}Ar$) in phase Q and ureilite diamonds respectively.

5.5 Role of Parent body processing in evolution of elemental and isotopic ratios

In addition to the diamond, that carries most of the noble gases in ureilite (see the mass balance calculations in previous chapter), another unknown carrier X having very different elemental ratios of noble gases had been proposed by Göbel *et al.*
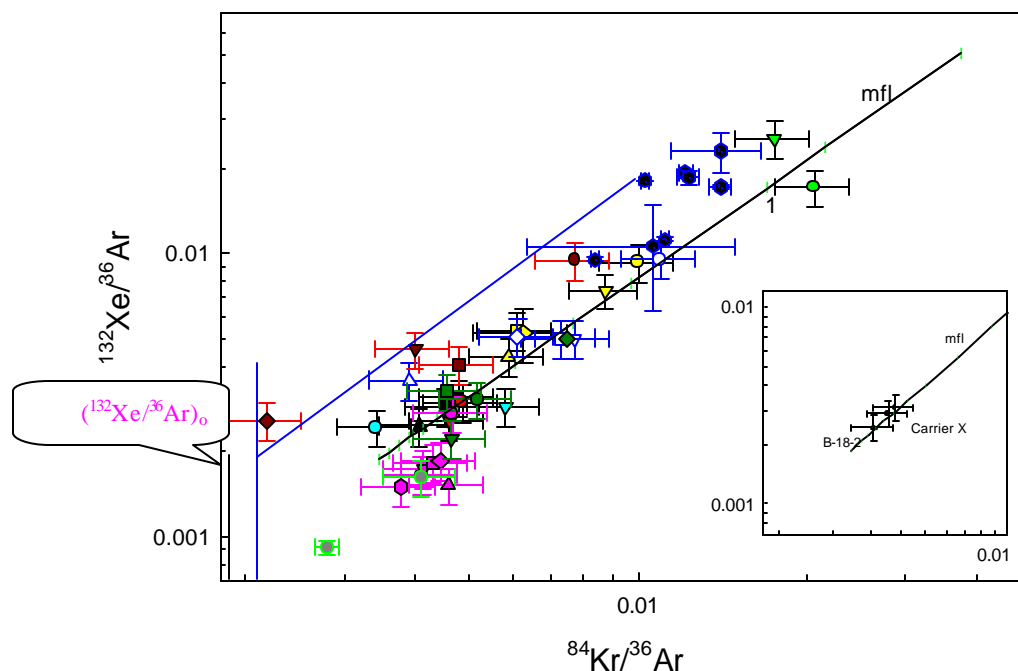
Fig 5.11 *Plot of $^{132}Xe/^{36}Ar$ vs $^{84}Kr/^{36}Ar$ ratios from acid residues as well as bulk samples of ureilites. The data fall along mass fractionation line. Inset showing the carrier X falls on the mass fractionation line passing through Haverö diamond (B-18-2). The data are from this work as well as from literature (Göbel et al., 1978, Wacker 1986, Wilkening and Marti (1976).*

(1978). Their choice was kamacite, which is present with an abundance of ~10%. They calculated the elemental ratios ($^{132}Xe/^{36}Ar$ and $^{84}Kr/^{36}Ar$) for the unknown carrier X of noble gas for the case of Haverö. In Fig 5.11 (inset), the elemental ratios of carrier X has been plotted with mass dependent fractionation line passing though $^{132}Xe/^{36}Ar$ and $^{84}Kr/^{36}Ar$ ratios of HF-HClO$_4$ residue (Haverö B-18-2, diamond rich). It can be seen clearly that the $^{132}Xe/^{36}Ar$ and $^{84}Kr/^{36}Ar$ ratios of carrier X exactly falling on mass dependent fractionation line (assuming Rayleigh Fractionation, *see* appendix), indicating that the noble gases in carrier X are related to that of diamond by mass fractionation. Ratios of $^{132}Xe/^{36}Ar$ and $^{84}Kr/^{36}Ar$ from all bulk ureilites as well as acid residue from all the ureilites as well as phase Q from primitive chondrites (not shown in the plot), show the same correlation, indicating that both the reservoirs of noble gases are related by mass fractionation. In general, bulk, HF-HCl and HF-HCl/HClO$_4$ residue data also fall along the line nearly parallel to the mass fractionation line indicating the presence of a carrier which has very different elemental ratio of noble gases but related to diamond by diffusion loss. Here we

propose that the unknown carrier X would have trapped the noble gases initially with composition similar to that of diamonds but lost a significant fraction of it through diffusion loss during parent body processing (heating). The mixing of this component with evolved elemental ratios with that of diamond, which being very refractory and hence least affected by the parent body processing, resulted in shifting along the fractionation line. The differences in elemental compositions in various aliquots of the same sample (two aliquots of the bulk samples, acid residue and oxidized residue), could be due to the heterogeneous distribution of these two carriers.

The presence of noble gases in comparable amount in diamond free ureilite ALH78019 (very lightly shocked), revealed another carrier of noble gases. Further studies of this ureilite suggested that the carrier of noble gases is fine grained carbonaceous material, which, like phase Q, survives the demineralization with HF-HCl but lost by $HClO_4$ treatment (Wacker 1986, Ott *et al.*, 1985b). Based on the similarities in release patterns (lower release temperature as compared to dia mond), nitrogen isotopic composition, behavior towards acid treatment, we propose the carrier of primordial noble gases in diamond free ureilites is fine grained amorphous carbon similar to that of phase Q from primitive chondrites.

$^{132}Xe/^{36}Ar$ and $^{84}Kr/^{36}Ar$ from ALH78019 plot very near to the left-hand (least altered) corner of the plot, indicating little evolution after trapping and it is quite expected because this ureilite is least shocked (*i.e.* least heated). Since the amorphous carbon is less refractory than diamonds, heating in parent body may lead to loss of trapped gases. We propose that the carrier X is amorphous carbon rather than kamacite, chromite or magnetite (the survival of these phases through acid treatment is difficult). The proportion of this amorphous carbon (carrier X) vary significantly from one ureilite to other and also within two aliquots of the same sample (the later is a consequence of sampling artifact). The amorphous carbon in diamond free ureilite is quite different from that of diamond bearing ureilites, the later ones lost most of their noble gases during body parent body processing.

If the diffusion loss of gases would have been responsible for evolution of elemental ratios, imprints of loss should be seen in isotopic composition. Since most of the amorphous carbon (in diamond bearing ureilites) combusting at lower temperature contain too small amount of noble gases for precise isotopic composition measurement, the expected small shifts in isotopic ratios (due to diffusion loss) might

be difficult to notice. However this contains significant amount of nitrogen and that is certainly heavier than that of diamonds but differences in nitrogen isotopic composition is too large to attribute solely to diffusion loss (see 4th chapter).

5.6 Noble gas elemental abundance and oxygen isotopic composition of ureilite

We have seen that elemental ratios $^{132}Xe/^{36}Ar$ and $^{84}Kr/^{36}Ar$ are mainly established by electron temperature of solar nebula with minor changes due to parent body processes superimposed on them. We have two elemental ratios, and the effect of parent body processing can be corrected to make the other ratio independent of diffusion loss. For this, we extrapolate one of the ratio ($^{132}Xe/^{36}Ar$) for all the bulk samples to a constant ratio of ($^{84}Kr/^{36}Ar$) ratio along the mass fractionation line (see Fig 5.11). In other
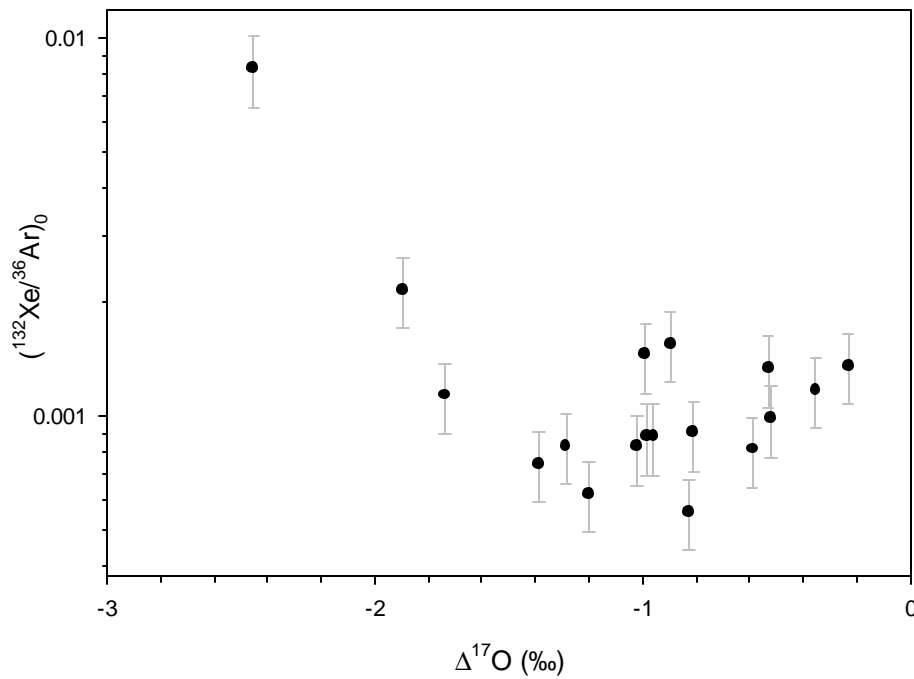
Fig 5.12 *The plot of ($^{132}Xe/^{36}Ar)_0$ (see text for definition) and $D^{17}O$ of various ureilites. A weak correlation can be seen between ureilite if two left most points have been included (ALH82130 have highest value of ($^{132}Xe/^{36}Ar)_0$ and lowest value of $D^{17}O$). Excluding these two points, a poor correlation is apparent, indicating that the carbon in ureilites, carrier of Xenon (noble gases as well), show no relation to the silicates, the major carrier of oxygen. (Oxygen data from Clayton and Mayeda, 1988; Ureilite data from this work; Gobel et al., 1978; Wacker 1986; Wilkening and Marti (1986).*

words, $(^{132}Xe/^{36}Ar)_0$ is the intercept on $^{132}Xe/^{36}Ar$ axis (ordinate) at a fixed value of $^{84}Kr/^{36}Ar$ (abscissa) by the line with slope defined by mass dependant Raleigh fractionation. The values of $(^{132}Xe/^{36}Ar)_0$ are supposed to be independent of parent body processing and represent the initial trapped value of this ratio. If noble gases are trapped by diamond under plasma, the elemental ratio $^{132}Xe/^{36}Ar$ is established by plasma temperature and can be used as measure of plasma temperature.

In three isotope plot of oxygen, like other achondrite, ureilites, do not fall along mass fractionation line with slope nearly half; instead they fall along slope 'one' defined by the dark inclusions of C3V carbonaceous chondrites (Clayton and Mayeda 1988). This means that each individual ureilite sample have different $\Delta^{17}O$. It has been argued that the $\Delta^{17}O$ of any meteorite is function of temperature that in turn related to location of meteorite formation. In ureilites, the majority of oxygen is carried by the silicates, therefore the $\Delta^{17}O$ of individual ureilite is characteristic (function of temperature) of their formation location. $(^{132}Xe/^{36}Ar)_o$ on the other hand, is also function of plasma temperature at their formation location that in turn related to origin of carbon. In order to see that relation between the carbon and silicate, it is interesting to look at the correlation of $(^{132}Xe/^{36}Ar)_o$ and $\Delta^{17}O$. In Fig 5.12, $(^{132}Xe/^{36}Ar)_o$ and $\Delta^{17}O$ have been plotted for individual ureilite, the poor correlation (excluding the two left most points) can be seen. This might be an indication that the origin of carbon in ureilite is not related to silicates in ureilites i.e. carbon would have never been a part of magma from which silicates have been crystallized. But the lowest value of $\Delta^{17}O$ shown by most reduced specimen among ureilites is intriguing.

Implications of Nitrogen Studies to the Nebular/Parent Body Processes

6.1 Introduction

In this chapter, various nitrogen components in ureilites and their origin will be discussed. Origin of diamonds in ureilites is not yet settled and study of nitrogen in bulk as well as acid residues provide some insight into this, as will be discussed in a later part of the chapter. There are three different forms of carbon present in ureilites: diamond, amorphous carbon and graphite. So far, we have seen that the acid resistant residues contain two isotopically very distinct major nitrogen components that primarily reside in diamonds and amorphous carbon. The nitrogen in diamonds is always accompanied by primordial noble gases while in amorphous carbon, the amount of noble gases associated with nitrogen is varying from negligible to very large amounts from one sample to other. These variations are most likely caused by secondary processes in side their parent body. Graphite, the most abundant form of carbon in ureilite, contains a significant amount of nitrogen but almost has no noble gases. In the previous chapters, we have shown that both diamonds, amorphous carbon (in diamond free ureilite as well as phase Q from primitive chondrites) and graphite are most likely early nebular condensates and trapped the noble gases from nebular plasma in the early solar system. If noble gases trapped in diamonds and phase Q are from the solar nebula, the accompanied nitrogen should also have similar origin and may represents nebular nitrogen composition provided no isotopic fractionation has occurred during trapping. In this chapter, this issue will also be discussed in detail.

6.2 Trapping of nitrogen into diamonds and amorphous C

Nitrogen analysis from all the acid residues can not simply be explained by only two nitrogen components. At least one more nitrogen component is needed with nearly air-like composition. This air-like nitrogen component is most likely captured by the
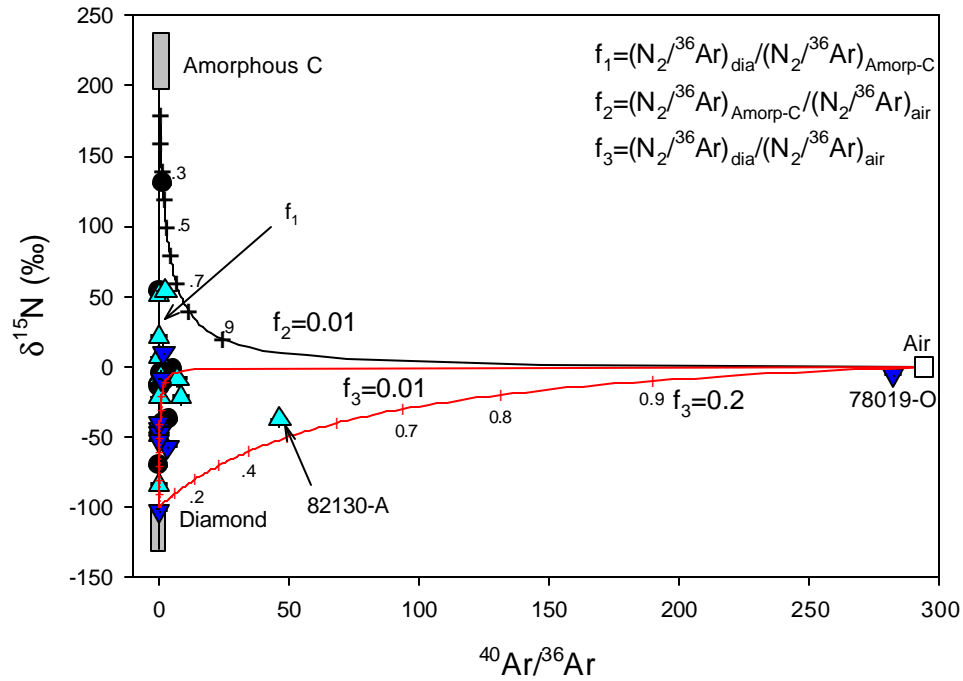
Fig 6.1 *Three component mixing diagram for nitrogen and argon. Two components are diamonds and amorphous carbon while third component is air like nitrogen most likely adsorbed during sample preparation. It can be seen clearly that the acid residues, in general, contain relatively more air-like nitrogen as compared to bulk samples. (Symbol: = HF/HCl residue; = $HClO_4$ residues and ●= Bulk samples. Each number below the line is fraction of air-like component present.*

acid residue during acid dissolution and is thus not an indigenous ureilitic component. In three component mixing diagram (Fig 6.1), most of the bulk samples fall along the mixing line of diamonds ($\delta^{15}N \leq -120$‰, $^{40}Ar/^{36}Ar \sim 0$) and amorphous carbon ($\delta^{15}N \geq 200$‰, $^{40}Ar/^{36}Ar \sim 0$) while the acid residues seem to be contaminated by air-like nitrogen and argon ($\delta^{15}N = 0$‰, $^{40}Ar/^{36}Ar \sim 295$). In all the measurements except two (ALH78019-O and ALH82130-A have more contribution from air like components), the contribution of air-like component is always less than 20 percent though the estimation of the fraction of air-like component strongly depends on the ratio of $N_2/^{36}Ar$ assumed (f_2 and f_3) in the two components. In Fig 6.2, $^{14}N/^{36}Ar$ has been plotted against reciprocal of ^{36}Ar concentration, higher concentration of ^{36}Ar (*i.e.*, lower value of $1/^{36}Ar$) can be used as indicator for the higher proportion of 'planetary' (or primordial) noble gases and hence the $^{14}N/^{36}Ar$ corresponding to $1/^{36}Ar$ 0, should more closely represent the planetary $^{14}N/^{36}Ar$ ratio. The shaded region in Fig 6.2 are the range of calculated values for singly ionized nitrogen to argon ratio ($^{28}N_2/^{36}Ar$ and
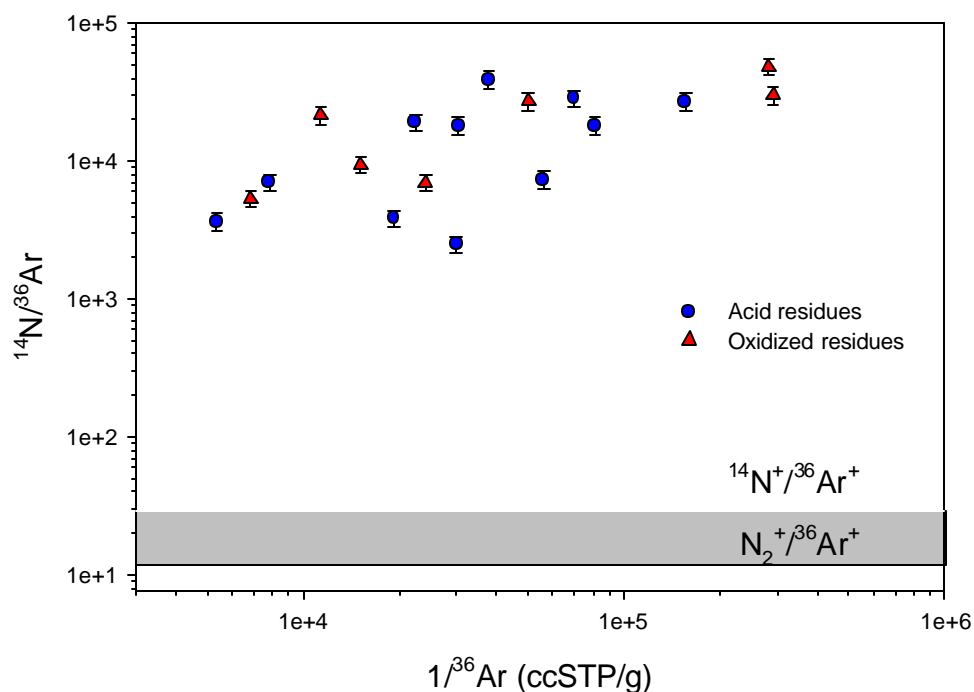
Fig 6.2 *Nitrogen to argon ratio for various acid residues as well as oxidized residues from ureilites as function of $1/^{36}Ar$. The shaded region is theoretically calculated nitrogen to argon ratios (singly ionized) for atomic and molecular nitrogen at electron temperature of 8000K in plasma. Higher ^{36}Ar amount is indicative of higher proportion of 'planetary' gases. The excess of nitrogen over argon than that expected for 'planetary' ratio can be seen.*

$^{14}N/^{36}Ar$ in assuming molecular or atomic nitrogen) that can be attained in the solar nebula for electron temperature of 8000K. It can be seen clearly that the $^{14}N/^{36}Ar$ ratios measured in ureilite residues are two to three orders of magnitude higher than that expected from 'planetary' gases. Similar enrichments have been observed for nitrogen implanted in pure ilmenite separate from lunar soil 71501 (Kerridge 1993). When nitrogen has been plotted as though ^{14}N were heavier noble gas than xenon, a smooth fractionation line has been observed and this is attributed to the chemical reactivity of nitrogen, which might cause it to be implanted with greater efficiency than a noble gas. In Fig 6.3, the elemental abundance of nitrogen and noble gases normalized to ^{36}Ar relative to solar abundance have been plotted for the acid residues from various ureilites and phase Q from Dhajala. The enrichment of nitrogen relative to noble gases can clearly be seen. It has already been established that most of the nitrogen and noble gases in lunar soils are solar wind implanted. The similarity of nitrogen and noble gases elemental abundance pattern for acid residues from ureilites to that of ilmenite separates from lunar soil argue that the enrichment of nitrogen as
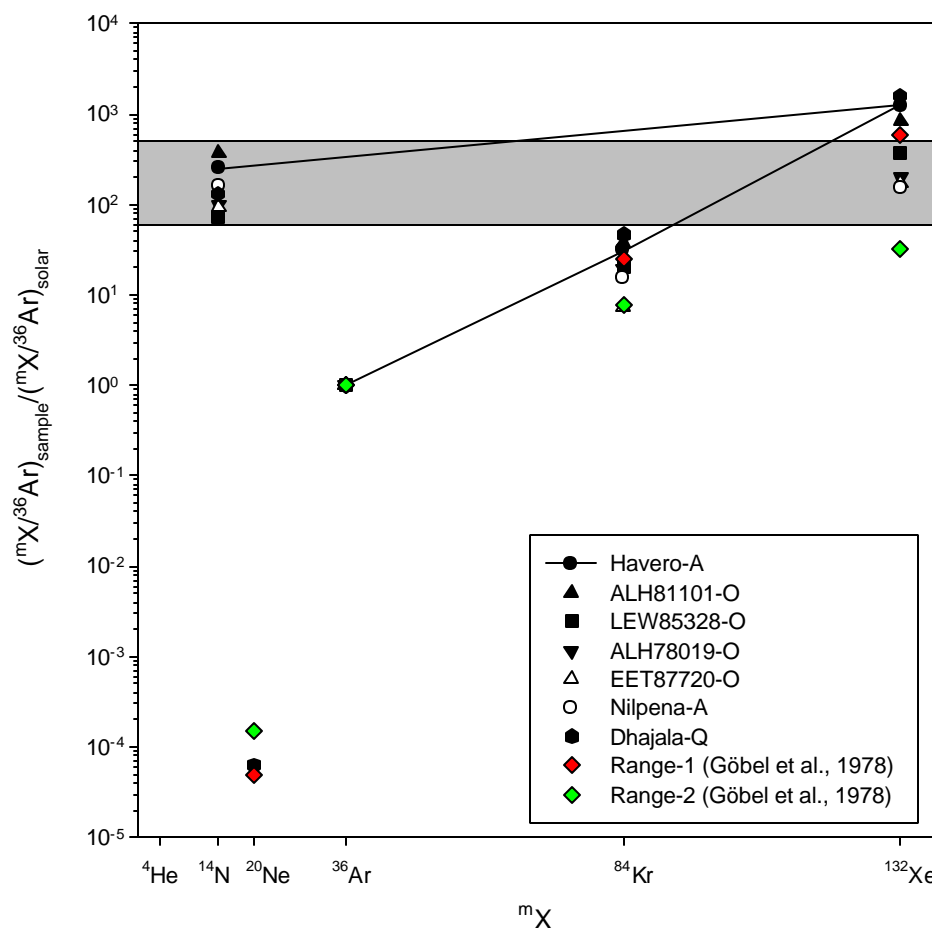
Fig 6.3 *Elemental abundance patterns of noble gases normalized to ^{36}Ar relative to solar abundance is plotted as function of mass for the acid residues of ureilites and phase Q from Dhajala. Nitrogen has also been included along with noble gases. A clear excess of nitrogen over noble gases can be seen for both phase Q and acid residues of ureilites.*

compared to noble gases is brought about by implantation mechanism. In other words the enrichment of nitrogen as compared to noble gases is suggesting the implantation as a mechanism of the noble gas (and nitrogen as well) trapping. In order to have better understanding of the mechanism of enrichment of nitrogen over noble gases during ion implantation, an appropriate laboratory simulation experiment is required.

6.3 Implications

6.3.1 Origin of diamonds in ureilites

Ever since the diamonds have been discovered in ureilites, their origin has been a puzzle for scientists. Many of the features of ureilites suggest that the diamonds were produced *in situ* by shock conversion of graphite. But the origin of gas rich diamonds

from gas poor graphite is difficult to explain (Göbel *et al.*, 1978). Though many of the ureilites show the evidence of shock, it is not clear whether the shock is really responsible for the production of the diamonds (by the conversion of graphite) or the diamonds were already present when ureilites have undergone the shock event. Irrespective of whether shock predates or postdates the formation of diamonds, the shock features shown by either ureilites or diamonds can be explained, but the noble gas characteristics argue against the *in situ* origin of diamonds and are in favor of the nebular origin of diamonds (Wilkening and Marti, 1976; Göbel *et al*, 1978; Wacker, 1986) through condensation in solar nebula. Laboratory simulation study on diamonds produced by CVD (Chemical vapor Deposition) process in artificial noble gas atmosphere under low pressure plasma also argue in favor of nebular origin of diamonds (Fukunaga *et al.*, 1987; Matsuda *et al.*, 1991; Fukunaga and Matsuda, 1996). In the present section, I will try to rationalize the origin of diamonds using nitrogen isotopes as a tracer.

Nitrogen in acid residue of ALH78019 showed the presence of two nitrogen components, one released along with primordial noble gases, having $\delta^{15}N = -21‰$ and the other having $\delta^{15}N=+19‰$, is free of trapped noble gases but accompanied by peak carbon combustion (graphite). Diamonds in all the ureilites have nitrogen with $\delta^{15}N$ of $\leq -100‰$. If diamonds were produced *in situ* by shock conversion of the precursor material similar to either gas rich carbon or graphite in ALH78019, then fractionation of nitrogen from +19‰ or −21‰ to $\leq$-100‰ is needed during the shock conversion of graphite (or gas rich amorphous carbon) to the diamonds. Since the conversion of graphite to diamonds is an instantaneous process, one hardly expects such a large change in nitrogen isotopic composition. Moreover, graphite in ureilites is found to be free of noble gases. Though the noble gas free graphite might still be reconcilable, with shock production of diamond (from graphite), as a left over material, the nitrogen isotopic data of graphite/amorphous carbon and diamond will be very difficult to be explained. This indicates that the diamonds in ureilites are not *in situ* produced by shock conversion of graphite or amorphous carbon. Rather, all the three C phases could have been produced independently from gas phase in the nebula and later incorporated into ureilites. The large difference in nitrogen compositions of bulk ureilites and their acid residues as well as the similar nitrogen composition of diamonds from monomict and polymict ureilites despite of large differences in their

bulk nitrogen isotopic compositions also argue against the *in situ* origin of diamonds in ureilite (Table 4.6 in chapter 4).

6.3.2 Origin of heavy and light nitrogen

Grady and Pillinger (1988) are the first to identify the heavy nitrogen in polymict ureilites and have suggested that the heavy nitrogen was of external origin and was most likely injected into the ureilites parent body by an impactor. Our results on monomict ureilites as well as some recent reports from literature (Rai *et al.*, 2000; Yamamoto *et al.*, 1998) have shown heavy nitrogen with $\delta^{15}N$ similar to that of polymict ureilites, necessitating a revaluation of impactor origin for heavy nitrogen. Heavy nitrogen is always present in significant amount in both monomict and polymict ureilites, except that it is relatively much heavier in polymict ureilites. The behavior of carriers of heavy and light nitrogen toward combustion release and towards acid treatment suggest the amorphous carbon as the most probable carrier of heavy nitrogen while diamond is the carrier of light nitrogen. There are at least three ways to understand the isotopic signatures of these two nitrogen components. One possibility is that both amorphous carbon and diamonds trapped their gases from solar nebula from different locations having different nitrogen isotopic compositions and are representing local nebular heterogeneity. Another possibility for the presence of heavy and light nitrogen could be due to fractionation during incorporation of nitrogen, brought about by slight change in the physicochemical conditions, which led to the formation of the three different forms of carbon. Since diamonds are formed in very narrow range of physicochemical conditions (Fukanaga and Matsuda, 1997), they show very narrow range of $\delta^{15}N$, while amorphous carbon, which can be formed in wider range of physicochemical conditions (Matsuda *et al.,* 1991) leading to broad range of $\delta^{15}N$. A third possibility could be due to differential loss of gases from some of the carrier phases after initially trapping the same composition in all the three carbon carriers leading to the observed variations in nitrogen composition. Our results suggest that the primary cause for these differences could be the changes in physicochemical conditions in the nebula, while a later partial loss due to parent body processes must have led to the finer changes that have been superimposed on these primary differences, in particular, between the heavy nitrogen phases of monomict and polymict ureilites. The presence of two carriers of noble gases, whose elemental compositions are related by mass dependent fractionation, as shown by covariance of

the elemental ratios $^{132}Xe/^{36}Ar$ and $^{84}Kr/^{36}Ar$ among various ureilites suggest that the loss of noble gases from one of the carrier could have occurred after trapping of gases from the same reservoir (Fig. 5.11).

6.3.3 Implications to nebular nitrogen composition

Despite a large number of nitrogen measurements from various classes of meteorites and planetary objects and from solar wind, the composition of nitrogen in early solar nebula is still not constrained (Fig 6.4). Primitive chondrites show large variations in N composition though they all showed a uniform reservoir of trapped primordial noble gases. Most of the trapped primordial noble gases in primitive chondrites are carried by the acid resistant phase named as 'phase Q' (Lewis *et al.*, 1975; Wieler *et al.*, 1991 & 1992; Busemann *et al.*, 2000). The determination of nitrogen composition of phase Q is difficult because of its inseparability from presolar grains with extremely anomalous nitrogen isotopic composition $\delta^{15}N = -340‰$) (Russell *et al.*, 1991). An alternative approach to determine the nitrogen composition is the measurement of solar wind nitrogen or solar energetic particles (SEP) nitrogen. The first *in situ* on board SOHO (Solar and Heliospheric Observatory) space craft measurement of nitrogen in solar wind showed a heavy nitrogen with $\delta^{15}N = 360 \pm 374‰$ (Kallenbach *et al.*, 1998). The solar wind implanted nitrogen from returned lunar samples showed 300‰ variation in $\delta^{15}N$ in the samples of different antiquities, which has been attributed to the secular change in solar convection shell that led to nitrogen fractionation (Becker and Clayton, 1977). Recent *in situ* ion probe measurement in lunar soil yielded nitrogen with $\delta^{15}N$ of $\leq -240‰$ that resides in surface layer of $\leq 100nm$ on ilmenite grains from lunar soil sample (79035), and hence attributed to implanted solar wind (Hashizume *et al.*, 2000).

The question is whether the present day solar wind nitrogen composition or the nitrogen implanted in lunar soil samples really represents nitrogen composition of early solar nebula. Nitrogen in early solar nebula means the nitrogen trapped (or implanted in grains) during condensation of solids from solar nebula that subsequently accreted to form meteorite parent body. Most of the meteorite parent bodies or planetesimal (accreted to form planets) trapped their gases from protosolar disk. The nitrogen in the solar wind is cycled through Sun and might have undergone compositional (isotopic) change to unknown degree during acceleration mechanism (Bochsler and Kallenbach, 1994) and probably may not be representative of the
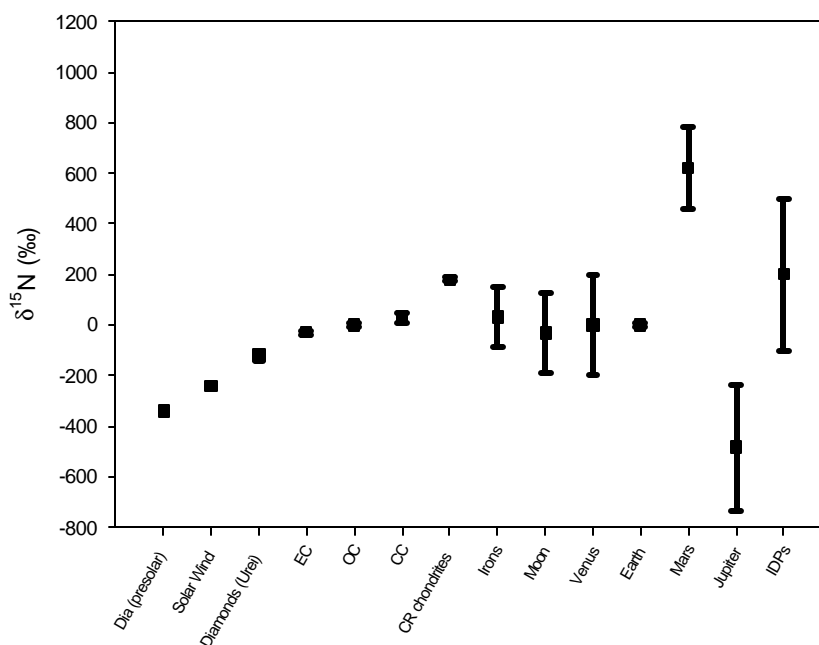
Fig 6.4 *Nitrogen compositions ($d^{15}N$) for various solar system objects. The error bars represent the range of $d^{15}N$ values measured [data from, this work (Ureilite diamond); Hashizume et al., 2000; Russell et al., 1991 (Insterstellar diamonds); Haffman et al., 1979 (Venus); Grady et al., 1986 (EC); Owen et al., 1977 (Mars); Thiemens and Clayton 1980; Becker and Clayton 1977 (Moon); Kung and Clayton 1978 (CC, OC and CR); Kerridge 1985 (CC & CR)].*

nitroge n composition in early solar nebula. In this connection, the nitrogen in the atmosphere of Jupiter might be a better representative of nebular nitrogen rather than solar wind nitrogen. Although a number of attempts have been made to measure the nitrogen composition of Jovian atmosphere, such data have not only shown very large variations but also had large uncertainty. A very heavy nitrogen has been reported for Jupiter with $\delta^{15}N$ of +660‰ based on $^{15}NH_3/^{14}NH_3$ measurement using IR spectra (Tokunaga *et al*., 1979 and Nier *et al.*, 1976). However, because of some basic problem with interpretation of IR spectra, Tokunaga and coworkers stated that the $^{15}N/^{14}N$ ratio could still be consistent with the terrestrial ratio. Recently, Fouchet *et al.* (2000) reported very light nitrogen with $\delta^{15}N$ value of -484^{+245}_{-272} ‰ for ammonia (at 400 mbar pressure) in Jovian atmosphere. But they suspected two processes could have plausibly caused the depletion of ^{15}N at pressure level of 400 mbar: the condensation of NH_3-ice and photo-dissociation from solar UV radiation. Therefore, the measured nitrogen composition of Jovian atmosphere may not provide the original nitrogen composition of solar nebula because of the two reasons; firstly the

measurements have very large uncertainty and secondly, it might have undergone fractionation to unknown extent either due to cloud formation or due to solar UV radiation. The ground based spectroscopic measurement of nitrogen composition of comet Hale Bopp (C/1995 O1) revealed $\delta^{15}N$ value of $-158 \pm 120‰$ along with carbon and sulfur isotopic composition that are consistent with of solar system values (Jewitt *et al.*, 1997). Based on this they concluded that comets have originated in the outer regions of the sun's proto-planetary disk. Though the isotopic composition of volatile elements (carbon and sulfur) in comets are consistent with solar system values, the large errors involved in spectroscopic measurements of isotopic compositions make these numbers of less importance. The $\delta^{15}N$ value for the IDPs (Interplanetary Dust Particles) range from -100 to $+500‰$, whereas a major population exhibits enrichment of ^{15}N associated with D rich hydrogen with δD values up to $25000‰$ (Messenger 2000).

We have seen that the phase Q and the diamonds from ureilites are the carriers of primordial noble gases in primitive chondrites and ureilites respectively. These gases have been trapped very early in solar nebula as indicated by the lower value of $^{40}Ar/^{36}Ar$. The study of nitrogen composition in these samples may provide its composition in early solar nebula. But the reliable measurement of nitrogen in phase Q is difficult due to presence of presolar grains with their extremely anomalous nitrogen isotopic composition. So far, only one successful measurement of nitrogen composition has been reported in phase Q of Dhajala, which fortunately does not contain presolar grains (Schelhaas *et al.*, 1990) and yielded $\delta^{15}N$ of $-15‰$ (Murty 1996). The diamonds (and the amorphous carbon in ALH78019) from ureilites have noble gases with elemental and isotopic composition similar to that of phase-Q. The nitrogen released along with primordial noble gases in the acid resistant residue from both monomict and polymict ureilites have yielded nitrogen with $\delta^{15}N$ of $\leq -100‰$, while the nitrogen in the amorphous carbon along with noble gases in the diamond free ureilite, is having $\delta^{15}N$ of $\leq -21‰$. Though all these carriers of primordial gases have more or less uniform isotopic compositions for the noble gases, the nitrogen isotopic compositions of these carriers are quite different. These variations in $\delta^{15}N$ may have two possible explanations. First one is that the solar nebula was heterogeneous with respect to nitrogen isotopic composition while the second one is due to fractionation during the trapping of nitrogen from a homogeneous solar nebula.

In order to understand the cause of fractionation of nitrogen in these carriers of primordial gases, a proper understanding of physico-chemical conditions during trapping of these gases are required. Since the elemental composition of noble gases most likely established by plasma temperature, the noble gases elemental ratio may provide the information about the electron temperature of plasma at the formation location of the carrier of these phases (Fig 5.6). It has been shown (in the previous chapter) that the higher plasma temperatures lead to lower elemental fractionation. The close look of elemental abundance pattern of noble gases in ureilite diamonds reveals that the noble gases in diamonds from ureilites are less fractionated than those of phases Q indicating that the primordial gases are trapped in diamonds at higher electron temperatures than that of Q phase. Since the gases are trapped in diamonds at higher plasma temperature as compared to phase Q, it is likely that higher temperature fractionates nitrogen towards lower $\delta^{15}N$. In other words, the elemental fractionation of heavy noble gases and nitrogen isotopic fractionation move in opposite direction. If this is true then the nitrogen from solar wind should have been even more fractionated because of its higher temperature origin either in corona or in solar photosphere and most probably that is what has already been observed (Hashizume *et al.*, 2000). The higher temperature origin of solar wind also be consistent by its nearly flat (little fractionated) noble gas elemental abundance pattern. The reason why nitrogen is being fractionated towards lighter $\delta^{15}N$ with higher electron temperature is not yet clear but it is an important aspect to be addressed by future laboratory simulation experiments.

6.3.4 Is the nebular nitrogen heavy or light?

The noble gases from solar wind or SEP are less fractionated because of its origin at higher temperature at solar corona or photosphere. Though the measurement of elements in solar wind matches reasonably well with spectroscopic measurements, the measured isotopic compositions show inconsistency e.g., the $^{20}Ne/^{22}Ne$ isotopic composition of solar wind and SEP are quite different though they both have originated in solar surface, but differing in mechanism of acceleration. In case of nitrogen, the scenario seems to be even more complex. Surface correlated nitrogen in lunar soils showed 35% variations (Becker and Clayton, 1977).

In early solar system, a significant proportion of the matter was in the form of plasma. In plasma, the elements are present in ionized state along with some neutral species as
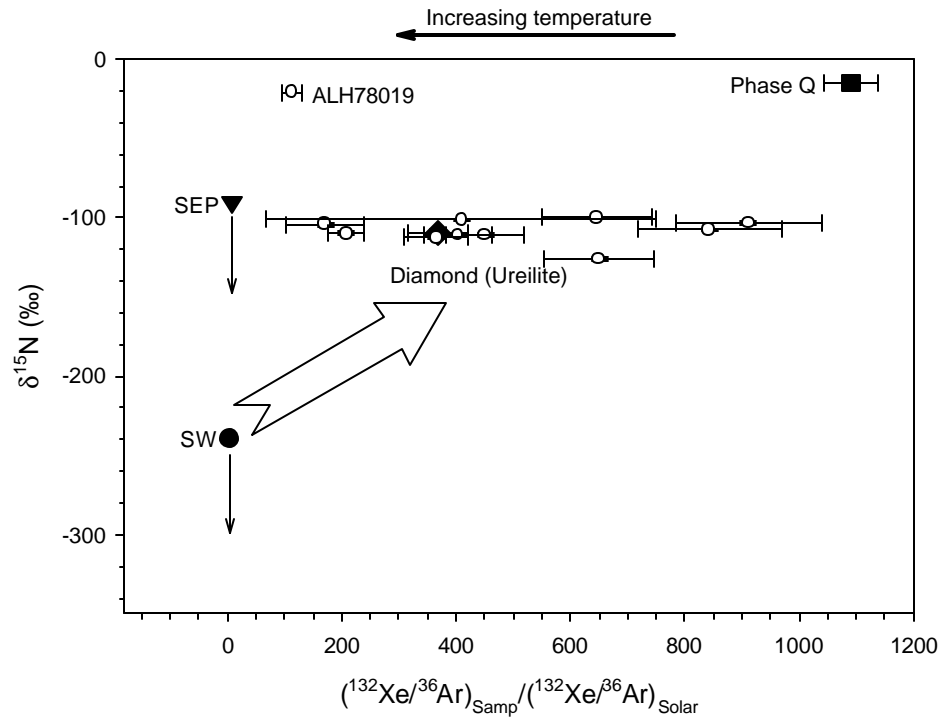
Fig 6.5 *d^{15}N of solar wind, SEP, phase Q and ureilitic diamonds as a function of corresponding $^{132}Xe/^{36}Ar$ ratios normalized to solar ratio. The abscissa is a measure of the electron temperature of the plasma, higher values corresponding to lower temperature. The* **d**^{15}N *of SW and SEP are the upper limit estimates. Open diamonds are individual ureilite diamonds data while the filled diamond is the mean value for all the measurements from diamond rich residues from ureilites. Data sources: Phase Q, Murty (1996); SW, Hashizume et al., (2000): SEP, Mathew et al. (1998) & Wieler and Baur (1995).*

well. The ionic composition of plasma approaches their elemental composition at very high temperature (electron). The major difference of nitrogen and noble gases are the tendency of former to form molecule. Nitrogen forms very stable diatomic molecule and is supposed to be second most stable molecule after CO in nebular condition. Most probably, because of this behavior, nitrogen is very sensitive to isotopic fractionation. It has been shown by various workers that nitrogen has undergone non-equilibrium isotopic fractionation in plasma (Arrhenius *et al.*, 1978). This could most likely be the cause for nitrogen fractionation in various classes of meteorites rather than heterogeneous solar nebula with respect to nitrogen isotopic composition. The $^{84}Kr/^{36}Ar$ and $^{132}Xe/^{36}Ar$ of diamonds from ureilites are relatively less fractionated as compared to that of phase Q from primitive meteorite. This implied that gases are trapped in diamonds at higher electron temperature than that of Q phase. The

difference in the $\delta^{15}N$ could most likely be due to this difference in trapping conditions. This mechanism not only explains the fractionation of nitrogen in these carriers but also explains very light nitrogen in solar wind as observed recently (Hashizume *et al.*, 2000). From the above discussion, it is clear that the high electron temperature favor low $\delta^{15}N$, indicating that the true nitrogen composition of solar nebula must be heavier than that shown by Q phase. In order to know the true nebular composition of nitrogen one has to look for a carrier phase that has formed at lower temperature rather than a carrier phase which has been formed in high temperature plasma in early solar nebula. An alternative way is the quantitative estimation of fractionation by a laboratory simulation study in artificial nitrogen and noble gas atmosphere. At this stage I could only say that the nebular nitrogen must be heavier than the -15‰ and could most probably be enriched up to a few hundred per mil in $\delta^{15}N$ (Fig 6.5). The relatively heavy nitrogen observed in carbonaceous chondrites may be real representative of nebular nitrogen composition. The nitrogen from CI and CM (excluding presolar component) are in general heavy and most likely represents nebular nitrogen composition.

Conclusions and Future work

7.1 Conclusions

Ten ureilite samples have been studied for nitrogen and noble gases. Out of these, HF-HCl resistant residues for eight samples and HF-HCl-HClO$_4$ resistant residues for seven samples have been prepared and analyzed either by pyrolysis or by combustion or by a combination of both. A few selected samples as well as acid residues have also been studied for elemental analyses by INAA.

The focus of this thesis is to decipher and understand the 'nitrogen components' in ureilites. The nitrogen components deciphered from this study have been plotted in Fig 7.1 for monomict, polymict and diamond free ureilites. The $\delta^{15}N$ of diamond from both monomict and polymict ureilites must be lower than -110‰ (shown by blue box within the diamond field). Slightly heavier (than -110‰) $\delta^{15}N$ for the other diamonds, most likely indicates co-release of nitrogen from graphite which is expected to be heavy. In case of amorphous C, the true $\delta^{15}N$ must be heavier than that shown in the box because it is most probably lowered by contamination by adsorbed air nitrogen. Based on the present study, the following conclusions can be drawn:

- At least two major nitrogen components are needed to explain the nitrogen isotopic systematics of ureilites in addition to two minor components. A light nitrogen with $\delta^{15}N\leq$-100‰, is carried by the diamonds present in both monomict and polymict ureilites and is also accompanied by primordial noble gases. Based on degree of secondary alteration inside their parent body, presence of two types of amorphous carbon carriers have been suggested in ureilites. The one present in diamond bearing ureilites, has lost a significant fraction of its trapped gases during
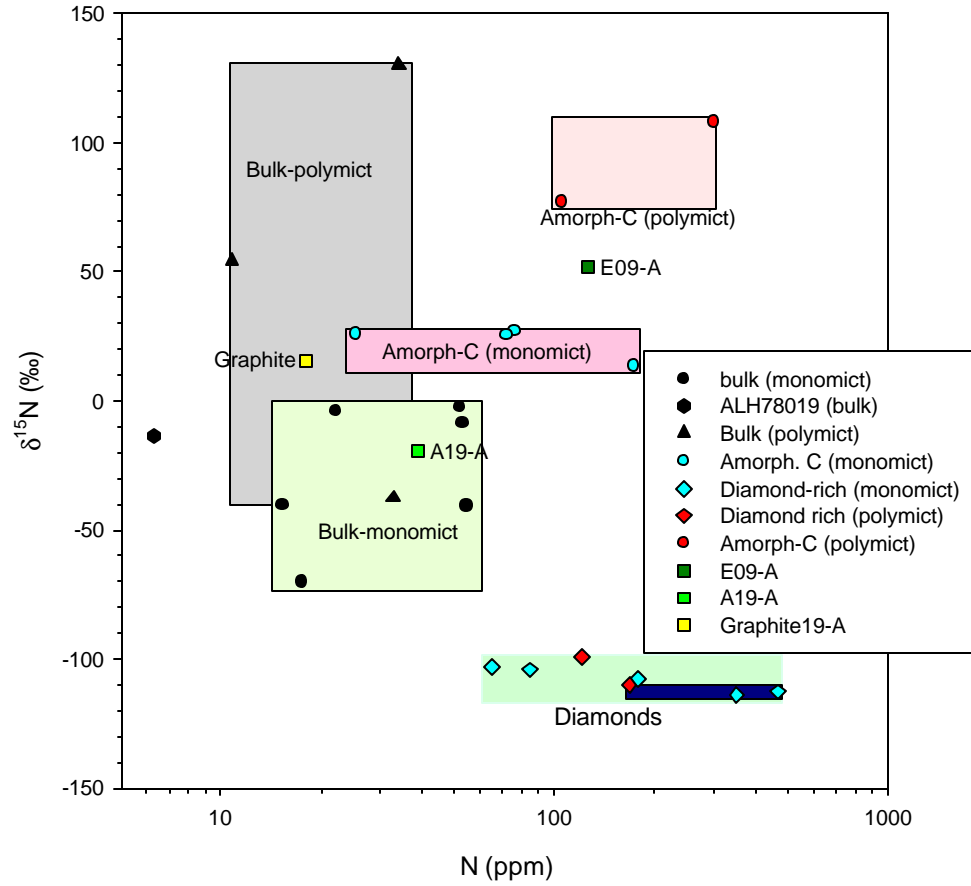
Fig 7.1 *Plot showing the range of nitrogen concentrations and isotopic compositions ($d^{15}N$) of various components (amorphous-C, graphite and diamond) of ureilites along with whole rock samples.*

parent body processing, while the other one is least affected by parent body processes and is present in only two diamond free ureilites (ALH78019 and EET83309). A relatively heavy nitrogen with variable $\delta^{15}N$ ($\geq 20\permil$) is carried by amorphous carbon from diamond bearing monomict ureilites, and this nitrogen is not associated with primordial noble gases (most likely lost during parent body processing). Amorphous C from diamond free ureilite, ALH78019 contains nitrogen with $\delta^{15}N \leq -21\permil$, and is accompanied by peak noble gas release. Based on absence of light nitrogen and low release temperature of nitrogen and noble gases (as observed in case of diamond free ureilite ALH78019), the polymict ureilite EET83309 also seems to be a diamond free ureilite and out of more than 50 ureilites known so far, this is the second diamond free ureilite and the first diamond free polymict ureilite. Most of the nitrogen released from this ureilite is relatively heavier.

- The presence of light nitrogen (with narrow range of $\delta^{15}N$) in diamonds from both monomict and polymict ureilites, having very large variations in their bulk nitrogen composition argues against the *in situ* origin of diamonds.

- Spread of heavy noble gas elemental ratios ($^{132}Xe/^{36}Ar$ and $^{84}Kr/^{36}Ar$) along mass dependant fractionation line, indicates the presence of two noble gas carriers, which have responded differently during parent body processing. The amorphous carbon being less refractory, lost a significant fraction of trapped gases and hence evolved to higher values of $^{132}Xe/^{36}Ar$ and $^{84}Kr/^{36}Ar$ ratios. The mixing of this to the gases trapped in diamonds that is little affected by these later processes, is most likely responsible for the observed spread in noble gas elemental ratios.

- It has been proposed earlier that the heavy nitrogen in polymict ureilites is of foreign origin, but the presence of heavy nitrogen in some of the monomict ureilites argues against it. It seems more likely that both heavy and light nitrogen produced by a non-equilibrium fractionation processes during trapping of these gases into their carriers in solar nebula due to difference in physicochemical conditions at their formation locations. A minor modification of nitrogen isotopic composition could also be possible due to secondary alteration inside their parent body.

- It has been shown that the diamonds and amorphous carbon (acid residues) in ureilites are highly enriched in refractory trace siderophile elements and accounts for the total inventory of these elements in ureilites. These are most likely incorporated in carbon phases directly from solar nebula.

- The depth profile of elemental ratios of heavy noble gases along with simulation of ion implantation study, indicate that the primordial noble gases and nitrogen have been incorporated into their carriers by ion implantation.

- By comparing $^{132}Xe/^{36}Ar$ and $^{84}Kr/^{36}Ar$ ratios between phase Q and diamond from ureilites, it is possible to infer the plasma temperature at which gases are ion implanted into these phases. We infer that phase Q has acquired its gases at lower temperature as compared to diamonds from ureilites.

- The primary reason for the differences between $\delta^{15}N$ of diamonds and amorphous carbon and graphite of ureilites, and of phase Q are due to the changes in physico-chemical conditions (possibly dominated by the plasma temperature) prevalent at the formation locations of these phases. Combining these results with nitrogen isotopic compositions of these carriers revealed that the nitrogen in solar nebula must be heavier than -15‰, and might be enriched in ^{15}N by a few tens of permil.

7.2 Scope of future work

- A simulation study is needed to understand nitrogen fractionation during trapping into diamonds and amorphous carbon from plasma. Understanding this process will also help in constraining the isotopic composition of solar nebula.

- Similar to nitrogen, boron is another element, which can replace carbon in diamonds lattice with ease and hence it is possible that diamonds and probably amorphous carbon and graphite in ureilites contain appreciable amount of boron. Like nitrogen, if boron also undergoes non-equilibrium isotopic fractionation, a study of boron isotopic composition in diamonds and amorphous carbon can offer clues to understand non-equilibrium processes operating in the nebula during trapping of volatile species.

- The closed system stepped etching (CSSE) experiment on diamond free ureilites might be useful to better constrain the carrier of noble gases in these ureilites.

- Measurement of halogens (Cl and I) in phase Q and acid resistant residues from ureilites would be very interesting to confirm the suggested preferential enrichment of halogens over noble gases in these carriers of primordial gases.

Appendix

A 1. Nitrogen isotopes: *the d notation*

Nitrogen has two stable isotopes, ^{14}N and ^{15}N, of which ^{14}N is far more abundant. The terrestrial atmosphere, with a uniform $^{15}N/^{14}N$ ratio of 0.003676, serves as the standard for the nitrogen isotopic measurements. The N isotopic composition of a sample is expressed as the deviation of the $^{15}N/^{14}N$ ratio from that in the terrestrial atmosphere (air). Symbolically it is represented as

$$\delta^{15}N\ (‰) = \left[\frac{\left(\frac{^{15}N}{^{14}N}\right)_{sample}}{\left(\frac{^{15}N}{^{14}N}\right)_{Air}} - 1 \right] \times 10^3 .$$

A 2. Neon in Ureilites
Table A1. The isotopic composition of neon in whole rock samples of ureilites.

Temp. (°C)	^{22}Ne 10^{-8}ccSTP/g	$^{20}Ne/^{22}Ne$	$^{21}Ne/^{22}Ne$	^{4}He 10^{6} ccSTP/g	$^{3}He/^{4}He$ ($\times 10^4$)
Kenna (bulk), 49.49 mg					
400	0.11	9.861	0.2232	0.69	187.9
		0.091	0.0019		15.4
800	0.75	0.829	0.8908	-	
		0.005	0.0064		
1000	1.58	1.803	0.7828	-	
		0.003	0.0069		
1200	1.25	2.414	0.7337	0.32	1140
		0.018	0.0066		94
1300	1.62	1.571	0.8321	-	
		0.015	0.0069		
1350	0.70	2.723	0.6679	-	
		0.048	0.0099		

1400	0.94	3.050	0.6605	-	
		0.020	0.0068		
1450	1.60	2.291	0.7433	-	-
		0.003	0.0066		
1451	0.86	4.161	0.4967	1.34	58.23
		0.072	0.0064		4.78
1452	0.57	4.099	0.5109	-	
		0.118	0.0068		
1500	1.66	2.311	0.7281	-	
		0.008	0.0082		
1600	4.31	1.770	0.7850	-	
		0.017	0.0055		
1850	0.48	9.378	0.0519	-	
		0.017	0.0009		
Total	16.43	2.461	0.7186	2.36	245.4
		0.021	0.0062		20.1

Lahrauli (bulk), 29.89 mg

300	0.15	9.440	0.0345	4.16	2.32
		0.145	0.0002		0.19
400	0.19	10.555	0.0607	3.91	14.48
		0.084	0.0010		1.19
500	0.15	14.276	0.1773	1.68	109.7
		0.395	0.0010		9.0
600	0.26	7.712	0.2476	4.05	79.76
		0.052	0.0060		6.54
700	0.23	6.608	0.3185	4.36	71.85
		0.010	0.0077		5.89
800	0.44	4.701	0.4586	3.64	129.5
		0.015	0.0081		10.6
900	0.50	3.679	0.5205	-	-
		0.051	0.0041		
1200	1.25	5.343	0.4014	4.78	207.1
		0.011	0.0036		17.0
1500	5.59	1.731	0.6897	-	-
		0.007	0.0019		
1850	3.39	3.371	0.5596	-	-
		0.002	0.0013		
Total	12.17	3.360	0.5675	26.58	88.32
		0.016	0.0024		7.25

ALH82130-bulk, 50.24 mg

400	0.17	9.789	0.0523	11.26	4.97
		0.048	0.0026		0.41
500	0.09	9.582	0.0803	-	-
		0.043	0.0026		
800	0.06	3.964	0.5417	10.63	9.02
		0.044	0.0205		0.74
1000	0.28	6.611	0.3397	8.83	5.94
		0.018	0.0040		0.49
1200	0.13	4.156	0.5204	5.92	5.81
		0.024	0.0143		0.48

1400	0.24	1.269	0.7551	0.15	90.16
		0.009	0.0162		7.40
1600	0.29	6.974	0.2905	9.30	0.55
		0.016	0.0050		0.05
1800	0.45	9.407	0.0310	9.08	0.01
		0.022	0.0012		0.01
1850	0.20	10.086	0.0299	12.12	0.02
		0.013	0.0004		0.01
Total	1.91	7.189	0.2602	68.31	3.78
		0.022	0.0057		0.31

ALH81101-bulk, 42.34 mg

400	0.17	8.476	0.0858	16.36	8.85
		0.120	0.0012		0.73
500	0.17	9.372	0.1207	67.05	4.58
		0.054	0.0022		0.38
800	0.53	4.562	0.5508	13.59	25.06
		0.025	0.0078		2.06
1000	0.32	1.475	0.8727	1.55	49.56
		0.020	0.0094		4.07
1200	0.62	1.788	0.8786	2.05	66.58
		0.005	0.0123		5.56
1400	2.09	2.387	0.7811	6.62	22.57
		0.002	0.0063		1.85
1600	1.85	3.003	0.7185	5.13	2.72
		0.009	0.0052		0.22
1850	0.55	9.673	0.0306	1.40	1.50
		0.020	0.003		0.12
Total	3.01	3.633	0.6557	113.7	10.29
		0.014	0.0061		0.84

LEW85328 –Bulk 77.04 mg

300	0.03	10.010	0.0815	24.35	1.38
		0.049	0.0013		0.11
400	-	-	-	20.97	7.25
					0.59
500	0.05	7.242	0.3485	26.78	10.69
		0.031	0.0042		0.88
800	0.33	4.576	0.4653	5.15	54.12
		0.002	0.0062		4.44
1000	0.73	3.385	0.5544	3.31	159.5
		0.015	0.0049		13.08
1200	0.88	3.217	0.5648	25.08	21.79
		0.016	0.0050		1.79
1400	2.39	1.867	0.6755	12.68	45.51
		0.002	0.0050		3.73
1401	0.63	4.113	0.4940	5.19	30.65
		0.048	0.0056		2.51
1450	0.49	4.190	0.4792	2.66	20.73
		0.015	0.0060		1.70
1500	0.75	3.558	0.5512	3.939	8.23
		0.016	0.0040		0.68

1600	2.35	1.870	0.6803	3.977	12.68
		0.04	0.0047		1.04
1850	0.30	9.765	0.0374	029	8.88
		0.046	0.0008		0.73
Total	8.94	2.974	0.5891	134.4	20.11
		0.012	0.0048		1.65

LEW85328 (bulk), Pyrolysis and Combustion, 26.33mg

300	0.18	9.999	0.0356	2.26	3.09
		0.049	0.0010		0.25
400	0.12	12.608	0.0700	1.80	27.38
		0.012	0.0025		2.25
450	0.18	10.032	0.0392	1.47	27.56
		0.25	0.0025		2.26
500	0.27	10.093	0.0696	2.83	52.98
		0.011	0.0002		4.35
600	0.27	9.082	0.1256	4.85	42.80
		0.061	0.0026		3.51
700	0.28	6.091	0.2718	3.02	58.47
		0.179	0.0085		4.80
800	0.49	6.827	0.1721	5.31	35.25
		0.041	0.0059		2.89
900	0.45	5.671	0.3475	-	-
		0.035	0.0039		
1000	0.33	4.278	0.4681	-	-
		0.045	0.0054		
1200	1.77	7.765	0.2153	8.96	47.32
		0.046	0.0018		3.88
1500	3.41	2.224	0.6303	-	-
		0.014	0.0018		
1850	2.61	4.584	0.4350	-	-
		0.020	0.0011		
Total	10.35	5.074	0.4068	30.50	40.72
		0.031	0.0022		3.34

Havero (bulk), 76.53 mg

400	0.07	6.097	0.2869	-	-
		0.422	0.0045		
1000	2.09	1.387	0.7837	2.60	955.9
		0.003	0.0034		63.2
1200	2.09	2.098	0.7162	0.72	508.5
		0.009	0.0036		33.6
1400	1.03	1.418	0.7779	0.91	722.9
		0.003	0.0033		47.8
1600	2.60	2.653	0.6714	0.69	55.64
		0.006	0.0045		3.68
1800	n.d.				
Total	10.88	1.803	0.7445	4.91	721.3
		0.007	0.0036		47.7

ALH78019 (bulk), 42.20 mg

400	15.98	9.179	0.0322	0.89	0.49
		0.040	0.0011		0.03

1000	17.36	8.676	0.0399	-	-
		0.168	0.0002		
1200	23.28	8.718	0.0368	-	-
		0.067	0.0002		
1400	55.12	9.265	0.0501	-	-
		0.045	0.0010		
1600	40.91	8.988	0.0833	-	-
		0.109	0.0017		
Total	152.7	9.088	0.0539	0.89	0.49
		0.079	0.0010		0.03
Nilpena-bulk, 49.15 mg					
300	0.15	10.557	0.0316	1.88	1.16
		0.081	0.0013		0.09
400	0.06	10.901	0.0630	83.85	27.19
		0.034	0.0017		2.23
500	0.14	8.962	0.1790	1.59	116.1
		0.009	0.0042		9.5
600	0.29	6.257	0.3554	3.29	45.71
		0.026	0.0063		3.75
700	0.33	3.535	0.5591	2.09	52.92
		0.010	0.0089		4.34
800	0.78	3.073	0.6070	3.30	52.62
		0.004	0.0056		4.32
900	0.66	3.549	0.5279	16.24	753.0
		0.017	0.0041		61.8
1000	0.56	3.926	0.5545	3.51	33.43
		0.022	0.0030		2.74
1001	0.27	5.751	0.3903	7.99	3.66
		0.024	0.0044		0.30
1200	0.57	6.327	0.4403	1.34	31.17
		0.541	0.0051		2.56
1500	1.51	2.994	0.5770	-	-
		0.012	0.0037		
1850	1.43	4.800	0.4799	-	-
		0.009	0.0008		
Total	6.74	4.430	0.5186	25.99	36.72
		0.059	0.0053		3.01
EET83309-Bulk, 45.90 mg					
300	0.18	9.875	0.0347	10.63	1.77
		0.010	0.0015		0.02
400	0.22	9.754	0.0836	16.77	7.59
		0.024	0.0007		0.62
500	0.34	6.401	0.3877	17.49	77.23
		0.027	0.0030		6.34
800	1.07	2.182	0.7670	6.46	272.9
		0.006	0.0075		22.4
1000	3.98	1.283	0.8466	2.33	673.2
		0.002	0.0067		55.2
1200	2.56	1.701	0.8028	1.85	250.8
		0.005	0.0079		20.6

1400	5.30	1.641	0.8158	2.77	64.57
		0.007	0.0056		5.30
1600	10.54	1.347	0.8417	18.27	2.81
		0.003	0.0058		0.23
1850	-	-			72.11
					2.92
Total	24.19	1.688	0.8101	76.56	72.11
		0.004	0.0061		2.92
EET87720-bulk, 71.41 mg					
300	0.05	9.997	0.0596	2.16	6.01
		0.082	0.002		0.49
400	0.09	9.118	0.1651	2.64	32.37
		0.104	0.0026		2.66
500	0.14	7.030	0.3347	4.75	52.16
		0.003	0.0026		4.28
800	0.69	3.762	0.6594	7.23	30.51
		0.013	0..65		2.50
1000	1.24	2.873	0.7148	2.79	20.88
		0.007	0.0051		1.71
1200	0.94	2.838	0.7336	1.29	16.04
		0.001	0.0064		1.32
1400	1.23	2.101	0.7617	1.04	12.81
		0.003	0.0063		1.05
1500	0.52	5.324	0.4318	0.55	17.61
		0.047	0.0036		1.44
1600	0.30	7.304	0.1891	2.40	3.51
		0.102	0.0018		0.29
1850	-				
Total	5.20	3.599	0.6365	24.84	27.25
		0.018	0.0053		2.24

A 3. Krypton in ureilites

Table A2. The abundance and isotopic compositions of Kr in ureilites.

Temp. (°C)	^{84}Kr 10^{-12} ccSTP/g	80	82	83	86
		84 =100			
Havero (bulk), 76.53 mg, (pyrolysis)					
400	30.5	4.005	22.24	21.88	31.69
		0.104	0.11	0.24	0.07
1000	64.5	5.133	21.41	20.91	31.84
		0.242	0.48	0.19	0.19
1200	158.6	4.503	20.82	21.31	31.47
		0.151	0.06	0.12	0.28
1400	818.1	4.109	20.14	20.52	31.14
		0.045	0.19	0.06	0.20
1600	2883.5	3.986	20.20	20.24	31.04
		0.014	0.04	0.01	0.03
Total	3955.2	4.051	20.25	20.37	31.10

	0.030	0.08	0.03	0.08

Havero (HF/HCl residue), 1.18 mg, (Combustion, 5 torr O₂)

300	72.4	4.329	21.30	20.68	30.53
		0.023	0.36	0.04	0.23
400	271.3	4.173	20.33	20.33	31.26
		0.053	0.18	0.01	0.03
450	160.1	4.223	20.35	20.28	31.01
		0.060	0.09	0.13	0.39
550	483.4	4.135	20.24	20.50	31.47
		0.008	0.05	0.16	0.08
650	1099.4	3.925	20.12	20.10	30.95
		0.050	0.03	0.10	0.07
800	946.9	4.118	20.21	20.31	31.36
		0.012	0.04	0.04	0.19
1000	30.8	3.115	21.05	20.04	32.43
		0.3036	0.25	0.38	0.82
Total	3064.2	4.056	20.24	20.27	31.19
		0.034	0.06	0.09	0.14

Havero (HClO₄ residue), 0.56 mg, (Combustion, 5 torr O₂)

400	35.7	4.372	15.26	21.59	33.50
		0.264	2.14	6.76	1.82
450	29.9	5.647	20.17	21.46	31.65
		0.158	0.43	0.77	1.10
550	269.9	4.242	20.43	20.14	31.34
		0.019	0.23	0.17	0.21
650	1073.7	3.960	20.37	20.22	31.04
		0.062	0.13	0.01	0.07
800	747.1	4.095	20.33	20.28	30.86
		0.017	0.07	0.34	0.07
1000	974.1	4.094	20.30	20.30	31.17
		0.078	0.089	0.03	0.26
Total	3130.4	4.079	20.29	20.28	31.10
		0.056	0.14	0.19	0.17
Total [14]	3064.8	4.061	20.34	20.25	31.06
		0.052	0.11	0.11	0.14

ALH78019 (bulk), 42.20mg, Pyrolysis

400	208.5	4.329	21.29	20.52	32.38
		0.037	0.01	0.28	0.21
1000	559.9	4.222	20.27	20.31	31.25
		0.095	0.07	0.07	0.13
1200	673.9	4.208	20.28	20.24	31.17
		0.016	0.26	0.04	0.05
1400	1673.8	4.013	20.43	20.38	31.19
		0.027	0.05	0.02	0.17
1600	851.5	4.263	20.64	20.61	30.84
		0.074	0.08	0.09	0.16
1800	27.2	6.904	22.37	20.72	34.76
		0.176	0.26	0.23	0.17

---

[14] neglecting steps before 550℃ step.

Total	3994.8	4.165	20.48	20.40	31.21
		0.046	0.10	0.06	0.15
Total [15]	3759.1	4.136	20.43	20.39	31.12
		0.046	0.10	0.05	0.14

ALH78019 (HF/HCl residue), 1.35mg, Combustion, 5 torr O$_2$

300	63.4	4.491	21.10	20.57	31.74
		0.061	0.07	0.33	0.22
400	577.1	4.148	20.22	20.37	31.01
		0.048	0.04	0.07	0.05
450	167.8	4.215	20.70	21.04	31.73
		0.017	0.02	0.08	0.03
550	120.2	4.215	21.00	20.11	31.49
		0.017	0.02	0.07	0.03
650	5.5	3.277	12.20	20.42	34.23
		0.482	2.88	1.92	0.39
800	83.0	4.371	20.13	20.38	30.81
		0.068	0.03	0.23	0.28
1000	18.7	4.389	21.07	20.89	32.67
		0.116	0.55	0.10	0.36
Total	1035.7	4.198	20.41	20.49	31.26
		0.044	0.06	0.11	0.08
Total [16]	1030.2	4.203	20.45	20.47	31.24
		0.042	0.05	0.10	0.08
Total [17]	1011.5	4.200	20.44	20.46	31.22
		0.040	0.04	0.10	0.07

ALH78019 (HClO$_4$ residue), 1.00 mg, Combustion, 5 torr O$_2$

400	27.7	5.234	21.81	22.19	33.51
		0.143	0.13	0.64	0.03
450	7.9	4.934	26.64	21.49	42.96
		0.993	2.35	2.35	2.70
700	60.2	4.092	21.46	20.58	30.13
		0.271	0.13	0.51	0.18
800	25.8	1.883	21.81	21.46	27.50
		0.643	0.19	0.10	0.86
1050	34.0	3.347	21.47	20.30	32.93
		0.093	0.11	0.30	0.22
Total	155.6	3.808	21.84	21.00	31.56
		0.307	0.26	0.51	0.40

LEW85328 (HF/HCl residue), 1.21 mg, combustion, 2 torr O$_2$

300	18.3	5.493	21.86	22.67	29.27
		0.016	0.03	0.02	0.04
400	134.6	3.859	20.25	20.04	30.82
		0.088	0.04	0.02	0.06
500	495.7	3.829	20.29	20.54	30.96
		0.047	0.07	0.03	0.19
600	2759.3	3.958	20.23	20.18	31.09

---

[15] Neglecting 400 & 1800°C steps.

[16] Neglecting 650 °C step.

[17] Neglecting 650 & 1000°C steps.

		0.014	0.03	0.05	0.04
700	2376.2	3.975	20.37	20.40	30.90
		0.016	0.07	0.02	0.05
800	572.2	4.012	20.15	20.10	3087
		0.023	0.03	0.04	0.06
900	8.7	6.954	23.62	17.15	38.03
		0.077	0.03	0.01	0.05
1000	4.2	9.885	29.00	20.03	35.03
		0.077	0.04	0.01	0.05
Total	6369.5	3.970	20.30	20.28	30.99
		0.020	0.05	0.04	0.06
Total [18]	6337.9	3.957	20.28	20.28	30.98
		0.020	0.05	0.04	0.06

LEW85328 (HClO$_4$ residue), 2.07 mg, combustion, 2 torr O$_2$

200	0.9				
300	3.1				
400	28.6	3.749	18.40	19.70	30.08
		0.089	0.33	0.24	0.06
500	61.5	4.003	20.46	20.61	31.16
		0.047	0.06	0.02	0.28
600	1543.7	3.993	20.16	20.21	30.88
		0.015	0.05	0.02	0.06
700	3026.5	3.958	20.20	20.10	30.84
		0.014	0.03	0.01	0.05
800	2656.1	3.984	20.25	20.23	30.92
		0.013	0.03	0.01	0.05
900	1583.3	3.943	20.24	20.21	30.87
		0.012	0.03	0.03	0.05
1000	3.5	7.666	22.56	20.43	36.84
		0.070	0.03	0.01	0.05
Total	8908.2	3.977	20.22	20.19	30.88
		0.014	0.03	0.02	0.05
Total [19]	8900.8	3.969	20.21	20.18	30.88
		0.014	0.03	0.02	0.05

EET87720 (HF/HCl residue), 1.76 mg, 2 torr O$_2$

300	2.7				
400	34.3	3.619	20.01	20.88	32.27
		0.064	0.17	0.35	0.23
500	148.2	3.896	20.22	20.31	31.13
		0.020	0.08	0.05	0.09
600	265.0	3.912	20.18	20.23	31.05
		0.062	0.09	0.02	0.10
700	306.0	4.120	20.26	19.92	30.68
		0.049	0.04	0.20	0.07
800	751.0	3.949	20.27	20.16	31.04
		0.022	0.03	0.04	0.05
1000	6.6	6.3535	26.83	22.30	32.48

---

[18] Neglecting 300, 900 & 1000°C steps
[19] Neglecting 200, 300 & 1000°C steps.

		0.042	0.04	0.016	0.05
Total	1513.8	3.996	20.28	20.18	31.02
		0.035	0.05	0.07	0.07
Total [20]	1504.5	3.964	20.24	20.15	31.01
		0.035	0.05	0.07	0.07
EET87720 (HClO$_4$ residue), 1.89 mg, 2 torr O$_2$					
400	3.1				
500	9.4	3.408	19.88	17.72	35.87
		0.670	0.47	0.15	0.50
600	67.7	4.008	20.01	19.70	31.80
		0.073	0.20	0.03	0.27
700	586.7	3.798	20.36	20.36	30.76
		0.016	0.03	0.07	0.06
800	243.6	3.971	20.78	20.25	31.03
		0.016	0.13	0.08	0.05
900	2.8	-	39.82	23.84	31.14
			0.06	0.02	0.04
Total	913.4	3.872	20.47	20.30	30.97
		0.027	0.08	0.07	0.08
Total [21]	907.7	3.856	20.38	20.25	30.96
		0.027	0.08	0.07	0.08

A 4. Xenon in ureilites

Table A3. Abundance and isotopic composition of xenon in ureilites and their residues

Temp. (°C)	^{132}Xe 10^{-10}ccSTP/g	124	126	128	129	130	131	134	136
					132 =	100			
LEW 85328 (HF/HCl residue) 1.21 mg									
300	14.8	-	-	9.113	102.6	14.38	80.16	38.65	33.20
				0.029	±0.3	0.02	0.06	0.06	0.10
400	161.8	0.5309	0.4871	8.423	103.1	16.29	81.18	37.70	31.50
		0.0067	0.0112	0.141	0.3	0.11	0.30	0.07	0.10
500	934.1	0.4944	0.4566	8.415	103.5	16.42	82.17	37.83	31.51
		0.0096	0.0071	0.040	0.3	0.05	0.10	0.06	0.11
600	3572.9	0.4730	0.4231	8.265	103.5	16.29	82.05	37.93	31.60
		0.0035	0.0126	0.035	0.3	0.03	0.07	0.08	0.10
700	4546.8	0.4689	0.4293	8.220	103.9	16.31	82.07	37.97	31.50
		0.0031	0.0043	0.028	0.3	0.04	0.07	0.06	0.10
800	1618.9	0.4600	0.4413	8.346	104.4	16.31	81.96	38.00	31.82
		0.0087	0.0023	0.028	0.3	0.03	0.11	0.07	0.12
900	6.5	-	-	-	-	-	-	-	-
1000	2.4	-	-	-	-	-	-	-	-
Total	10858	0.4711	0.4313	8.276	103.8	16.31	82.04	37.95	31.58
		0.0047	0.0071	0.032	0.3	0.04	0.08	0.07	0.10
Total [22]	10835	0.4721	0.4323	8.275	103.8	16.31	82.04	37.95	31.58

[20] Neglecting 300 & 1000°C steps.
[21] Neglecting 400, 900°C steps

		0.0047	0.0071	0.032	0.3	0.04	0.08	0.07	0.10
LEW 85328 (HClO₄ residue) 2.07 mg									
300	4.3	-	-	-	-	-	-	-	-
400	56.3	0.5804	0.5774	9.087	102.6	16.81	81.90	39.07	32.52
		0.0193	0.0229	0.054	0.5	0.13	0.53	0.44	0.28
500	128.8	0.5665	0.4892	8.589	103.6	16.63	82.41	38.50	32.15
		0.0082	0.0332	0.125	0.5	0.17	0.20	0.17	0.29
600	1459.1	0.3788	0.4851	8.268	103.6	16.27	81.67	37.98	31.55
		0.0065	0.0031	0.029	0.3	0.03	0.10	0.06	0.10
700	2481.5	0.3929	0.4788	8.246	103.7	16.17	81.98	37.89	31.65
		0.0026	0.0031	0.030	0.25	0.05	0.11	0.06	0.10
800	2163.9	0.4374	0.4776	8.239	103.7	16.39	82.20	37.94	31.69
		0.0044	0.0092	0.036	0.3	0.03	0.10	0.07	0.10
900	1504.1	0.4822	0.4271	8.330	103.5	16.45	82.19	37.96	31.47
		0.0032	0.0029	0.029	0.3	0.52	0.13	0.07	0.10
1000	2.3	-	-	16.196	124.4	21.10	95.76	43.89	39.27
				0.052	0.05	0.03	0.08	0.07	0.12
Total	7800.4	0.4237	0.4702	8.279	103.6	16.32	82.03	37.95	31.64
		0.0042	0.0054	0.033	0.3	0.04	0.11	0.07	0.11
Total[23]	7793.8	0.4241	0.4706	8.276	103.6	16.31	82.03	37.95	31.62
		0.0042	0.0054	0.033	0.3	0.04	0.11	0.07	0.11
EET 87720 (HF/HCl residue) 1.76 mg									
300	2.4	-	-	-	-	-	-	-	-
400	63.3	0.7295	0.6964	8.762	102.8	16.733	81.10	37.55	31.40
		0.0497	0.0198	0.086	0.6	0.239	0.39	0.41	0.15
500	275.9	0.5412	0.4970	8.333	103.4	16.335	81.88	37.20	30.93
		0.0059	0.0042	0.105	0.4	0.043	0.15	0.10	0.11
600	435.0	0.5332	0.4378	8.295	103.6	16.399	81.86	37.52	31.25
		0.017	0.0095	0.044	0.4	0.059	0.07	0.07	0.11
700	5070.6	0.5367	0.4697	8.246	103.1	16.392	81.89	38.04	31.83
		0.0048	0.0029	0.062	0.3	0.065	0.07	0.09	0.16
800	548.6	0.5213	0.4493	8.363	103.5	16.236	81.71	37.60	31.80
		0.0035	0.0119	0.030	0.4	0.045	0.29	0.06	0.10
900	204.9	0.5307	0.4644	8.454	103.7	15.966	82.28	37.90	31.53
		0.0111	0.0040	0.153	0.3	0.096	0.08	0.25	0.19
1000	2.8	-	-	-	-	-	-	-	-
Total	6603.5	0.5366	0.4687	8.275	103.20	16.366	81.873	37.93	31.74
		0.0061	0.0043	0.063	0.31	0.065	0.099	0.10	0.15
Total[24]	6598.2	0.5371	0.4691	8.274	103.21	16.367	81.874	37.93	31.74
		0.0061	0.0043	0.063	0.31	0.065	0.099	0.10	0.15
EET 87720 (HClO₄ residue) 1.89 mg									
400	3.3	-	-	-	-	-	-	-	-
500	16.0	1.1733	0.8468	9.817	106.8	17.20	83.17	39.04	32.43
		0.0010	0.0259	0.032	0.3	0.34	1.04	0.47	0.13
600	219.5	0.5454	0.4988	8.383	104.2	16.37	81.66	38.15	31.88
		0.0065	0.0061	0.114	0.3	0.03	0.07	0.06	0.14

---

[22] After neglecting 300, 900 & 1000°C steps.

[23] After neglecting 300 & 1000°C steps.

[24] Neglecting 300 & 1000°C steps.

700	580.1	0.4995	0.4550	8.353	104.2	16.39	82.34	38.12	31.89
		0.0033	0.0097	0.047	0.3	0.03	0.17	0.06	0.12
800	246.4	0.4668	0.4662	8.453	103.6	16.63	81.91	37.78	31.66
		0.0094	0.0059	0.027	0.5	0.06	0.20	0.22	0.10
900	1.1	-	-	-	-	-	-	-	-
Total	1066.26	0.5595	0.4707	8.412	104.1	16.46	82.12	38.08	31.87
		0.0068	0.0083	0.058	0.3	0.06	0.18	0.11	0.12
Total[25]	1061.93	0.5116	0.4726	8.405	104.1	16.46	82.11	38.06	31.84
		0.0069	0.0084	0.056	0.3	0.06	0.17	0.11	0.12
Havero (bulk) 76.52 mg									
1000	0.8	0.6269	0.6066	8.115	101.4	16.40	80.90	38.74	32.56
		0.0186	0.0348	0.261	0.5	0.03	0.07	0.07	0.10
1200	1.5	0.2263	0.0948	7.585	102.8	16.17	82.29	37.88	30.75
		0.0592	0.0461	0.044	0.3	0.08	0.07	0.22	0.11
1400	4.5	0.4979	0.4628	8.538	103.2	16.57	81.94	37.83	31.43
		0.0435	0.0057	0.032	0.3	0.03	0.07	0.12	0.10
1600	17.5	0.4999	0.4640	8.245	103.6	16.38	82.12	37.78	31.52
		0.0033	0.0057	0.039	0.3	0.05	0.07	0.06	0.10
Total	24.3	0.4875	0.4465	8.255	103.4	16.40	82.06	37.83	31.49
		0.0146	0.0089	0.045	0.3	0.04	0.08	0.08	0.10
Havero (HF/HCl residue) 1.18 mg									
300	8.7	0.5341	0.5252	7.884	102.3	16.29	80.53	39.02	33.81
		0.0539	0.0125	0.013	0.6	0.09	0.74	0.06	0.18
400	396.3	0.4649	0.4060	7.951	101.3	16.00	80.52	38.30	32.32
		0.0057	0.0308	0.060	0.3	0.18	0.34	0.11	0.18
450	201.6	0.4020	0.4387	7.967	101.2	16.48	81.28	38.57	32.89
		0.0106	0.0097	0.075	0.3	0.24	0.09	0.09	0.25
550	540.2	0.6200	0.3980	8.146	102.0	16.31	81.02	37.61	32.15
		0.0381	0.0097	0.480	0.5	0.03	0.08	0.08	0.15
650	1582.9	0.5041	0.4680	8.265	103.2	16.42	82.14	37.96	31.92
		0.0130	0.0092	0.038	0.25	0.04	0.07	0.09	0.10
800	2878.1	0.4732	0.4823	8.497	103.4	16.55	82.34	38.38	32.18
		0.0090	0.0146	0.052	0.3	0.04	0.28	0.07	0.10
1000	220.7	0.3840	0.5849	9.091	103.7	16.46	82.33	38.83	33.25
		0.1260	0.0111	0.249	0.3	0.43	0.14	0.10	0.11
Total	5906.6	0.4895	0.4686	8.361	103.2	16.45	81.98	38.22	32.21
		0.0177	0.0135	0.058	0.3	0.07	0.20	0.08	0.12
Havero (HClO$_4$ residue), 0.56 mg.									
400	15.7	0.2597	0.6408	9.756	102.9	17.83	84.96	37.63	35.42
		0.3313	0.0827	1.496	1.5	0.24	3.05	1.30	0.41
450	30.1	0.1736	0.3782	8.693	103.4	17.57	85.57	38.21	33.44
		0.1114	0.0525	0.124	0.3	0.23	1.34	0.07	0.11
550	233.2	0.7239	0.5592	8.560	103.7	16.35	81.85	37.80	31.34
		0.1166	0.0140	0.081	0.6	0.03	0.07	0.06	0.10
650	553.5	0.5461	0.4615	8.620	103.5	16.41	81.56	38.22	32.11
		0.0149	0.0090	0.035	0.3	0.03	0.41	0.12	0.11
800	466.7	0.7317	0.4669	8.356	103.2	16.59	81.84	37.44	32.31

---

[25] Neglecting 400 & 900°C steps.

		0.0271	0.0084	0.063	0.4	0.032	0.07	0.11	0.30
1000	391.0	0.5654	0.4552	8.287	104.5	16.53	82.10	38.48	31.61
		0.0531	0.0077	0.061	0.4	0.04	0.13	0.07	0.15
Total	1690.2	0.6170	0.4752	8.473	103.7	16.51	81.91	38.00	32.00
		0.0458	0.0107	0.067	0.4	0.04	0.24	0.11	0.17
ALH 78019 (bulk) , 42.20 mg.									
400	0.2	-	-	-	104.2	18.31	84.29	39.45	33.85
					0.3	0.14	0.21	0.71	1.08
1000	3.8	0.5620	0.5483	8.136	102.7	16.16	81.65	37.65	31.93
		0.0238	0.0435	0.056	0.6	0.09	0.09	0.19	0.14
1200	3.7	0.3593	0.1865	8.469	103.4	16.52	82.77	37.80	30.91
		0.0946	0.0223	0.049	0.4	0.16	0.07	0.12	0.10
1400	10.4	0.5039	0.4559	8.358	103.4	16.34	81.83	38.15	31.41
		0.0115	0.0024	0.029	0.3	0.14	0.10	0.06	0.12
1600	8.7	0.5751	0.3829	8.377	103.2	16.65	81.74	37.89	31.77
		0.0216	0.0049	0.027	0.3	0.12	0.30	0.06	0.10
1800	0.2	1.5689	0.9117	5.561	100.1	16.85	79.99	39.47	31.77
		0.0803	0.0371	0.167	1.4	0.67	1.07	0.70	0.10
Total	26.7	0.5382	0.4321	8.343	103.2	16.46	81.90	37.99	31.56
		0.0282	0.0137	0.036	0.4	0.13	0.17	0.10	0.15
ALH 78019 (HF/HCl residue) , 1.35 mg									
300	60.0	0.5163	0.5958	8.597	104.7	16.82	82.78	38.47	31.80
		0.0315	0.0584	0.063	0.3	0.21	0.22	0.30	0.10
400	130.2	0.4585	0.5930	8.605	105.2	16.77	83.29	38.27	31.20
		0.0136	0.0061	0.031	0.6	0.63	0.11	0.31	0.10
450	77.1	0.7005	0.4388	8.478	103.5	16.25	81.70	38.14	31.92
		0.0693	0.0294	0.171	0.3	0.06	0.13	0.09	0.34
550	90.0	0.5049	0.5532	8.710	103.0	16.57	81.15	37.84	31.78
		0.0277	0.0236	0.087	0.3	0.20	0.20	0.37	0.28
650	57.3	0.6930	0.5796	8.857	103.6	16.72	81.95	39.55	32.26
		0.0127	0.0132	0.154	0.3	0.10	0.12	0.67	0.41
800	66.3	0.6514	0.7015	8.833	104.0	16.59	81.78	39.08	32.01
		0.0065	0.0172	0.048	0.4	0.10	0.11	0.10	0.13
1000	30.4	0.7359	0.7755	8.837	104.4	16.99	82.15	39.61	32.32
		0.0817	0.0596	0.107	0.3	0.14	0.84	0.15	0.24
Total	511.1	0.5777	0.5864	8.675	104.1	16.64	82.20	38.52	31.77
		0.0296	0.0242	0.086	0.4	0.12	0.19	0.29	0.22

A 5. Details of simulation of ion implantation

Simulation of ion implantation in spherical diamond grains has been done using SRIM code (Stopping and Range of Ions in Matters). The calculations have been done using an input data file (TRIM.DAT), which supplies the energy of ions, angle of incidence of ions (cosines), coordinates or starting (initial positions) of ions, *etc*. The initial positions of ions are set in such a way that they start from surface of sphere (with radius equal to grain radius under consideration) in random directions. The energy of each ion is distributed randomly between two energies (chosen externally).

Similar calculations have been done for all the noble gases (He to Xe) for 10^6 ions each. Subsequently the grain of diamond is divided into a number of (*e.g.*~500) spherical cells of equal δr' and the number of atoms in each of the cells has been counted for all the noble gases. The ratio of number of atoms in corresponding cells provides the distributions of elemental ratio as a function of radial depth (*see* Fig 5.4). The volume of each spherical cell can be calculated, the ratio of this volume to the total volume of the grain (diamond) provide relative fraction of carbon that resides in each cell. This has been used to calculate the distribution of noble gases (ratios) with percent of carbon combusted.

A 6. Mass dependent Rayleigh fractionation for noble gases

Noble gases are chemically inactive elements and behave as isotopes in the natural system. Therefore, the elemental composition of noble gas can be used as tracer to understand evolution of planets and planetesimals. The major difference between noble gases and isotopes of a particular noble gas element are their atomic sizes. They all have different atomic radii while the isotopes of the same element have similar atomic radii. The advantage is the large differences of masses among different noble gases that lead to larger changes in elemental ratios (as compared to isotopic composition) during the evolution, making the detection easier.

If meteorite parent body lost a fraction of noble gases during secondary processing, the elemental composition of noble gases evolves depending on their masses (and sizes). Let R_o be the initial ratio of two noble gas elements ($^{132}Xe/^{36}Ar$) and *f* be the fraction noble gases remaining after loss. Then the evolved ratio R will be given by

$$R = R_o . f^{\alpha-1}$$

Where, α is the fractionation factor.

Approximately, α is inversely proportional to the square-root of their masses.

A slight variation from the above equation could be expected because in natural system the atomic size will also play an important role that is not considered in the above equation.

A 7. d($^{36}Ar/^{38}Ar$) defined as:

$$d\left({}^{36}Ar\middle/{}^{38}Ar\right)=\left[\frac{\left({}^{36}Ar\middle/{}^{38}Ar\right)_Q}{\left({}^{36}Ar\middle/{}^{38}Ar\right)_{Ureilite}}-1\right]\times 1000 \qquad (‰)$$

References

Alaerts L., Lewis R. S. and Anders E. (1979a) Isotopic anomalies of noble gases in meteorites and their origins-III. LL chondrites. *Geochim. Cosmochim. Acta* **43**, 1399-1415.

Alaerts L., Lewis R. S. and Anders E. (1979b) Isotopic anomalies of noble gases in meteorites and their origins-IV. C3 (Oranans) carbonaceous chondrites. *Geochim. Cosmochim. Acta* **43**, 1421-1432.

Amari S., Lewis R. S. and Anders E. (1994) Interstellar grains in meteorites. I. Isolation of SiC, graphite and diamond; size distribution of SiC and graphite. *Geochim. Cosmochim. Acta* **58**, 459-470.

Anders E. and Grevesse N. (1989) Abundance of elements: Meteoritic and solar. *Geochim. Cosmochim. Acta* **53**,197-214.

Anders E., Higuchi H., Takahashi H. and Morgan J. W. (1975) Extinct superheavy element in the Allende meteorites. *Science* **190**, 1262-1271.

Antarctic Meteorite Newslatter (1983) #2, NASA, JSC, Houston, Texas.

Antarctic Meteorite Newslatter (1987) #10, NASA, JSC, Houston, Texas.

Antarctic Meteorite Newslatter (1990) #13, NASA, JSC, Houston, Texas.

Arden J. W., Ash R. W., Grady M. M., Wright I. P. and Pillinger C. T. (1989) Further studies on the isotopic composition of interstellar grains in Allende: I Diamonds. *Lunar Planet. Sci. XX*, 21-22.

Arrhenius R., Fitzgerald, Markus S. and Simpson C. (1978) Isotope fractionation under simulated space conditions. *Astrphys. Space Sci.* **55**, 285-297.

Baseford J. R., Dragon J. C., Pepin R. O., Coscio Jr. M. R. and Murthy V. R. (1973) Krypton and Xenon in lunar fines. *Proc. of 4th Lunar Sci. Conf.*, 1915-1955.

Becker R. H. and Clayton R. N. (1977) Nitrogen isotopes in lunar soils as a measure of cosmic-ray and rigolith history. *Proc 8th Lunar Sci. Conf.* Houston. **3**, 3685-3704.

Becker R. H., Schlutter D. J., Rider P. E. and Pepin R. O. (1998) An acid-etch study of the Kapoeta achondrite: Implications for the $^{36}Ar/^{38}Ar$ ratio in the solar wind. *Meteorit. Planet. Sci.* **33**, 109-113.

Begemann F., Weber H. W. and Hintenberger H. (1976) On the primordial abundance of argon-40. *Ap. J.* (Letters) **157**, L155-L157.

Benkert J. P., Baur H., Signer P. and Wieler R. (1993) He, Ne, and Ar from the solar wind and solar energetic particles in lunar ilmenites and pyroxenes. *Journ. Geophysi. Res.* 98(E7), 13147-13162.

Berkley J.L. (1986) Four Antarctic ureilites: Petrology and observations on ureilite petrogenesis. *Meteoritcs* **21**, 169-189.

Berkley J. L., Brown H. G., Keil K., Carter N. L. Mercier J-C. C. and Huss G. (1976) The Kenna ureilite: An ultramafic rock with evidence for igneous, metamorphic and shock origin. *Geochim. Cosmochem. Acta* **40**, 1429-1437.

Berkley J.L., Goodrich C. A., and Keil K. (1985) The unique ureilite, ALHA 82106-82130: Evidence for progressive reduction during ureilite magmatic differentiation (abstract). *Meteoritics* **20**, 607-608.

Berkley J.L. and Jones J.H. (1982) Primary igneous carbon in ureilites : Petrological implications. *Proc. Lunar Planet. Sci Conf.* ***XIII***, A353-A364.

Berkley J. L. and Prinz M. (1992) CI chondrite-like clasts in the Nilpena polymict ureilite: Implications for aqueous alteration processes in CI chondrites. *Geochim. Cosmochem. Acta* **56**, 1373-1386.

Berkley J. L., Taylor G. J., Keil K., Harlow G. E. and Prinz M. (1980) The nature and origin of ureilites. *Geochim. Cosmochem. Acta* **44**, 1579-1597.

Berkley J. L. (1989) Precision minor element analyses of silicates minerals in ureilites (abstract). *Lunar planet. Sci.* ***XX***, 61-62.

Bhandari N., Shah V. G., and Graham A. (1981) The Lahrauli ureilite. *Meteoritics* **16**, 185-191.

Bochsler P. and Kallenbach R. (1994) Fractionation of nitrogen isotopes in solar energetic particles. *Meteoritics* **29**, 653-658.

Bogard D. D., Gibson E. K., Jr., Moore D. R., Turner T. L. and Wilkin R. B. (1973) Noble gase and carbon abundances of Havero, Dingo Pup Donga and North Haig ureilites. *Geochim. Cosmochem. Acta* **37**, 547-557.

Boynton W. V., Starzyk P. M. and Schmitt R. A. (1976) Chemical evidence for the genesis of the ureilites, the achondrites Chessigny and the Nakhlites. *Geochim. Cosmochem. Acta* **40**, 1439-1447

Browne J. C. and Berman B. L. (1973) Neutron-capture cross-sections for ^{128}Te and ^{130}Te and xenon anomaly in old tellurium ores. *Phys. Rev.* **C8**, 2405-2411.

Busemann H., Baur H. and Wieler R. (2000) Primordial noble gases in "phase Q" in carbonaceous and ordinary chondrite studied by closed-system stepped etching. *Meteorit. Planet. Sci.* **35**, 949-973.

Cameron A. G. W. (1973) Abundance of elements in the solar system. *Space Sci. Rev.* **15**, 121-146.

Carr L. P., Wright I. P. and Pillinger C. T. (1985) Nitrogen content and isotopic composition of lunar breccia 79135: A high resolution study. *Meteoritics* **20**, 622-623.

Clayton R. N. and Mayeda T. K. (1988) Formation of ureilite by nebular process. *Geochim. Cosmochim. Acta* **52**, 1313-1318.

Clayton R. N. and Thiemens M. H. (1980) Lunar nitrogen: Evidence for secular changes in the solar wind. *Proc. Conf. Anc. Sun*. 463-473.

Donahue T. M., Hoffman, J. H. and Hodges, Jr. R. R. (1981) Krypton and xenon in atmosphere of Venus. *Geophys. Res. Lett.* **8**, 513-516.

Elwert G. Über die Ionisations- und Rekombinationsprozesse in einem Plasma und die ionisationsformel der Sonnenkorona, Z. *Naturforsch., 7a*, **432**. 1952.

Eugster O., Eberhardt P. and Geiss J. (1967) Krypton and Xenon isotopic composition in three carbonaceous chaondrites. Earth planet. Sci. Lett. 3, 249-256.

Eugster O. and Weigel A. (1993) Xe-Q in lodranites and a hint for Xe-L. FRO 940011 another lodranite? (abstract) *Luner Planet. Sci.* **24**, 453-454.

Farquhar J. Jackson T. L. and Thiemens M. H. (2000) A ^{33}S enrichment in ureilite meteorites: Evidence for a nebular sulfur component. *Geochim. Cosmochim. Acta* **64**, 1819-1825.

Fanale F. P. and Cannon W. A. ((1972) Origin of planetary primordial rare gas: the possible role of adsorption, *Geochim. Cosmochim. Acta* **36**, 319-328.

Fouchet T., Lellouch E., Bézard B., Encrenaz T., Drossart P., Feuchtgruber H. and Graauw T. D. (2000) ISO-SWS observations of Jupiter: Measurement of the ammonia tropospheric profile and of the ^{15}N/^{14}N isotopic ratio. *Icarus* **143**, 223-243.

Franchi I. A., Wright I. P. and Pillinger C. T. (1986) Heavy nitrogen in Bencubbin–A light element isotopic anomaly in a stony-iron meteorite. Nature 323, 138-140.

Franchi I. A., Wright I. P. and Pillinger C. T. (1993) Constraints on the formation conditions of iron meteorites based on concentrations and isotopic compositions of nitrogen. *Geochim. Cosmochim. Acta* **57**, 3105-3121.

Frick U. and Chang S. (1978) Elimination of chromite and novel sulfides as important carriers of noble gases in carbonaceous chondrites. *Meteoritics* **13**, 465-470.

Frick U. and Pepin R. O. (1981) On the distribution of noble gases in Allende: A differential oxidation study. *Earth and Planet. Sci Lett.* **56,** 45-63.

Fukanaga K. and Matsuda J. (1997) Vapor growth carbon and the origin of carbonaceous material in ureilites. *Geochemical Journal*, **31**, 263-273.

Fukanaga K., Matsuda J., Nagao K., Miyamoto M. and Ito K. (1987) Noble gas enrichment in vapor-growth diamonds and origin of diamonds in ureilites. *Nature* **328**, 141-143.

Geiss J. and Boschsler P. (1981) On abundance of rare ions in the solar wind. In *Solar Wind Four*, Ed. H. Rosenbauer, (Garching: Max-Planck Institut), pp. 403-414.

Geiss J. and Reeves H. (1972) Cosmic and solar system abundances of duterium and helium-3. *Astron. Astrophys.* **18**, 126-132.

Göbel R., Begemann F. and Ott U. (1982) On neutron-induced and other noble gases in Allnede inclusions. *Geochim. Cosmochim. Acta* **46**, 1777-1792.

Göbel R., Ott U. and Begemann F. (1978) On trapped noble gases in ureilites. *J. Geophys. Res.* **83**, 855-867.

Goodrich C. A. (1992) Ureilites: A critical review. *Meteoritics* **27**, 327-352.

Goodrich C. A., Jones J. H. and Berkley J. L. (1987) Origin and evolution of the ureilite parent magmas: Multy stage igneous activity on a large parent body. *Geochim. Cosmochim. Acta* **51**, 2255-2273.

Grady M. M., Pillinger C. T. (1986) The ALHA 82130 ureilites: Its light element stable isotope composition and relationship to other ureilites (abstract). *Meteoritics*, **23**, 375.

Grady M. M., Pillinger C. T. (1987) The EET 83309 polymict ureilites: Its relationship to other ureilites on the basis of stable isotope measurements (abstract). *Lunar Planet. Sci. Conf.* **XVIII**, 353.

Grady M. M., Pillinger C. T. (1988) ^{15}N enriched nitrogen in polymict ureilite and its bearing on their formation. *Nature* **331**, 321-323.

Grady M. M. and Pillinger C. T. (1990) ALH 85058: nitrogen isotope analysis of a highly unusual primitive chondrite. *Earth Planet. Sci. Lett.* **97**, 29-40.

Grady M. M., Wright I. P., Carr L. P. and Pillinger C. T. (1985) The carbon and nitrogen isotopic composition of ureilites: Implications for their genesis. *Geochim. Cosmochim. Acta* **49**, 903-915.

Grady M. M., Wright I. P., Swart P. K. and Pillinger C. T. (1986) Compositional differences in enstatite chondrites based on carbon and nitrogen stable isotope measurements. *Geochim. Cosmochim. Acta* **50**, 2799-2813.

Haffmann J. H., Hodges R. R. Jr., McElroy M. B., Donahue T. M. and Kolpin M. (1979) Composition and structure of the Venus atmosphere: Results from Pioneer Venus. *Science* **205**, 49-52.

Hashizume K., Chaussidon M., Marty B. and Robert F. (2000) Solar wind record on the Moon: Deciphering presolar from planetary nitrogen. *Science* **290**, 1142-1145.

Higuchi H., Morgan J. W., Ganpathi R. and Anders E. (1976) Chemical variations in meteorite–X. Ureilites. *Geochim. Cosmochim. Acta* **40**, 1563-1571.

Huss G. R. and Lewis R. S. (1994a) Noble gases in presolar diamonds I: Three distinct components and their implications for diamond origins. *Meteoritics* **29**, 791-810.

Huss G. R. and Lewis R. S. (1994b) Noble gases in presolar diamonds II: Components abundances reflect thermal processing. *Meteoritics* **29**, 811-829.

Huss G. R., Lewis R. S. and Hemkin S. (1996) The "Normal planetary" noble gas component in primitive chondrites: Compositions, carrier, and metomorphic history. *Geochim. Cosmochim. Acta* **60**, 3311-3340.

Janssens M-J. Hertogen J., Wolf R., Ebihara M. and Anders E. (1987) Ureilites: Trace element clues to their origin. *Geochim. Cosmochim. Acta* **51**, 2275-2283.

Jaques A. L. and Fitzgerald M. J. (1982) The Nilpena ureilite, an unusual polymict breccia: Implications for the origin. *Geochim. Cosmochim. Acta* **46**, 893-900.

Jewitt D., Matthews H. E., Owen T. and Meier R. (1997) Measurements of $^{12}C/^{13}C$, $^{14}N/^{15}N$, and $^{32}S/^{34}S$ Ratios in Commet Hale-Bopp (C/1995 O1). *Science* **278**, 90-93.

Jokipii J. R. (1964) The distribution of gases in the protoplanetary nebula. *Icarus* **3**, 248-252.

Jorden J. and Pernicka E. (1981) Search for extinct ^{36}Cl in Allnede. *Meteoritics* **16**, 332-333.

Kallenbach R., Geiss J., Ipavich F. M., Gloeckler G., Bochsler P., Gliem F., Hefti S., Hilchenbach M. and Hovestadt D. (1998) Isotopic composition of solar wind nitrogen: First in situ determination with the CELIAS/MTOF spectrometer on board *SOHO*. *Astrophys. J.* **507**, L185-L188.

Kerridge J. F. (1985) Carbon, hydrogen and nitrogen in carbonaceous chondrites: abundance and isotopic compositions in bulk samples. *Geochim. Cosmochim. Acta* **49**, 1707-1714.

Kerridge J. F. (1993) Long-term compositional variation in solar corpuscular radiation: Evidence from nitrogen isotopes in the lunar regolith. *Rev. Geophys.* **31**, 423-437.

Kung C.C. and Clayton R. N. (1978) Nitrogen abundances and isotopic compositions in stony meteorites. *Earth Planet. Sci Lett.* **38**, 421-435.

Lewis R. S. and Anders E. (1981) Isotopically anomalous xenon in mete orite: A new clue to its origin. *Astrophys. J.* **247**, 1122-1127.

Lewis R. S., Srinivasan B. and Anders E. (1975) Host phase of a strange Xe component in Allende. *Science 190*, 1251-1262.

Lewis R. S., Tang M., Wacker J. F., Anders E. and Steel E. (1987) Interstellar diamonds in meteorites. *Nature* **326**, 160-162.

Lipschutz M. E. (1964) Origin of diamonds in ureilites. *Science* **143**,1431-1434.

Malhotra P. D. (1962) A note on composition of Basti meteorite. *Records Geol. Sur. India* **89**, 479-481.

Mathew K. J., Kerridge J. F. and Marti K. (1998) Nitrogen in solar energetic particles: Isotopically distinct from solar wind. *Geophys. Res. Lett.* **25**, 4293-4296.

Matsuda J., Fukanaga K., and Ito K. (1991) Noble gas study in vapor growth diamonds: Comparison with shock produced diamonds and the origin of diamonds in ureilites. *Geochim. Cosmochim. Acta* **55**, 2011-2023.

Matsuda J., Kusumi A., Yajima H. and Syono Y. (1995) Noble gas studies in diamonds synthesized by shock loading in the laboratory and their implications to the origin of diamonds in ureilites. *Geochim. Cosmochim. Acta* **59**, 2011-2023.

Matsuda J. and Maekawa T. (1992) Noble gas implantation in glow discharge: Comparison between diamond and graphite. *Geochemical J.* **26**, 251-259.

Messenger S. (2000) Identification of molecular-cloud material in interplanetary dust particle. Nature 404, 968-971.

Marti K. (1969) Solar-type xenon: and new isotopic composition of xenon in the Pesyanoe meteorite. Science 166, 1263-1265.

McCoy T. J., Clayton R. N., Mayeda T. K., Bogard D. D., Garrison D. H., Huss G. R., Hutcheon I. D. and Wieler R. (1996) A petrologic, chemical, and isotopic study of Monument Draw and comparison with other acapulcoites: Evidence for formation by incipient partial melting. *Geochim. Cosmochim. Acta* **60**, 2681-2708.

Murty S. V. S. (1996) Isotopic composition of nitrogen in 'phase Q'. *Earth Planet. Sci. Lett.* **141**, 307-313.

Murty S. V. S. (1994) Interstellar verses ureilitic diamonds: Nitrogen and noble gas systematics. *Meteoritics* **29**, 507.

Murty S. V. S. and Bhandari N. (1992) Noble gases and nitrogen in Lahrauli Ureilite. *7th Symposium on Antarctic Meteorites.* 86-1– 86-3.

Murty S. V. S., Goswami J. N. and Shukolyukov Yu. A. (1997) Excess ^{36}Cl in the Efremovka meteorite: A strong hint for the presence of ^{36}Cl in the early solar system. *Astrophys. Journ.* **475**, L65-L68.

Murty S. V. S., Rai V. K. and Ott U. (1999) Nitrogen and noble gases in the diamond free ureilite ALH78019 (abstract). *Meteorit. Planet. Sci.* **34**, A85.

Murty S. V. S. and Wasserburg, G. J. (1996) Search for extinct ^{36}Cl in a halogen-rich chondrule from Allnede (abstract). *Meteorit. Planet. Sci.* **31**, A94.

Neuvonen K. J., Ohlson B., Papuen T. A., Häkli T. A. and Ramdohr P. (1972) The Haverö ureilite. *Meteoritics* **7**, 515-531.

Niemann H. B., Atreya S. K., Carignan G. R., Donahue T. M., Habermann J. A., Harpold D. N., Hartle R. E., Hunten D. M., Kasprzak W. T., Mahaffy P. R., Owen T. C., Spencer N. W. and Way S. H. (1996) The Galileo probe mass spectrometer: composition of Jupiter's atmosphere. *Science* **272**, 846-849.

Nier A. O. (1950) A redetermination of the relative abundances of the isotopes of neon, kryptopn, rubidium, xenon and murcury. **79**, 450-454.

Nier A. O., McElroy M. B. and Yung Y. L. (1976) Isotopic composition of Martian atmosphere. *Science* **194**, 68-70.

Norris S. J., Swart P. K., Wright I. P., Grady M. M. and Pillinger C. T. (1983) A search for correlatable, isotopically light carbon and nitrogen components in lunar soils and breccias. *J. Geophys. Res.* **88**, B200-B210.

Ott U., Löhr H. P., and Begemann F. (1984) Ureilites: the case of missing diamonds and a new neon component (abstract). *Meteoritics* **19**, 287-288.

Ott U., Löhr H. P., and Begemann F. (1985a) Trapped neon in ureilites – a new component. *In isotopic ratios in the solar system/ Rapports isotopiques dans le systeme solaire*, 129-136. Centre National d'Etudes Spatiales, Peris, 19-22 June 84/19-22 Juin 84.

Ott U., Löhr H. P., and Begemann F. (1985b) Trapped noble gases in 5 more ureilites and the possible role of Q. *Lunar and Planet. Sci. Conf. XVI*, 639-640.

Ott U., Löhr H. P., and Begemann F. (1990) EET83309: A ureilite with solar noble gases. *Meteoritics* **25**, 396.

Ott U., Löhr H. P., and Begemann F. (1993) Solar noble gases in polymict ureilites and an update on ureilite noble gas data. *Meteoritics* **28**, 415-416.

Ott U., Mack R. and Chang S. (1981) Noble-gas-rich separates from the Allende meteorite. *Geochim. Cosmochim. Acta* **45**, 1751-1788.

Ott U. (1996) Interstellar diamond xenon and timescales of supernova ejecta. *Astrophys. Jour.* **463**, 344-348.

Owen T., Biemann K., Rushneck D. R., Biller J. E., Howarth D. W. and Lafleur A. L. (1977) The composition of atmosphere at the surface of Mars. *Jour. Geophys. Res.* **82** 4635-4639.

Ozima M. and Nakazawa K. (1980) Origin of rare gases in the Earth, *Nature* **284**, 313-316.

Ozima M. and Podosek F. A. (1983) *Noble gas geochemistry*. Cambridge University Press, Cambridge.

Ozima M., Wieler R., Marti B., and Podosek F. A. (1998) Comparative study of solar, Q-gases and terrestrial noble gases, and implications on the evolution of the solar nebula. . *Geochim. Cosmochim. Acta* **62**, 301-314.

Ozima M. and Zahnle K. (1993) Mantle degassing and atmospheric evolution: Noble gas view. *Geochemical J.* **27**, 185-200.

Pepin R. O. (1967) Trapped neon in meteorites. *Earth planet Sci. Lett.* **2**, 13-18.

Pepin R. O. (1991) On the origin and early evolution of terrestrial planet atmosphere and meteorite volatiles. Icarus 92, 2-79.

Pepin R. O. (1992) Origin of noble gases in terrestrial planets. *Ann. Rev. Earth Planet. Sci.* **20**, 389-830.

Pepin R. O. and Phinny D. (1978) Components of xenon in the solar system. Preprint. University of Minnesotta.

Podosek F. A. and Swindle T. D. (1988) Extinct radionuclides. *Meteorites and Early Solar System.* (Eds. Kerridge J. F. and Mattews M. S.) , The University of Arizona Press, Tucson.

Pollack J. B. and Black D. C. (1982) Noble gases in planetary atmosphere: Implications for the origin and evolution of atmosphere. *Icarus* **51**, 169-198.

Prinz M., Weisberg M. K., Nehru C. E. and Delaney J. S. (1987) EET83309, a polymict ureilite: Recognition of a new group (abstract). *Lunar and Planet. Sci. Conf.* **XIX**, 947-948.

Prombo C. A. and Clayton R. N. (1985) A striking nitrogen isotopic anomaly in the Bencubbin and Weatherford meteorites. *Science* **230**, 935-937.

Prombo C. A. and Clayton R. N. (1993) Nitrogen isotopic composition of iron meteorites. *Geochim. Cosmochim. Acta* **57**, 3749-3761.

Rai V. K., Murty S. V. S. and Ott U. (2000) EET83309: A polymict ureilite having similarities with diamond free ureilite, ALH78019 (abstract). *Meteorit. Planet. Sci.* **35**, A133.

Rai V. K., Murty S. V. S. and Ott U. (2000) LEW 85328: A monomict ureilite containing both heavy and light nitrogen (abstract). *Meteorit. Planet. Sci.* **35**, A132.

Reynolds J. H., Frick U., Neil J. M. and Phinney D. L. (1978) Rare-gas-rich separates from carbonaceous chondrites. *Geochim. Cosmochim. Acta* **42**, 1775-1797.

Rooke G. P., Frainchi I. A., Verchovsky A. B. and Pillinger C. T. (1998) Relationship between noble gases and the heavy nitrogen in polymict ureilites (abstract). *Lunar Planet. Sci. Conf.* **XXIX**, 1744.pdf (disc).

Rooke G. P., Frainchi I. A., Verchovsky A. B. and Pillinger C. T. (1998) Nitrogen-15-rich nitrogen in meteorites: Polymict ureilites and Bencubbin (abstract). *Meteorit. Planet. Sci.* **33**, A130.

Russell S. S., Arden J. W. and Pillinger C. T. (1991) Evidence for multiple source of diamonds from primitive chondrites. *Science* **254**, 1188-1191.

Russell S. S., Arden J. W., Franchi I. A. and Pillinger C. T. (1993) A carbon and nitrogen isotope study of carbonaceous veins material in ureilites (abstract). *Lunar Planet. Sci. Conf. XXIV*, 1221-1222.

Rubin A. E. (1988) Formation of ureilites by impact-melting of carbonaceous chondritic material. *Meteoritics* **23**, 333-337.

Saito J. and Takeda H. (1989) Minerological study of LEW85328 ureilite (abstract). *Lunar Planet. Sci XX*, 938-939.

Saito J. and Takeda H. (1990) Information of elemental distributions in heavily shocked ureilites as a guide to deduce the ureilite formation process. *Lunar Planet. Sci XXI*, 1063-1064.

Schelhaas N., Ott U. and Begemann F. (1990) Trapped noble gases in unequilibrated ordianary chondrites. *Geochim. Cosmochim. Acta* **54**, 2869-2882.

Schulz L. and Freundel M. (1985) On the production rate of ^{21}Ne in ordinary chondrites. In Isotopic Ratios in the Solar System (Ed. Centre National d'Etudes Spatiales). pp 27-33, Cepadues-Editions, Toulouse, France.

Scott E. R. D., Taylor G. and Keil K. (1993) Origin of ureilite meteorites and implications for planetary accretion. *Geophys. Res. Lett.* **20**, 415-418.

Signer P. and Suess H. E. (1963) Rare gases in Sun, in the atmosphere, and in meteorites. *In Earth Science and Meteorites* (Eds. J. Geiss and E. D. Goldberg), pp. 241-272.

Smith C. L., Franchi I. A., Wright I. P., Grady M. M. Verchovsky A. B. and Pillinger C. T. (1999) A preliminary noble gas and light element stable isotopic study of the FOR 90228 Low-carbon ureilite. *Meteorit. Planet. Sci.* **33**, 31-48.

Smith S. P., Huneke J. C., Rajan R. S., and Wasserburg G. J. (1977) Neon and argon in the Allende meteorite. *Geochim. Cosmochim. Acta* **41**, 627-647.

Spitz A. H. (1992) ICP-MS trace element analysis of ureilites: Evidence for mixing of distinct components (abstract) Lunar Planet. Sci Conf. XXIII, 1339-1340.

Spitz A. H. and Boynton W. V. (1991) Trace element analysis of ureilites: New constraints on their petrogenesis. *Geochim. Cosmochim. Acta* **55**, 3417-3430.

Srinivasan G., Sahijpal S., Ulyanove, A. A. and Goswami J. N. (1996) Ion microprobe studies of Efremovka CAIs: II. Potessium isotope composition and ^{41}Ca in the early solar system. *Geochim. Cosmochim. Acta* **60**, 1823-1835.

Swindle T. D., Kring D. A., Burkland M. K., Hill D. H. and Boynton W. V. (1998) Noble gas, bulk chemistry, and petrography of olivine-rich achondrite Eagle Nest and Lewis Cliff 88763: comparison to brachinites. *Meteorit. Planet. Sci.* **33**, 31-48.

Takeda H. (1987) Mineralogy of antarctic ureilites and a working hypothesis for their origin and evolution. *Earth Planet. Sci. Lett.* **81**, 358-370.

Takeda H. (1989) Mineralogy of coexisting pyroxenes in magnesian ureilites and their formation conditions. *Earth Planet. Sci. Lett.* **93**, 181-194.

Takeda H., Mori H., Yanai K. and Shiraishi K. (1980) Mineralogical examination of Allen Hill achondrites and their bearing on the parent bodies. *Proc. 5th symp on Antarctic Meteorites, Nat. Inst. Polar Research, Spec. Issue* **17**, 119-144.

Takeda H., Mori H. and Ogata H. (1989) Mineralogy of augite-bearing ureilite and the origin of their chemical trends. *Meteoritics* **24**, 73-81.

Thiemens M. H. and Clayton R. N. (1980) Ancient solar wind in lunar microbreccias. *Earth Planet. Sci. Lett.* **47**, 34-42.

Tokunaga A. T., Knacke R. F., Ridgway S.T. and Wallace L. (1979) High-resolution spectra of Jupiter in the 744980 inverse centimeter spectral range. *Astrophys. J.* **232**, 603-615.

Vdovykin G. P. (1970) Ureilites. *Space Sci. Rev.* **10**, 483-510.

Vdovykin G. P. (1972) The forms of carbon in the new Haverö ureilite of Finland. Meteoritics, 7, 547-552.

Vdovykin G. P. (1976) The Haverö ureilite. *Space Sci. Rev.* 18, 749-776.

Wacker J. F. (1984) Noble gases in the unshocked ureilite Allen Hills 78019 (abstract). *Meteoritics* **19**, 326-327.

Wacker J. F. (1986) Noble gases in diamond free ureilite, ALHA 78019: The role of shock and nebular processes. *Geochim. Cosmochim. Acta* **50**, 633-642.

Wacker J. F., Zadnic M. G. and Anders E. (1985) Laboratory simulation of meteoritic noble gases. I Sorption of Xe on carbon: Trapping experiment. *Geochim. Cosmochim. Acta* **49**, 1035-1048.

Wacker J. F. (1989) Laboratory simulation of meteoritic noble gases. III Sorption of neon, argon, krypton, and xenon on carbon: elemental fractionation. *Geochim. Cosmochim. Acta* **53**, 1421-1433.

Wacker J. F. (1986) Noble gases in diamond free ureilite, ALH78019: The role of shock and nebular processes. *Geochim. Cosmochim. Acta* **50**, 633-642.

Walker D. and Groove T. (1993) Ureilite smelting. *Meteoritics* **28**, 629-636.

Wänke H., Baddenhausen H., Spettel B, Teschke F, Quuano-Rico M., Dreibus G. and Palme H. (1972) The chemistry of Haverö ureilite. *Meteoritics* **7**, 579-590.

Warren P. H. and Kallemeyn G. W. (1989) Geochemistry of polymcit ureilite EET 83309, and a partially-disruptive impact model for ureilite origin. *Meteoritics* **24**, 233-246.

Warren P. H. and Kallemeyn G. W. (1991) Geochemistry of unique achondrite MAC88177: Comparison with polymict ureilite EET87720 (abstract). *Lunar Planet. Sci.* **XXII**, 1467-1468.

Wasson J. T. (1985) Meteorites: Their records of early-solar system history. (New York: W. H. Freemann).

Wasson J. T., Chou C. L., Bild R. W. and Baedecker P. A. (1976) Classification of and elemental fractionation among ureilites. *Geochim. Cosmochim. Acta* **40**, 1449-1458.

Weber H. W., Hintenberger H. and Begemann F. (1971) Noble gases in the Haverö ureilite. *Earth Planet. Sci. Lett.* **13**, 205-209.

Weber H. W., Begemann F. and Hintenberger H. (1976) Primordial gases in graphite-diamond-kamacite inclusions from the Haverö ureilites. *Earth Planet. Sci. Lett.* **29**, 81-90.

Wieler R., Anders E., Baur H., Lewis R. S. and Signer P (1991) Noble gases in " Phase Q": Closed system etching of an Allende residue. *Geochim. Cosmochim. Acta* **55**, 1709-1722.

Wieler R., Anders E., Baur H., Lewis R. S. and Signer P (1992) Characterization of Q gases and other noble gas components in the Murchison Meteorite. *Geochim. Cosmochim. Acta* **56**, 2907-2921.

Wieler R. and Baur H. (1995) Fractionation of Xe, Kr, and Ar in the solar corpuscular radiation deduced by closed system etching of lunar soils. *Astrophys. J.* **456**, 987-997.

Wilkening L. L. and Marti K. (1976) Rare gases and fossil tracks in the Kenna ureilite. *Geochim. Cosmochim. Acta* **40**, 1265-1473.

Yamamoto T., Hashizume K., Matsuda J. and Kase T. (1998) Multiple nitrogen components coexisting in ureilites. *Meteorit. Planet. Sci.* **33**, 857-870.

Zadnic M. G., Wacker J. F. and Lewis R. S. (1985) Laboratory simulation of meteorite noble gases. II. Sorption of xenon on carbon: etching experiments. *Geochim. Cosmochim. Acta* **49**, 1049-1059.

Zahnle K. (1993) Planetary noble gases. *In Protostars and Planets III* (eds. (E. H. Levy and I Lunine), pp 1305-1338. The University of Arizona Press, Tucson.

Zahnle K., Pollak J. B. and Kasting J. F. (1990) Xenon fractionation in porous planetesimals. *Geochim. Cosmochim. Acta* **54**, 2577-2586.

Ziegler's home page, 2000,
http://www.research.ibm.com.ionbeams/SRIM/SRIMNTR.HTM.

Zinner E., Tang M. and Anders E. (1989) Interstellar SiC in the Murchison and Murray meteorites: Isotopic compositions of Ne, Xe, Si, C, and N. *Geochim. Cosmochim. Acta* **53**, 3273-3290.